

FROM WEARABLE TOWARDS EPIDERMAL COMPUTING

Soft Wearable Devices for Rich Interaction on the Skin



UNIVERSITÄT
DES
SAARLANDES

A dissertation submitted towards the degree
Doctor of Engineering (Dr.-Ing.)
of the Faculty of Mathematics and Computer Science
of Saarland University

ADITYA SHEKHAR NITTALA

Saarbrücken 2021

Date of the Colloquium: 11th Feb 2022
Dean of the Faculty: Univ.-Prof. Dr. Thomas Schuster

Chair of the Committee: Prof. Dr. Martina Maggio

Reporters

First Reviewer: Prof. Dr. Jürgen Steimle
(Saarland University, Germany)

Second Reviewer: Prof. Dr. Stefanie Mueller
(MIT CSAIL, USA)

Third Reviewer: Dr. Alex Olwal
(Google Research, USA)

Academic Assistant: Dr. Dimitar Valkov
(DFKI, Germany)

Dedicated to my wife Aparna and our son Abhiram Shekhar whose presence has ushered a new joy into my life.

To my brother Krishna Chaitanya and his wife, my parents Ramakrishna and Lakshmi.

ABSTRACT

Human skin provides a large, always available, and easy to access real-estate for interaction. Recent advances in new materials, electronics, and human-computer interaction have led to the emergence of electronic devices that reside directly on the user's skin. These conformal devices, referred to as *Epidermal Devices*, have mechanical properties compatible with human skin: they are very thin, often thinner than human hair; they elastically deform when the body is moving, and stretch with the user's skin.

Firstly, this thesis provides a conceptual understanding of Epidermal Devices in the HCI literature. We compare and contrast them with other technical approaches that enable novel on-skin interactions. Then, through a multi-disciplinary analysis of Epidermal Devices, we identify the design goals and challenges that need to be addressed for advancing this emerging research area in HCI. Following this, our fundamental empirical research investigated how epidermal devices of different rigidity levels affect passive and active tactile perception. Generally, a correlation was found between the device rigidity and tactile sensitivity thresholds as well as roughness discrimination ability. Based on these findings, we derive design recommendations for realizing epidermal devices.

Secondly, this thesis contributes novel *Epidermal Devices* that enable rich on-body interaction. *SkinMarks* contributes to the fabrication and design of novel Epidermal Devices that are highly skin-conformal and enable touch, squeeze, and bend sensing with co-located visual output. These devices can be deployed on highly challenging body locations, enabling novel interaction techniques and expanding the design space of on-body interaction. *Multi-Touch Skin* enables high-resolution multi-touch input on the body. We present the first non-rectangular and high-resolution multi-touch sensor overlays for use on skin and introduce a design tool that generates such sensors in custom shapes and sizes. Empirical results from two technical evaluations confirm that the sensor achieves a high signal-to-noise ratio on the body under various grounding conditions and has a high spatial accuracy even when subjected to strong deformations.

Thirdly, Epidermal Devices are in contact with the skin, they offer opportunities for sensing rich physiological signals from the body. To leverage this unique property, this thesis presents rapid fabrication and computational design techniques for realizing *Multi-Modal Epidermal Devices* that can measure multiple physiological signals from the human body. Devices fabricated through these techniques can measure ECG (Electrocardiogram), EMG (Electromyogram), and EDA (Electro-Dermal Activity). We also contribute a computational design and optimization method based on underlying human anatomical models to create optimized device designs that provide an optimal trade-off between physiological

signal acquisition capability and device size. The graphical tool allows for easily specifying design preferences and to visually analyze the generated designs in real-time, enabling designer-in-the-loop optimization. Experimental results show high quantitative agreement between the prediction of the optimizer and experimentally collected physiological data.

Finally, taking a multi-disciplinary perspective, we outline the roadmap for future research in this area by highlighting the next important steps, opportunities, and challenges. Taken together, this thesis contributes towards a holistic understanding of *Epidermal Devices*: it provides an empirical and conceptual understanding as well as technical insights through contributions in DIY (Do-It-Yourself), rapid fabrication, and computational design techniques.

ZUSAMMENFASSUNG

Die menschliche Haut bietet eine große, stets verfügbare und leicht zugängliche Fläche für Interaktion. Jüngste Fortschritte in den Bereichen Materialwissenschaft, Elektronik und Mensch-Computer-Interaktion (Human-Computer-Interaction, HCI) [so that you can later use the English abbreviation] haben zur Entwicklung elektronischer Geräte geführt, die sich direkt auf der Haut des Benutzers befinden. Diese sogenannten *Epidermisgeräte* haben mechanische Eigenschaften, die mit der menschlichen Haut kompatibel sind: Sie sind sehr dünn, oft dünner als ein menschliches Haar; sie verformen sich elastisch, wenn sich der Körper bewegt, und dehnen sich mit der Haut des Benutzers.

Diese Thesis bietet, erstens, ein konzeptionelles Verständnis von Epidermisgeräten in der HCI-Literatur. Wir vergleichen sie mit anderen technischen Ansätzen, die neuartige Interaktionen auf der Haut ermöglichen. Dann identifizieren wir durch eine multidisziplinäre Analyse von Epidermisgeräten die Designziele und Herausforderungen, die angegangen werden müssen, um diesen aufstrebenden Forschungsbereich voranzubringen. Im Anschluss daran untersuchten wir in unserer empirischen Grundlagenforschung, wie epidermale Geräte unterschiedlicher Steifigkeit die passive und aktive taktile Wahrnehmung beeinflussen. Im Allgemeinen wurde eine Korrelation zwischen der Steifigkeit des Geräts und den taktilen Empfindlichkeitsschwellen sowie der Fähigkeit zur Rauheitsunterscheidung festgestellt. Basierend auf diesen Ergebnissen leiten wir Designempfehlungen für die Realisierung epidermaler Geräte ab.

Zweitens trägt diese Thesis zu neuartigen *Epidermisgeräten* bei, die eine reichhaltige Interaktion am Körper ermöglichen. *SkinMarks* trägt zur Herstellung und zum Design neuartiger Epidermisgeräte bei, die hochgradig an die Haut angepasst sind und Berührungs-, Quetsch- und Biegesensoren mit gleichzeitiger visueller Ausgabe ermöglichen. Diese Geräte können an sehr schwierigen Körperstellen eingesetzt werden, ermöglichen neuartige Interaktionstechniken und erweitern den Designraum für die Interaktion am Körper. *Multi-Touch Skin* ermöglicht hochauflösende Multi-Touch-Eingaben am Körper. Wir präsentieren die ersten nicht-rechteckigen und hochauflösenden Multi-Touch-Sensor-Overlays zur Verwendung auf der Haut und stellen ein Design-Tool vor, das solche Sensoren in benutzerdefinierten Formen und Größen erzeugt. Empirische Ergebnisse aus zwei technischen Evaluierungen bestätigen, dass der Sensor auf dem Körper unter verschiedenen Bedingungen ein hohes Signal-Rausch-Verhältnis erreicht und eine hohe räumliche Auflösung aufweist, selbst wenn er starken Verformungen ausgesetzt ist.

Drittens, da Epidermisgeräte in Kontakt mit der Haut stehen, bieten sie die Möglichkeit, reichhaltige physiologische Signale des Körpers zu erfassen. Um

diese einzigartige Eigenschaft zu nutzen, werden in dieser Arbeit Techniken zur schnellen Herstellung und zum computergestützten Design von multimodalen Epidermisgeräten vorgestellt, die mehrere physiologische Signale des menschlichen Körpers messen können. Die mit diesen Techniken hergestellten Geräte können EKG (Elektrokardiogramm), EMG (Elektromyogramm) und EDA (elektrodermale Aktivität) messen. Darüber hinaus stellen wir eine computergestützte Design- und Optimierungsmethode vor, die auf den zugrunde liegenden anatomischen Modellen des Menschen basiert, um optimierte Gerätedesigns zu erstellen. Diese Designs bieten einen optimalen Kompromiss zwischen der Fähigkeit zur Erfassung physiologischer Signale und der Größe des Geräts. Das grafische Tool ermöglicht die einfache Festlegung von Designpräferenzen und die visuelle Analyse der generierten Designs in Echtzeit, was eine Optimierung durch den Designer im laufenden Betrieb ermöglicht. Experimentelle Ergebnisse zeigen eine hohe quantitative Übereinstimmung zwischen den Vorhersagen des Optimierers und den experimentell erfassten physiologischen Daten.

Schließlich skizzieren wir aus einer multidisziplinären Perspektive einen Fahrplan für zukünftige Forschung in diesem Bereich, indem wir die nächsten wichtigen Schritte, Möglichkeiten und Herausforderungen hervorheben. Insgesamt trägt diese Arbeit zu einem ganzheitlichen Verständnis von *Epidermisgeräten* bei: Sie liefert ein empirisches und konzeptionelles Verständnis sowie technische Einblicke durch Beiträge zu DIY (Do-It-Yourself), schneller Fertigung und computergestützten Entwurfstechniken.

ACKNOWLEDGMENTS

This thesis would not have been possible without the support of several friends, colleagues and family. I am grateful for the support and the many positive experiences that have had a profound impact not only on my research but have shaped me personally.

Firstly, I would like to thank my advisor Jürgen Steimle. His guidance, mentoring, and unwavering support during challenging times have been phenomenal. I have learned a lot from our several invaluable discussions that pushed the boundaries of science and helped me mature as a researcher. I also would like to thank my committee members Stefanie Mueller and Alex Olwal who have been very supportive during this journey. I will cherish all those invaluable and insightful discussions we had with Alex during the *SkinMarks* project. I also would like to thank all the Ph.D. students and post-docs at the HCI lab for creating a wonderful and fun environment to work in. I would like to thank Martin Weigel and Daniel Groeger who has been my amazing lab-mates during the first years of my Ph.D. I also would like to Anusha Withana and Joan Sol Roo for being such wonderful post-docs, imparting their knowledge, and sharing their experiences with me. It was a great experience working with Marion Koelle, Paul Strohmeier, Marc Teyssier and Bruno Fruchard. I really enjoyed the discussions we used to have and the recent project with Madalina.

A big thanks to Adwait Sharma who has been a wonderful colleague, and an awesome friend. His help and support during the deadlines have been invaluable. From his days as a very polite intern to a very strong Ph.D. candidate, I have learned a lot from him. I wish him lots of success in his future. While we have collaborated on research projects, I will forever cherish the personal relationship with him that has developed over the years.

Over the past years, I had the opportunity to meet and collaborate with amazing researchers not only from the CS department of Saarland University but also with scientists from the INM-Leibniz institute for new materials. A special thanks to Klaus Kruttwig for helping me understand the material-related aspects of my research. I also would like to thank Arshad Khan who has immensely helped me with his expertise in functional materials, inkjet printing, and for his great support in the PhysioSkin project. Special thanks to Prof. Tobias Kraus and Prof. Roland Bennewitz, who with their deep knowledge in materials and experimental physics respectively have always inspired me. My conversations working with them on the Like a Second Skin and our recent Nature Communications article paper have been very rewarding.

I am grateful to my other collaborators and mentors in the HCI community. Specifically, I would like to thank my former advisors and mentors during my

Masters: Ehud Sharlin, Xing-Dong Yang, Mario Costa Sousa and Teddy Seyed for priming me towards academic research. Working with Xing-Dong and his team including Jun Gong and Zheer Xu on TipText project was very exciting and I hope to continue having such wonderful collaborations.

I also would like to thank all the students I was fortunate to work with: Narjes Pourjafarian, Rukmini Manoz Banda, Elif Ataka, Leon Sauerwald, Tejaswani Verma, Anusha Gadepalli. The best part of academic research is that you always continue to learn not only from your colleagues and seniors but also from students you mentor. I can say that I have learnt a lot through my mentoring experiences. Narjes who worked with me for their masters thesis turned out to be a very nice PhD lab mate. A special mention to Manoz Banda who in addition to working with me on his masters thesis has also been a great roommate and a great friend.

A big thanks to the administrative staff and assistants at the Cluster of Excellence, MMCI and HCI lab: Mona Linn, Natalia Weise, Polina Quaranta, Asel Bojarski and Anne Bardesano-Kopsel, Kathrin Keim. I am grateful for their help in the paper work and logistics on several occasions.

I would like to thank the members of the cricket fraternity at Saarbruecken. It has been such a wonderful experience playing for the university cricket team and winning national championships. Thanks to Ramgopal Balijepalli and Axel Koch for letting me be part of this and giving me the opportunity to lead a team full of enthusiastic players who were students at Saarland University.

I would like to thank my parents and brother for showing support and faith in me, always encouraging me to pursue things of my interest. A special mention to my wife Aparna who has been my pillar of strength and support during this entire journey. On the personal front, her addition to my life has had a deep impact on me. I also would like to thank my sister-in-law for her support and encouragement. She has been a vital part of this journey. Last but not the least, I would like to thank my father-in-law GDS Sastry and my mother-in-law Sujatha Gadepalli. They have been additional pillars of support during this journey. I have always appreciated their constant support and encouragement.

CONTENTS

1	INTRODUCTION	21
1.1	Skin as an Interactive Medium	21
1.2	Epidermal Computing	22
1.3	Research Challenges and Contributions	23
1.4	Structure of the Thesis	27
I	Part One - Understanding Epidermal Computing and Skin Coformality	33
2	BACKGROUND	35
2.1	Functions and Anatomy of Skin	35
2.1.1	Layers of Skin	36
2.1.2	Skin as a Sense Organ	37
2.2	Multi-Disciplinary Analysis of Epidermal Devices	38
2.3	Materials	40
2.3.1	Substrates	40
2.3.2	Functional Materials	42
2.3.3	Skin Adhesives	43
2.4	Fabrication	44
2.4.1	Fabrication Methods	45
2.4.2	Computational Design and Optimization	46
2.4.3	Aesthetics	46
2.5	Functionality of Devices	47
2.5.1	Input	48
2.5.2	Output	51
2.5.3	Computation and Communication	52
2.5.4	Energy Harvesting	53
2.6	Evaluation Methods and Strategies	54
2.6.1	Technical Evaluations	54
2.6.2	Empirical Studies and User Experiments	55
2.7	Applications and Real-World Deployments	56
2.7.1	Health Monitoring and Diagnosis	57
2.7.2	Assistive Technologies	57
2.7.3	Sports and Fitness	57
2.7.4	Affective Communication	58
2.7.5	Mobile Computing	58
2.8	Positioning Epidermal Computing in HCI Literature	58
2.8.1	Overview of Sensing Techniques for On-Body Interaction	59

2.8.2	Other Technologies from the Taxonomy of On-Body Interaction	64
2.9	Summary	68
2.9.1	Material Exploration	69
2.9.2	Enriching Sensing Capabilities of Epidermal Devices	69
2.9.3	Easy and Rapid Fabrication Methods couples with Computational Design Approaches	70
2.9.4	Empirical Studies to Inform Device Design	70
3	UNDERSTANDING HOW EPIDERMAL DEVICES AFFECT TACTILE PERCEPTION	71
3.1	Classification Of Epidermal Devices	72
3.1.1	Flexural Rigidity	72
3.1.2	Classification of Prior Work	74
3.2	Experiment Overview	76
3.2.1	Rigidity Levels and Materials	76
3.2.2	Body Locations	78
3.2.3	Participants	78
3.2.4	Experiment Design	78
3.2.5	Analysis	79
3.3	Experiment 1: Tactile Sensitivity	80
3.3.1	Apparatus	80
3.3.2	Design and Procedure	81
3.3.3	Results	81
3.3.4	Discussion	82
3.4	Experiment 2: Two-Point Orientation Discrimination	84
3.4.1	Apparatus	84
3.4.2	Design and Procedure	84
3.4.3	Results	85
3.4.4	Discussion	85
3.5	Experiment 3: Tactile Discrimination of Textured Surfaces	87
3.5.1	Apparatus	87
3.5.2	Design and Procedure	88
3.5.3	Results	89
3.5.4	Discussion	89
3.6	Overall Discussion and Design Implications	89
3.6.1	Effect of Epidermal Devices on Tactile Perception	89
3.6.2	Mechanical Robustness of Materials	91
3.6.3	Re-Usability and Adhesion	91
3.7	Limitations	92
3.8	Conclusion	93

II Part Two - Epidermal Devices for Rich On-Body Interaction 95

4	FABRICATION OF SKIN-CONFORMAL ELECTRONICS FOR EXPRESSIVE INTERACTION	97
4.1	Fabrication of SkinMarks	99
4.1.1	Multi-layer Functional Inks on Tattoo Paper	99
4.1.2	Conformal Interactive Tattoos: Slim and Stretchable	99
4.1.3	Touch Sensing	100
4.1.4	Squeeze and Bend Sensing	101
4.1.5	Conformal Touch-sensitive Displays	101
4.2	Expressive On-Body Interaction With SkinMarks	102
4.2.1	Leveraging Tactile Cues on Bony Regions	102
4.2.2	Precise Touch Input on Skin Microstructures	103
4.2.3	Expressive Deformation on Elastic Body Locations	104
4.2.4	Dynamic Visual Cues Leveraging Visual Variations on Skin	105
4.2.5	Interaction on Passive Accessories	106
4.3	Technical Evaluation	106
4.3.1	Conformal Form Factor	108
4.3.2	Precise Localization: Touch Input and Tattoo Application	108
4.4	Discussion, Limitations and Future Work	110
4.5	Conclusion	111
5	EPIDERMAL DEVICES FOR HIGH-RESOLUTION TOUCH SENSING	113
5.1	Design Requirements for Multi-Touch Skin	115
5.1.1	Compatible with deformable properties of skin	115
5.1.2	Robust to electro-capacitive effects of body	115
5.1.3	Leveraging unique affordances of the body	115
5.2	Sensor Fabrication	115
5.2.1	Mutual Capacitance Touch Sensing on Skin	116
5.2.2	Material Choices and Sensor Design	117
5.2.3	Scalability	119
5.3	Customized Form Factors	121
5.3.1	Generating Custom-Shaped Multi-Touch Sensor Designs	121
5.3.2	Design Tool	123
5.4	Interfacing and Data Processing	124
5.5	Tactile Input Modalities	125
5.5.1	Classifying Input Modalities	127
5.6	Evaluation	128
5.6.1	Study 1: Guarding Against Body Capacitance	128
5.6.2	Study 2: Flexibility and Scalability	130
5.6.3	Study 3: Evaluating Tactile Input Modalities	133
5.7	Application Examples	135
5.7.1	Multi-Touch Input on the Forearm	135

5.7.2	Multi-Touch EarStrap	136
5.7.3	One-Handed Input while Holding an Object	136
5.7.4	Multi-Touch Bracelet	138
5.7.5	Eyes-Free Text-Entry on a Fingertip Keyboard	138
5.8	Discussion, Limitations and Future Work	142
5.9	Conclusion	143

III Part Three - Epidermal Devices for Physiological Sensing 145

6	RAPID FABRICATION OF SKIN-CONFORMAL PHYSIOLOGICAL INTER-FACES	147
6.1	Recommendations for Digital Design	149
6.2	Fabrication	150
6.2.1	Hardware and Interfacing	152
6.3	Accuracy of Electro-Physiological Sensing	154
6.3.1	Method	154
6.3.2	Analysis	155
6.3.3	Results	155
6.3.4	SNR of EMG Signals	156
6.3.5	SNR of EDA Signals	156
6.3.6	SNR of ECG Signals	156
6.4	Example Applications	156
6.4.1	Fitness Tracking Sportswear	156
6.4.2	Interactive Heart Rate Sensing Tattoo	160
6.4.3	Arousal Logging in Virtual Reality Interaction	160
6.5	Discussion, Limitations and Future Work	161
6.6	Conclusion	162
7	COMPUTATIONAL DESIGN AND OPTIMIZATION OF ELECTRO-PHYSIOLOGICAL SENSORS	163
7.1	Informal Study to Understand Electrode Placement	166
7.1.1	Participants	166
7.1.2	Method	166
7.1.3	Observations	167
7.1.4	Design Implications and Requirements for Design Tools	167
7.2	Integrated Predictive Model	170
7.2.1	Predictive Model for EMG Electrodes	171
7.2.2	Predictive Model for EDA Electrodes	174
7.2.3	Predictive Model for ECG Electrodes	175
7.2.4	Predictive Model for Area	175
7.3	Computational Optimization	176
7.3.1	Weight-Based Optimization	176
7.3.2	Lower-Bound Based Optimization	177

7.4	Conception of an Interactive Optimizer with a Web-Based Software Tool	178
7.4.1	Inputs and Constraints	178
7.4.2	Selection of Search Space	181
7.4.3	Optimizer Results	181
7.4.4	Electrode-Agnostic Design	182
7.5	Comparison of Optimizer Results with Conventional Designs	182
7.5.1	Validation of Optimizer	183
7.5.2	Results	184
7.6	Experimental Validation of Optimizer's Results	187
7.6.1	Experimental Data Collection	188
7.6.2	Accuracy of Optimizer Prediction with Gel Electrodes	189
7.6.3	Accuracy of Optimizer Predictions for Dry Electrodes	193
7.7	Applications	197
7.8	Discussion	200
7.9	Conclusion	202

IV Part Four - Next Steps in Epidermal Computing **205**

8	NEXT STEPS FOR EPIDERMAL COMPUTING	207
8.1	Themes for Future Research	207
8.2	Materials	208
8.2.1	Sustainable Materials	208
8.2.2	Stretchable Conductors	209
8.2.3	Robust Ultra-Thin Materials	209
8.2.4	Technical and Safety Challenges for Handling Materials	210
8.3	Fabrication	211
8.3.1	Computational Fabrication	211
8.3.2	Fabricating for Large Body Areas	211
8.3.3	Supporting High Resolution and Complex Aesthetic Patterns	212
8.3.4	Mass Fabrication Techniques	212
8.3.5	On-Demand Fabrication Techniques	213
8.4	Functionality of Devices	213
8.4.1	Pressure, Shear and Deformation Input	213
8.4.2	Output with Visual Displays and Haptic Displays	214
8.4.3	Bio-Signals and Electro-Chemical Sensing	214
8.4.4	Energy Harvesting and Self-Powered Devices	215
8.4.5	Connections and Tethering	215
8.5	Evaluation Methods and Strategies	215
8.5.1	Understanding Skin-Specific Interactions	215
8.5.2	Performance Studies	216
8.5.3	Durability and In-the-wild Studies	216

8.5.4	Social Acceptability Studies	216
8.6	Applications and Real-World Deployments	217
8.6.1	Assistive Technologies	217
8.6.2	Health Monitoring and Diagnosis	217
8.6.3	Sports, Fitness, and Rehabilitation	218
8.6.4	Human-Robot Interaction	218
8.6.5	Mobile Computing	219
8.6.6	Ethics, Security, and Privacy	219
8.7	Conclusion	219
9	CONCLUSION	221
9.1	Summary	221
	BIBLIOGRAPHY	225

LIST OF FIGURES

- Figure 1 SEM images of epidermal devices of different thickness, showing its effect on skin conformality, reproduced with permission from [196]. 23
- Figure 2 Overview of the contributions of this Thesis. (a) Empirical experiments for better understanding of *Epidermal Devices* (b) *SkinMarks* presents novel highly skin-conformal Epidermal Devices for rich on-body interaction. (c) *Multi-Touch Skin* enables high-resolution multi-touch sensing on the skin. The sensors can be fabricated in custom shapes to support diverse body locations. (d) *PhysioSkin* presents a rapid fabrication approach for realizing physiological interfaces with a simple desktop inkjet printer loaded with functional inks (e) extending this, we contribute a computational design and optimization approach for realizing multi-modal electro-physiological patches. 24
- Figure 3 Structure of this Thesis. 29
- Figure 4 The four main sensory receptors Merkel cell (Tactile disc), Meissner corpuscle (Tactile corpuscle), Ruffini endings (Ruffini corpuscle), and Pacinian corpuscle (Lamellated corpuscle) underlying in the different layers of the Skin. (Source: Medical gallery of Blausen [508] 37
- Figure 5 On-body touch sensing enabled by state-of-the-art Epidermal Devices. (a) iSkin [498] is a soft stretchable device that uses carbon-doped PDMS to enable touch sensing. (b) Skintillates [287] uses screen-printed silver traces on temporary rub-on tattoos to enable self-capacitance-based touch sensing. (c) DuoSkin [215] uses gold-leaf as the conductive material to create a touch matrix for continuous 2D touch input. (d) AnimSkin [491] uses PDMS as the base material and conductive layers of ITO to enable touch sensing. 49

- Figure 6 Empirical studies on understanding on-skin gestures and on-skin devices. (a) More Than Touch [499] used an elicitation study to understand gestural interaction on specific body locations such as the forearm. (b) Kao et al. [210] used a mixed-methods approach with online surveys and in-lab interviews to investigate the means by which on-skin notification displays are perceived by the general public. (c) You et al. [543] investigated the third person perceptions of a user's interactions with an on-skin touch sensor. 56
- Figure 7 Positioning Epidermal Devices within the broad scope of Body-Based Interaction in HCI. This taxonomy of on-body technologies is adopted from prior work [285, 380]. 59
- Figure 8 Sensing on the skin using optical approaches using cameras mounted on the body. (a) Omnitouch [153] uses a depth camera and a projection setup to enable input on the body. (b) CyclopsRing [51] uses a camera with a fish-eye lens placed between the finger webbing to enable gestural interaction (c) WatchSense [425] uses a depth camera mounted on a wrist to enable interaction on and around the body (d) FingerInput [419] uses a depth camera mounted either on the shoulder or head to enable a wide range of finger microgestures. 60
- Figure 9 Sensing on skin using optical approaches using IR emitters and reflectors mounted on the body. (a) *Senskin* [344] uses an array of IR reflective sensors to sense skin deformations. (b) Nakatsuma et al. [334] demonstrated a wrist worn device consisting of IR sensors to sense 2D touch input on the back of the hand (c) *CheekInput* [527] uses a depth camera mounted inside HMD device to enable input on the cheek. (d) *LumiWatch* [517] uses a an array of 1D depth sensors and projector housed inside a smart watch casing to enable input and output on the body. 61

- Figure 10 Body has been used as a medium for the propagation of acoustic and high-frequency waves. (a) *Humantenna* [73] uses the human body as an antenna for sensing whole-body gestures (b) *Sound of Touch* uses transdermal low-frequency ultrasound propagation for sensing pressure-aware continuous touch input as well as arm-grasping hand gestures on the human body. (c) *SkinTrack* [553] uses the human body as an electromagnetic waveguide and transmits an 80MHz wave through the body. (d) *EarBuddy* [523] uses commodity wireless earbuds to detect face and cheek gestures. The working principle of this technology uses acoustic waves propagated through the body while performing the face gestures. 62
- Figure 11 Magnetic approaches can be used for sensing input and delivering haptic output on skin. (a) *FingerPad* [53] uses hall-effect sensors and a magnet attached to the thumb for sensing subtle thumb to fingertip gestures. (b) *Magnetips* [312] uses a magnetometer array and a copper coil for tracking continuous finger movements and delivering haptic feedback. (c) *MagnetIO* [309] provide haptic feedback through soft haptic patches that can be affixed to any object or surface. (d) *Auraring* [356] enables continuous motion tracking of the finger. 63
- Figure 12 Electric field sensing approaches can be used for sensing input on skin. (a) *ActiTouch* [552] uses transmit and receive electrode pairs for sensing touch input on the skin. (b) *AuraSense* [558] uses electric field sensing to enable expressive around-smartwatch interactions. (c) *Electroring's* [227] uses active electrical sensing approach sensing both touch and release events. There is a step-function-like change in the raw signal which can be easily detected using only basic signal processing techniques. (d) *EnhancedTouchX* [142] is a bracelet-type interpersonal body area network device, which detects and quantifies interpersonal hand-to-hand touch interactions through electric field sensing. 64
- Figure 13 Classification of prior work based on flexural rigidity (ranges shown for devices made of multiple materials). Vertical axis shows total device thickness. 73

- Figure 14 Overview of the three experiments. (a) Von-Frey monofilaments were applied to measure sensitivity, (b) tips of the digital calipers for Two-Point Orientation Discrimination Task, (c) Participants performed the roughness discrimination experiment by exploring two surfaces with different spacing between "dots" (the surface on the left is the baseline). 75
- Figure 15 Experimental determination of the flexural rigidity of composite films: (A) Schematic representation of the experimental analysis of the flexible rigidity of composite PDMS films. L indicates the length of the film and h the thickness. (B) MEDIUM RIGIDITY and (C) HIGH RIGIDITY patches were investigated. The scale bar represents 2.5 mm. N = 3 independent manufactured films with a total of 9 samples for each condition were analyzed. 79
- Figure 16 Three patch conditions with varying levels of flexural rigidity: (a) Patch with low rigidity level ($\sim 1.7 \times 10^{-9}$), (b) medium rigidity ($\sim 1.3 \times 10^{-7}$), (c) high rigidity ($\sim 1.7 \times 10^{-5}$). Patches were applied on (a) the *Fingertip*, (d) *Hand* and (e) *Forearm*. (f) Participant performing roughness-discrimination task. 80
- Figure 17 Von-Frey Filaments used in the Tactile Sensitivity experiment. Each of the filaments has a force profile starting with the lowest force of 0.008 grams to 4.0 grams. 81
- Figure 18 Tactile Sensitivity thresholds for all skin sites and all the patch conditions, with 95% confidence intervals. Lower thresholds mean higher sensitivity. 83
- Figure 19 Normalized Tactile Sensitivity levels relative to the Bare Skin condition, with 95% confidence intervals. Lower thresholds mean higher sensitivity. 83
- Figure 20 Two-Point Orientation Discrimination thresholds (in mm) for all skin sites and patch conditions, with 95% confidence intervals. Lower thresholds mean higher spatial acuity. 86
- Figure 21 Normalized Two-Point Orientation Discrimination thresholds (in mm) for all skin sites and patch conditions, with 95% confidence intervals. Lower thresholds mean higher spatial acuity. 86

- Figure 22 (a) Absolute Surface Offset Thresholds of tactile roughness discrimination task for all patch conditions, with 95% confidence intervals. (b) Normalized Tactile Roughness Discrimination levels relative to the Bare Skin condition, with 95% confidence intervals. Lower thresholds mean higher capability to discriminate surfaces. 88
- Figure 23 (a) Patches of the Low RIGIDITY condition were damaged during the surface discrimination task for 10 participants. (b) 4 patches of the Medium Rigidity condition were damaged. 90
- Figure 24 *SkinMarks* are conformal on-skin sensors and displays. They enable interaction on complex and challenging body locations: (a) bony regions with high curvature, (b) skin microstructures that are fine and narrow, (c) elastic locations, (d) visual elements on the skin such as birthmarks, and (e) body-worn accessories. 98
- Figure 25 *SkinMarks* supports: (a) capacitive touch buttons and sliders, (b) squeeze sensors, (c) bend sensors, and (d) electroluminescent displays. 100
- Figure 26 Interaction on challenging, highly curved skeletal landmarks: (a) tapping the peaks and valleys for discrete input; (b) sliding along the knuckles for continuous input. 103
- Figure 27 Using body posture to dynamically change functionality: (a) Straight finger for linear movements, e.g. to control volume, (b) bent finger for discrete touch areas. 104
- Figure 28 *SkinMarks* allow for precise touch input on skin microstructures: (a) wrinkle slider and (b) wrinkle toggle. (c) Interacting on an body location that is highly stretchable. 105
- Figure 29 *SkinMarks* can augment personal locations on the skin, e.g. birthmarks (a–b), and passive accessories, e.g. a ring (c). 106
- Figure 30 *SkinMarks* conform to wrinkles: (a) a tattoo with PEDOT:PSS conductor; (b) tattoo with EL display. (c) Cross-section of a tattoo with printed EL display, taken with a scanning electron microscope (SEM). 107
- Figure 31 Study setup: (a) evaluation of touch on submillimeter electrodes and (b) of precise tattoo application. 109

- Figure 32 The thin and flexible multi-touch sensor can be customized in size and shape to fit various locations on the body: a) multi-touch input on the forearm for remote communication (inset shows capacitive image); b) multi-touch-enabled bracelet with an art-layer for aesthetic customization; c) input behind the ear; d) input on the palm with busy hands. 114
- Figure 33 (a) Basic electrode design. (b) Layer-by-layer overview of the Multi-Touch Skin sensor. 117
- Figure 34 Overview of all the components required for preparing the interfacing the multi-touch sensor sandwich. The receiver, transmitter, and shielding layers are screen-printed onto a tattoo paper substrate. Conductive Z-axis tape is used for connecting the printed routings to a flat flexible cable (FFC) which is used for interfacing to the touch controller. 120
- Figure 35 Multi-Touch Skin sensors with varying thickness and materials: (a) thinnest version of the sensor with tattoo-paper substrates ($\sim 70 - 80\mu m$); (b) screen-printed sensor with a thicker PET film as the substrate ($\sim 150 - 160\mu m$) (c) ink-jet printed sensor on transparent PET film ($\sim 400\mu m$) 121
- Figure 36 Screenshot of the design tool. (left) The designer specifies the touch-sensitive area S (green), the outer shape O of the full sensor sheet (gray) and the desired location of the connector C (black). (right) The tool generates the multi-touch sensor and provides the corresponding receiver, transmitter and shielding layers. 122
- Figure 37 Functional sensor prototypes of custom rectangular and non-rectangular shapes. 124
- Figure 38 Detecting multi-touch input: a) minimum distance between two fingers which results in two distinct blobs, and the corresponding interpolated capacitive image and the extracted blobs; b) full finger placed on the sensor; c) the wearable hardware setup includes a Raspberry Pi Zero, the touch controller board and the Multi-Touch Skin Sensor. 126
- Figure 39 Tactile input modalities supported by Multi-Touch Skin. For each input modality, the interpolated, masked images are generated followed by blob extraction. Higher-level features such as major axis, minor axis, and intensity levels are extracted from the blobs and fed to a BayesNet machine learning classifier. 129
- Figure 40 Signal-to-noise ratio of touch sensing on the body with and without the shielding layer. 130

- Figure 41 Illustration of the three different curvature conditions evaluated for investigating the flexibility of the sensor. Each of the curvature condition reflects placement on forearm, wrist and finger respectively. 131
- Figure 42 (a) Spatial accuracy of touch contact for different sensor sizes and curvatures. (b) The green dots show the locations on the sensor matrix which were used for evaluating the spatial accuracy. 132
- Figure 43 Confusion matrix showing the accuracy of all the input modalities. 134
- Figure 44 Multi-Touch Skin can be customized to multiple body locations. Four different body locations which were used for deploying Multi-Touch Skin 135
- Figure 45 Multi-Touch Skin deployed on the forearm can be utilized for expressive remote communication. In this specific example, a remote user wearing a multi-touch sensor on his forearm performs a "grasp" gesture (covering his entire sensors with his hand) to send an invite to his friend for a party. 136
- Figure 46 Multi-Touch Skin deployed on the ear to support quick access to music control. In this specific scenario, the user can perform a simple vertical and horizontal swipes to control volume or to switch music tracks. 137
- Figure 47 Multi-Touch Skin deployed on the palm to support quick and always available input while the hands are busy. In this specific scenario, the user can perform a multi-finger tap to accept or reject calls. 137
- Figure 48 Multi-Touch Skin deployed on the wrist as a bracelet can be deployed in Smart Home applications. Through the Multi-Touch Bracelet, the user can control the brightness of the lamp through expressive multi-touch gestures (inset). 138
- Figure 49 (a) first prototype with PET film; (b) second prototype with FPC (flexible printed circuit); (c) third prototype on temporary tattoo paper. 141
- Figure 50 (a) first prototype with PET film; (b) second prototype with FPC (flexible printed circuit); (c) third prototype on temporary tattoo paper. 141

- Figure 51 (a) PhysioSkin enables digital fabrication of custom electro-physiological sensing patches for monitoring EMG, ECG and EDA. (b) A custom made skin-conformal sensor. (c) A fitness tracking sportswear tracks heart rate and muscle movements. (d) Raw signal of the heart rate recorded from a temporary tattoo. 148
- Figure 52 Overview of fabrication options with Soft inkjet and Instant inkjet printing. 151
- Figure 53 Conformal skin contact made by the electrodes fabricated on all the substrates. 153
- Figure 54 (a) Raw EMG signals for each of the six substrate conditions. (b) SNR levels for each of the conditions calculated for all the participants. Error bars indicate standard deviation. 157
- Figure 55 (a) Raw EDA signals for each of the six substrate conditions. (b) Pearson Correlation coefficients between the substrate conditions measured with respect to the commercial gel electrodes. Error bars indicate standard deviation. 158
- Figure 56 (a) Raw ECG signals for each of the six substrate conditions. (b) SNR levels for each of the conditions calculated for all the participants. Error bars indicate standard deviation. 159
- Figure 57 A fitness tracking vest with electrodes for EMG and ECG sensing. 160
- Figure 58 Overview of the concept of computational design and optimization of electro-physiological sensors. An integrated predictive model is presented which encapsulates three bio-signal modalities (EMG, EDA, and ECG). This model along with inputs from the user is fed to an optimizer which generates an optimized layout that optimally trades off between desired device size and sensing quality. An interactive software tool assists the user in specifying desired properties and inspecting the generated design in real-time. The design can be further fine-tuned by an expert while interactively inspecting its quality, allowing for a "human-in-the-loop" optimization process. The optimized device can then be realized using commercial gel electrodes or through dry electrodes fabricated on a temporary tattoo. 165
- Figure 59 Physical muscular models with annotated landmarks and textbooks with placement guides used by experts in the study for placing electrodes. 168

- Figure 60 Key points generated for each of the muscles on the anterior side of the forearm. The electrodes need to be placed symmetrically along this key point. ("x" denotes the length of the muscle line). The four measurements a , b , c , d for the forearm form the basis for the calculation of the muscle keypoints on the anterior side of the forearm. 172
- Figure 61 Total area covered between and under two EDA electrodes. 174
- Figure 62 Key points for ECG electrode placement on the forearm and empirically measured signal quality for combinations of key points. 176
- Figure 63 Screenshot of the graphical design tool for interactively generating and inspecting optimized results. (a) Input panel for selecting the modalities and muscles, setting forearm dimensions, and setting the lower bounds. (b) The canvas area where the generated designs are visualized. Designs can be fine-tuned by drawing a desired location and shape or dragging individual electrodes. (c) Panel for choosing the optimization type, weights for each of the modalities, and overall sensor area. (d) Shape customization panel for fine-tuning the properties related to the sensor shape. Additionally, this panel also allows for uploading existing designs and exporting the current designs. (e) Buttons for one-click automatic generation of the layout. The result is displayed in real-time in the canvas area. (f) Panel visualizing quality metrics for the generated layout. Advanced functionality for use by experts can be accessed through drop-down panels. This includes functions for adjusting and editing the electrodes in the generated solution, adjusting the internal parameters of the model, tweaking the optimization parameters, and adjusting the appearance of the forearm polygon. The workflow for using the tool is shown in Supplementary Video 1. 179
- Figure 64 (a) High resolution sampling of the anterior side of the forearm in 1 mm increments starting near the wrist. (b) Scatter plot showing the entire spectrum of solutions generated by varying the search space on the forearm. The solutions have been plotted with respect to their size. 185

- Figure 65 Comparison of the optimizer results with conventional designs and the experimentally collected physiological data. (a) Visual representation of the generated designs for the uni-modal combination, involving EMG with three muscles, alongside their area and quality score predicated by the optimizer (values are normalized w.r.t. the baseline solution). (b) Comparison of model prediction with empirically measured quality scores of EMG sensing. The model is able to accurately predict the sensing quality (values are normalized w.r.t the baseline solution). (c) Visual representation of the generated designs for the multi-modal combination, involving EMG with five muscles, EDA and ECG. (d, e, f) Modality-wise comparison of model prediction with empirically measured quality scores, for EMG, EDA, and ECG sensing, showing the model accurately predicts the sensing quality. Note: The optimizer score ranges between 0 and 1 with 0 being the best. For better clarity, the graphs plot the complement value ($1 - \text{Optimizer Score}$) which gives a direct measure of the quality predicted. 186
- Figure 66 Average rectified EMG signals for the uni-modal combination consisting of three muscles. For each of the sensor design condition and the muscle, the predicted vs. the measured qualities have been labelled. 191
- Figure 67 Average Rectified EMG signals for each of the muscles for all sensor design solutions in the multi-modal case. 191
- Figure 68 Raw signals of the EDA measurements for a participant for all the sensor design solutions. During each measurement, a reference measurement of skin conductance was taken by placing the electrodes on the fingertips. 192
- Figure 69 Raw signals of the ECG measurements for a participant for all four solutions. 192
- Figure 70 Accuracy of optimizer predictions for gel electrodes and dry electrodes for the AREA OPTIMIZED solution. (a) Comparison of EMG signal quality predicted by the optimizer and normalized experimental measurement, for gel electrodes and dry electrodes. (b) Comparison of EMG signal quality predicted by the optimizer and normalized experimental measurement, for gel electrodes and dry electrodes (c) Comparison of EMG signal quality predicted by the optimizer and normalized experimental measurement, for gel electrodes and dry electrodes. 195

- Figure 71 (a) Raw ARV signals of EMG measurements for each of the five muscles. (a) Raw ARV signals for GEL ELECTRODES -BASELINE and GEL ELECTRODES - AREA OPTIMIZED CONDITIONS. (b) Raw ARV signals for Same signals obtained with dry electrodes. 196
- Figure 72 Magnitude of the raw ARV signals of EMG measurements for five muscles (a) Pair-wise comparison of the ARVs for the gel electrodes for BASELINE and AREA OPTIMIZED placement conditions (b) Pair-wise comparison of the ARVs for the dry electrodes for BASELINE and AREA OPTIMIZED conditions. 197
- Figure 73 Raw signals of EDA measurements. (a) Skin conductance levels for the gel electrode in BASELINE and AREA OPTIMIZED conditions. (b) Skin conductance levels in the BASELINE and AREA OPTIMIZED CONDITIONS FOR THE DRY ELECTRODES. 197
- Figure 74 Raw signals of the ECG measurements showing the comparison of signals with Gel Electrodes and Dry Electrodes on the forearm. 198
- Figure 75 Example applications. (a) Ultra-thin temporary tattoo with compact sensor layout generated by the optimizer and fabricated with an off-the-shelf desktop ink-jet printer. (b) Augmented reality exercising application: a virtual character performs push-up motion when the user performs a push-up. (c) A virtual reality game in which EMG-sensed gestures are used for controlling the virtual character in a first-person shooter game. (d) Raw signals of the EMG signals when performing a push-up exercise. (e) Increase in the skin conductivity levels before and after the push-ups. The shaded region represents the standard deviation. (f) Difference in the heart rate before and after performing the push-ups. (g) Raw EMG signals of the five muscles for each of the gestures used in the virtual reality game. 199
- Figure 76 Opportunities and challenges for Epidermal Computing span aspects of materials, fabrication, functionality, evaluation methods, and applications. 208
- Figure 77 Most commonly used functional materials for epidermal devices, plotted against their respective electrical conductivity and Young's modulus. A key opportunity for further research is to develop highly stretchable materials that possess high electrical conductivity. Note: Young's modulus is inversely proportional to stretchability. 210

- Figure 78 Key research themes for Fabricating Epidermal Devices. A number of rapid and easy-to-perform fabrication methods have been explored in HCI. For each of the fabrication methods and computational design approaches, representative research works from physical sciences and HCI research are shown. The next steps (highlighted) include the exploration of fabrication methods that leverage traditional art and handcraft-based workflows (e.g. henna tattoos) and exploration of mass manufacturing techniques. For computational design techniques, advanced design tools incorporating material properties, FEM analysis, and widely accessible fabrication methods are the next crucial steps. [212](#)
- Figure 79 Current Epidermal devices are limited to a few centimeters in size. The next step is to create skin-conformable epidermal devices that cover large body areas. Representative research works from physical sciences and the HCI research community are shown. [213](#)
- Figure 80 **Epidermal IoT** - In the future, we can envision Epidermal Devices to be an integral part of our body. These devices (highlighted in green) can be easily worn at multiple locations on the body custom-designed for a specific purpose. As a collective, they present us with an ecosystem of Epidermal Devices enabling new opportunities for sensing, computing, and interaction, in addition to giving us a holistic picture of the state of our body. [223](#)

LIST OF TABLES

- Table 1 Table with different sensory receptors and their properties such as location, adapting speed, frequency range, and respective sensing capability[65]. The size of the receptive field typically relates to the depth of the receptor in the skin – the closer the cell is to the surface, the smaller the corresponding receptive field. Fast adapting receptors react to changes in stimulus, while slow adapting receptors react to the presence of a stimulus. Note: Different sources report minor differences in the frequency ranges that each receptor responds to. This table relies on [65, 123, 201, 203] [39](#)

Table 2	Commonly used electro-physiological modalities along with the key parameters (location and spatial configuration) influencing the signal acquisition. 50
Table 3	Results from exploration of material combinations. Recommended combinations are highlighted in bold font. 116
Table 4	Five muscles used for the experimental condition and their corresponding voluntary contraction identified from literature [506] 188

INTRODUCTION

1.1 SKIN AS AN INTERACTIVE MEDIUM

The extraordinary properties of skin make it an appealing user interface. First, the presence of mechanoreceptors that capture nuanced tactile sensations afford dexterous tactile input techniques and rich haptic output, which can be further enhanced using the materiality of soft and deformable skin. Moreover, as the skin is the largest human organ, it offers a large real estate for input and output. It is always with us and easily accessible supporting direct, subtle, and discreet interactions. This is applicable for a variety of mobile activities, including walking, running, carrying shopping bags, riding a bike, or driving a car. Lastly, skin is inherently multi-modal. In addition to its haptic aspects and its function of visual display, it can also act as a biological interface for sensing bio-signals.

The HCI community has explored diverse technical approaches for turning human skin into an interface. Amongst others, these comprise optical [153], bio-acoustic [159, 326], magnetic [53, 181], radar-based [484] and ultrasound imaging techniques [311]. Additionally, a number of body locations have also been investigated in HCI literature which enable rich and expressive interactions. These include forearm [153, 159, 215, 498], palm [138, 153], fingertips [53, 126], nails [214], hair [92], ear [281], belly [474], wrist [137, 475, 503], back [287], eyelids [216, 292]. A recent stream of work, at the intersection of material science, biomedical engineering and HCI, has created the foundations for **Epidermal Computing** – a new form of wearable computing platform that is characterized by ultra-thin devices which are noninvasive, offer intimate integration with the curved surfaces of the body and have physical and mechanical properties that are akin to skin.

These Epidermal Devices, often also referred to as Electronic Skin or Epidermal Electronic Systems (EES), open up a wide range of possibilities by augmenting the human skin with electronic functionality. They enable sensing of tactile input [215, 287, 498], highly-articulated body movements [232, 559], and physiological signals [27, 105, 206, 568]. They provide haptic output [510, 541, 545] or augment the body with visual displays [215, 287]. Moreover, Epidermal Devices enable non-invasive testing of contagious viruses such as COVID-19 [462] and offer non-invasive drug delivery [482]. Last but not least, they can harvest energy from bio-mechanical activities like walking [532] or even human sweat [199].

1.2 EPIDERMAL COMPUTING

In the past few decades computing has evolved from large room-scale computers where operators had to manually load the programs, to more portable and wearable devices that we have today. Continuing with this trend, in the near future, we will be transitioning towards interaction that is going to seamlessly merge with our body and utilize our intricate perceptual, mental, motor, and proprioceptive capabilities.

The vision for **Epidermal Computing** is to intimately couple sensing, computation, and interaction to the outermost layer of the human body (the epidermis) by means of Epidermal Devices. These devices are soft, of minimal thickness, highly stretchable and flexible, to adapt to complex body geometries and ideally conform to the relief of the skin's surface. Furthermore, Epidermal Devices are non-invasive and should be made of bio-compatible materials. They leverage perceptual, biological, social, and emotional properties associated with human skin, in order to support multimodal interactions, physiological sensing, health diagnostics, and treatment.

One of the key properties that define *Epidermal Devices* is skin conformality. This is a crucial property that defines how well a device adapts to the complex relief of the skin. Figure 1 shows SEM (scanning electron microscope) scans of devices of various thickness levels and their skin-conformable property. It can be noticed that thick devices having a thickness of $500\mu\text{m}$ do not have conformal skin contact. When a device of $\sim 100\mu\text{m}$ is applied to the skin, the device very well adapts to the contours of the skin but fails to penetrate into the deepest creases and pits. Reducing the device thickness further creates highly skin-conformal contact with the device adapting to the fine microstructures of the skin.

The skin-conformal contact has many advantages in various domains. Firstly, from an ergonomics perspective, skin-conformal devices can be very comfortable and minimally invasive, promoting long-term use [228]. Secondly, a device that is highly skin-conformal minimally attenuates our natural tactile perception capabilities. Tactile cues can be transmitted through these devices to the underlying mechanoreceptors, which enables us to feel natural tactile sensations despite the presence of these devices on the body [339]. Thirdly, many bio-signals such as EEG, ECG, or EOG are captured with skin-mounted sensing electrodes that need to be in close contact with the skin for acquiring high-quality signals. Similarly, this is a very attractive property for applications in sports and fitness where devices need to be tightly coupled to the body for measuring athletic performance [526].

The degree of skin conformality allows to broadly subdivide Epidermal Computing Devices into two groups: (a) *Skin stickers* are somewhat thicker ($\sim 100\mu\text{m}$ – $700\mu\text{m}$) and therefore can be easily worn, removed from the body surface, and re-applied. A few examples of such devices that have been presented in the HCI literature are iSkin [498], Electrodermis [304], Springlets [149] and Multi-Touch

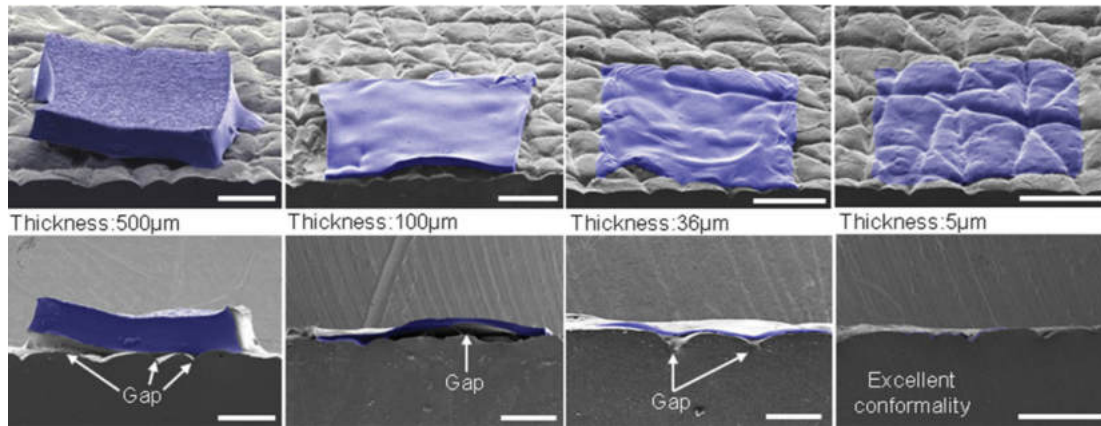


Figure 1: SEM images of epidermal devices of different thickness, showing its effect on skin conformity, reproduced with permission from [196].

Skin [341] (presented in Chapter 5). (b) *Skin-conformal devices* are ultra-thin (ranging between $\sim 1\mu\text{m}$ and $100\mu\text{m}$). This enables them to be tightly coupled to the skin, in some cases even without any additional adhesives by van der Waals forces alone. They are extremely stretchable, flexible, and adapt very well onto strongly curved and deforming body geometries. Few examples of such devices in the HCI literature are SkinMarks [500] (presented in Chapter 4), DuoSkin [215], Skintillates [287], Tacttoo [510] and Tip-Tap [221].

1.3 RESEARCH CHALLENGES AND CONTRIBUTIONS

While Epidermal Electronic Devices have been explored in various other research communities, there are important research challenges that need to be addressed for deploying these devices for applications in HCI.

1. Empirical Understanding of Epidermal Devices

The current mobile and personal computers have matured over the years because of numerous studies and experiments that focused on understanding and improving interaction with them. Prior work reported on various input modalities and user preferences for on-skin input [499], identified user strategies for creating on-body gestures [346] and revealed that on-skin input increased the sense of agency [34].

While these empirical studies in HCI evaluated on-body interaction techniques, there is very limited work that studied epidermal devices. Since epidermal devices reside on the human skin, a deeper understanding of their mechanical and tactile transmissive properties is very crucial for the design of future epidermal devices.

Contributions

To address this research challenge, this thesis contributes a **novel inter-disciplinary classification system for Epidermal Devices** and **proposes the metric of flexural**

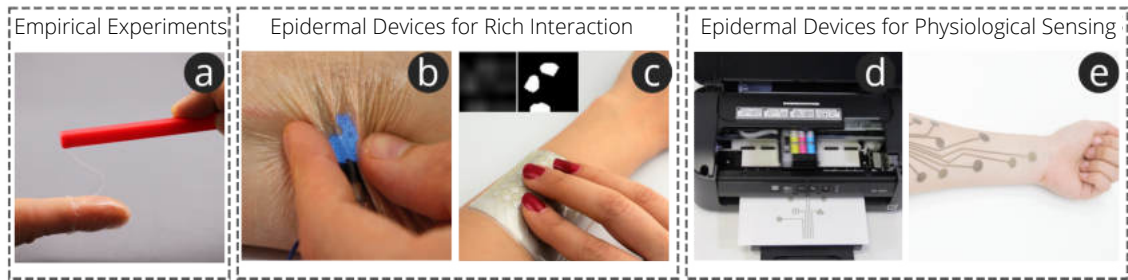


Figure 2: Overview of the contributions of this Thesis. (a) Empirical experiments for better understanding of *Epidermal Devices* (b) *SkinMarks* presents novel highly skin-conformal Epidermal Devices for rich on-body interaction. (c) *Multi-Touch Skin* enables high-resolution multi-touch sensing on the skin. The sensors can be fabricated in custom shapes to support diverse body locations. (d) *PhysioSkin* presents a rapid fabrication approach for realizing physiological interfaces with a simple desktop inkjet printer loaded with functional inks (e) extending this, we contribute a computational design and optimization approach for realizing multi-modal electro-physiological patches.

rigidity to characterize their tactile performance. Based on this metric, we tested and evaluated advanced adhesive and substrate materials that are used for the fabrication of Epidermal Devices. **We conducted three psychophysical experiments that investigated the effect of rigidity levels of Epidermal Devices on passive and active tactile perception.** We analyzed human tactile sensitivity thresholds, two-point discrimination thresholds, and roughness discrimination abilities on three body locations (fingertip, hand, forearm). Based on our findings, we derive design recommendations for Epidermal Devices that combine tactile perception with device robustness.

2. Epidermal Devices for Rich On-Skin Interaction

Epidermal Devices can exploit the interaction benefits that our body offers resulting in highly expressive interactions. However, there are challenges with respect to sensing, fabrication, and design approaches that need to be addressed.

2.1. Sensing Skin-Specific and High-Resolution Touch Input

While Epidermal devices have opened up new opportunities for interaction on the body, they suffer from several major limitations. Firstly, they mostly assume interactive elements to be rather large and only slightly curved. However, there are locations on our body that have complex geometries and support rich tactile touch input (e.g. knuckles and flexure lines on palm [138]). Secondly, the resolution of touch input supported by these devices is very low and supports only single-touch input. This low touch resolution limits the richness of interactions that can be possible. Empirical studies also show that our body affords a wider variety of

touch-based interactions [499]. However, these interactions require high-resolution multi-touch input.

2.2. Rapid and Easy Fabrication

While Epidermal Devices have been developed in physical sciences research communities, they entail complex fabrication processes requiring sophisticated lab equipment and infrastructure. This restricts the availability of these devices to a larger audience that includes hobbyists, practitioners, and researchers from other communities.

2.3. Computational Design Approaches for Epidermal Devices

Realizing current Epidermal Devices involves a two-step design and fabrication process. Firstly, standard vector graphics editors or similar tools are used for creating a device design. Once the design is complete, in the second step, the devices are fabricated. There are limitations to this workflow. Firstly, designing Epidermal Devices is an iterative process where designs evolve over multiple iterations. Hence, manually re-designing and fabricating the devices is time-consuming. Secondly, realizing these devices requires expertise and technical knowledge in multiple disciplines such as electrical engineering, materials science, and digital fabrication. This is a barrier for novice users and designers who need to acquaint themselves with the prerequisite technical skills. Finally, unlike the commercial devices that offer limited customization, Epidermal devices should be highly customizable since they are worn on the body. The customization should be in terms of the shape of the device to support a specific body location, the thickness/rigidity levels for supporting specific applications, and the aesthetics and visual appeal of the device. Leveraging computational design techniques can alleviate all these challenges since these design tools can be very powerful in abstracting the designer from the lower level technical detail. They also support a rapid iterative design process, since designs need not be manually generated every time. Finally, they also enable easy and quick customization of the devices.

Contributions

To address these research challenges, this thesis contributes easy and rapid fabrication techniques to realize Epidermal Devices through *SkinMarks* and *Multi-Touch Skin*. These devices enable rich interactions - interactions that leverage the natural affordances offered by human skin.

***SkinMarks* are novel skin-worn I/O devices for precisely localized input and output on highly challenging body locations.** *SkinMarks* comprise skin electronics on temporary rub-on tattoos. They conform to fine wrinkles and are compatible with strongly curved and elastic body locations. We demonstrate novel interaction techniques that leverage *SkinMarks*' unique touch, squeeze and bend sensing with integrated visual output. Our technical evaluations show that *SkinMarks* are highly skin-conformal with displays ranging in thickness from 31-46 μm and touch sensors being 1-4 μm thick. Taken together, *SkinMarks* expands the on-body

interaction space to more detailed, highly curved, and challenging areas on the body

Multi-Touch Skin presents a **highly flexible and thin high-resolution multi-touch sensor** for enabling expressive on-body interactions. Through a systematic materials exploration, we identify the material combinations and fabrication approaches for printing thin and flexible multi-touch sensors. To support deployment on diverse body geometries and locations, **we present the first non-rectangular multi-touch epidermal devices**. To enable rapid design and fabrication, we introduce a design tool that generates such sensors in custom shapes and sizes. To validate the feasibility and versatility of our approach, we present four application examples and empirical results from two technical evaluations. They confirm that the sensor achieves a high signal-to-noise ratio on the body under various grounding conditions and has a high spatial accuracy even when subjected to strong deformations.

3. Epidermal Devices for Physiological Sensing

Since Epidermal Devices are present on the skin, they offer us the unique opportunity of measuring rich physiological signals from our body that can determine the state of health. However, there are challenges with respect to fabrication, placement of the devices, and design approaches that need to be addressed.

3.1. Fabrication of Electro-Physiological Sensors

While electro-physiological sensing devices have become increasingly common in diverse applications due to the availability of rapid prototyping platforms to a larger audience, they still rely on off-the-shelf gel electrodes for capturing bio-signals. These electrodes are thick, non-conformal, unergonomic, and prohibit usage over long durations. They are also not customizable and are not aesthetically pleasing. While the physical sciences research community has contributed highly skin-conformal electro-physiological sensors, they typically entail complex fabrication processes and require sophisticated infrastructure.

3.2. Computational Design of Electro-Physiological Sensors

Designing Electro-Physiological sensors in compact form factors and capturing high-quality signals is a challenging task even for experts, is typically done using heuristics, and requires extensive training. This becomes even more challenging when multiple bio-signal modalities need to be sensed with a single device.

Contributions

To solve these fabrication and computational design challenges for electrophysiological sensors, this thesis contributes *PhysioSkin* and proposes a computational design and optimization technique for creating highly compact sensing patches that can measure multiple bio-signal modalities with high accuracy.

PhysioSkin, is a **rapid, do-it-yourself prototyping method for fabricating custom multi-modal physiological sensors, using commercial materials and a commodity desktop inkjet printer**. It realizes ultrathin skin-conformal patches (~ 1

μm) and interactive textiles that capture sEMG, EDA, and ECG signals. It further supports fabricating devices with custom levels of thickness and stretchability. We present detailed fabrication explorations on multiple substrate materials, functional inks, and skin adhesive materials. Informed from the literature, we also provide design recommendations for each of the modalities. Evaluation results show that the sensor patches achieve a high signal-to-noise ratio. Example applications demonstrate the functionality and versatility of our approach for prototyping the next generation of physiological devices that intimately couple with the human body.

To address the second challenge, this thesis proposes the **first computational approach for designing and optimizing multi-modal electro-physiological sensors**. By employing an optimization-based approach alongside an integrated predictive model for multiple modalities, compact sensors can be created which offer an optimal trade-off between high signal quality and small device size. The task is assisted by a graphical tool that allows to easily specify design preferences and to visually analyze the generated designs in real-time, enabling designer-in-the-loop optimization. Experimental results show high quantitative agreement between the prediction of the optimizer and experimentally collected physiological data. They demonstrate that generated designs can achieve an optimal balance between the size of the sensor and its signal acquisition capability outperforming expert-generated solutions.

1.4 STRUCTURE OF THE THESIS

This thesis is structured into four parts and is organized as follows:

1. **Part 1: Understanding Epidermal Computing and Skin Conformality**

The first part of this thesis gives a broad overview of human skin, state-of-the-art Epidermal Devices in HCI, reviews other technical approaches that enable on-body interaction, and presents results from empirical experiments which give us a better understanding of skin-conformality and how it is influenced by Epidermal Devices.

Chapter 2 gives a background on human skin and details of its anatomy, its sense of touch, and the underlying mechanoreceptors that are responsible for tactile perception. It then presents the state-of-the-art in various technological approaches and platforms that have been investigated for enabling on-skin computing, comparing and contrasting them with Epidermal Computing.

Chapter 3 presents the results from the empirical experiments which we conducted to understand how epidermal devices affect human tactile perception. Based on the results from these experiments, a set of design guidelines are then derived which can inform the design of next-generation epidermal devices.

2. Part 2: Design and Fabrication of Epidermal Devices for Rich On-Body Interaction

The second part of this thesis contributes to the design and fabrication of epidermal devices that enable rich interactions.

Chapter 4 presents *SkinMarks*, highly conformal skin electronics. They are based on very thin temporary rub-on tattoos and made for interaction on highly curved, deformable, and small body locations. They support touch, squeeze, and bend sensing with integrated visual output. The chapter details the fabrication of these devices using simple lab equipment and also presents an evaluation of the high level of conformality that can be achieved through these devices.

Chapter 5 presents *Multi-Touch Skin*, the first thin and flexible epidermal device that enables high-resolution multi-touch sensing on the body. Contrary to the conventional touch screen and mobile devices, *Multi-Touch Skin* can be easily fabricated in various non-rectangular shapes. The chapter details the fabrication explorations and experiments for realizing the sensor. This was also the first instance where a computational design approach has been employed for designing and realizing epidermal devices.

3. Part 3: Design and Fabrication of Epidermal Devices for Electro-Physiological Sensing

Physiological sensing is becoming more ubiquitous with open-source toolkits enabling hobbyists, makers, practitioners, and HCI experts to deploy custom electro-physiological sensing systems. However, the electrodes used for capturing the bio-signals are usually commercial gel-based wet electrodes or metallic dry electrodes which cannot be customized and are unergonomic, prohibiting long-term use. While sensing bio-signals through epidermal devices has been widely explored in various engineering and physical science communities such as Materials Science, Electrical Engineering, Bio-Medical Engineering, the fabrication techniques and infrastructure required for realizing these devices prohibit widespread use. Extending beyond the rich interaction, this thesis contributes computational design and rapid fabrication techniques for realizing custom electro-physiological sensors.

Chapter 6 presents *PhysioSkin*, a rapid fabrication technique to realize custom electro-physiological sensors. These sensors can measure multiple modalities of bio-signals such as EMG (Electromyogram), ECG (Electrocardiogram), and EDA (Electro-Dermal Activity) and work with off-the-shelf open-source bio-signal acquisition hardware platforms.

Chapter 7 presents a computational design and optimization approach for realizing multi-modal electro-physiological sensing patches. Placement of electrodes



Figure 3: Structure of this Thesis.

at the appropriate skin site is very crucial for high-quality bio-signal acquisition. And this issue becomes even more complicated if the overall sensor design needs to have a minimal size while having high bio-signal acquisition capability. This chapter addresses this challenge by contributing a computational design tool that automatically generates electrode layouts that can provide a good trade-off between the size of the overall device and the capability to measure multiple bio-signals with high quality.

4. Part 4: Exploring Applications and Identifying next steps for Epidermal Computing

This part of the thesis looks at potential applications and domains where deploying epidermal devices can have a significant impact. It also identifies the next steps in epidermal computing and concludes the thesis by summarizing the main findings.

Chapter 8 presents the next steps for future research in Epidermal Computing. By providing a multi-disciplinary analysis of epidermal devices, the chapter identifies opportunities for future research in this area.

Chapter 9 presents the concluding remarks and summarizes the main findings of this work.

PUBLICATIONS

The ideas and figures in this dissertation have appeared previously in the following publications:

- P1.** **Aditya Shekhar Nittala** and Jürgen Steimle. *Next Steps for Epidermal Computing: Opportunities and Challenges for Soft On-Skin Devices*. In Proceedings of the 2022 CHI Conference on Human Factors in Computing Systems (ACM CHI '22).
- P2.** **Aditya Shekhar Nittala**, Andreas Karrenbauer, Arshad Khan, Tobias Kraus, and Jürgen Steimle. *Computational Design and Optimization of Electro-Physiological Sensors*. In Nature Communications (2021).
- P3.** **Aditya Shekhar Nittala**, Arshad Khan, Klaus Kruttwig, Tobias Kraus, and Jürgen Steimle. *PhysioSkin: Rapid Fabrication of Skin-Conformal Physiological Interfaces*. In Proceedings of the 2020 CHI Conference on Human Factors in Computing Systems (ACM CHI '20).
- P4.** **Aditya Shekhar Nittala**, Klaus Kruttwig, Jaeyeon Lee, Roland Bennewitz, Eduard Arzt, and Jürgen Steimle. *Like A Second Skin: Understanding How Epidermal Devices Affect Human Tactile Perception*. In Proceedings of the 2019 CHI Conference on Human Factors in Computing Systems (ACM CHI '19). **ACM CHI 2019 Honorable Mention Award.**
- P5.** **Aditya Shekhar Nittala**, Anusha Withana, Narjes Pourjafarian, and Jürgen Steimle. *Multi-Touch Skin: A Thin and Flexible Multi-Touch Sensor for On-Skin Input*. In Proceedings of the 2018 CHI Conference on Human Factors in Computing Systems (ACM CHI '18).
- P6.** Martin Weigel, **Aditya Shekhar Nittala**, Alex Olwal, and Jürgen Steimle. *SkinMarks: Enabling Interactions on Body Landmarks Using Conformal Skin Electronics*. In Proceedings of the SIGCHI Conference on Human Factors in Computing Systems (ACM CHI '17).
- P7.** Zheer Xu, Pui Chung Wong, Jun Gong, Te-Yen Wu, **Aditya Shekhar Nittala**, Xiaojun Bi, Jürgen Steimle, Hongbo Fu, Kening Zhu, and Xing-Dong Yang. *TipText: Eyes-Free Text Entry on a Fingertip Keyboard*. In Proceedings of the 32nd Annual ACM Symposium on User Interface Software and Technology (ACM UIST '19). **Best Paper Award.**
- P8.** Jürgen Steimle, Joanna Bergstrom-Lehtovirta, Martin Weigel, **Aditya Shekhar Nittala**, Sebastian Boring, Alex Olwal, and Kasper Hornbæk. *On-skin interaction using body landmarks*. In IEEE Computer (2017), pp. 19-27.

In addition to these, the the author contributed to the following publications on Epidermal Computing which are under review:

- P9.** Marion Koelle, Madalina Nicolae, **Aditya Shekhar Nittala**, Marc Teyssier and Jürgen Steimle. *(Im)perfectly Sustainable: Prototyping of Soft Devices with Bio-based and Bio-degradable Materials*. Under Review.

The research has been published at premiere journals and conferences. The research has been published as five papers at the ACM Conference on Human Factors in Computing Systems (CHI) [P1, P3, P4, P5, P6] which includes an Honorable mention award, one paper at the ACM Symposium on User Interface Software and Technology (UIST) [P7], and one journal article in the Nature Communications [P2].

In addition to the main publications, the following list shows publications of relevant workshop papers, and demos:

- P10.** **Aditya Shekhar Nittala**, Arshad Khan and Jürgen Steimle. *Conformal Wearable Devices for Expressive On-Skin Interaction*. In Proceedings of the ACM Augmented Humans International Conference. (AHs'20).
- P11.** **Aditya Shekhar Nittala** and Jürgen Steimle. *Digital Fabrication Pipeline for On-Body Sensors: Design Goals and Challenges*. In Proceedings of the 2016 ACM International Joint Conference on Pervasive and Ubiquitous Computing: Adjunct. (UbiComp '16).

Part I

Part One - Understanding Epidermal Computing and Skin Coformality

BACKGROUND

Contrary to conventional computing devices, Epidermal Devices need to be in conformal contact with the skin. Hence a basic understanding of the anatomical properties of skin is crucial, and this knowledge informs the design of Epidermal Devices. This chapter will present an overview of the anatomy and physiology of human skin. Epidermal Computing is a multidisciplinary area at the intersection of Materials Science, Bio-Medical Engineering, and HCI. Taking this into account, this chapter presents a detailed literature review in two parts¹: in the first part, we present a broad overview of Epidermal Computing by discussing the state-of-the-art Epidermal Devices across multiple research disciplines (HCI, Materials Science, Nanotechnology, Bio-medical, Electronics) and focus on the HCI-specific questions and research directions that other works have not reviewed. By comparing and contrasting research from prior work, we identify challenges and opportunities across five major themes that are central for the development of Epidermal Computing Devices from an HCI perspective: (1) Materials, (2) Fabrication, (3) Devices and their functionality, (4) Technical and Empirical studies, and (5) Applications and real-world deployments. The second part of the literature review positions Epidermal Computing within the realm of HCI. To inform the reader, firstly, it provides an overview of the sensing techniques that have been explored for enabling input on the body. Then we compare and contrast Epidermal Devices with other on-body interaction technologies such as wearables and interactive textiles.

2.1 FUNCTIONS AND ANATOMY OF SKIN

Skin is the natural interface that connects the environment to our body. Covering almost 2 square meters and weighing approximately 3.6 kilograms, it is the largest human organ. In total, the skin accounts for about 5.5% of body mass [165]. This organ is present in all mammals [189] and it is the first organ that develops in the womb. It plays a vital role in maintaining the health and well-being of the body. For this it serves multiple functionalities: it serves as a protective barrier, a regulation interface, and a medium for enabling exploration of the environment [383].

Protective Barrier: Skin protects our internal body organs from external factors. This waterproof layer protects our vital organs from being directly exposed to harmful elements such as radiation, and chemicals. It acts as an anatomical barrier

¹ This chapter is based on a research paper that has been submitted for ACM CHI'22. I performed the literature survey. I and my advisor Jürgen Steimle framed the definition of Epidermal Computing, derived the challenges and opportunities, and wrote the paper.

against damages from pathogens such as microbes and viruses. It also enables us to feel various sensations such as heat, pressure, enabling us to act safely and adapt to our environment.

Regulatory Interface: Skin serves as a thermal insulator for heat regulation, and enables our body to precisely control the loss of energy through radiation, convection, and conduction. Vitamin and other vital chemical syntheses are also formulated in the skin. Finally, lipids and water which help in regulating the body are stored in the skin.

Medium for Environment Exploration: Due to the presence of a number of inherent natural mechanoreceptors, skin equips us with the “sense of touch”. This capability enables us to sense and explore our environment and feel a number of sensations such as temperature, pressure, textures, etc. For instance, we can feel minute forces, discriminate roughness of surfaces, textures, or the warmth of natural elements or objects. Overall, by transmitting tactile and kinesthetic cues, the skin provides us with a better understanding of our environment.

2.1.1 Layers of Skin

The human skin is comprised of three main layers: Epidermis, Dermis, and hypodermis.

Epidermis is the outermost layer of the skin that forms the boundary between the human body and the external environment. It acts as a protective barrier against the external environment and also as a regulatory interface. The total thickness of the epidermis varies between different body parts ranging from very thin ($\sim 50 \mu\text{m}$ near eyelids) or forming thicker protection on the palms of the hand ($\sim 547 \mu\text{m}$), and foot soles ($1159 \mu\text{m}$) [165]. The Epidermis also secretes melanin which protects the skin cells from harmful UV radiations. This production of melanin results in the creation of different skin pigments such as tan marks, birthmarks, freckles, and age spots at various locations on the body. These visual elements on the skin can be exploited for interaction as they serve as visual cues for on-skin input as demonstrated in Chapter 4.

The layer beneath the Epidermis is the *dermis*. This layer constitutes dense irregular connective tissues that absorb shocks thereby cushioning the body from external stress and strain. Collagen, elastic fibers, and extracellular matrix form the structural components of the dermis. The collagen gives tensile strength and elastic fibers allow for recoil. This allows the skin to revert back to its original form even after twisting and deforming [426]. These elastic deformable properties of skin can be utilized for interaction with input modalities such as twisting, pulling, squeezing in addition to conventional touch input. The dermis also contains hair follicles, lymph, blood vessels as well as sebum, and sweat glands. A common physiological signal, skin conductance is usually captured by monitoring the sweat gland activity (also referred to as Electro-dermal activity) and can be used for deciphering the emotional state of a person. Part 3 of this thesis shows the

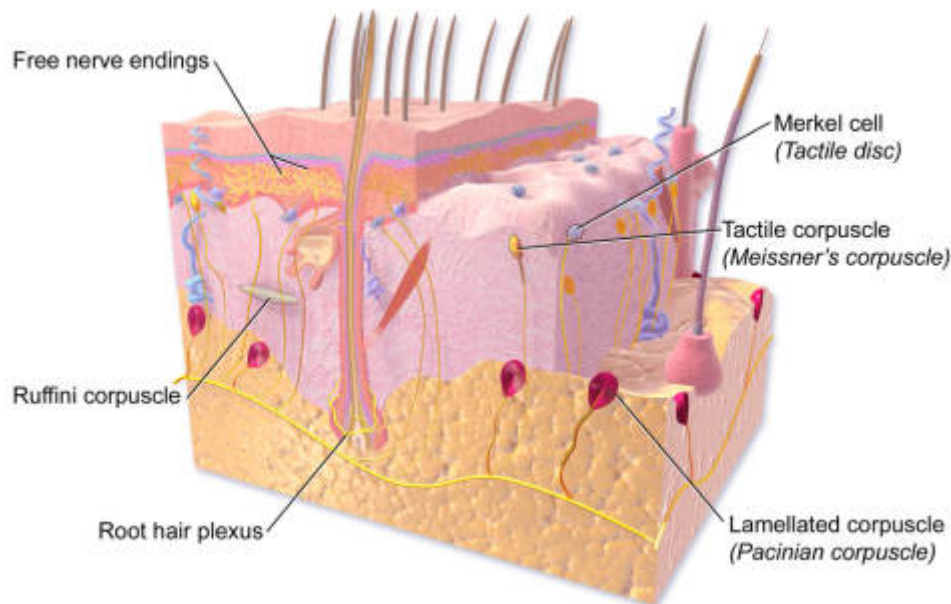


Figure 4: The four main sensory receptors Merkel cell (Tactile disc), Meissner corpuscle (Tactile corpuscle), Ruffini endings (Ruffini corpuscle), and Pacinian corpuscle (Lamellated corpuscle) underlying in the different layers of the Skin. (Source: Medical gallery of Blausen [508])

computational design and fabrication of epidermal interfaces for capturing skin conductance. Apart from these many vital components, the dermis layer is also home to the tactile sensory units which enable us to feel various tactile sensations such as touch, pressure, vibration, temperature, and pain.

The deepest layer of skin is the hypodermis or the subcutaneous tissue. This layer contains adipose tissues which are used for storing body fat and connects the blood and lymph vessels with the rest of the body. The composition of this layer is also very crucial for physiological sensing since signals such as EMG (Electromyogram) that are used for measuring muscle activity are influenced by the body fat that is stored in the hypodermis.

2.1.2 Skin as a Sense Organ

Skin is one of the five sensor organs of our body. It equips us with the sense of touch. This allows us to feel tactile cues during on-skin input with our fingertips and the touched surface. The tactile feedback allows for natural eyes-free interaction on the body [138]. One of the most established frameworks in tactile perception is the four-channel theory: glabrous (non-hairy) human skin contains four types of mechanoreceptors (sensory cells that detect skin deformation) [119]. The four receptors are Merkel cells, Meissner corpuscles, Pacinian corpuscles, and Ruffini corpuscles as shown in Table 1.

- Merkel Discs are located closer to the surface of the skin and can be found on the epidermis [251]. They are slow-adapting receptors and react to sustained signals. They typically respond to pressure, tension and sense fine details such as texture.
- Similar to Merkel Discs, Ruffini corpuscles are slowly adapting mechanoreceptors that sense stretch of skin, sustained pressure on the skin, and tension.
- Pacinian Corpuscles are located in the deeper layers of the skin typically in dermis [251]. They respond to changes in pressure, vibration, and are responsible for texture perception.
- Meissner Corpuscles are similar in structure to Pacinian Corpuscles, but are located closer to the surface of the skin and are typically associated with the perception of fine surface features, edges, and contours. They are responsive to lower frequency vibration from ~ 5 Hz to ~ 50 Hz (sometimes referred to as flutter-vibration [445]).

Since these mechanoreceptors vary in density across the body, there is a difference in the spatial acuity and tactile perception capabilities at different body locations. For example, the number of receptors on the glabrous region of the hand is estimated to be 17,000 [15]. And even on the hand, there is a variation in the density: Fingertips have the higher density (~ 211 per cm^2), while palms have a lower density (~ 33 per cm^2). Hence, the fingertips are one of the most sensitive regions of the body. They provide high-resolution tactile feedback when exploring surfaces and have high spatial acuity which is a direct measure of spatial resolution. Chapter 3 of this thesis also discusses these aspects with respect to how the tactile perception is influenced based on the body location and the rigidity of an epidermal patch.

2.2 MULTI-DISCIPLINARY ANALYSIS OF EPIDERMAL DEVICES

The field of HCI has seen rapid growth in the development of Epidermal Devices in the past few years. Starting with iSkin [498] which introduced Epidermal Devices in HCI for enabling touch input on the body, the devices have become slimmer [215, 287], enable continuous 2D touch input [215], provide visual output [215, 287] and deliver novel haptic sensations [149–151, 510]. The physical sciences research community has been investigating Epidermal Devices for more than a decade longer than HCI. The majority of their work focuses on creating and formulating new materials, advanced fabrication techniques, and developing sensors and actuators, which typically involve using sophisticated lab equipment. The learnings and research innovations from those communities have in parts been taken up by the HCI community, which in turn has led to the development of new interactive devices, along with more accessible fabrication techniques.

Receptors	Depth	Adapting Speed	Receptive Field	Frequency (Hz)	Sensing Property
Merkel's discs	I	Slow	Small	5–15	Pressure, Fine details
Ruffini endings	II	Slow	Large	15–400	Stretch
Meissner's corpuscles	I	Fast	Small	20–50	Stroke, Fluttering
Pacinian corpuscles	II	Fast	Large	~10–500	Vibration

Table 1: Table with different sensory receptors and their properties such as location, adapting speed, frequency range, and respective sensing capability[65]. The size of the receptive field typically relates to the depth of the receptor in the skin – the closer the cell is to the surface, the smaller the corresponding receptive field. Fast adapting receptors react to changes in stimulus, while slow adapting receptors react to the presence of a stimulus. Note: Different sources report minor differences in the frequency ranges that each receptor responds to. This table relies on [65, 123, 201, 203]

To synthesize the opportunities and challenges, we performed a literature analysis across multiple disciplines by analyzing research articles published at top-tier journals and conferences which include: Nature (Nature, Nature Communications, Nature Electronics, Nature Nanotechnology, Nature Materials), Science (Science, Science Advances), Wiley (Advanced Materials, Advanced Functional Materials, Advanced Healthcare Materials), American Chemical Society (ACS Sensors, ACS Applied Material Interfaces, ACS Nano), Royal Society of Chemistry and the ACM Digital Library for research articles in HCI/Computer Science. By performing a thematic analysis of these research works across disciplines, we present a synthesis of challenges and opportunities for driving research in this area. While this thesis addresses important contributions across four thematic areas, the following sections present the broad landscape of research opportunities that can drive the growth of Epidermal Computing.

- **Functional Materials:** We analyze the functional materials that commonly are used for building Epidermal Devices across disciplines. Based on this, we identify opportunities and challenges for sustainable materials, stretchable conductors, safety, and handling of materials.
- **Fabrication and Design Workflows:** By analyzing and understanding the fabrication mechanisms and design workflows used for realizing Epidermal Devices, we identify potential opportunities and challenges for devising new techniques that better support rapid prototyping, require only simple lab equipment, and enable easy fabrication of devices.
- **Devices and their functionality:** We compare and contrast the devices across disciplines based on their functionality and the interactions that are supported.

By understanding and analyzing several device types, we identify future device functionalities that can be developed by the HCI community.

- **Evaluation Methods and Strategies:** We compare methods of evaluating technical aspects, human factors, and user interaction of Epidermal Computing Devices across disciplines. We identify the next steps with regard to fundamental empirical experiments for understanding skin-specific interactions, social acceptability, and in-the-wild studies of Epidermal Computing.
- **Applications and Real-World Deployments:** By comparing and contrasting the applications and deployments that have been targeted, we identify opportunities for potential applications that future Epidermal Devices can target.

In the following sections, we will discuss these thematic areas in turn.

2.3 MATERIALS

Epidermal Devices are typically fabricated as a multi-material sandwich. Selection of materials is critical, as they need to comply with the demanding mechanical requirements (notably, being soft, stretchable, mechanically robust despite a very low diameter, and adhering to the skin) and offer the required functional properties for the embedded electronics. We will now discuss materials for substrates and functional layers that have been commonly investigated in HCI and Material sciences communities.

2.3.1 Substrates

Substrates usually form the base material onto which functional materials are coated for creating the device sandwich.

2.3.1.1 PDMS

PDMS (poly (dimethyl) siloxane) is one of the most commonly used substrate materials for fabricating epidermal devices. It is optically transparent (240 – 1100 nm wave length) [46, 310, 427], flexible [202, 513], highly stretchable and biocompatible [145, 513]. It can be fabricated in a range of thicknesses between $\sim 10 - 700\mu\text{m}$ for Epidermal Devices, allowing for trading-off between conformality and mechanical durability for a given application case.

PDMS offers additional advantages because of its low cost and rapid prototyping capability. This makes PDMS not only widely used in physical sciences research [69, 197, 230, 358], but it has also been used in the HCI community to create epidermal touch sensors [498], thermochromic displays [491] and for creating haptic sensations using micro-fluidic channels [151, 490].

2.3.1.2 *Tattoo Decal Paper*

Tattoo Decal or Temporary Tattoo paper is another commonly used substrate material for fabricating ultrathin Epidermal Devices. The main constituents of tattoos are polymers, having low Young's modulus [105, 305] and the overall thickness is submicrometric [105]. These two peculiar characteristics make it an ideal substrate material for obtaining conformal adhesion to the skin [230]. Temporary Tattoo paper is composed of ultrathin ($<1\mu\text{m}$) carrier film, water-soluble polyvinyl alcohol (PVA) layer, and backing paper for ease of handling. Functional layers can be easily created on the substrate through inkjet printing [225, 289] or screen printing [287]. Once the devices are printed they can be transferred to the human skin through water transfer: when water is applied to the temporary tattoo paper, the carrier film separates from the paper leaving behind an ultrathin layer composed of functional layers that easily adapt to the body surface.

Temporary tattoo paper has been extensively used in physical sciences research for fabricating various devices such as skin-conforming electrodes for electrophysiology [27, 105, 206, 289, 450], emotion sensing [190], transistors and edible electronics [39], wireless communication [466], energy harvesting on skin [199] and for organic indoor photovoltaics [370]. Temporary tattoo paper has also been extensively used in the HCI community for creating various devices such as touch sensors [287], 2D touch matrices [215], battery-less 2D touch input [221], electro-tactile actuators [510], displays [215, 287], and on-skin PCBs [213].

2.3.1.3 *Hydrogels*

Hydrogels and ionogels are another promising class of stretchable active materials, noteworthy because they closely mimic the mechanical, chemical, and optical properties of biological tissues [529]. Due to the advantages of their 3D structure, biocompatibility, and biodegradability, hydrogels have been used for a wide variety of applications such as tissue engineering [277], and highly stretchable printed electronics [546]. We are seeing first explorations of hydrogels in the HCI community for epidermal devices which change their texture and stiffness through joule heating [212].

2.3.1.4 *Substrate-Less or Water-Soluble Substrates*

Depositing functional materials directly onto the skin has been another way that has been explored in physical sciences research. This is typically done through a water-soluble substrate that dissolves during wet transfer [493, 494].

2.3.1.5 *Textile Patches*

While e-textile research is a substantial research area on its own with multiple research communities actively exploring the field, a few research works in HCI

have investigated the use of e-textiles as on-skin interfaces. This includes augmenting the skin by adhering soft textile patches [429, 431] as well as using weaving or machine embroidery for creating patches with unique visual-haptic properties [183, 200, 439].

2.3.2 Functional Materials

2.3.2.1 Conductors

Epidermal Devices typically require one or more conductive layers on a base substrate for performing a specific function. Multiple approaches and materials have been explored for coating conductive layers. The most commonly used functional materials are:

- *Metallic Conductors*: Metallic conductors are one of the most commonly used functional materials because of their high conductivity and ease of processing. Silver and gold have been used very commonly in the HCI community either in form of screen-printing pastes [287] or through thin films [215]. These are also very commonly used materials in physical sciences research [322, 493]. Metallic conductors in the form of silver nano-particles (AgNp) can also be deposited through ink-jet printing methods [222]. Additionally, they are also used in the form of nanowires and nanoparticles [169, 243].
- *Intrinsically Stretchable Polymers*: By comparison to metallic conductors that have high Young's modulus and hence are very brittle, intrinsically stretchable polymers have attractive mechanical properties such as high stretchability and deformability. A well-studied conductive polymer is poly(3,4-ethylenedioxythiophene) polystyrenesulfonate (PEDOT:PSS) [485]. It has been widely used in the physical sciences research community for creating Epidermal Devices which measure physiological signals such as EMG, ECG, and EEG [105, 270]. PEDOT:PSS has also been widely used in the HCI community for creating stretchable interactive devices [131, 503], pressure sensing foils [388] and soft sensors [333]. Physical sciences research has also explored other stretchable polymers that offer superior deformability, such as a compound material formed from the copolymerization of poly(3-hexylthiophene) (P3HT) and polyethylene (PE) to obtain (P3HT-PE) which offers up to 600% stretchability [328].
- *Carbon Composites*: Carbon and its composites like graphite, graphene, or activated charcoal have been successfully used for creating Epidermal Devices [206, 238, 524]. Carbon composites have received lesser attention in the HCI community, with only a few works using them [498]. A key advantage is that they are low-cost when compared to metallic conductors which have limited reserves and are expensive. Some of the allotropes of carbon used for fabrication purposes are graphite [387] and graphene [106]. Graphene has received wide

attention because of its electrical conductivity, mechanical properties [384] and the “thinnest” known material [106] and as result has been used in realizing a number of Epidermal Devices [182, 206, 265]. However, since graphene is expensive [106], Graphite has been viewed as another alternative since it is a low-cost material, and offers the advantage of bio-compatibility [54]. It has relatively low conductivity but is also a popular choice to develop devices for biomedical applications [330].

- *Nanowires, Nanomeshes, and Nano-Tubes*: Nanoparticles typically in the form of nanowires (NWs), nano-meshes or nano-tubes are another class of conductive materials that have been extensively used [47, 533]. Multi-walled carbon nanotubes have also been recently introduced in HCI for realizing self-healing interfaces [335, 379]. A key advantage of using nanomeshes is that they can be realized in highly thin form factors while being stretchable achieving superior conformal contact in comparison to the planar polymeric substrates [207, 488]. However, a key challenge for using nanomeshes and nanowires is the complex fabrication process which often requires sophisticated equipment.
- *Liquid Metals*: Liquid metals are another class of conductors that offer the benefits of high deformability [560] and high electrical conductivity [567]. Most prior research that utilized liquid metals have employed gallium-based liquid metals to develop epidermal devices that measure strain [359] and pressure [536]. They have also been used for creating capacitive touch and pressure [9] sensors, resistive strain sensors [352, 360], for measuring the angle of body joints [313] and for self-healing robots [303]. Liquid metals are also becoming increasingly popular in the HCI community [400, 457, 458, 477], however with only very little work investigating their use in Epidermal Devices [331].

2.3.2.2 *Insulators and Dielectrics*

Dielectrics and insulating materials are necessary for creating devices that are composed of multi-material layers and for insulating the device from its environment. One common approach is to embed silicone elastomers as flat or textured sheets [498, 533]. Another approach is to print fine layers of dielectric materials [225, 347] or use multiple layers of the base material as an insulating material.

2.3.3 *Skin Adhesives*

Skin adhesives are typically used to achieve stronger adhesion of the device onto the skin. In some cases, the high stretchability and very low thickness levels of the devices make them bond to the skin through just van der Waals forces without the need for external adhesives [230]. Other approaches typically include using commercially available solutions such as water-soluble tape [196], commercial

medical grade adhesives [304], tattoo-paper adhesive [215, 287], acrylic [240], spray bandage [537], and mastic [498].

Contributions in Material Exploration

While the physical sciences research community has explored a wide range of materials including the substrate, functional and adhesive materials, the material exploration for fabricating Epidermal Devices in the HCI community is limited in comparison. The functional materials that have been typically used in HCI for fabricating Epidermal Devices have been predominantly metallic [215, 287, 373, 491], with a few works using carbon [498] and liquid metals [331]. Metallic conductors provide high conductivity but it comes at the cost of low stretchability. This prohibits their usage at highly challenging body locations that can deform and stretch. Hence, investigating new materials and material compounds that offer a good balance between high electrical conductivity is of prime importance. This thesis investigates the use of PEDOT: PSS, an intrinsically stretchable polymer for realizing Epidermal Devices. To the best of our knowledge, SkinMarks [500] (Chapter 4) is the first work that introduced this material for touch sensing². This enables sensing expressive touch interactions on highly challenging body locations such as knuckles, and flexure lines of the finger.

In addition to introducing intrinsically stretchable polymers for sensing touch, this thesis also explores using a compound material sandwich comprising a metallic conductor and intrinsically stretchable polymer. In Chapters 4, 5, 6, for enhancing the mechanical robustness of conductive silver traces, we cover the highly conductive device designs made of silver with a second layer of PEDOT: PSS containing the same design. This allows the devices to remain functional, even when the silver connection breaks at a few locations.³

In addition to functional materials, this thesis also explores skin adhesives for epidermal devices. Chapter 3 explores commercial medical-grade adhesives with silicone to create patches of desired stiffness and thickness levels. Chapter 6 examines the compatibility of various off-the-shelf adhesives with different substrate materials.

2.4 FABRICATION

The fabrication of Epidermal Devices not only involves identifying the right set of methods, tools, and equipment for creating the multi-material sandwich. It also

² While PEDOT: PSS has been used previously in HCI [333, 388] its exploration for sensing touch on the body has not been explored.

³ A detailed study examining this effect through comprehensive stress and stretch tests has been conducted by my colleague Dr. Arshad Khan who is a material scientist. I am one of the co-authors of the journal article which is under preparation (not part of this thesis). These experiments confirm our hypothesis of PEDOT: PSS particles bridging the gaps between broken silver traces.

involves challenges regarding the design of layouts that are fabricable and comply with a user's aesthetic preferences.

2.4.1 *Fabrication Methods*

2.4.1.1 *Additive Methods*

Typical additive fabrication methods use printing to pattern a sheet of the substrate material with functional ink. The arguably most commonly used approach is screen printing, as it allows for convenient deposition of a very wide range of materials with fine-tuned layer thicknesses and sufficiently good resolution [184, 275, 554]. Due to the simplicity of fabrication, it has been widely used in the HCI community [287, 347, 503]. However, the approach is manual and requires creating a negative mask, which makes it slower than alternative techniques. A rapid approach for creating high-resolution patterns is inkjet printing with functional inks. Physical sciences research typically uses specialized industrial inkjet printers [105], which are very expensive and not easily accessible to hobbyists, practitioners, and many HCI research labs. Recent research in HCI has contributed inkjet printing and transfer approaches that are simple and can be deployed with inexpensive commodity inkjet printers [61, 225]. In addition to these, *Direct On-Skin Printing* techniques involve directly printing functional layers on the skin [134]. Recent research in HCI has demonstrated this via pen-based devices which used computational guides for inking [373] and through wearable plotters that deposit ink based on the target design provided through a design tool [66].

2.4.1.2 *Subtractive Methods*

Typical subtractive methods involve cutting a substrate or film of functional materials into a patterned structure, by cutting out residual materials and leaving behind the desired pattern on the substrate. Commonly used tools are mechanical plotter cuts [215] or more advanced laser cutting such as CO₂ [291, 498] or UV laser micromachining [304].

2.4.1.3 *Mixed Methods*

Another recently introduced technique that uses a mix of additive and subtractive methods is the "cut-and-paste" method [531] which involves using a mechanical plotter to cut a specific design on a functional layer. The resultant functional layer is then transferred onto the desired substrate. This technique has been widely used in the Materials Science community with variants of this approach being actively pursued [493]. A similar approach uses a doctor blade to incrementally add functional layers and use CNC milling to have the device in custom shape [491].

While the HCI community majorly focuses on fabrication techniques that are easy, rapid, and can be performed with simple lab equipment, the physical sciences

research community employs various other approaches involving more complex procedures and equipment such as electrospinning and vacuum depositions [322], microfabrication, and thermal deposition techniques [168].

2.4.2 *Computational Design and Optimization*

Optimizing designs for targeting a specific functionality is a common practice in HCI and physical sciences research communities. This involves optimizing electrical, physical, and mechanical parameters, for instance for withstanding high strain [196], or for specific electronic functionality such as the design of antennas for near-field communication (NFC) [240]. One of the areas, where the HCI community has made rapid advances in the use of computational design approaches for creating personalized device designs that are optimized for a user's body, often using interactive design tools. This includes, for instance, a custom design tool for creating non-rectangular touch sensor designs that fit on desired body parts [341] (presented in Chapter 5), or a design tool for controlling the aesthetics of an Epidermal Device [304]. Chapter 6 presents a computational design and optimization approach for creating multi-modal Epidermal Devices that can sense multiple physiological signals.

2.4.3 *Aesthetics*

Skin acts as a social display that signals traits related to personality, demographics, health, and social status [444]. Diverse forms of aesthetic skin decoration, such as henna, make-up, jewellery and tattoos, are wide-spread across cultures [80, 252, 353]. If worn visibly, Epidermal Devices become an element of social display, possibly even a fashion item. Therefore, their visual and material aesthetics are central aspects for user adoption. Research in HCI is considering this aspect increasingly, while it still remains rarely addressed in materials science and physical sciences [133].

The current state of the art of fabrication incorporates aesthetics in the following ways:

- **Using Aesthetic Materials:** Metallic materials such as gold or silver have been used for decorative purposes. Using these materials for fabricating Epidermal Devices has enabled the devices to be intrinsically attractive. A common way to use them is with temporary tattoos [215] or through interactive cosmetics and make-up materials [216, 472].
- **Art Layers:** Art layers are one of the commonly used techniques to add aesthetically pleasing graphics on top of the device, which is typically hiding the device's internal structure. This is often done by using a dedicated layer of temporary tattoo [287, 292, 341, 500] or molded onto the device [304].

- **Aesthetic Functional Designs:** A third approach does not hide the device's inner functional structure, but rather designs it to be visually attractive. Electrical circuits or functional elements of sensors are laid out in ornamental shapes that create a desired visual aesthetics [498]. Prior work has achieved this through laser cutting [498], CNC milling [491], a cutting plotter [215], and free inking [373].

Recent work in HCI involves interactive computational tools for creating aesthetic on-skin devices, such as creating devices decorated with custom Voronoi patterns [304] or creating functional and aesthetic epidermal circuits with computer-assisted free-form sketching [373].

Contributions in Fabrication

This thesis explores all the fabrication methods (additive, subtractive, and mixed methods) that were previously described. Chapter 4 uses screenprinting (additive method) to print functional layers on top of each other to create a multi-layer device sandwich. The devices created through this process can sense touch, squeeze, and bend while also providing visual output through displays. Chapter 5 also uses an additive fabrication method, it utilizes screenprinting to create functional layers. Insulating materials are printed or stacked between the functional layers to create the multi-layer sandwich. Subtractive fabrication is also explored in this chapter where a cutting plotter creates the individual functional layers made of gold leaf. To support rapid prototyping, this thesis also explores conductive inkjet printing to create Epidermal Devices. Chapter 6 explores a mixed-methods approach to first print the device design on a textile transfer sheet, then a laser cutter is used to remove the excess material, then the design is transferred through an iron-on process.

In addition to these techniques, this thesis presents the first computational design approach for creating Epidermal Device designs.⁴ Chapter 5, presents a design tool for creating multi-touch sensor designs in custom shape. Chapter 7 presents a computational design and optimization approach for designing and optimizing multi-modal electro-physiological sensors. By employing an optimization-based approach alongside an integrated predictive model for multiple modalities, compact sensors can be created which offer an optimal trade-off between high signal quality and small device size. Both these design tools assist designers in generating functional sensor designs for desired custom shapes.

2.5 FUNCTIONALITY OF DEVICES

Epidermal Devices can serve multiple functions: they can act as input devices through touch, pressure, and gestural input, provide multi-sensory haptic feed-

⁴ While ElectroDermis [304] presented a design tool for creating Epidermal Devices, Chapter 5 (Multi-Touch Skin [341]) is the first work which investigated using computational design approach for Epidermal Devices.

back and visual output, monitor physiological signals, and offer a promising platform for health monitoring and diagnostics.

2.5.1 *Input*

2.5.1.1 *Tactile Sensing*

Recent advances in materials and fabrication techniques have enabled the interaction on the body through thin, flexible, and stretchable epidermal devices which reside on the human skin [498] (Figure 5 (a)). iSkin [498] is the first Epidermal Device introduced in the HCI literature. It used stretchable bio-compatible silicone known as PDMS (polydimethylsiloxane) as the base material. Carbon-doped PDMS was used as an elastic conductor enabling touch sensing and also for sensing pressure. Similarly, AnimSkin [491] (Figure 5 (d)) and Stretchis [503] used PDMS as the base material along with conductive layers made of ITO and PEDOT:PSS respectively for implementing touch sensing. Lo et al. [287] (Figure 5 (b)) presented tattoo-based devices that could sense touch input. Building on this, prior research presented tattoo-based epidermal devices that allow for continuous 2D interpolated touch input [215, 221]. In addition to soft epidermal devices based on PDMS or tattoo-based substrates, prior work has also explored the use of soft textile patches [429, 431] as well as using weaving or machine embroidery for creating patches with unique visuo-haptic properties [183, 200, 439].

While prior work in HCI has explored epidermal devices fabricated through various substrate materials, the resolution of touch sensing that is enabled through these devices has been limited. It is restricted to sensing single-touch contact. However, the current wearable and mobile devices have touch sensing capabilities that go beyond this. In addition to this, human skin also affords various types of expressive touch interactions [499] that require high-resolution multi-touch sensing.

2.5.1.2 *Kinematic Sensing*

Epidermal Devices that capture dynamic motions of the human body can provide critical insights across a broad range of applications, from clinical diagnostics (movement disorders [268, 448], neurological disorders [192]) to athletic performance monitoring [526, 550]. Sensing of body motions through Epidermal devices has also been widely explored in the HCI community [287, 304, 338, 500]. In addition to precise movement tracking, kinematic sensing also allows for using body movements for interactive applications such as gesture detection [559]. Typically epidermal kinematic sensing is deployed through strain sensors, IMUs, or EMG approaches.

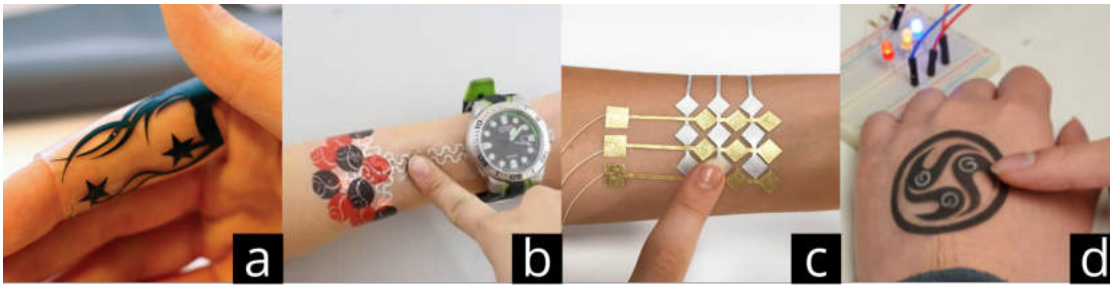


Figure 5: On-body touch sensing enabled by state-of-the-art Epidermal Devices. (a) iSkin [498] is a soft stretchable device that uses carbon-doped PDMS to enable touch sensing. (b) Skintillates [287] uses screen-printed silver traces on temporary rub-on tattoos to enable self-capacitance-based touch sensing. (c) DuoSkin [215] uses gold-leaf as the conductive material to create a touch matrix for continuous 2D touch input. (d) AnimSkin [491] uses PDMS as the base material and conductive layers of ITO to enable touch sensing.

2.5.1.3 Physiological Sensing

Physiological signals are readings or measurements that are produced by the physiological processes that happen in the human body, e.g., voltage potential changes that happen during a heartbeat (Electrocardiogram), the voltage generated during muscle movements (Electromyogram), changes in the skin conductance levels due to activity of sweat glands (Electro-Dermal activity), or the electrical signals generated due to the activity of the brain (Electroencephalogram). Electrophysiology is the branch of physiology that studies the electrical properties of biological processes that happen in the body. It involves measurements of voltage changes or electric current to capture the physiological state of the body. Typically, these electro-physiological signals are measured by placing multiple electrodes at dedicated locations on the body to capture bio-signals. These electrodes need to have a specific spatial configuration depending on the modality of the bio-signal measured. An overview of the commonly used electro-physiological modalities is shown in the table below.

Design and fabrication of sensors for physiological monitoring has been subject of intense research in the materials and bio-medical engineering communities. Thin epidermal devices have been presented that monitor various physiological signals such as ECG [537], EMG [105, 537], pulse oximetry [239], sweat and thermal characterization [185, 497]. Alternatively, textile sensors have been extensively explored as well [70], including for ECG [521], EMG [107], and EEG [288].

The HCI community has also explored a number of ways to use bio-signals for interaction. This involved the use of EMG signals for gesture recognition [8, 404, 405]. Apart from this, various other bio-signals such as electro-dermal activity, heart-rate activity, electrooculography have also been explored [36, 121]. More recent research is also looking into the area of continuous health monitoring by tracking various activities such as blood pressure levels [480]. This involves

#	Modality	Measurement	Where (Location)	How (Spatial Configuration)
1	Electromyography (EMG)	Muscle activity through voltage generated from muscle movements.	Key-Points located along the muscle [566]	Three electrodes placed on the body. Two for measuring the potential and the third electrode is a reference electrode.
2	Electro-Dermal Activity (EDA)	Sweat gland activity through measurement of skin resistance	Area with high concentration of sweat glands (e.g. palms, fingertips, foot sole, forehead) [43, 109]	Two electrodes placed on the body with the same dermatome (area innervated by single spinal nerve) [109].
3	Electrocardiogram (ECG)	ECG refers to the recording of electrical changes that occur in the heart during a cardiac cycle.	12-lead ECG electrode placement near the heart [198]. However, other alternate placement strategies have been experimented for ambulatory recording [2, 101, 294, 530]	The configuration varies from a medical-grade setup with 12 leads/electrodes placed near the heart to a more simpler setup with three electrodes. In the three-electrodes setup, two electrodes act as the measuring electrodes while the third one is a reference electrode. The typical placement of these electrodes follows Einthoven's triangle [99] for good signal acquisition.
4	Electroencephalogram (EEG)	Measures the spontaneous electrical activity of the brain	Typically on the scalp	The electrodes are placed on the scale according to the 10-20 electrode placement standard [246].
5	Electrooculography (EOG)	Measures the potential between front and back of the human eye	placement is around the eye	Many placement configurations are possible. The minimal configuration is with 4 electrodes with one electrode being a reference and three electrodes placed near the eye (left, right and top of eye) to measure left-up and right-up potentials. For more configurations refer to [290]
6	Impedance Pneumography	Measures the respiratory rate. Implemented using two electrodes or four-electrode system, the technique measures changes in electrical impedance of the person's thorax caused by respiration or breathing	The location is typically near chest (Thorax)	The precise placement of electrodes is required. The placements are described in [293]. The best placement location for the two-electrode system was to have electrodes placed symmetrically on the anterior and posterior sides of the thorax. The electrodes should be on the midpoint between the left and right second intercostal spaces on the sternum.

Table 2: Commonly used electro-physiological modalities along with the key parameters (location and spatial configuration) influencing the signal acquisition.

either using off-the-shelf devices (e.g. smart-phones) for continuous health monitoring [479, 480] or developing custom-made devices which strategically place sensors for signal collection [48, 83, 84, 177, 304].

Electro-chemical sensors are another class of devices that convert information associated with biochemical processes that happen in the body. They can also be used for detecting viruses and pathogens in the body [462]. A wide range of electro-chemical Epidermal Devices have been developed which measure blood glucose levels [237], hemoglobin [239] or characterize sweat [20] with various compounds such as pH levels [77] or trace metals [236].

2.5.1.4 *Environmental Sensing*

The interaction of the human body with external environmental signals can be a good indicator of health. These environmental factors include exposure to UV light, pollutants, and gases which can be hazardous. Prior research has contributed Epidermal Devices for sensing various environmental elements such as UV exposure [117, 301, 463], harmful gases like ammonia [116], humidity levels [464], and exposure to explosives and gunshot residues [24]. While there has been extensive research in physical sciences, environmental sensing so far has received very limited attention in HCI, with pioneering work investigating the fabrication of chemical UV sensors [301].

2.5.2 *Output*

2.5.2.1 *Visual Displays*

Visual displays on the skin can serve multiple purposes. Firstly they can provide subtle notifications to the user [215, 500]; second, they can be embedded with tattoo art to add further aesthetic value to the devices [287]; third, in a medical context, they can be utilized for healing wounds on the skin [193]. Prior work on epidermal displays from the physical sciences includes a high-resolution display matrix made of LEDs [168], electro-luminescent displays [233, 554], stretchable organic LEDs [193, 194], thermochromic [234], and electrochromic displays [68, 357]. Research in HCI built onto some of these findings to focus on more accessible fabrication approaches in a simple lab or DIY settings. Approaches comprise the fabrication of Epidermal Devices that consist of SMD LEDs [287], stretchable electro-luminescent displays [500, 503] and thermochromic displays [215, 491].

2.5.2.2 *Actuation*

Stretchable epidermal actuators attached closely to human skin can act as devices that produce haptic output on the body through targeted stimulations. A large number of epidermal haptic output devices have been presented across research communities. Various technologies have been successfully employed. The

approach that allows for the most minimal form factor uses electro-tactile stimulation. Two or more electrodes in direct contact with the skin deliver a controlled electrical pulse to directly stimulate nerve stems of mechanoreceptors, which can be perceived as vibrations. These types of actuators have been extensively explored both in the physical sciences [412] and HCI research communities [220, 510]. Various other approaches have been explored for creating haptic sensations based on mechanical movement. These include the use of dielectric elastomers [447, 541], magnetic actuation [308, 545], piezoelectric actuation [555], mechanical actuation with shape memory alloys [62, 149] and actuation through microfluidic channels [150, 151]. A key observation here is that both the HCI community and physical sciences research community are very active in designing actuator devices, with competitive results. However, the communities complement each other in the evaluation approaches: the HCI community's focus on psychophysical studies to validate the actuation principle and corresponding human perception can go hand-in-hand with the materials and fabrication-centered evaluations that are typically performed in the physical sciences research community.

2.5.2.3 *Drug Delivery*

Drug delivery devices are another class of output devices that non-invasively and transcutaneously inject drugs. This is achieved through multiple approaches including the use of microneedles [266], electrical methods [520], ultrasound methods [423] and thermal ablation [17]. A more detailed discussion of various types of drug delivery mechanisms (not all are compatible with Epidermal Devices) can be found in [374].

2.5.3 *Computation and Communication*

In addition to means for input and output, prior research has also investigated components that are central for on-device computation and communication.

2.5.3.1 *Electronic Components and Fully Integrated Devices*

Electronic components such as transistors, memory devices that are building blocks of computing. Prior literature in physical science research community has developed fully printed capacitors [16], transistors [351], dense transistors arrays [78, 486], memory and logic devices [420]. In addition to these components, the design and fabrication of fully-integrated devices is a very active research topic [115, 265, 393]. Self-contained devices are also being actively pursued in the HCI community [304, 331], with even computational capability for running on-device neural network models being imbued into devices via off-the-shelf FPGAs [19].

2.5.3.2 *Communication Components*

Often Epidermal Devices are coupled with wireless communication modules to send data to a remote computer or a mobile device for further processing. These strategies typically involve using on-device antennas for wireless communication [230]. Epidermal devices with wireless transmission capabilities have been developed for power transfer [186], near-field communication [215, 240], radiofrequency communication [396] and wireless bluetooth communication [183].

2.5.4 *Energy Harvesting*

While extensive efforts have been devoted to the development of wearable health and fitness monitoring systems, limited efforts have focused on developing body-worn energy harvesting and energy storage for powering these sensing systems. Most of the work on energy harvesting devices has been contributed in the physical sciences research community by using electro-chemical approaches [23]. Pioneering work from HCI has been using commercial supercapacitors for energy harvesting [183].

Triboelectric generators (commonly termed as TENGs) are one of the most commonly used techniques and utilize the principles of tribocharging to harvest mechanical energy and convert it into electricity in a simple and low-cost manner [103]. Energy harvesting through triboelectric generators has also received attention in the HCI community recently. They have been used for powering paper-based interfaces [55], microphones and acoustic sensing [13] and for interactive cords and textiles [127, 410]. Moreover, biofuel cells (BFCs) have been explored in the physical sciences research community. These are devices that convert chemical energy into electricity through biocatalytic reactions. They are a promising source for generating sustainable electrical energy [23, 144, 548]. Epidermal BFCs have been successfully deployed to harvest energy from human sweat [21, 25, 199, 438]. Finally, thin-film alkaline batteries [557] that use water-based electrolytes can be used for powering on-skin electronics [32, 255].

Contributions in Functionality of Devices

This thesis majorly focuses on the input aspect of Epidermal Devices. Touch and its contact information have been the most frequently investigated forms of input for Epidermal Devices in both HCI and physical sciences research. This thesis contributes to Epidermal Devices with enhanced input capabilities. *SkinMarks* (Chapter 4) contributes touch sensors with sub-millimeter electrode sizes that allow for higher-resolution touch sensing along with enabling touch input on challenging body geometries. To further enhance touch input, Chapter 5 presents *Multi-Touch Skin*, a thin and flexible multi-touch sensor that can sense high-resolution multi-touch input. The device can also detect the touch contact information enabling the sensing of various tactile input modalities (e.g. touch,

grab, knuckle, touch pressure, etc.). For kinematic sensing, this thesis contributes bend sensors (Chapter 4) through strain gauges that can be placed at various challenging locations on the body. For physiological sensing, Chapter 6 presents easy and rapid fabrication methods for fabricating multi-modal Epidermal Devices. To the best of our knowledge, it is the first work that integrates custom touch input controls with bio-sensing electrodes within a single device.

In all disciplines, empirical studies are conducted to better understand the performance and characteristics of Epidermal Devices. Yet, the research questions, methods, and study designs strongly differ across disciplines. In this section, we will review what are common evaluation methods and will contrast the typical methods and strategies used in HCI with those employed in other disciplines.

2.6 EVALUATION METHODS AND STRATEGIES

2.6.1 *Technical Evaluations*

Technical evaluations typically include experiments designed to understand the functionality of the device, its mechanical characteristics, and material behavior.

2.6.1.1 *Evaluating Device Functionality*

For input devices involving tactile sensing and physiological sensing, typical measurements representing the quality of signal acquisition include measuring signal-to-noise levels [105, 498]. For displays, these involve optical characterization [193]. In the case of actuators, these measurements typically include psychophysical studies to understand the stimulation thresholds and just-noticeable differences (JNDs). Recent work has also been using psychophysical methods to characterize the feel-through characteristics, a key property of Epidermal Devices [150, 510]. In most cases, the methods for measuring device functionality have been similar across the HCI community and physical sciences research.

2.6.1.2 *Microscopic Analysis*

Microscopic analysis usually involves SEM (Scanning Electron Microscope) scans of the device to accurately measure the device thickness [531, 537]. These evaluations also show the quality of deposited functional traces and layers in the device. Microscopic analysis is less common in the HCI literature, with only a few works reporting this analyses [287]. Microscopic analyses should be more commonly adopted in HCI work since they can provide insights into various aspects of real-world usages, such as the initial quality of functional layers and for measuring the degradation of the material after continued use.

2.6.2 *Empirical Studies and User Experiments*

The HCI community has made fundamental contributions to understanding the use of the human body for interaction. Most of the empirical research and controlled experiments with users are centered around three themes: (a) User Strategies and mappings, (b) elicitation Studies, and (c) social acceptability studies.

2.6.2.1 *User Strategies and Mappings*

Understanding on-body interaction is an active research topic in HCI. Several empirical studies focused on the body-centric interaction space [155, 476], identified user strategies for creating on-body gestures [346] and revealed that on-skin input increased the sense of agency [34]. Moreover, previous research has investigated mapping strategies for input elements on the skin. These include salient features on the palm [90, 138, 478], targets placed on the forearm [278], visual and tactile anatomical landmarks [33, 500] as well as mappings between skin and an off-skin display [35].

2.6.2.2 *Elicitation Studies*

Several elicitation studies have been conducted to understand gestural interaction on specific body locations such as ears [59], fingers [50, 411], forearm [42, 499], nose [378], belly [474], head and shoulders [469]. In addition to gestural input on body locations, elicitation studies have also been reported for skin-specific input modalities and user preferences for on-skin input [42, 499].

2.6.2.3 *Social Acceptability*

In recent years, we witness an increasing focus on social acceptability and social perception of body-worn devices. Social acceptability studies have initially been focused on wearable devices [249, 250] and interactive textiles [88, 218]. They have investigated how e-textiles might alter the wearer's social image and perception by others during everyday activities [88, 247, 377, 459]. More recent work has tried to understand the social perception of using on-skin interfaces in public. You et al. [543] studies a third person's perception of a user's interactions with an on-skin touch sensor. In their survey, participants had to look at a series of videos of a user interacting with an epidermal touch sensor placed at seven on-body locations. The authors examined social perceptions that correspond to the different body locations, as well as gestural interactions performed on the device. The study was conducted in the United States and Taiwan to examine cross-cultural attitudes towards device usage. Similarly, a follow-up study investigated social perceptions towards interacting with a color-changing on-skin display [210, 542]. In addition to these these studies, prior work also studied gestural input performed on

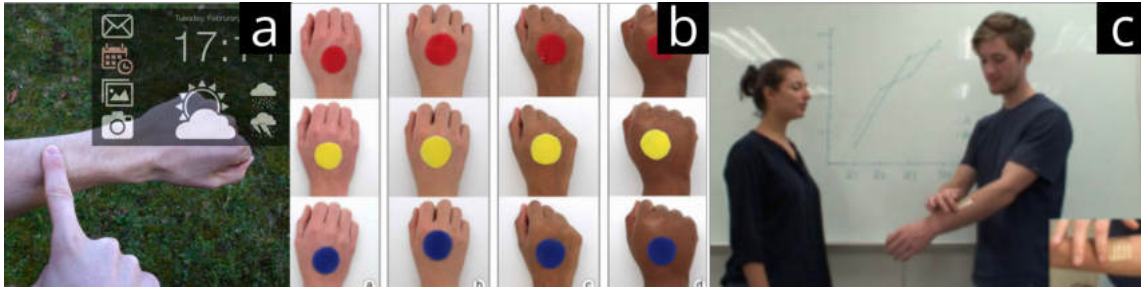


Figure 6: Empirical studies on understanding on-skin gestures and on-skin devices. (a) More Than Touch [499] used an elicitation study to understand gestural interaction on specific body locations such as the forearm. (b) Kao et al. [210] used a mixed-methods approach with online surveys and in-lab interviews to investigate the means by which on-skin notification displays are perceived by the general public. (c) You et al. [543] investigated the third person perceptions of a user's interactions with an on-skin touch sensor.

the body [345, 375], on epidermal interfaces [543] or directly on skin [499] and evaluated appropriate body locations for on-body computing [542, 543, 547].

This thesis employs the standard technical evaluations that have been reported in prior literature. To evaluate the device functionality, this thesis reports on experiments that measure SNR levels of touch sensors (Chapters 4 and 5) and physiological sensors (Chapter 6). In addition to measuring the SNR of touch sensing under varying ground conditions, Chapter 5 also presents an evaluation method for measuring the spatial resolution of the sensor under varying deformation conditions. Microscopic analysis involving SEM scans is very limited in HCI literature. This thesis takes a step in this direction by analyzing devices using an SEM scan (Chapter 4). In addition to these evaluation methods, this thesis takes the first steps in understanding the psychophysical aspects of Epidermal Devices which to the best of our knowledge, have not been explored in prior literature. Investigating the psychophysical aspects of Epidermal Devices is very crucial as this determines their tactile performance i.e. how well they can transmit the tactile cues to the mechanoreceptors in our skin. Chapter 3 investigates this aspect through three psychophysical studies that measure the influence of the stiffness of a patch on tactile perception capability.

2.7 APPLICATIONS AND REAL-WORLD DEPLOYMENTS

Due to their unique form factor, intimate integration with the user's body, and low cost, Epidermal Devices open up a range of opportunities for applications and real-world deployments. These span a wide range of areas, ranging from general mobile computing and communication to supporting a user's bodily activities in sports and fitness, and ranging from health monitoring and diagnosis for the masses to more specialized areas such as assistive technologies. Exemplary

application scenarios are one area where the HCI research community trumps over the physical sciences research community.

2.7.1 *Health Monitoring and Diagnosis*

A key advantage of Epidermal Devices is that, since they are directly present in the body, they have direct access to the biophysical and biochemical features of the body. Using these devices to continuously monitor bio-signals promises to reduce diagnostic hospital visits and can also facilitate early diagnosis and prevention of illnesses. Epidermal Devices have been deployed for non-invasive drug delivery [17, 266, 423, 482] and wound healing [193, 194, 520]. This application area provides an exciting opportunity, with first interactive physiological devices already being developed in the HCI community [304, 338].

2.7.2 *Assistive Technologies*

Assistive technologies and accessibility are key application areas where Epidermal Devices can be deployed for creating societal impact. Studies have demonstrated the benefits of body-based interaction for eyes-free and accessible interaction [138, 346]. Wearable accessories have already been developed in the HCI community for accessible computing on the go [414]. Furthermore, epidermal exoskeletons promise support for applications such as assisting the physically disabled [212] or restoring the ability to pinch and grasp objects after having suffered a spinal cord injury [209].

2.7.3 *Sports and Fitness*

Epidermal Devices offer new integrated platforms for continuous monitoring of both biophysical and biochemical signals, which can be of interest in sports analytics and fitness monitoring. Prior work includes strain sensors that can detect human motion [526] and precise body movements during athletic training [550]. Furthermore, traditional electronic components such as accelerometers and strain gauges can be encapsulated within stretchable casings and shells to realize devices that are more mechanically robust and can be deployed for monitoring during a workout [263]. In addition to motion sensing, other physiological parameters such as EMG [531], ECG [269], temperature [465], respiration, and electrochemical signals such as glucose and sweat composition [23] are essential for evaluating an individual's overall physiological state and are thus topics of intense academic interest in sports science and performance. Epidermal Devices from the HCI community have also demonstrated body motion sensing [304, 338]. However, these are typically limited to a single body location or movement.

2.7.4 *Affective Communication*

The multisensory nature of human touch makes Epidermal Devices a promising choice for enhancing affective communication between people over the distance. Propositions from prior research include remote communication with a partner using on-skin multi-touch gestures [338, 341] (presented in Chapters 5 and 6) or sending affective haptic signals to a remote user [545]. Sharing of biosignals as a means for intimate communication between users [282] is another promising direction.

2.7.5 *Mobile Computing*

A vastly explored application area for Epidermal Devices in HCI is mobile computing. Epidermal Devices have been used for designing novel techniques that enable interaction in demanding mobility conditions. This includes mobile on-body text entry [498, 525], eyes-free micro gestures control [221], smart control of IoT devices [242, 341], physical interaction with mobile devices [150], display of subtle notifications [215, 287, 500, 510], and gestures that can be performed when hands are busy holding objects [341] (presented in Chapter 5). In addition to supporting interaction in mobile scenarios, Epidermal Devices have also been deployed in the context of other interactive applications such as in AR/VR [510, 545].

This thesis makes initial explorations in identifying and deploying Epidermal Devices in multiple application scenarios. Multi-Touch Skin (Chapter 5) and PhysioSkin (Chapter 6) propose using on-skin touch sensing for remote communication with a partner. For enhancing interaction in mobile scenarios, Multi-Touch Skin sensors have been used for enabling eyes-free text entry on a fingertip, performing gestural input when hands are busy holding objects, and for controlling IoT devices (presented in Chapter 5). To explore applications in the context of health monitoring and fitness Chapter 6 presents devices embedded with physiological sensing electrodes that can sense body motions and heart rate.

2.8 POSITIONING EPIDERMAL COMPUTING IN HCI LITERATURE

Figure 7 shows the taxonomy of wearable technologies that classifies each technology based on its location on the body surface. Technology can be on the body or on the surface of the skin (such as wearables), inside the body (such as implants and pacemakers), and carried on the body (such as smartphones and tablets). The main difference between technology that can be carried and wearables is that the former often demands full attention from the user, is typically carried and not worn, and requires using both hands for operating [365]. Wearables can be worn on the body as devices (e.g. smartwatches, smart glasses) or integrated into

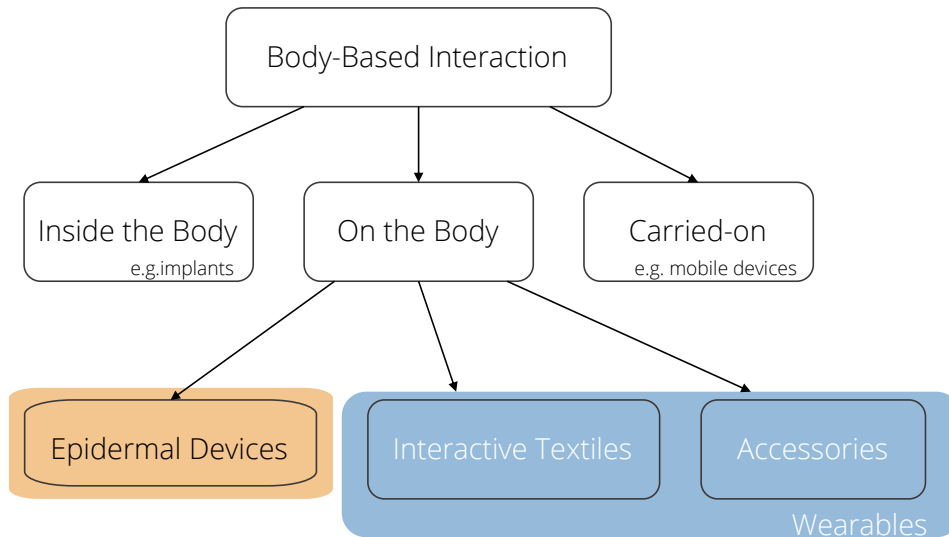


Figure 7: Positioning Epidermal Devices within the broad scope of Body-Based Interaction in HCI. This taxonomy of on-body technologies is adopted from prior work [285, 380].

textiles. Epidermal Devices, the focus of this thesis, are present on the surface of the skin.

In the remaining sections of this chapter, we firstly present an overview of the sensing techniques that have been explored in the HCI community for enabling interaction on the body. We compare and contrast them with the techniques that have been explored in this thesis. We then present state-of-the-art in other on-body technologies that have been investigated in HCI literature.

2.8.1 Overview of Sensing Techniques for On-Body Interaction

Input sensing on the skin has received a lot of attention in the HCI community. Many technical approaches have been investigated to enable touch input on the skin including microgestures. This section reviews those various technical approaches.

2.8.1.1 Optical Approaches

The most common approach employed in the HCI literature to sense input on the skin is the optical sensing approach. It uses cameras. Prior work sensed input on the skin using RGB cameras [51, 320, 446], depth cameras [90, 141, 153, 156, 231, 425] or infrared sensors [126, 437, 535] for gesture recognition on or around the body. The camera is either mounted on the shoulder [153, 419], to the ceiling [156], on the wrist [425, 535], hand webbings [51], head [320, 446], or on an external tripod behind the person [90, 141]. This allows for direct interaction on the skin,

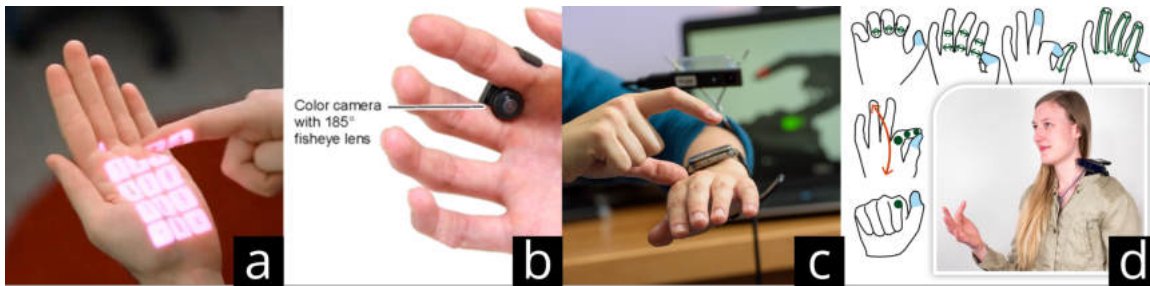


Figure 8: Sensing on the skin using optical approaches using cameras mounted on the body. (a) Omnitouch [153] uses a depth camera and a projection setup to enable input on the body. (b) CyclopsRing [51] uses a camera with a fish-eye lens placed between the finger webbing to enable gestural interaction (c) WatchSense [425] uses a depth camera mounted on a wrist to enable interaction on and around the body (d) FingerInput [419] uses a depth camera mounted either on the shoulder or head to enable a wide range of finger microgestures.

however it requires direct line-of-sight to the camera and can be susceptible to lighting conditions.

An alternative approach that has been explored is to attach lightweight optical sensors close to the skin. These optical sensors typically include one or multiple photo-reflective or IR sensors that can be easily packaged into a wearable form factor. They also often require less computational processing than typical camera setups. Ni and Baudisch propose the use of a Phidgets light sensor and an inverted optical mouse to capture finger scanning and finger movements [336]. Butler et al. [45] used Infrared (IR) proximity sensors embedded along the sides of a mobile device to sense touch input around small devices. Similarly, prior work used IR reflectors and emitters to enable expressive interaction with wearable devices [258, 511, 528]. Nakatsuma et al. [334] built a custom wristwatch-sized device that consists of IR reflectors and a piezoelectric sensor to track 2D finger movements on the back of the hand. Similarly, IR sensors and emitters have been incorporated into HMDs for enabling input on the cheek [527] and on the forearm for sensing skin deformations [344]. *LumiWatch* is a custom-made smartwatch that uses an array of 1-D depth sensors and a pico projector to project the interface onto the skin. The 1D depth-sensing array is used to track fingers on or very near to the surface of the arm [517]. Sensors attached to the fingernails have also been utilized for sensing deformations [307].

2.8.1.2 *Wave-Propagation through the Body*

The human body in addition to being electrically conductive also serves as an ideal medium for transmitting acoustic and electromagnetic waves [549]. By using through-body electrical signals, Capacitive Fingerprinting [157] and Biometric Touch Sensing [176] can differentiate between users. Passive techniques such as *Humantenna* [72, 73] and *EM-Sense* [259] monitor electromagnetic noise absorbed

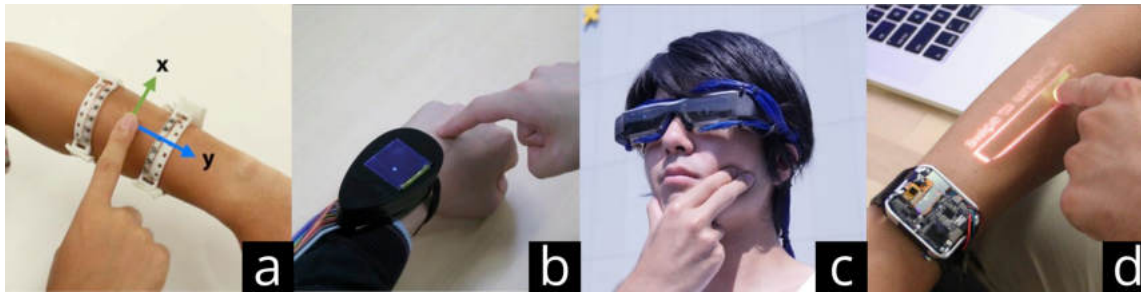


Figure 9: Sensing on skin using optical approaches using IR emitters and reflectors mounted on the body. (a) *Senskin* [344] uses an array of IR reflective sensors to sense skin deformations. (b) Nakatsuma et al. [334] demonstrated a wrist worn device consisting of IR sensors to sense 2D touch input on the back of the hand (c) *CheekInput* [527] uses a depth camera mounted inside HMD device to enable input on the cheek. (d) *LumiWatch* [517] uses an array of 1D depth sensors and projector housed inside a smart watch casing to enable input and output on the body.

by the human body for gesture and object recognition. *Skinput* [159] proposed bio-acoustic sensing for on-skin touch sensing. Vibrations resulting from firm touches propagate through the skin. These vibrations can be with an array of piezo sensors to localize the touch contact. Similarly, *EarBuddy* [523] senses taps and touch contact near the face and the ears using commercial wireless earbuds.

Active signal propagation can be used for personal area networks [166, 563] and to transmit audio signals [113]. Mujibiya et al. [326] showed that touch and pressure on the skin can be sensed through the transdermal propagation of ultrasound signals. A transducer placed perpendicular to the skin results in surface wave propagation which is captured using a finger-worn receiver. Zhang et al. used a high-frequency AC signal (80MHz) generated by a finger-worn ring that this transmitted through the body and is sensed using a wristband [553]. The two electrodes on the wristband measure the received signal and the phase delay are computed for 2D localization of the finger on the arm. This system had a mean positional error of 7.6mm. In comparison to camera solutions, they do not suffer from occlusion problems. However, they do not support the full range of multi-touch interactions that are enabled through capacitive sensing techniques employed in smartphones and touchscreens.

2.8.1.3 Magnetic and Electric Field Sensing

Another approach that has been used for input sensing is magnetic field sensing. Typically, this approach uses magnets in conjunction with magnetometers or hall-effect sensor grids to track the position of the magnet. *Abracadabra* provides an additional input modality to smartwatches through a magnet affixed to the finger [154]. *Nenya* provides subtle eyes-free input interaction with smartwatches. It utilizes the magnetometers that are found in smartphones [14, 356]. Hall-effect

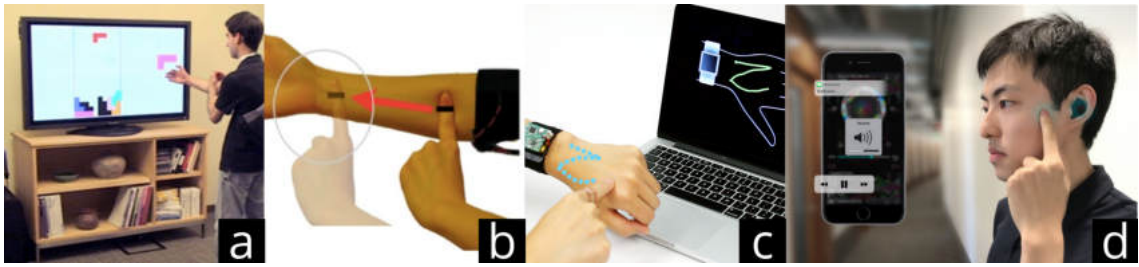


Figure 10: Body has been used as a medium for the propagation of acoustic and high-frequency waves. (a) *Humantenna* [73] uses the human body as an antenna for sensing whole-body gestures (b) *Sound of Touch* uses transdermal low-frequency ultrasound propagation for sensing pressure-aware continuous touch input as well as arm-grasping hand gestures on the human body. (c) *SkinTrack* [553] uses the human body as an electromagnetic waveguide and transmits an 80MHz wave through the body. (d) *EarBuddy* [523] uses commodity wireless earbuds to detect face and cheek gestures. The working principle of this technology uses acoustic waves propagated through the body while performing the face gestures.

sensor grids have been used to sense subtle thumb to fingertip gestures [53, 181]. More recent work has also investigated the use of magnets for providing haptic feedback. *Magnetips* [312] utilizes a magnetometer array and a copper coil for enabling continuous finger-tracking and haptic feedback. *MagnetIO* provides ubiquitous haptic feedback through soft haptic patches that can be affixed to any object or surface. The system comprises of a voice-coil worn on the user's fingernail and any number of interactive soft patches regions doped with polarized neodymium powder that can be attached to any surface (everyday objects, user's body, appliances, etc.) [309]. All of these approaches use a magnet mounted onto the fingertip [295, 356] to enable continuous motion tracking of the finger which in turn results in expanding the interaction space. Magnetic sensing enables subtle and eyes-free interaction through gestures and continuous finger tracking. However, one limitation of this sensing approach is the precise tracking of touch-down and touch-up events. Another limitation is that in all of these research works, the magnet or an actuation coil has often been affixed to the nail of the index finger or in the form of a ring [14]. Magnet being a very rigid object is not skin-conformal and cannot be easily transferred to other challenging body locations.

Similar to magnetic field sensing, another complementary approach that has been investigated for on-body input is electric field sensing [565]. EF sensing is a well-explored technique in HCI and has been previously explored for gestures [100, 261, 509], motion sensing [71], and even activity tracking [327]. Three configurations are common. In Loading-Mode sensing, an electric signal is injected into an electrode and the capacitive coupling between the electrode and an object of interest is measured. In Transmit-mode, a signal is passed through the human

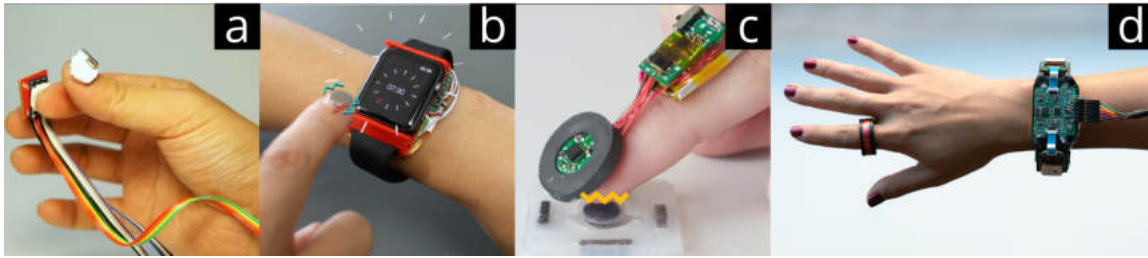


Figure 11: Magnetic approaches can be used for sensing input and delivering haptic output on skin. (a) FingerPad [53] uses hall-effect sensors and a magnet attached to the thumb for sensing subtle thumb to fingertip gestures. (b) Magnetips [312] uses a magnetometer array and a copper coil for tracking continuous finger movements and delivering haptic feedback. (c) MagnetIO [309] provide haptic feedback through soft haptic patches that can be affixed to any object or surface. (d) Auraring [356] enables continuous motion tracking of the finger.

body; the signal is captured by a receiver electrode touched by the user. Finally, shunt-mode uses emitting and receiving electrode pairs and measure the disturbance when a conductive object (e.g., a finger) interferes with the electric field. All of these approaches exploit the inherent electrical conductivity of the human body. A more detailed comparison of these three configurations can be found in [418].

Electric field sensing has been employed for sensing touch input on the skin for enhancing input on smartwatches and in the context of AR/VR [552, 558]. Taking this concept further, *ElectroRing*[227] employs electric field sensing through transmitting and receiving electrodes embedded onto a ring along with a shield electrode that separates the transmit and receive electrodes. Electric field sensing has also been used for sensing inter-personal touch through a wearable bracelet [142, 441].

2.8.1.4 Radar and Ultrasound Techniques

Radar-based sensing techniques use high-frequency short-range radio-frequency signals for sensing fine-grained motions with high temporal resolution [484, 534]. It enables sensing of motion, range, and velocity, which can be used for detecting gestures with a quick motion, e.g. swiping and rubbing. By employing machine learning approaches, a wide range of materials can also be classified including various body parts [534]. A key drawback is that tracking precise spatial configurations e.g. touch location and type of touch contact is difficult. Ultrasonic sensors and transducers attached to the skin can also be used for sensing gestures and interaction on the body [191, 278]. These techniques require line of sight[278] with the interacting finger and support a set of discrete gestures. Realizing high-resolution multi-touch interaction is challenging with these sensing techniques.

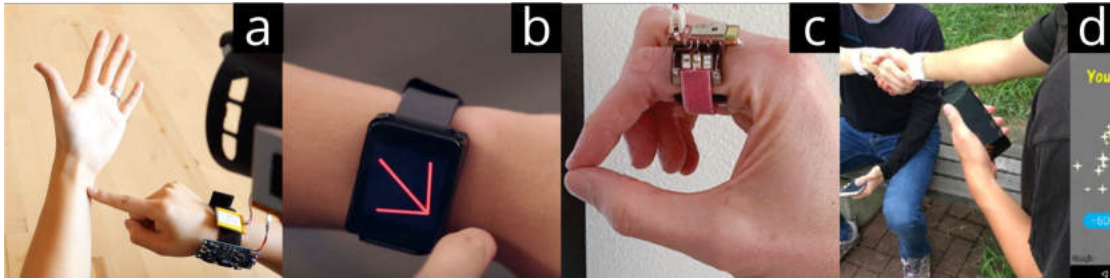


Figure 12: Electric field sensing approaches can be used for sensing input on skin. (a) ActiTouch [552] uses transmit and receive electrode pairs for sensing touch input on the skin. (b) AuraSense [558] uses electric field sensing to enable expressive around-smartwatch interactions. (c) Electroring's [227] uses active electrical sensing approach sensing both touch and release events. There is a step-function-like change in the raw signal which can be easily detected using only basic signal processing techniques. (d) EnhancedTouchX [142] is a bracelet-type interpersonal body area network device, which detects and quantifies interpersonal hand-to-hand touch interactions through electric field sensing.

2.8.2 Other Technologies from the Taxonomy of On-Body Interaction

Figure 7 shows the taxonomy of the on-body technologies that have been explored in HCI. This section reviews the state-of-the-art in other alternate technologies that have been explored in HCI literature. These include (1) implants, (2) wearable devices and interaction techniques with them, and (3) interactive textiles.

2.8.2.1 Implants

Implants are electronic devices that are placed inside the body (under the surface of the skin). This technology already exists in the form of medical devices such as pacemakers, insulin pumps, and cochlear implants. In addition to medical applications, implants have been used for enabling novel forms of input and output [430], identification through RFID, to control remote robots [496] and to permanently augment senses with technology [495]. Holz et al. [175] investigated implanted user interfaces to study how these devices function through the skin. The devices implanted include touch, tap, microphone for sensing touch and audio input, LEDs, vibration motors and speakers for providing output, bluetooth for evaluating the communication, and inductive charging for energy harvesting. Another interesting approach is implanting silicon-based devices [229], tattooing functional inks [37] and using ingestible devices for exploring novel forms of interactive gameplay [273, 274]. In addition to these technical implementations, studies have been reported that investigate the use of implants among hobbyist populations [160]. Overall, implants are a very promising technology and offer a wide range of opportunities for advancing the capabilities of humans. However,

these technologies often require surgery, need medical expertise and supervision while implanting devices for intrusive modification of the body. In contrast, the devices proposed in this thesis are all temporarily attached to the skin and are easy to attach and detach by the user. The fabrication and design approaches presented in this thesis also enable a wider audience including hobbyists, practitioners to realize custom devices.

2.8.2.2 *Interaction with Wearable Devices*

Wearable devices have been an active research topic for a long time. The first instances of wearable devices appeared in 1966 when Thorp and Shannons built a timing device to predict roulette [456]. Subsequently, many other devices followed that include a wrist-worn calculator [302] and a general-purpose wearable computer featuring a head-mounted display and chorded keyboard [300]. Recent advances in low-power processors, wireless communication, and miniaturization of sensor technologies have enabled the commercialization of wearable computing devices. However, wearable devices suffer from interaction problems. The HCI community has explored several technical approaches and interaction techniques to solve these issues. The following section discusses the approaches that have been explored in this regard.

Body-Worn Devices for Interaction with Wearables Commercial wearable devices (e.g. smartwatches, smart glasses, fitness trackers, portable head-mounted displays) offer superior wearability by sacrificing real-estate for interaction. As a result, precise touch input is demanding because the size of the touch targets is diminished to account for smaller screen real-estate. Additionally, there is also the occlusion problem due to the finger present on the touchscreen.

In addition to designing device-centric interaction techniques such as pan, twist and click interactions [518], tapping gestures [342, 397], cross-device [58, 409] and bezel-based interactions [253, 514], prior work addressed this problem through various body-worn devices [501]. Ashbrook et al. presented a magnetically tracked finger ring to enable subtle eyes-free mobile input [14]. Xia et al. used a finger-worn nano-stylus to enhance precise touch input on a small-screen display [516]. Interaction with smartwatches has also been enhanced by embedding them with miniature projectors and infrared proximity sensors for extending interaction onto the skin [258, 517]. Finger-worn wearable devices are an active research area in HCI for supporting rich natural interactions with wearable devices [415]. These include nail-worn displays [436], nail-worn input devices [180, 214, 264] that have been developed for enhancing interaction with wearable devices. In addition to input, body-worn output devices have also been used for augmenting interaction with wearables. Roumen et al. conducted an empirical investigation of wearable interactive rings to compare the noticeability of four instantaneous notification modalities (light, vibration, sound, poke) [398]. Additional output modalities such

as wind and thermal feedback have also been investigated by integrating them in a wrist-worn device form factor suitable for smartwatches [364, 416].

Device-centric interactions offer new means of interaction with wearable devices, however, they do not leverage the natural affordances of human skin. Body-worn devices that have been explored in the HCI literature fill this gap. However, they are rigid or bulky restricting (similar to traditional ornaments) them to a few locations on the body such as nails, wrist, and fingers.

Free-Form Body Gestures Contact-less or gestural interaction is an alternative method that enables input on and around the devices. Gestural input is performed by making a motion around the large, 3D space around the device. One of the early works investigated mid-air swipe gestures for simple number entry for mobile and wearable devices [316]. Building on this, Kim et al. [241] enabled input above a smartwatch with multi-directional gestures. Gestural interaction on mobile devices and smartwatches has been explored through in-air gestures [421, 422] and wrist gestures [125]. Besides these techniques, magnetic sensing techniques have also been explored for continuous tracking of a finger around a device [154, 312, 356]. μ Track tracks the 3D position of the thumb using magnetic sensing [56]. Similarly, Finexus [57] tracks precise motions of multiple fingers using magnetic sensing. Imaginary interfaces allow for spatial and gestural interactions without a screen. They support in-air gestures expanding the interaction space around a small device [140]. Radar-based sensing techniques also allow for in-air gestures around a device [484]. A key limitation of mid-air gestures is that they do not provide tactile feedback to the user. This is in contrast to on-skin interaction, where gestural interaction on the skin provides natural tactile feedback of the finger performing the gesture at a specific location on the body.

In addition to using precise finger motions for gestural input, arms and hands also afford gestural interaction with mobile and wearable devices. Hand gestures can be detected through a chest-worn infrared camera [428]. Similarly, Sixth Sense supports in-air gestures and drawing [319]. Shifting the camera position to the shoe provides a new perspective to sense body gestures [18]. Armura [156] investigated the interaction space of hand gestures with and without visual output. Going beyond the upper limbs, Cyclops [52] uses a fish-eye lens on a chest-mounted camera to capture full-body gestures.

Data gloves capture the rich dexterity and articulated finger movements that can be utilized for human-computer interactions [94, 435]. These gloves are typically worn on the hand to capture hand movements and hand pose [564]. Gloves are a promising technology for capturing intricate details of hand and finger movements. However, they can be bulky, and not suitable for scenarios demanding high mobility. As a reason, glove-less systems are being actively investigated for hand-gesture recognition. Typically this can be done using wrist-worn sensors using capacitive sensing [385], photo reflectors [112], electrical impedance tomography [551], bio-acoustic sensing [6, 89] and pressure sensors [85]. Tracking the skin motion of the back of the hand can also provide an estimation of finger

angles [276]. Optical sensors worn on the finger, wrist, or body can also be used for sensing hand pose. Finally, bio-signals such as surface electromyography (sEMG) has also been used for sensing finger and hand gestures [8, 404].

The design and implementation of free-form body gestures is an exciting research area in HCI that opens a wide range of opportunities in various application domains. While technical approaches such as magnetic sensing, radar-based sensing, and optical sensing allow for mid-air gestural interaction, they are usually restricted to interaction with specific body sites or need to be re-calibrated to support interaction at a different body site (for instance, radar-based sensing was explored for in-air gestures around a mobile device [484] but it remains to be seen how well it can work for sensing skin-specific gestures). It remains to be seen how these technologies can be leveraged for interaction on multiple body sites, for instance, optical approaches may fail to detect an interacting finger behind the ear because of occlusion problems. Epidermal Devices offer the advantage of quickly deploying it on different body locations to augment a body site with rich input capabilities.

2.8.2.3 *Interactive Textiles*

Clothing and interactive textiles (more broadly termed as e-textiles in other research communities like Materials, Textile engineering) has been one of the active research areas in HCI and other disciplines [49, 60, 64]. Recent advances in conductive yarns allow for weaving of touch sensing electrodes into textiles on a large scale through industrial manufacturing processes [372]. Multiple interactive sensing approaches such as capacitive touch [171], mutual-capacitive touch [348], resistive [162], pressure [5, 556], strain [539], body-pose sensing [284] and inductive sensing [515] have been successfully implemented through interactive textiles.

Interactive textiles also have been deployed on various body locations in form-factors such as sleeves on the forearm [361], pockets [96, 403, 515], on fingers [539], socks [111], belt [95], hair extensions [92, 473] and prosthetic limbs [271]. In addition to augmenting textiles with conductive yarns [362] and embroidery techniques [148], another commonly employed approach in HCI has been to augment the skin with soft textile patches. For instance, zPatches are e-textile patches that can sense touch, hover, and pressure input through resistive and capacitive sensing [429]. Similarly, SkinLace [200] uses free-standing laces fabricated with machine embroidery. These laces can be embedded with touch sensors, LEDs, and RFID chips for interactive applications. Strohmeier et al. [431] use pretreated kinesiology tape, which is made piezo-resistive material for creating textile patches on the skin that can sense touch, pressure, and stretch.

The HCI community has also explored various fabrication strategies for realizing customized e-textiles. Klamka et al. [244] use heat-activated adhesive materials consisting of smart textiles and printed electronics, which can be flexibly ironed onto the fabric to create custom interface functionality. Honnet et al. [178] use

in-situ polymerization for enabling arbitrary textiles to sense pressure and deformation. Devendorf et al. used weaving and yarn plying techniques to realize smart textiles [87]. Sun et al. introduce a weaving-based fabrication approach to create on-skin patches. They leverage the skin-friendly material of PVA, which enables on-skin adherence of textile patches [439]. Using embroidery techniques is another way in which smart textiles have been realized for custom applications [148, 391].

Many interaction techniques with interactive textiles have also been explored. Olwal et al. explored microinteractions with flick, slide and grasp gestures [349]. Parzer et al. explored deformation gestures with a interactive textile sleeve [361]. Schneegass et al. [406] investigated different gestures such as stroke based gestures or taps using a touch enabled textile. Many other interaction techniques have been explored such as eyes-free interaction [218, 540], menu selection [146], contextual interactions [124],

Compared to Epidermal Devices, e-textiles and smart textiles have been explored very widely in multiple research communities. The challenges with respect to sensing and fabrication of devices through textiles are also fundamentally different from Epidermal Devices. From an interaction design perspective, the physical and functional affordances provided by the skin are different from textiles. The haptic cues and surface textures are different and hence the interaction technique designed for skin does not directly translate to skin and vice-versa. Textiles also do not offer the same level of tactile transparency as Epidermal Devices, this is because usually, the thickness levels of textile are very high when compared to Epidermal Devices. Fabrication-wise, smart clothing, and interactive textiles are mostly based on conductive yarn and thread, which integrate into the common fabrication processes for which manufacturing equipment and machinery already exist such as weaving and embroidery [87, 200, 372, 439]. Such techniques and fabrication processes do not directly transfer to Epidermal Devices. Hence, there is a need for exploring new fabrication techniques and computational design approaches for Epidermal Devices. While this thesis does not address and focus on interactive textiles, there is one exploration with respect to this area. PhysioSkin [338] (Chapter 6) presents a fabrication technique for embedding physiological sensing electrodes into textiles.

2.9 SUMMARY

This chapter presented a detailed literature review on multiple fronts. Firstly, it provided an overview of the anatomy and physiology of human skin which is essential for the design, development, and deployment of Epidermal Devices. Taking a multi-disciplinary approach, this chapter reviewed prior work that contributed to Epidermal Devices across disciplines. Following this, Epidermal Computing as an emerging area is positioned within the context of technologies that enable on-body interaction in HCI. A key insight from these broad literature reviews is that there are several open challenges and research directions for advancing Epi-

dermal Computing. This thesis majorly focuses on important research challenges that need to be addressed from an HCI perspective.

2.9.1 *Material Exploration*

Material exploration is an important step that guides the design of Epidermal Devices, from an HCI perspective. While there have been advanced materials and material formulations that have been developed in Materials Science communities, oftentimes these entail complex fabrication processes and require expertise prohibiting a wider scale audience to adopt these methods. Hence, a systematic exploration of materials that are commercially available or can be formulated with simple lab equipment is essential for enabling rapid prototyping and development of Epidermal Devices. Material exploration is also important because conventional materials used in commercial touchscreen devices are not compatible for deployment on the body. Unlike commercial wearable devices, the human body is soft, malleable, and supports strong deformations. In addition to identifying material combinations that are stretchable while possessing high electrical conductivity, identifying other suitable materials such as insulators and skin adhesives is crucial. Chapters 4, 5, and 6 highlight these aspects. Chapter 5 explores various material combinations including conductors and insulators suitable for creating the sensor sandwich for sensing high-resolution multi-touch input. Chapter 6 highlights the importance of skin adhesives for creating tight electrical contact with the skin for acquiring bio-signals. Through diverse material explorations, this thesis helps in better understanding the properties of functional materials that are vital for fabricating various types of Epidermal Devices.

2.9.2 *Enriching Sensing Capabilities of Epidermal Devices*

Touch is one of the primary input modalities that we use for interacting with computing devices. Human skin affords rich touch input modalities [499]. However, the resolution of touch sensing that is enabled by Epidermal Devices has thus far been limited to low-resolution single-touch input [215, 287]. One key research direction this thesis explores is in improving touch resolution. Chapter 4 presents early endeavors in this regard through the design of touch electrodes that are an order of magnitude thinner than prior work [215, 287]. Chapter 5 then presents the design and fabrication of Epidermal Devices that can sense high-resolution multi-touch input. It presents the first non-rectangular multi-touch Epidermal Devices that can be deployed at various locations on the body. In addition to enriching sensing through high-resolution touch sensing, this thesis also contributes Epidermal Devices that can sense multiple bio-signals enriching the sensing capabilities of Epidermal Devices.

2.9.3 *Easy and Rapid Fabrication Methods couples with Computational Design Approaches*

Creating easy and rapid fabrication techniques is very vital for promoting the development of custom Epidermal Devices to a wider audience including researchers, practitioners, makers, and hobbyists. The primary goal of fabrication techniques used in this thesis has been to use off-the-shelf materials and simple lab equipment that is easily accessible. Screen printing was the technique used in Chapter 4 for fabricating *SkinMarks* devices. Chapter 5 explored screen printing along with the use of other techniques such as vinyl-cutting. It also explored a hybrid method where conductive ink-jet printing was used for rapid prototyping and testing the designs while using screen printing for higher-fidelity prototypes. Chapter 6 builds on multi-functional ink-jet printing introduced in prior work [225] to create Epidermal devices for measuring electro-physiological signals. It explores multiple approaches for creating fully functional devices that comprise conductive and insulating layers. It also provides diverse fabrication strategies that are compatible with various types of base substrate materials.

In addition to simple and easy fabrication strategies, this thesis also contributes computational design approaches for further speed-up the design process. The computational design approaches also enable the designer to focus on the device design abstracting her from the lower-level technical details that require experience and expertise in multiple domains. Chapters 5 and 7 present computational design tools for creating multi-touch Epidermal Devices in custom shapes and multi-modal electro-physiological devices respectively.

2.9.4 *Empirical Studies to Inform Device Design*

An empirical understanding of Epidermal Devices is crucial since this informs novel device designs. While there have been various types of technical evaluations on Epidermal Devices and empirical experiments in form of elicitation studies, social acceptability studies, identifying user strategies, and mappings, there is very limited work that empirically studies Epidermal Devices. You et al. [542, 543] present the first investigations in this regard where they evaluate social acceptability of Epidermal Devices and Withana et al. [510] present initial explorations into the psychophysics aspects of Epidermal Devices. However, to the best of our knowledge, a systematic, comprehensive psychophysical evaluation of Epidermal Devices measuring their tactile performance and capability to transmit tactile cues has not been explored. Chapter 3 presents the first such investigation where firstly, the tactile performance of a device is quantified by proposing the metric of flexural rigidity - which not takes into account the thickness of the device but also other properties such as elastic modulus which influence the stretchability of the device. Subsequently, the chapter presents three psychophysical experiments that measure the influence of the stiffness of the device on tactile perception capability.

UNDERSTANDING HOW EPIDERMAL DEVICES AFFECT TACTILE PERCEPTION

Epidermal devices open up opportunities for a broad range of important applications. For use in health and fitness, epidermal sensors can continuously monitor physiological parameters [104, 185, 537] in a device form factor that is ergonomic to wear and compatible with demanding body locations [208, 538]. For use in rehabilitation, electronic skin can add human-like sensory capabilities to flexible membranes, for instance, to be integrated with prostheses [67, 350]. For applications in computing, epidermal devices can augment the skin with interactive input and output capabilities, and hence seamlessly integrate the user interface of a computer system with the human body [215, 287, 341, 498, 500].

Very promising pioneering work has been presented and first devices have been made commercially available [296]. This development makes it very plausible that epidermal devices will soon have more widespread use. At the same time, materials and fabrication techniques have matured and are now accessible to interface designers through various rapid prototyping platforms [215, 287, 331, 341, 498]. Moving beyond basic technical studies, interface designers and domain experts can now start exploring designs of devices that offer high usability and user experience.

In this context, envisioning that epidermal devices will be ubiquitous in the near future, one central question that remains is how a skin-worn device affects the natural tactile perception of the skin. An ideal device would leave the user's natural perception undiminished, i.e., the device would be fully transparent to tactile stimuli. Indeed, very slim sub-micron devices have been presented that may come close to this property [104, 205, 497]. However, the thin form factor comes at the cost of more complicated handling and considerably reduced durability of typically less than one day. This limitation can make thicker devices the preferred choice in many cases. As a consequence, designers are confronted with complex, multi-factorial design space. Choosing the best material option is a difficult design decision made more difficult because so far very little is known about the impact of epidermal devices on the user's tactile perception.

This chapter contributes empirical results from the first systematic psychophysical investigation of the effects of epidermal devices on human tactile perception¹.

¹ This chapter is based on [339]. As the first author, I led the experimental design, created the classification of epidermal devices across disciplines, conducted the experiments, analyzed the results, performed the statistical analyses, identified the implications for design and discussion of results. Klaus Kruttwig helped in the fabrication of soft skin silicone adhesive patches that were used in the experiment and conducted the experiments for measuring the flexural rigidity of the patches used in experiments. Roland Bennewitz helped in interpreting the results and

Based on our findings, we derive recommendations that can guide designers of epidermal devices and skin-based interfaces in choosing the appropriate device form factor and materials. We start by proposing the metric of flexural rigidity for capturing the mechanical properties of an epidermal device that affect tactile perception. We contribute the first systematic classification of epidermal devices from the literature in material science, mechanical engineering, nanotechnology, biomedical engineering, robotics, and HCI based on this metric. Our results allow us to identify common properties and to draw comparisons between devices. We also use the classification to inform our experimental conditions.

The main contribution of this chapter are results from three psychophysical experiments that shed new light on the design of epidermal devices. We investigated the effect of device rigidity (mediated by device thickness and elasticity) on human tactile sensitivity thresholds, spatial acuity, and roughness discrimination abilities. We also studied the variations across multiple body locations, on fingertip, hand, and forearm. Results from our experiments show a significant effect of device rigidity on tactile sensitivity and roughness-discrimination abilities; more rigid devices increased the tactile sensitivity thresholds by up to 390% and roughness-discrimination thresholds by up to 490% compared with bare skin. Device rigidity had a considerably less strong effect on spatial acuity. On the sensitive fingertip, spatial acuity thresholds moderately increased by up to 50%, whereas the thresholds remained fairly unchanged on the less sensitive body locations.

Finally, based on the results of our experiments, we contribute recommendations that can inform the design of future epidermal devices. We also highlight the important trade-offs between material properties, mechanical robustness, and tactile perception that designers need to take into consideration when designing epidermal devices.

3.1 CLASSIFICATION OF EPIDERMAL DEVICES

We propose to use flexural rigidity as a metric for mechanical characterization of epidermal devices regarding their expected effects on tactile acuity.

This metric allows us to provide the first systematic classification of prior work, to identify common properties, and to draw comparisons between devices.

3.1.1 *Flexural Rigidity*

The key metric reported in prior research in HCI is device thickness (e.g. [215, 287, 331, 498, 500]). Rarely do papers report on material properties such as maximum

in connecting them to the underlying theoretical foundations in physics. Jaeyeon Lee helped in designing the surface discrimination task. My supervisor Jürgen Steimle advised me on the conceptual design, evaluation, and identifying the design implications for the results we obtained. He further contributed to the structure and writing of the publication.

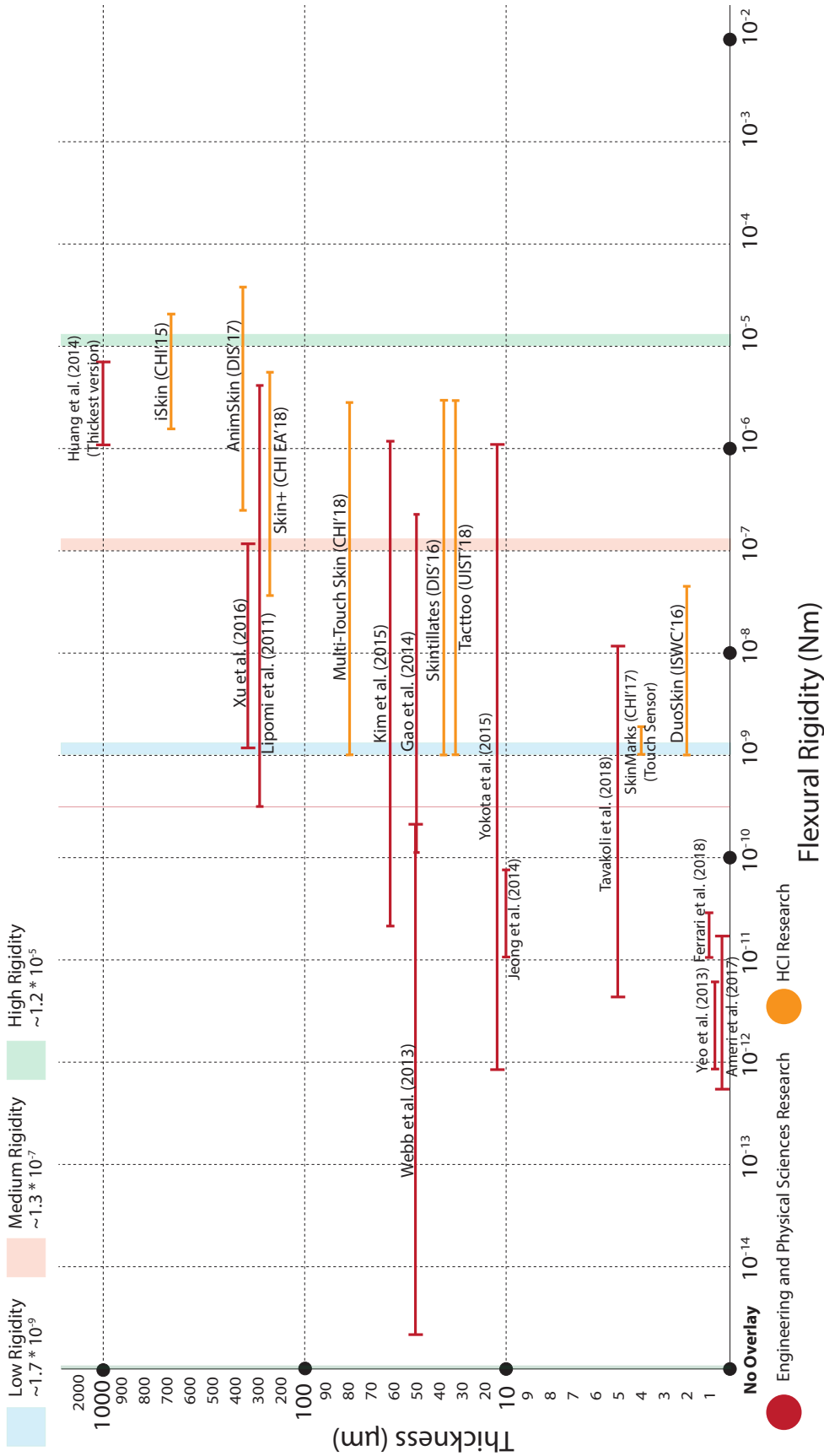


Figure 13: Classification of prior work based on flexural rigidity (ranges shown for devices made of multiple materials). Vertical axis shows total device thickness.

stretchability [498] or the elastic modulus [286]. The property of device thickness alone is not sufficient to characterize or to compare the tactile performance of devices. For instance, a piece of PET plastic foil is certainly more transmissive to tactile cues than a metal plate of the same thickness. Rather than the device's thickness, it is its resistance to bending that limits how well a tactile cue (i.e. localized mechanical stress applied on its outer side) is transmitted through the device. Let us consider a localized force acting from outside on the device. The thicker the device and the higher the elastic modulus of its material, the lower is the maximum stress on the skin and the larger is the area of stress redistribution [471]. For a less rigid device made of a soft material, the localized force is transmitted as a similarly localized stress on the skin.

The resistance to bending is formalized in solid mechanics as flexural rigidity and has been previously used for calculating rigidity of thin films [257, 279]

$$FR = \frac{E * h^3}{12(1 - \nu^2)} \quad (1)$$

Flexural rigidity depends on the thickness of the device h , the material's constant Young's modulus E and its Poisson ratio ν . Despite the cubic influence of thickness, the effect of elastic modulus should not be underestimated, as the differences in elastic moduli of commonly used materials span more than four orders of magnitude. This implies that both the thickness and the material properties of a device are key parameters defining its effects on tactile acuity. We recommend reporting on these parameters for future work that contributes novel epidermal devices.

3.1.2 Classification of Prior Work

To provide an overview of the mechanical properties of state-of-the-art epidermal devices, we use the metric of flexural rigidity to systematically classify prior work from material science, mechanical engineering, nanotechnology, biomedical engineering, robotics, and HCI. While presenting a fully exhaustive list would be beyond the scope of this paper, we consider the most recent devices (last 7 years) from research groups that are pioneers in the field. This focus allows us to identify common levels of flexural rigidity achieved in prior work and helps us to compare advances in materials with the state-of-the-art in HCI. Figure 13 presents the classification of prior work following its approximate flexural rigidity. For orientation of the reader, we plot in addition the overall thickness of the respective devices.

An epidermal device typically consists of a multi-material sandwich. These materials often have largely different elastic moduli. Elastomers, for instance, which are frequently used as substrate materials, have low elastic moduli (e.g., PDMS: \sim 2-5 MPa), whereas metallic conductors have elastic moduli approximately four orders of magnitude higher (e.g., Copper: 130 GPa). Calculating the exact flexural



Figure 14: Overview of the three experiments. (a) Von-Frey monofilaments were applied to measure sensitivity, (b) tips of the digital calipers for Two-Point Orientation Discrimination Task, (c) Participants performed the roughness discrimination experiment by exploring two surfaces with different spacing between "dots" (the surface on the left is the baseline).

rigidity of an entire multi-layer epidermal device sandwich requires a complex experimental setup along with FEM (Finite Element Methods) analyses, which is beyond the scope of this work. Also, oftentimes, the prior research does not report on all the parameters required for calculating the flexural rigidity, which makes it even harder to calculate the exact levels of flexural rigidity.

For instance, DuoSkin [215] consists of a layer of tattoo decal substrate covered with a layer of gold leaf ($\sim 2 \mu\text{m}$, 79 GPa). This combination leads to flexural rigidity ranging from $\sim [1 \times 10^{-10} - 6 \times 10^{-8}] \text{Nm}$. Typically, the most rigid layer of the material sandwich has the strongest influence on the transmission of tactile stimuli. Hence, it is the upper end of the denoted range that is qualitatively capturing the behavior expected from a given device.

Figure 13 shows that the flexural rigidity of epidermal devices ranges between $[\sim 10^{-5} - 10^{-15}] \text{Nm}$. The majority of work, including all work from the HCI community, is situated in the area of $[\sim 10^{-5} - 10^{-9}] \text{Nm}$. Some pioneering work from materials science extends further to extremely soft devices of down to $\sim 10^{-15} \text{Nm}$. The total thickness of devices ranges from less than $1 \mu\text{m}$ up to $\sim 1000 \mu\text{m}$, while the vast majority of devices are $1 \mu\text{m} - 100 \mu\text{m}$ thick.

By clustering devices using their upper end of flexural rigidity (which has the strongest effect on tactile acuity), we identified three main clusters:

- **Flexible Devices ($[10^{-5}, 10^{-7}] \text{Nm}$):** Most of the current day epidermal devices in HCI and some work from material science fall into this category [185, 489, 492, 498]. These devices are made of elastomers of considerable thickness (e.g. $\sim 240-700 \mu\text{m}$ in [489, 492, 498]) or contain layers of metallic conductors that are relatively thick (e.g., $20-30 \mu\text{m}$ in [287, 341, 500, 510]).
- **Highly-Flexible Devices ($[10^{-7}, 10^{-9}] \text{Nm}$):** Devices in this region are highly flexible, conforming well even to smaller wrinkles on the skin. They are typically thinner than $5 \mu\text{m}$. The limitation of these devices comes from using functional materials of high moduli that are still fairly thick (e.g., DuoSkin [215] uses $\sim 2 \mu\text{m}$ thick gold-leaf) or their use of a substrate material with a high elastic modulus, e.g., [215, 500], which use a temporary tattoo

paper substrate with a high elastic modulus ($\sim 0.8 - 1\text{GPa}$) that can be a few microns thick.

- **Ultra-Flexible Devices ($\leq 10^{-9}\text{ Nm}$):** Devices in this category possess very low flexural rigidity levels and hence are very stretchable and flexible. Typically, these devices use polymers (e.g. PEDOT: PSS) or very thin metallic layers ($<1\mu\text{m}$) as functional materials [104, 205, 537]. It is interesting to note that though the devices reported by Webb et al. [497] have a high thickness ($\sim 50\mu\text{m}$), they have very low flexural rigidity. This is because they use low-elastic modulus substrate ($\sim 30\text{kPa}$), which is roughly 30 times less than the elastic modulus of a commercial temporary tattoo paper used in [215, 287, 500, 510]. The functional materials used in Webb et al. [497] are also elastomeric (Silicon nanomembranes), due to which the overall flexural rigidity is very low. This example proves that thickness should not be the only metric considered when evaluating the overall flexibility of an epidermal device. The material conditions for our experiments were informed from these clusters.

3.2 EXPERIMENT OVERVIEW

To investigate how epidermal devices affect a user's natural tactile perception abilities, we conducted a series of three psychophysical experiments. We designed the experiments to measure three specific aspects of tactile perception and to involve both active and passive tasks: (1) tactile sensitivity to a single stimulus (passive), (2) distance threshold (spatial acuity) between two stimuli (passive), and (3) tactile roughness discrimination capability (active). We compared the results from bare skin with skin-worn patches of different flexural rigidity to quantify the effects of the flexural rigidity of an epidermal device.

3.2.1 Rigidity Levels and Materials

We chose three conditions of flexural rigidity to be tested in our experiments based on the representative levels of flexural rigidity we identified in the classification of state-of-the-art epidermal devices shown in Figure 13. These conditions are: **High Rigidity** Material: $\sim 10^{-5}\text{ Nm}$, **Medium Rigidity** Material: $\sim 10^{-7}\text{ Nm}$, **Low Rigidity** Material: $\sim 10^{-9}\text{ Nm}$, and Baseline condition: **Bare Skin**.

3.2.1.1 Material Choice and Fabrication

To represent epidermal devices of those levels of flexural rigidity, we engineered passive patches of elastomers to exhibit the respective rigidity levels. As materials, we chose the most commonly used substrate materials for epidermal devices in the HCI and materials science communities. These materials are temporary tattoo decal paper (Silhouette Inkjet Printable Tattoo paper, Young's modulus of $\sim 1\text{GPa}$

and thickness of $\sim 2.5\mu\text{m}$) used for electronic rub-on tattoos in [104, 205, 215, 287, 449, 500, 510] and poly(dimethylsiloxane) (PDMS), which is a biocompatible, elastic material actively used for the design of epidermal devices [Nagels2018, 114, 185, 240, 487, 497, 498]. We intentionally opted for using passive patches rather than functional epidermal devices, as this allowed us to more carefully control the rigidity properties of the material.

Polymer films were manufactured by a doctor blade technique with an automatic film applicator (AFA-IV, MTI Corp, USA). For fabricating the MEDIUM RIGIDITY patch Sylgard 184 was used (2.7MPa, Dow Corning, USA), and OE-6550 (5.1MPa, Dow Corning) was used for the HIGH RIGIDITY patch. The silicone layer was deposited on polyethyleneterephthalat (PET) films and cured at 95°C for 1 hour.

Previous work in HCI [215, 287, 341, 498] used external adhesives such as mastic or temporary tattoo paper adhesive. Here, we chose to use commercially available soft-skin adhesive (MG7-1010, Dow Corning), a subclass of PDMS. It was deposited on top of the first layer and cured again for 1 hour at 95°C . The thickness of the patches was determined with an optical microscope (Olympus). The thickness values were $40 \pm 9\mu\text{m}$ for the MEDIUM RIGIDITY patch and $390 \pm 70\mu\text{m}$ for the HIGH RIGIDITY patch. The thickness values for the SSA layer were $144 \pm 27\mu\text{m}$ for the MEDIUM RIGIDITY patch and $177 \pm 58\mu\text{m}$ for the HIGH RIGIDITY patch.

3.2.1.2 Experimental Verification of Flexural Rigidity

The material characteristics of commercially available Temporary Tattoo Paper have been reported in previous literature [104, 306], giving a flexural rigidity of $\sim 1.7 \times 10^{-9}\text{Nm}$. In contrast, as the PDMS-based patches were custom-fabricated and composed of two different layers for this experiment, we analyzed their flexural rigidity, experimentally determined by measuring deflection under their weight. Samples with a constant width have been excised and placed at the edge of a microscope slide. The length L and deflection angle α of the films were determined from photographs, as shown in Figure 15. The entire thickness h for each individual sample has been analyzed with optical microscopy. The flexural rigidity was then calculated as:

$$FR = \frac{\rho * g * L^3 * h}{6(1 - \nu^2) \tan \alpha} \quad (2)$$

with density $\rho = 1000 \text{ kg m}^{-3}$ (Sylgard 184 = 936 kg m^{-3} ; OE6550 = 1109 kg m^{-3} ; MG7-1010 = 994 kg m^{-3}); ν (Poisson's ratio)=0.48; $g = 9.81 \text{ m s}^{-2}$. The experimental values obtained for the MEDIUM RIGIDITY and HIGH RIGIDITY version of the PDMS substrates, including the adhesive SSA layer, were $1.3 \pm 0.62 \times 10^{-7} \text{ Nm}$ and $1.2 \pm 0.5 \times 10^{-5} \text{ Nm}$ respectively.

3.2.2 *Body Locations*

For the Two-Point Orientation Discrimination and Tactile Sensitivity experiments we chose three locations: the tip of the index finger (*Fingertip*) (Figure 16 (a, b, c)), the dorsal side of the hand (*Hand*), and the volar side of the forearm (*Forearm*), as shown in Figure 16(d & e). The main reason for choosing three body locations was to understand how tactile perception with epidermal devices varies depending on the natural sensitivity and acuity of skin sites. The locations have varying levels of cutaneous receptors (fingertip > hand > forearm) [299], which allows us to study epidermal devices for varied inherent sensitivity levels of the human body.

We chose locations on the upper limb because this body part is commonly used in prior work on epidermal devices [53, 185, 235, 276, 341, 498, 500]. Apart from this, hand and forearm are very commonly used for various activities where unimpaired tactile perception is essential. As an input and output space, the hands and forearm have been considered as promising candidates in HCI. Researchers used the dorsal side of the hand and the forearm as an extended input space for smartwatches [517] and explored the potential of expressive input using skin deformation on the forearm [343, 500]. We expected that not only proprioception but also the cutaneous sensation generated when tapping at a certain position, drawing gestures on the skin, or squeezing skin would play an important role in the usability of epidermal interfaces. As an output space, hands and forearm have been considered as preferable target locations for wearable interfaces, as they have a relatively high sensory capacity and provide large and flat surfaces on which a display can be mounted [187, 369].

For the roughness discrimination task, we chose only one body location, the Fingertip, because this task is typically performed with the fingertip [245, 256]. We conducted the experiment on the fingertip of the dominant hand.

3.2.3 *Participants*

We recruited 16 participants (9 female, mean age: 27.4, SD: 3.1) from the local university. Participation was voluntary. Each participant received compensation of \$30 for completing the three experiments.

3.2.4 *Experiment Design*

All experiments were performed in a silent room with participants blind-folded (Figure 16 (f)). To eliminate any potential auditory cues, the participants were wearing noise-canceling headphones. The patch dimensions (4.5 x 4.5 cm) were kept constant for all materials. Responses for all the experiments were logged on a laptop computer.

We randomized the order of three experiments and the body locations across all participants. For experiments 1 and 2, which were administered on three different

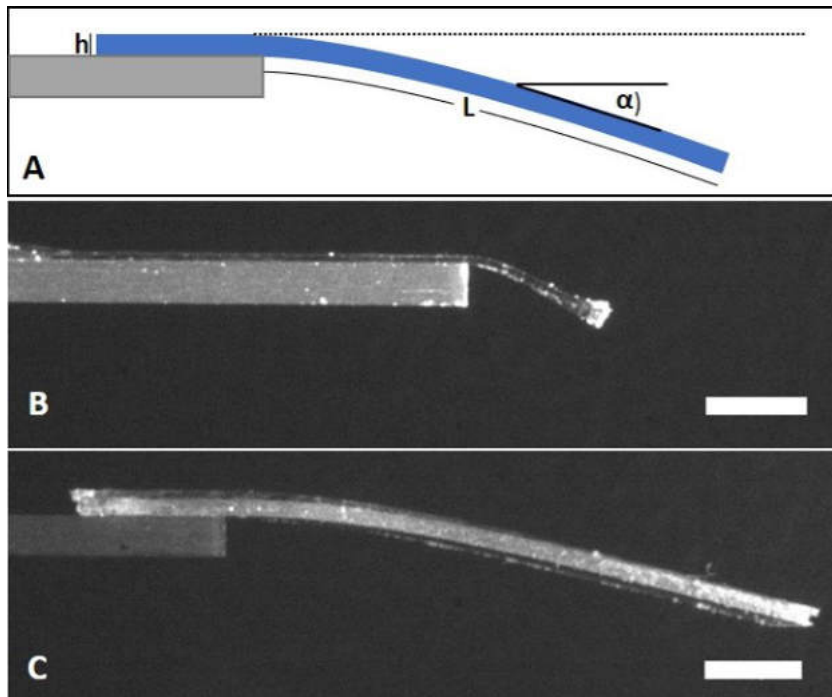


Figure 15: Experimental determination of the flexural rigidity of composite films: (A) Schematic representation of the experimental analysis of the flexible rigidity of composite PDMS films. L indicates the length of the film and h the thickness. (B) MEDIUM RIGIDITY and (C) HIGH RIGIDITY patches were investigated. The scale bar represents 2.5 mm. $N = 3$ independent manufactured films with a total of 9 samples for each condition were analyzed.

skin sites, the order of skin sites was randomized. There were a total of 4 (material) \times 3 (skin sites) = 12 conditions for experiments 1 and 2. For experiment 3, which was administered only on the *Fingertip*, there were a total of 4 (material) conditions. The series of three experiments took 3-3.5 hours in total (\sim 70-90 minutes each for experiments 1 and 2 and \sim 45-60 minutes for experiment 3). To avoid fatigue, the experiments were conducted in three independent sessions, on separate days. For all the experiments, the participants were free to take breaks in between. After every experiment, we conducted a semi-structured interview to gather qualitative feedback. The interviews were audio-recorded.

3.2.5 Analysis

To counter the inherent interpersonal variation of tactile perception abilities between participants, we established the BARE SKIN condition as the baseline. For each participant, we calculated the thresholds of all patch conditions on the same body site relative to this personal baseline. This resulted in a normalized measure for the relative increase of tactile thresholds generated by a material condition.

Since our data did not have a normal distribution, we performed the Aligned Ranked Transform from Wobbrock et al. [512]. For each experiment, the normal-

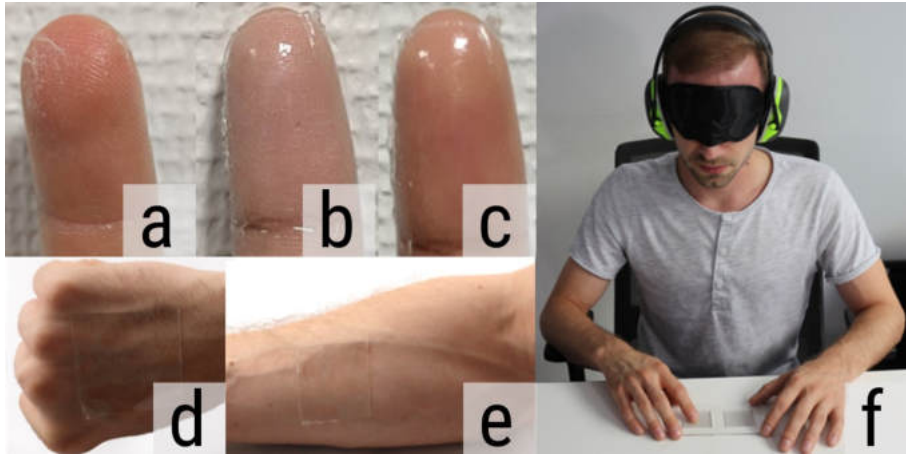


Figure 16: Three patch conditions with varying levels of flexural rigidity: (a) Patch with low rigidity level ($\sim 1.7 \times 10^{-9}$), (b) medium rigidity ($\sim 1.3 \times 10^{-7}$), (c) high rigidity ($\sim 1.7 \times 10^{-5}$). Patches were applied on (a) the *Fingertip*, (d) *Hand* and (e) *Forearm*. (f) Participant performing roughness-discrimination task.

ized data were first ranked and aligned by the ART tool [512] followed by a repeated-measures ANOVA, after which the Tukey HSD (Honestly Significant Difference) post-hoc test was run, with 95% confidence level. Mauchly's test showed no sphericity.

3.3 EXPERIMENT 1: TACTILE SENSITIVITY

Experiment 1 identified threshold force detection levels on three skin sites using patches with three different levels of flexural rigidity and bare skin as a baseline.

3.3.1 Apparatus

The tactile sensitivity measurements are used to get an estimate of how well we can perceive the minutest of the deformations that the human skin undergoes. Traditionally, this is done through Von-Frey filaments, which measure the sensitivity at given skin sites. This method is widely used in the research literature, is easily reproducible, and is a quick and easy way for measuring tactile sensitivity [3, 30].

To impart constant and known levels of forces we used the Von-Frey Filaments. Von Frey filaments rely on the principle that an elastic column, in compression, will buckle elastically at a specific force, dependent on the length, diameter, and modulus of the material. Once buckled, the force imparted by the column is fairly constant, irrespective of the degree of buckling [110]. These filaments were developed by Von-Frey in 1896 are still actively used for testing tactile sensitivity. The filaments may therefore be used to provide a range of forces on a given body site.



Figure 17: Von-Frey Filaments used in the Tactile Sensitivity experiment. Each of the filaments has a force profile starting with the lowest force of 0.008 grams to 4.0 grams.

Commercially available Von-Frey filaments² were used for delivering constant force stimuli [3, 30]. A total of eleven calibrated monofilaments was chosen for all locations: 0.008g, 0.02g, 0.04g, 0.07g, 0.16g, 0.4, 0.6g, 1g, 1.4 g, 2.0g, and 4.0g (1 gram force = 9.8 mN) (as shown in Figure 17).

3.3.2 Design and Procedure

We used the Method of Limit [30, 119, 204] with Yes/No paradigm. Each condition consisted of 4 series of trials with alternating ascending or descending forces. The starting series (ascending or descending) was chosen randomly. Since the participants are administered very low force levels, before each trial the experimenter gently tapped with a finger on the test location to indicate the start of the trial. This helped the participants to focus and accurately count the number of stimuli.

For each trial, a monofilament of the respective force value to be tested was pressed five times against the selected skin site, for approximately 1 s with a 1 s gap between presses. After administering five stimuli, the experimenter asked the participant how many presses she had felt. The force level was deemed to be detected if the participant reported having felt at least four of the five stimuli.

3.3.3 Results

The average Tactile Sensitivity thresholds for all skin locations and rigidity conditions are shown in Figure 18. The results from the Bare Skin condition on the fingertip are in-line with sensitivity thresholds reported in previous research ($0.06g \pm 0.09$) [44]. As expected, the thresholds increased with increasing rigidity of the patch, on all skin locations.

Figure 19 depicts the normalized tactile sensitivity for each patch condition. The results show that the average increase in intensity for all body locations was 34.76% for the LOW RIGIDITY PATCH, 97.6% for the MEDIUM RIGIDITY PATCH and

² <http://www.danmicglobal.com/semmesweinsteinmonofilament.aspx>

221.6% for the HIGH RIGIDITY PATCH. *Hand* showed the highest and lowest levels of increase (26.3% for the low rigidity patch and 392% for the high rigidity patch).

One-way repeated measures ANOVA showed a significant effect of FLEXURAL RIGIDITY on tactile sensitivity for all skin sites ($F_{3,60} = 26.31$, $p = 5.48 \times 10^{-11}$, $F_{3,60} = 18.85$, $p = 9.09 \times 10^{-9}$, $F_{3,60} = 13.9$, $p = 5.45 \times 10^{-7}$ for *Fingertip*, *Hand*, *Forearm* respectively). For the *Fingertip*, the Tukey HSD post-hoc test showed significant difference among all the patch pairs ($p < 0.012$) except for the BARE SKIN-LOW RIGIDITY pair ($p = 0.26$). For the *Hand* condition, the Tukey HSD post-hoc test showed significant difference between all patch pairs ($p < 0.006$) except for the BARE SKIN-LOW RIGIDITY and the MEDIUM RIGIDITY-LOW RIGIDITY pairs ($p = 0.36$ and $p = 0.28$ respectively). For the *Forearm* condition, the Tukey HSD post-hoc test showed significant difference between all patch pairs ($p < 0.032$) except for the MEDIUM RIGIDITY-LOW RIGIDITY and the MEDIUM RIGIDITY-HIGH RIGIDITY pairs ($p = 0.46$ and $p = 0.52$ respectively).

On the most sensitive skin site, the *Fingertip*, the LOW RIGIDITY patch showed an increase of 30.3% compared to BARE SKIN. The relative difference in thresholds between LOW RIGIDITY and MEDIUM RIGIDITY conditions was 87.3% while the difference between the MEDIUM RIGIDITY and HIGH RIGIDITY patches was 71.5%. It is worth noting that the relative difference between the LOW RIGIDITY and the MEDIUM RIGIDITY patch is always of the order to 50%, which is acceptable given that the MEDIUM RIGIDITY patch has a 100x higher flexural rigidity.

3.3.4 Discussion

Results from Experiment 1 show that epidermal devices of different rigidity considerably affect tactile sensitivity levels. While the LOW RIGIDITY tattoo patch had a comparably small effect on tactile thresholds, with less than 50% increase on all body locations, the most rigid patch showed increases of up to almost 400%. The results further show that the skin site is a major influencing factor. For example, on the *Fingertip*, it can be observed that there is significant difference between the LOW RIGIDITY and both MEDIUM and HIGH RIGIDITY patches. For the less sensitive regions, however, our results show a considerably lower relative increase in thresholds, which was statistically not significant. One of the key implications of this observation is that on less sensitive body locations, a more rigid and robust PDMS overlay can be used without overly compromising on tactile sensitivity. The range of tactile sensitivity between participants varied from 0.011 to 0.07g for the BARE SKIN condition. Compared to this, the maximum difference in intensity thresholds between the BARE SKIN and the LOW RIGIDITY conditions for all the participants was lower (0.02g).

It is very interesting to note that the intensity thresholds we have identified with our most rigid patch condition $\sim 0.12\text{g}$ ($SD=0.032$) are more than three times lower than values reported in prior work for surgical gloves $\sim 0.4\text{g}$ ($SD = 0.6$) [44]. Those gloves are used by surgeons for high-precision activities during surgeries.

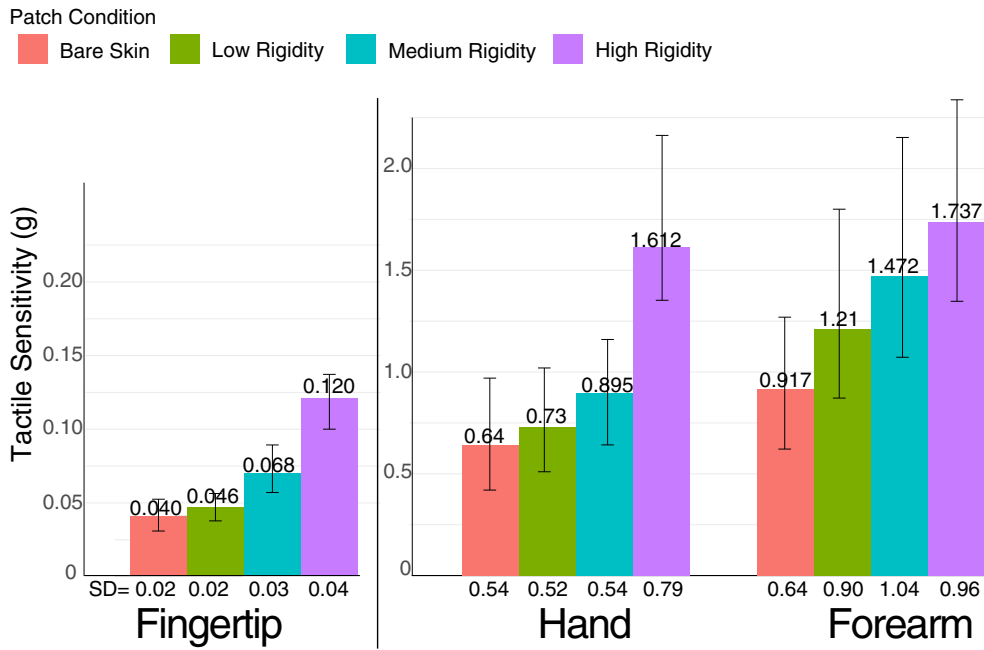


Figure 18: Tactile Sensitivity thresholds for all skin sites and all the patch conditions, with 95% confidence intervals. Lower thresholds mean higher sensitivity.

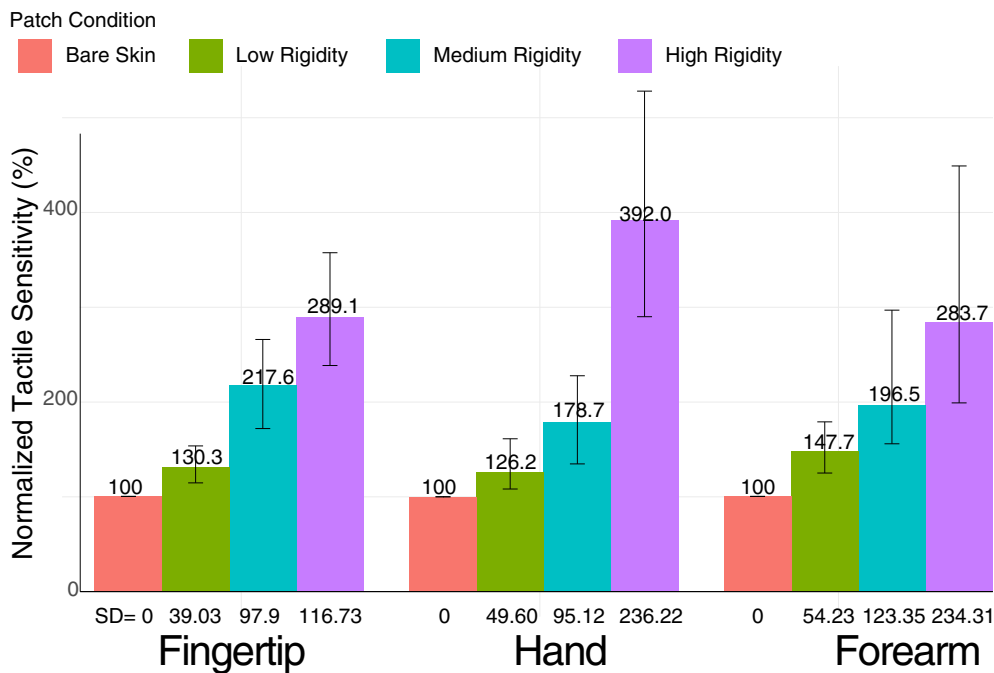


Figure 19: Normalized Tactile Sensitivity levels relative to the Bare Skin condition, with 95% confidence intervals. Lower thresholds mean higher sensitivity.

We conclude that epidermal devices with flexural rigidity levels corresponding to our most rigid patch condition retain a superb level of tactile sensitivity sufficient for high-precision manual activities.

Furthermore, these findings confirm our initial hypothesis that thickness alone is not a sufficient parameter for predicting an effect on tactile sensation, as the surgical gloves tested in [44] were considerably thinner ($\sim 260\mu\text{m}$) than our most rigid patch condition ($\sim 390\mu\text{m}$). This highlights the relevance of other material properties. The E modulus of natural rubber latex is [0.01-0.1] GPa, multiple times higher than our thickest sample. One additional factor contributing to the inferior behavior of gloves might also be that they enclose small air gaps, whereas our patches had skin-conformal skin contact.

3.4 EXPERIMENT 2: TWO-POINT ORIENTATION DISCRIMINATION

This experiment tested spatial acuity levels using a 2-point orientation discrimination [460] with a two-interval forced-choice (2IFC) paradigm on three skin sites using patches with three different levels of flexural rigidity and bare skin as a baseline.

3.4.1 Apparatus

We used a standard, commercially available two-point discriminator (Digital Vernier Calipers, Mitutoyo Corp). The tactile stimuli were the tips of the two-point discriminator. The width of each tip was 1 mm and the thickness was approximately 1 mm. The stimulus was manually applied by the experimenter [299, 460]. The spacing intervals were adopted from previous literature [460]. Based on pilot tests, we used 10 tip separations from 0 to 5mm (0, 0.5, 1.0, ...) for the *Fingertip*. For *Hand* and *Forearm*, we used 2.5 mm spacing intervals (0, 2.5mm, 5mm, 7.5mm .. 45mm). The upper limit was determined from literature [299, 460] and pilot tests.

3.4.2 Design and Procedure

We used the Method of Limits [204] to determine the thresholds. A total of four alternating ascending or descending series was administered. The starting series (ascending or descending) was chosen randomly. To reduce the cognitive load on the participants, the experimenter informed them of the location where the stimulus was to be applied so that the participant could concentrate on the stimuli being presented at the specified site.

3 <https://www.molnlycke.ca/SysSiteAssets/master-and-local-markets/documents/canada/biogel-surgeons.pdf>

For each trial, the stimuli were presented consecutively in randomized order, once with the two points oriented along the arm and once oriented perpendicular to the arm. The stimuli were applied for one second; the inter-stimuli interval between horizontal and vertical stimuli was 3 seconds. Then the participant was asked to report whether she had perceived the points that were oriented along the arm before or after the perpendicularly oriented points.

Before the actual experiment, there was a training phase wherein the experimenter provided stimuli multiple times against the three skin sites, allowing the participant to become familiar with the experiment and ensuring that the stimuli were non-nociceptive.

3.4.3 Results

The average two-point orientation discrimination thresholds for all skin locations and rigidity conditions are shown in Figure 20. The thresholds from the BARE SKIN condition are in-line with the literature [299, 460]. For the normalized thresholds (Figure 21), the average increase in spatial acuity thresholds for all body locations was 2.43% for the LOW RIGIDITY patch, 11.56% for the MEDIUM RIGIDITY patch and 21.36% for the HIGH RIGIDITY patch.

Fingertip (Figure 20 and Figure 21) showed the highest increase in the spatial acuity thresholds. The LOW RIGIDITY patch showed a relatively small increase of 6.7 %, while the most rigid patch showed the highest difference when compared to BARE SKIN (increase of 53.8 %).

The less sensitive skin sites, *Hand* and *Forearm* showed only small increases in thresholds. Even the most rigid patch (which is four orders of magnitude more rigid than the LOW RIGIDITY patch) showed only a 4.0% increase for *Hand* and 6.3% for the *Forearm* when compared to bare skin.

This is also evidenced by one of the comments from a participant: "It does not make a difference between the patches, as long the distance between the needles is the same." [P14].

One-way repeated measures ANOVA showed significant effect of FLEXURAL RIGIDITY on tactile acuity for *Fingertip* ($F_{3,58} = 5.649$, $p = 0.00187$). The Tukey HSD post-hoc test did not show any significant difference between all patch pairs ($p < 0.36$) except for the BARE SKIN-HIGH RIGIDITY pair ($p = 0.0008$). However, the difference was noticeable for BARE SKIN-MEDIUM RIGIDITY pair, yet not significant ($p = 0.081$). For *Hand* and *Forearm* one-way repeated measures ANOVA did not show any significant effect of FLEXURAL RIGIDITY on spatial acuity ($F_{3,56} = 1.25$, $p = 0.3$ and $F_{3,56} = 1.269$, $p = 0.294$ respectively).

3.4.4 Discussion

Our results show that the skin site is a key influencing factor for the effect of epidermal devices on spatial acuity. On the *Fingertip*, more rigid patches resulted

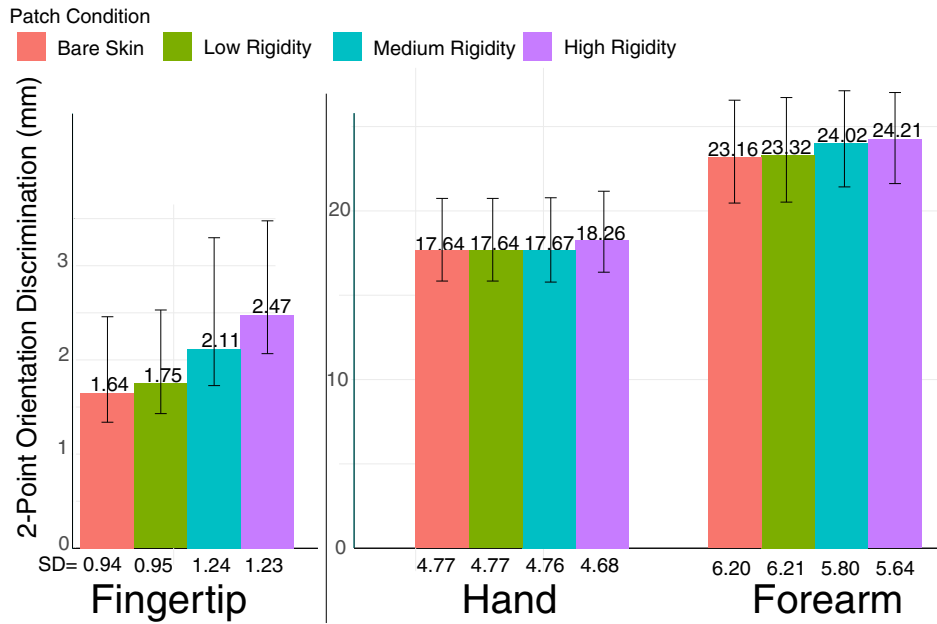


Figure 20: Two-Point Orientation Discrimination thresholds (in mm) for all skin sites and patch conditions, with 95% confidence intervals. Lower thresholds mean higher spatial acuity.

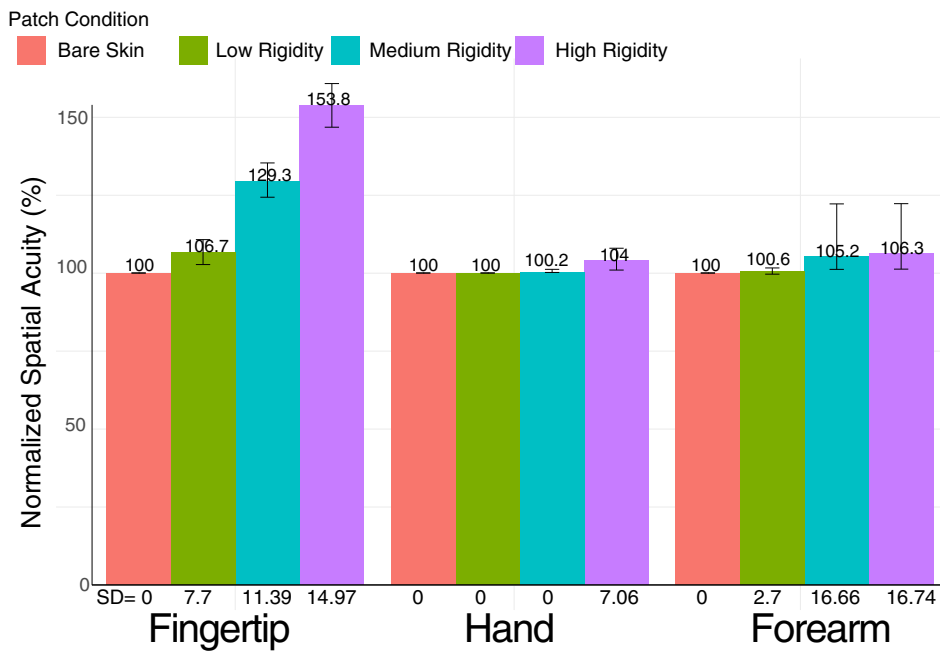


Figure 21: Normalized Two-Point Orientation Discrimination thresholds (in mm) for all skin sites and patch conditions, with 95% confidence intervals. Lower thresholds mean higher spatial acuity.

in a moderate increase of thresholds by up to 54%. This result is in line with the previous research, which showed a significant difference in tactile acuity on the fingertip for surgical gloves with $\sim 100\mu\text{m}$ thickness. On the less sensitive skin sites, however, the rigidity of the patch had only a very little effect. This is because, for tip distances as large as $\sim 20\text{ mm}$, patches with the rigidities considered here do not reduce the separation of the stress maxima transferred from the tips to the skin. For tip distances of $\sim 1.5\text{ mm}$, which are perceived as separated by bare skin, the more rigid patches blur the stress maxima such that only larger distances are perceived as separated. The spatial acuity thresholds varied from 1mm to 5mm among our participants. Considering this large interpersonal variation, the difference in the thresholds between BARE SKIN-LOW RIGIDITY condition are much smaller (avg=6.7%) with an increase of [0-16.7%].

Since our results for the fingertip showed a significant difference in spatial acuity between both the PDMS patches and bare skin, we recommended using LOW RIGIDITY devices on the fingertip if exquisite spatial discrimination abilities are desired. On less sensitive skin sites with spatial acuity thresholds similar to the *Hand* or below, a more rigid and mechanically robust patch of any of our rigidity levels can be used without generating any practically relevant decrease in spatial acuity.

3.5 EXPERIMENT 3: TACTILE DISCRIMINATION OF TEXTURED SURFACES

The purpose of Experiment 3 is to analyze how the human sensory information processing varies with different patch conditions for varying surface textures. This test is administered only on the fingertip since it has the largest concentration of cutaneous receptors and is typically used for active tactile perception tasks. We adopted this task from the classical roughness discrimination experiment [256].

3.5.1 Apparatus

Square surfaces of 4x4cm with grids of raised "dots" were fabricated using a 3D printer (Objet Connex 260). The baseline surface had a center-to-center spacing of dots of 1.0mm. The modified surfaces had increasing dot spacing in intervals of 5% up to 100%. These intervals are similar to those used in previous work [256] while extending to larger intervals to account for the effect of the patch conditions. The dots were 0.65mm high and the diameter was one-third of the spacing. This design of surfaces was based on previous work, which showed that spacing of dots plays a larger role than dot size in the roughness discrimination task [256, 262, 451]. An acrylic plate was laser cut to form a frame for holding both the surfaces, as shown in Figure 14 (c).

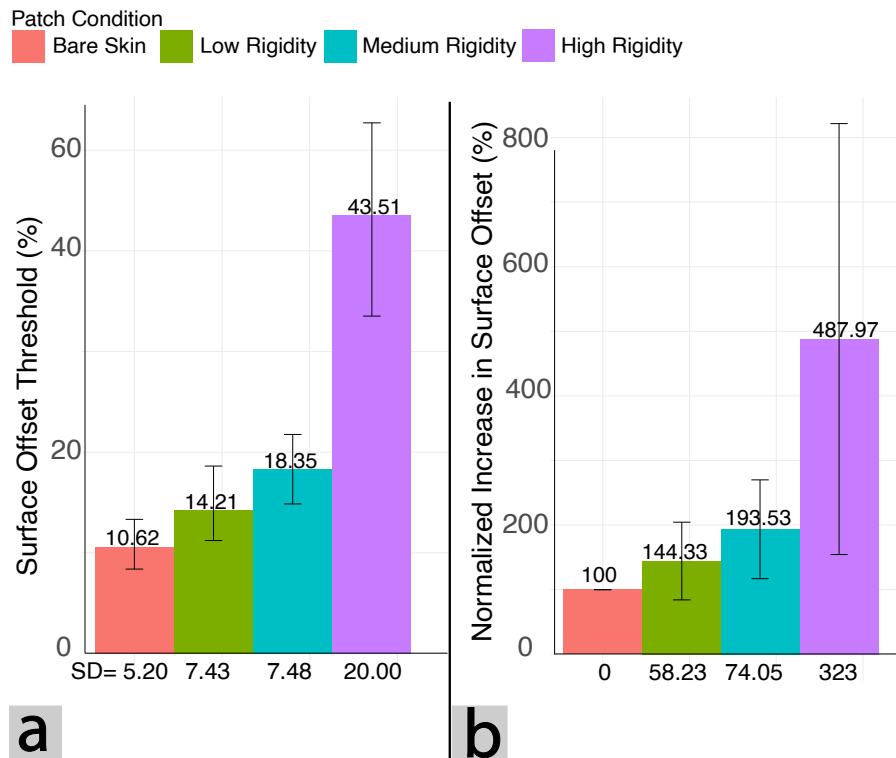


Figure 22: (a) Absolute Surface Offset Thresholds of tactile roughness discrimination task for all patch conditions, with 95% confidence intervals. (b) Normalized Tactile Roughness Discrimination levels relative to the Bare Skin condition, with 95% confidence intervals. Lower thresholds mean higher capability to discriminate surfaces.

3.5.2 Design and Procedure

The patches were administered on the *Fingertip* of the dominant hand. We used the method of limits [204] to determine the surface offset threshold. Each patch condition had a total of 4 sets (2 ascending and 2 descending) of trials with alternating ascending or descending forces. The starting series was randomly chosen.

For each trial, a two-alternative discrimination paradigm was used. Surfaces were presented in pairs (one of the baseline) and the participants were asked to respond whether the surfaces were similar or different after consecutively feeling the two surfaces with the fingertip of the dominant hand. Participants were free to explore the surfaces in any pattern (horizontal, vertical, diagonal, random, etc.) of their choice. There was no time limit for performing each trial.

Since the patches might tear or rip off the skin, visual inspection of the patch was carried out before each trial. If a patch was damaged, a photo of the torn patch was captured (Fig.23), a new patch was applied and the trial was repeated.

3.5.3 Results

The average surface offset threshold that the participants could discriminate relative to the baseline surface is shown in Figure 22 a. As expected, the threshold increased with the increasing rigidity of the patch. The relative increase compared to the bare skin performance, normalized per participant, is shown in Figure 22 b. The results revealed a 44.3% increase in the surface offset threshold for the LOW RIGIDITY device and 93.5% increase for the MEDIUM RIGIDITY patch. The HIGH RIGIDITY performed the worst with an average increase of 487.7%. This is the highest relative increase found in all our experiments.

One-Way repeated measures ANOVA ($F_{3,60} = 36.69$, $p = 1.35 \times 10^{-13}$) revealed significant difference between the patch conditions. The Tukey HSD post-hoc test showed significant differences between all patch-pairs ($p < 0.01$) except the LOW-RIGIDITY AND MEDIUM-RIGIDITY pair.

3.5.4 Discussion

One of the key material properties of epidermal devices required for the tactile roughness discrimination task is high tactile transfer capability, i.e, the capability of the material to transmit the underlying tactile roughness information to the cutaneous receptors. This is specifically more important for the roughness discrimination task since there is high-frequency tactile information resulting from lateral exploration of the surface that needs to be transmitted to the cutaneous receptors. For devices with high flexural rigidity, the area of stress distribution is larger [22]. Hence the detailed information of the surface is not transmitted accurately to the underlying receptors.

Results from the roughness discrimination task indicate that there is a significant reduction in the tactile roughness perception with both the PDMS patches, while the LOW-RIGIDITY patch condition only showed a moderate effect. Particularly the most rigid patch showed a very strong increase with an almost five times higher offset than bare skin. This suggests that the flexible patch is not an appropriate choice for performing activities that require high-resolution exploration of surfaces. As the difference between the LOW RIGIDITY patch and MEDIUM RIGIDITY patch is not very large, the latter is a good trade-off between active tactile perception and mechanical robustness.

3.6 OVERALL DISCUSSION AND DESIGN IMPLICATIONS

3.6.1 Effect of Epidermal Devices on Tactile Perception

The results of all three experiments have shown that the rigidity of epidermal devices has a significant effect on human tactile perception abilities. It is hence a critical factor that needs to be considered in the design of epidermal devices.



Figure 23: (a) Patches of the Low RIGIDITY condition were damaged during the surface discrimination task for 10 participants. (b) 4 patches of the Medium Rigidity condition were damaged.

As expected, tactile perception abilities decrease with increasing rigidity of the epidermal device. The most flexible patch condition resulted in comparably small effects on tactile sensitivity, tactile acuity, and surface roughness perception on all skin sites, with a relative increase of thresholds ranging between 6.7–47.7 %. In contrast, our most rigid device condition resulted in considerably larger increases of up to almost four times for intensity thresholds and almost five times for roughness discrimination offsets. In consequence, we can recommend *ultra-flexible* devices for all tactile tasks and all body locations if tactile perception abilities are key.

The results further revealed that skin location is a major influencing factor. On the highly sensitive fingertip, the LOW RIGIDITY patch performed significantly better for tactile intensity perception than the more rigid patches. In contrast, on the less sensitive *Hand* and *Forearm*, we identified a less pronounced effect. On these skin sites, a more rigid device can be chosen, offering a good trade-off between tactile perception and mechanical robustness. This contrast is even more pronounced for spatial acuity, where we did not identify any practically relevant difference between our device conditions on the hand and forearm. This implies that a device of any rigidity level amongst the ones tested in our experiment can be used in situations where spatial discrimination abilities are required on less sensitive skin sites, while tactile intensity is less relevant. For instance, this finding can be relevant for tactile output devices that spatially encode information, for instance using a matrix of taxels.

For active tactile perception, more rigid devices should be avoided if possible, as they considerably increase perception thresholds. However, *highly flexible* devices perform almost as well as *ultra-flexible* ones, presenting an attractive trade-off between roughness discrimination and mechanical robustness.

It is worth highlighting that our most rigid device condition yields considerably better results for tactile sensitivity and tactile acuity than thin surgical gloves studied in related work [44]. This finding suggests that despite the considerable increase in thresholds identified in our experiment, devices of this rigidity might still retain superb performance for high-precision manual tasks, such as surgeries.

3.6.2 *Mechanical Robustness of Materials*

One of the key observations we made during the roughness discrimination task was that the mechanical robustness of the patch varied considerably based on its rigidity. The lateral movements required for the active roughness discrimination task caused mechanical damage to the patches. The damage was more pronounced for the LOW-RIGIDITY patch. The tattoo patch ripped off for 10 participants (once for 8 users and 4 times for 2 users). Figure 23 shows the structural damage before the patch was replaced. It can be seen that the level of damage varied from small cracks to complete damage of the patch. In contrast, the MEDIUM RIGIDITY patch, which had higher flexural rigidity compared to the *Low Rigidity* patch, showed considerably higher durability, ripping off for 4 participants. Our most rigid patch was the most mechanically durable and was not damaged for any participant.

3.6.3 *Re-Usability and Adhesion*

The flexural rigidity of the device also determines its re-usability. In our case, the overlay with the highest rigidity was the most re-usable. In contrast, the LOW RIGIDITY tattoo material is usually a single-use device. Once applied on the skin, it is very hard to remove from the skin without damaging the patch. Moreover, in some cases removing the tattoo material caused participants discomfort when it was applied on a non-glabrous area on the forearm or hand.

Qualitative observations from our experiments further highlight the relevance of the adhesive. We found that adhesive properties of the epidermal devices are important criteria for re-usability. In general, silicones are a versatile class of polymeric materials exhibiting low surface energy, high flexibility of the silicone network and high permeability to water vapor [454, 455]. SSAs differ from analogous silicone elastomers by the absence of reinforcing silica filler and the exhibition of a minimal viscous component [455]. After the application of deformation pressure, only minimal energy dissipation occurs, resulting in a rapid debonding process [455]. In conjunction, these properties allow a sensitive, less traumatic removal of skin adhesives, which is particularly important for the attachment to the sensitive skin of neonates or the skin of elderly people [217, 260]. Hence, it was very easy for the participant to remove the patch without discomfort even on skin sites with body hair and without any visible residues. Designers should take these aspects into account while realizing epidermal devices. For example, for long-term physiological monitoring that might require expensive and re-usable sensors to be placed on the body, a device with higher flexural rigidity can be developed. However, for an inexpensive device such as touch sensors [215, 287, 500], which can be easily fabricated with off-the-shelf materials, the flexural rigidity can be very low and the device dispensable.

3.7 LIMITATIONS

Flexural Rigidity Classification: Our classification of epidermal devices from prior work indicates ranges of flexural rigidity rather than absolute points. Calculating the latter would require FEM-based modeling of the material sandwich of a device including the exact coverage of functional material for each layer, which is rarely reported. We take a conservative approach by assuming that the entire layer is covered by the functional material. The effective flexural rigidity is hence within the limits of the range indicated in our classification.

Rigidity Levels: We tested three levels of flexural rigidity representative of today's devices. As materials and fabrication techniques have matured, we believe it is safe to expect that these levels will also be appropriate representatives for devices we may see in the future. Moreover, even if future devices were to reach considerably lower levels of flexural rigidity, our results provide some close indication of their performance, which would be situated between our baseline and low rigidity conditions.

Cutaneous Stimuli: Our experiments investigated the types of tactile stimuli most commonly chosen in psychophysical studies. Future work should investigate the effect of epidermal devices on other cutaneous modalities, such as vibrotactile or thermal cues.

Participants and Body Location: We have conducted our experiments with healthy adults in their twenties. It remains to be studied how epidermal devices affect the tactile perception abilities of people with lower sensitivity, such as the elderly. Our findings are limited to locations on the upper limb. Future work should address additional skin sites.

Analytical Model: We have not developed a generalized model of how flexural rigidity affects human thresholds of perception. While our work provides the first empirical results that can be used in future work to inform or validate an analytical model, deriving such a model is beyond the scope of this paper. Modeling the flexural rigidity of layered patches with no-slip conditions at the interfaces requires finite-element numerical modeling [471]. Simplified analytical models would then have to be parameterized based on numerical results.

Flexural Rigidity vs Thickness: In our experiments, we modified thickness and elastic modulus to fabricate patches of varying rigidity levels. However, it would also be interesting to explore the independent variation of flexural rigidity at a constant thickness. For this, the elastic modulus needs to be scaled drastically and would require the fabrication of multi-layer patches, which in turn risks affecting other properties (e.g. adhesion, friction coefficient) of the samples.

Duplex Model for Tactile Perception: The perception of textures is duplex in nature, influenced by two components of stimulation: vibrational and spatial stimuli [172]. For discriminating very fine surfaces (particle sizes $< \sim 20\mu\text{m}$) with a lateral exploration of the surface, vibrational cues resulting from the friction of the surface play a vital role. The surfaces used in our experiments had larger particle

sizes ($\sim 300\mu\text{m}$ in radius); hence the experiments focused on the spatial cues, with vibrational cues having a lesser impact. Future experiments should test the vibrational component of texture perception, as done for instance by Fagiani et al. [102].

3.8 CONCLUSION

This chapter contributes the results from the first set of psychophysical experiments conducted on epidermal devices. As mentioned in chapter 1, gaining an understanding of epidermal devices guides the design of next-generation epidermal devices thereby pushing the boundaries of Epidermal Computing. The trade-off between superior tactile performance and mechanical robustness is very crucial for a number of applications and this chapter studies these aspects in detail.

Firstly, this chapter proposes the use of Flexural Rigidity as the metric characterizing the tactile performance of epidermal devices. Then the first classification of epidermal devices is presented based on their thickness and flexural rigidity. Based on this classification, three patches were fabricated with different rigidity levels: LOW RIGIDITY, MEDIUM RIGIDITY and HIGH RIGIDITY each representing the class of devices derived in the classification system. Through these patches, three psychophysical experiments were conducted to study the effect of flexural rigidity level on passive and active tactile perception.

Results from our experiments show a significant effect of device rigidity on tactile sensitivity and roughness-discrimination abilities; more rigid devices increased the tactile sensitivity thresholds by up to 390% and roughness-discrimination thresholds by up to 490% compared with bare skin. Device rigidity had a considerably less strong effect on spatial acuity. On the sensitive fingertip, spatial discrimination thresholds moderately increased by up to 50%, whereas the thresholds remained fairly unchanged on less sensitive body locations. Our results offer the opportunity for an informed choice of device materials when a compromise between tactile performance and mechanical durability is to be found.

Future work should investigate how epidermal devices affect other natural functions of skin (e.g. body movement, thermal management) and their effect on other cutaneous stimuli. It will also be important to study the usability and durability of epidermal devices during long-term user deployments.

Part II

Part Two - Epidermal Devices for Rich On-Body Interaction

FABRICATION OF SKIN-CONFORMAL ELECTRONICS FOR EXPRESSIVE INTERACTION

Prior research in HCI has contributed *Epidermal Devices* that augment the human skin with input and output capabilities. However, one key limitation of these devices is that they assume the interactive elements to be rather large and only slightly curved.

However, the human body has several locations that are non-planar and vary in size curvature and elastic properties. These locations open up unique possibilities for interaction due to their inherent tactile and visual properties. For example, protruding bony regions such as knuckles provide physical affordances for touching and circling them. Prior work in HCI has also explored the use of such unique body features for interaction. Gustafson et al. [138, 139] propose using the segments of fingers as distinct input buttons. There is very limited work that has explored the use of unique body features for interaction. This is due to the technical challenges and the lack of enabling technology that makes interaction on such challenging body locations possible.

On-Skin devices that need to conform to complex and challenging body locations should have high levels of stretchability and flexibility. The fabrication processes needed for realizing these devices should support customization in terms of shape and size. This enables the devices to be deployed on a wide variety of challenging body locations such as knuckles or other bony regions, flexure lines, birthmarks, elastic regions such as hypothenar eminence near the palm. Additionally, these devices can be integrated into body-worn accessories such as rings.

This chapter presents *SkinMarks*, an enabling technology for interaction on challenging body locations. *SkinMarks* are highly conformal interactive tattoos, which enable precisely localized input and output on the body.

*SkinMarks*¹ are inspired by recent research on slim, skin-worn sensors and displays [215, 287, 498]. We extend beyond prior work by contributing highly

¹ This chapter is based on publication at ACM CHI'17 [500]. This work was done along with my colleague Dr. Martin Weigel. Dr. Martin Weigel contributed to the classification of the body landmarks, fabrication of the *SkinMarks* prototypes, interaction techniques, and design of the empirical experiments. I assisted Dr. Martin Weigel in performing the literature survey to classify body landmarks, contributed to the fabrication of *SkinMarks* prototypes, implemented the application examples, and performed the technical experiments. Dr. Alex Olwal contributed to the classification of body landmarks, design of interaction techniques and evaluation methods, helped in framing the paper, and provided critical inputs that helped improve the paper. My advisor Jürgen Steimle advised on the conceptual design, fabrication, design of interaction techniques. He further contributed to the framing and writing of the publication. Chaithin Anil Kumar assisted in setting up the screen printing pipeline and in running fabrication experiments.

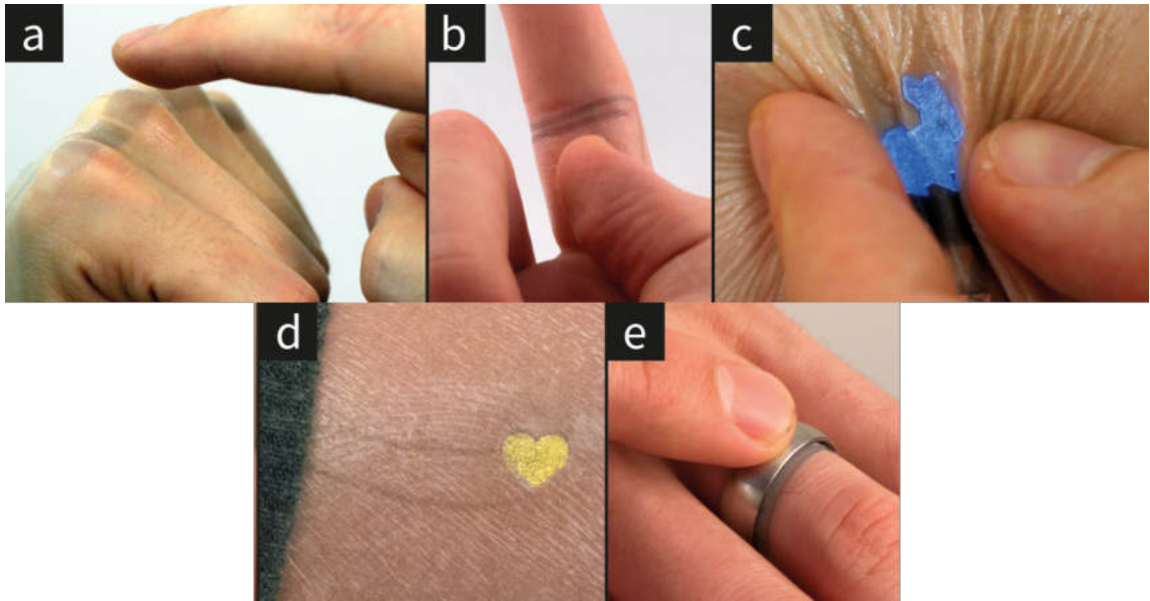


Figure 24: *SkinMarks* are conformal on-skin sensors and displays. They enable interaction on complex and challenging body locations: (a) bony regions with high curvature, (b) skin microstructures that are fine and narrow, (c) elastic locations, (d) visual elements on the skin such as birthmarks, and (e) body-worn accessories.

conformal skin electronics with co-located input and output, which are compatible with strongly curved, elastic, and tiny body locations. These make it possible to use the plethora of tactile and visual cues on the body for direct, eyes-free, and expressive interaction.

This chapter makes the following contributions:

1. We introduce *SkinMarks*, novel skin-worn I/O devices with co-located input and output, which are enabled through highly conformal and precisely localized skin electronics.
2. We describe the implementation of *SkinMarks* based on temporary rub-on tattoos. It allows for custom-shaped, slim, and stretchable devices that conform to challenging body locations.
3. We demonstrate interaction techniques on body landmarks that leverage *SkinMarks'* unique touch, squeeze and bend sensing with integrated visual output.
4. We present results from technical evaluations and user studies that validate conformity ($4\ \mu\text{m}$ to $46\ \mu\text{m}$ thin), precise localization, and touch input on sub-millimeter electrodes.

4.1 FABRICATION OF SKINMARKS

In this section we present our implementation of *SkinMarks* based on temporary rub-on tattoos. We start by providing an overview of our fabrication approach. Then we detail our technical contributions to make *SkinMarks* conformal on challenging geometries. Finally, we describe the implementation of precisely localized, co-located input and output surfaces for sensing of touch, bend and squeeze input and for visual display.

4.1.1 *Multi-layer Functional Inks on Tattoo Paper*

The human body possesses a large variety of locations with varying physical properties such as size, curvature, and elasticity. To support these locations, we base our implementation of *SkinMarks* on screen-printed electronics. We chose this fabrication technique since it is a flexible method to create small volumes of thin-film sensors and displays that feature a custom shape and a high print resolution [347].

To fabricate an interactive tattoo, we use commercially available temporary tattoo paper (Tattoo Decal Paper) as the substrate, as proposed in recent work [215, 287]. We screenprint one or multiple layers of functional inks onto it. After printing each layer, the ink is heat cured with a heat gun (130° Celsius, 3 minutes). After adding a thin adhesive layer, the tattoo is ready to be transferred onto the skin.

SkinMarks are powered and controlled using an Arduino microcontroller. We recommend placing the microcontroller at a body location that offers enough space and undergoes little mechanical strain, for instance, the wrist. For connecting the tattoo with this location, we extend the tattoo by printed conductive traces that each end with a printed connector surface close to the microcontroller. We solder a conventional wire onto copper tape and adhere the tape to the isolation layer, under the printed connector.

4.1.2 *Conformal Interactive Tattoos: Slim and Stretchable*

To ensure that an interactive tattoo is conformal on challenging landmark geometries and robust to stretching, we set out to minimize the thickness of printed functional layers (as suggested in [196]) and to use intrinsically stretchable materials. Layer thickness is mainly influenced by two factors: screen density and ink viscosity. We minimized the layer thickness by printing with a dense screen (140TT). We further reduced the thickness of conductive structures by printing a conducting polymer (PEDOT: PSS translucent conductor, Gwent C2100629D1, 500-700 /sq). Compared to silver ink, which was used in prior work [287], the ink is less viscous and results in considerably thinner layers. The thickness of a screen-printed layer of PEDOT: PSS conductor is approximately 1 μm , a magni-

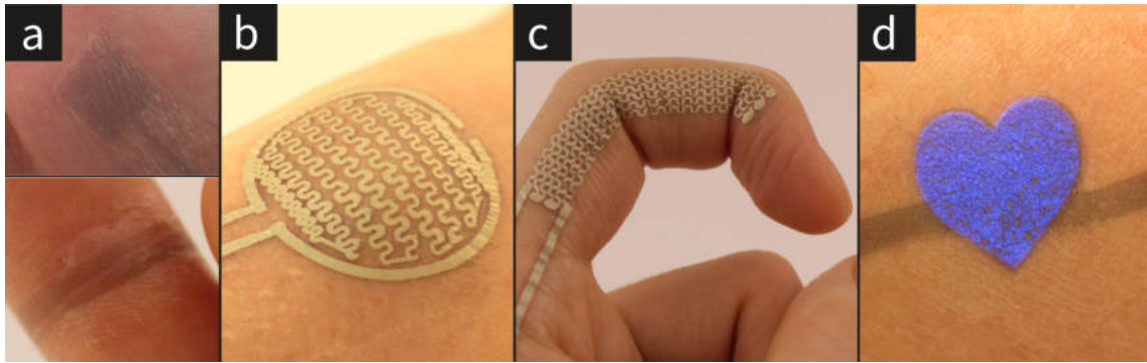


Figure 25: *SkinMarks* supports: (a) capacitive touch buttons and sliders, (b) squeeze sensors, (c) bend sensors, and (d) electroluminescent displays.

tude slimmer than screen-printed silver in prior work ($\sim 16 \mu\text{m}$ [287]). A tattoo with a touch sensor measures approximately $4 \mu\text{m}$. A tattoo with visual output measures $31 \mu\text{m}$ to $46 \mu\text{m}$, including the tattoo paper. This allows us to introduce temporary tattoos for tactile user input and visual output on highly challenging locations, such as the knuckles.

PEDOT: PSS conducting polymer has an additional important advantage over conductors made of metal, such as silver ink [287] or gold leaf [215]: it is intrinsically stretchable [280]. This does not only make the conductor conform better to challenging geometries; it also makes it considerably more robust to mechanical strain [280]. To further improve the robustness, we recommend laying out conductors in a horse-shoe pattern [170] in locations that are subject to extensive strain (e.g., knuckles, webbing, or wrist) or route traces around such areas, if possible. Based on these principles, we show conformal touch, bend and squeeze sensors and conformal EL displays that allow for interaction on body landmarks (see Figure 25).

4.1.3 Touch Sensing

Touch has been identified as an important input modality for on-skin electronics [215, 287, 498]. Solutions from prior work used fingertip-sized electrodes [215, 287, 498]. However, these large electrode sizes are not compatible with all the body locations. For instance, to support precisely localized interaction on flexure lines of the finger which provide natural tactile cues, smaller electrode sizes are required.

We use capacitive loading mode sensing (single capacitance) to measure touch contact and sliding (Figure 25(a)). The touch-sensitive electrodes are printed with one conductive layer of PEDOT: PSS and are connected to a commercial capacitive touch controller (Adafruit MPR121). Each tattoo can contain one or multiple custom-shaped electrodes, which can be printed close to each other. They support

interpolation and allow for slider sensor designs [79]. Our evaluation of touch sensors shows that *SkinMarks* allows for electrodes with a width of 0.25 mm and hence supports small landmarks. This is by an order of magnitude smaller than prior on-skin touch sensors [215, 287, 498].

4.1.4 Squeeze and Bend Sensing

Skin allows for deformation input as a further modality for tactile on-body interactions, as recommended in [499]. Deformation interaction can be used on various landmarks but is especially interesting for elastic landmarks to leverage their intrinsic deformability. We present an embedded sensor for capturing squeeze input on the skin, based on a printed strain gauge. Squeezing deforms the skin and results in compressive strain on the strain gauge. We found that the intrinsic stretchability of PEDOT: PSS prevents the strain gauge from giving precise readings. Therefore, we use silver ink (Flexible Silver Ink, Gwent C2131014D3). However, our initial tests showed that the brittle silver tends to break easily. To increase the robustness for high-stress areas on the body, we cover the silver pattern with a second layer of PEDOT: PSS containing the same pattern. This allows the strain gauge to remain functional, even when the silver connection breaks at a few locations because the second layer bridges the breaks. We implemented two squeeze sensor designs. They have a trace width of 0.75 mm. The larger one, designed for the forearm, has a dimension of 60×21 mm with 13 parallel lines laid out in a horseshoe pattern. The smaller one (Figure 25(b)) was designed for the head of the ulna, is dimensioned 21×21 mm, and features 9 parallel lines.

We evaluated the robustness of squeeze input by measuring the signal to noise ratio [79]. For a sample with a dimension of 60×21 mm, we calculated the average SNR of six squeeze sensors. They were deployed on six locations on the upper limb of five participants, chosen to cover a wide range of skinfolds (2–23mm; measured with an EagleFit Slim Guide Caliper). Each sensor was squeezed 20 times. The squeeze sensors achieved an average SNR of 17.0 (SD=7.97).

Furthermore, *SkinMarks* supports bend sensing, similar to prior work [287]. We use this principle to detect dynamic pose changes of skeletal locations of the body to allow for dynamic interface elements. The bend sensor on the finger measures 72×8 mm and features 6 parallel lines with the horseshoe pattern. Again, the additional layer of PEDOT: PSS prevents the strain gauge from breaking in case of tiny cracks in the silver layer. We show this principle on the finger (see Figure 25(c)).

4.1.5 Conformal Touch-sensitive Displays

We contribute tattoo-embedded active displays to allow for custom-shaped, co-located input and visual output on *SkinMarks*. Our displays have a faster response time than thermochromic displays [215] and are considerably slimmer than prior

body-worn LEDs [287] and EL displays [503]. They are thin and robust enough to conform to challenging body locations, such as knuckles or the flexure lines of the palm. The overall thickness of the display is between 31 μm to 46 μm . It is deformable and captures touch input (see Figure 1c, 25d, and 4).

We base our implementation on electroluminescent (EL) displays, which feature high update rates and energy efficiency. The implementation follows the basic principle introduced by PrintScreen [347]. In contrast, our displays use two electrodes made of a PEDOT-based translucent conductor. As discussed earlier, this allows for thinner and more robust layers. Between the electrodes is one layer of phosphor paste that determines the color of the display. We further reduce the thickness of the display by replacing the dielectric paste used in prior work with a transparent resin binder (Gwent R2070613P2). The resin binder is used as a dielectric and allows for printing thinner layers. Furthermore, it is completely transparent to avoid visible margins, as presented in prior work [347]. The EL display is driven with a Rogers D355B Electroluminescent Lamp Driver IC (145 V; max. 1 mA). It allows for integrated touch sensing by time-multiplexing a display cycle and a capacitive sensing cycle, as introduced in previous work [347].

4.2 EXPRESSIVE ON-BODY INTERACTION WITH SKINMARKS

SkinMarks enable new forms of on-body interaction. We present novel interaction techniques for five different types of body locations that exhibit unique tactile and visual properties.

4.2.1 Leveraging Tactile Cues on Bony Regions

The inherent skeletal structure of our body creates distinct locations on the body which have a high degree of curvature. Examples of such locations include knuckles, elbow, radius bone, etc. These locations create distinct tactile and visual cues which can be leveraged for expressive on-body interaction. For one, cues can help the user to memorize mappings; for instance, the user can associate an input element with a specific knuckle. Second, cues can also help localize the input element while looking at it or feeling the geometry through the touching finger. In addition, different geometries afford different interactions. Last but not least, unique geometries can also be formed by a group of multiple adjacent bony regions, such as the four knuckles of a hand.

We demonstrate these benefits for on-body interaction by deploying a touch-sensitive *SkinMark* sensor on the knuckles (Figure 26). *SkinMarks* allow for input on the knuckles (knuckle peaks) and around the knuckles (knuckle valleys), both areas with high curvature. These can be used to distinguish multiple different input elements that are associated with either a valley or a peak. We demonstrate that the knuckles can be used as discreet touch elements (fist) or as a slider that provides small tactile ticks (flat hand).

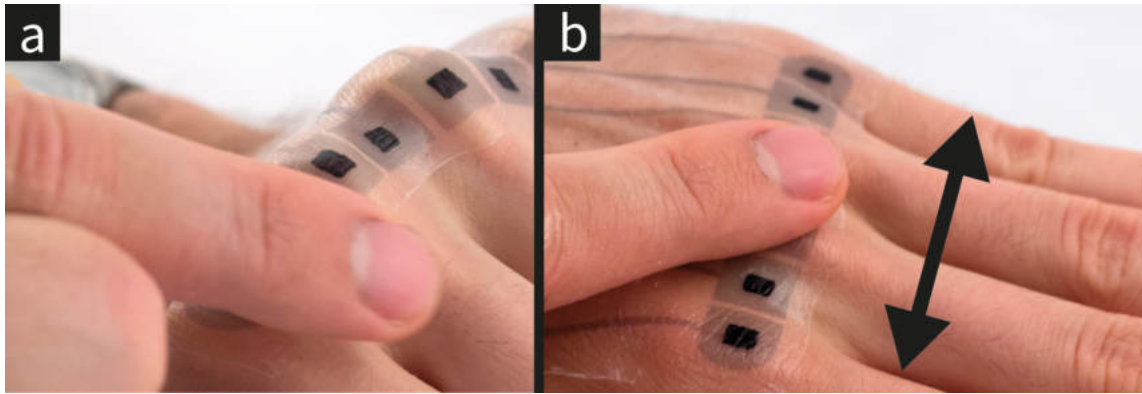


Figure 26: Interaction on challenging, highly curved skeletal landmarks: (a) tapping the peaks and valleys for discrete input; (b) sliding along the knuckles for continuous input.

4.2.1.1 *Dynamic Interface Elements Using Pose-Based Input*

Body movement allows for dynamic interface elements using pose-based input on skeletal body landmarks. The ability to change the pose on demand enables various novel interactions. For instance, when the user is making a fist the knuckles have a high curvature, clearly exposing the knuckle peaks. This allows for precisely locating discrete touch buttons. In contrast, while doing a flat hand, the knuckles form a relatively flat surface, which allows for continuous sliding (see Figure 26).

SkinMarks can capture the current body pose and change the interface dynamically. To illustrate this, we implemented a music player control, which is worn on the side of the index finger (Figure 27). It contains a printed bend sensor overlaid with touch-sensitive display elements. Those elements change their functionality based on the pose of the finger. When the index finger is straight, it affords continuous and linear movement along with the finger (Figure 27 (a)). It then acts as a volume slider. When it is bent, the flexure lines at the joints become more prominent; they visually and tactually split the input area into three distinct areas (Figure 27 (b)).

These afford discrete touch input. Therefore, when bent, the interface switches to three discrete buttons for play/pause, next song, and previous song. The integrated displays show which mode is active, either by illuminating the buttons or the slider. Switching between these modes is fast, easy, and discreet to perform.

4.2.2 *Precise Touch Input on Skin Microstructures*

To accommodate for joint movement the dermis layer of human skin has folds. These manifest as flexure lines on the surface of the skin and are present at various locations on the body such as fingers, toes, palms. These skin microstructures provide unique tactile cues for interaction. Our temporary tattoos allow for precise

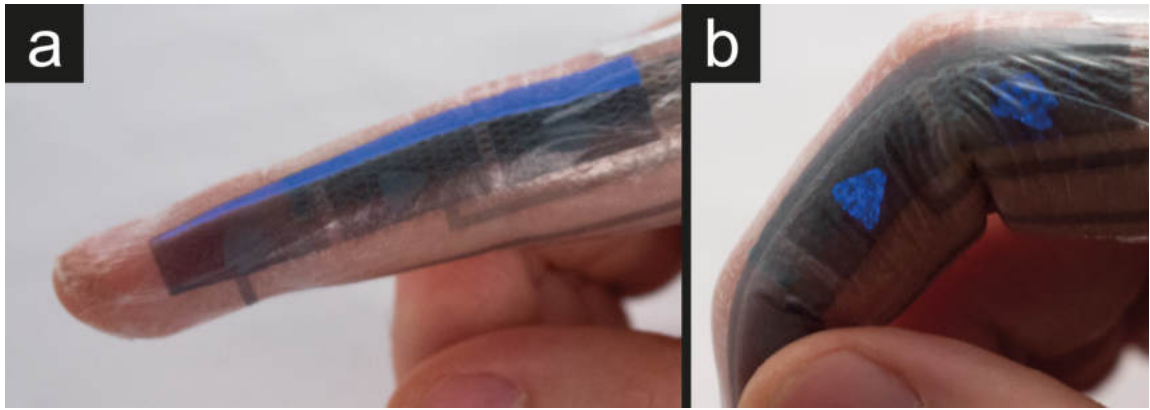


Figure 27: Using body posture to dynamically change functionality: (a) Straight finger for linear movements, e.g. to control volume, (b) bent finger for discrete touch areas.

application on these fine skin microstructures and precise touch elements. This allows for sensing touch input precisely on the tiny area of a skin microstructure and exploiting its distinct tactile properties for interaction.

We demonstrate this with a new interaction technique that makes use of tactile skin surface-structure: The *Wrinkle Slide* interaction technique. A touch sensor augments one or multiple flexure lines (the larger wrinkles) on a finger. By sliding along the flexure line, the user can continuously adjust a value. A selection can be made by tapping. The precise tactile cues of the flexure line allow for tactile localization and guide the user during sliding, without requiring visual attention. The technique also allows for one-handed input using the thumb of the same hand (thumb-to-finger input). Therefore, it can support interactions in busy mobile scenarios, e.g., while running. We demonstrate its use as a one-handed remote to control the volume of a mobile music player.

The wrinkle slider contains two triangular printed electrodes, which together measure 30×4.5 mm (Figure 28a). They are used for capacitive touch sensing. Interpolation allows capturing the touch location on the slider. *SkinMarks* are thin enough to closely conform to flexure lines and allow the feeling of the wrinkle through the sensor tattoo.

4.2.3 Expressive Deformation on Elastic Body Locations

The elasticity of skin varies across the body locations, depending on the amount of elastin in the dermis layer [251]. For example, finger webbing has considerably higher elasticity than its surrounding. These soft landmarks afford localized skin deformations, such as shearing, stretching, and squeezing, for continuous and expressive on-body input.

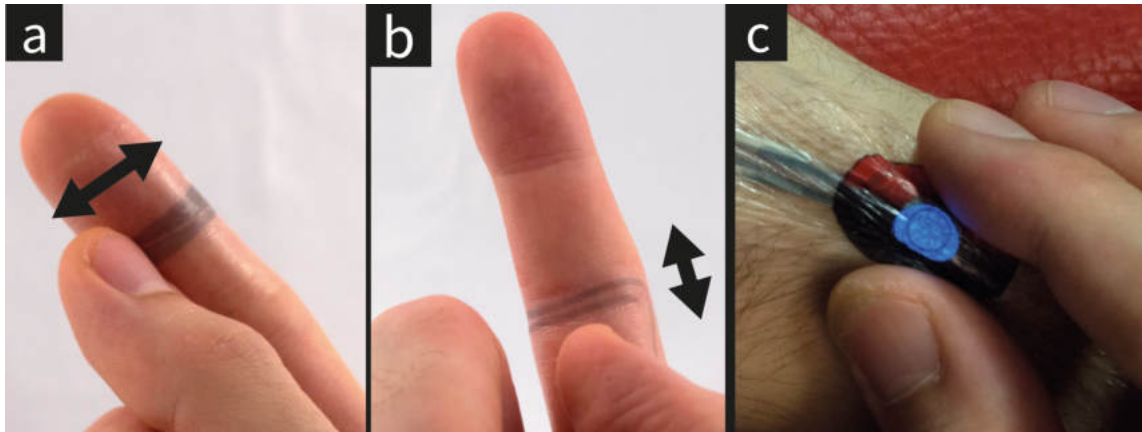


Figure 28: *SkinMarks* allow for precise touch input on skin microstructures: (a) wrinkle slider and (b) wrinkle toggle. (c) Interacting on an body location that is highly stretchable.

Localized deformation at such elastic locations can enrich the input vocabulary enabling expressive on-body interactions. For example, an interface can distinguish between touch input and squeeze input to trigger different commands. We demonstrate deformation input on the circular protrusion on the wrist created by the head of the ulna bone. This location is easily localizable through its visual and tactile cues. We implemented a *CaptureMark* (Figure 28c). The *CaptureMark* is a circular ball for capturing virtual objects in augmented reality games, e.g. treasures or Pokemon. The user is notified about virtual objects with audio feedback. The user can attempt catching it by squeezing the tattoo. Afterward, the *CaptureMark* blinks and finally lights up for a few seconds to notify the user that the virtual object is caught.

4.2.4 *Dynamic Visual Cues Leveraging Visual Variations on Skin*

Skin varies in its pigmentation and therefore offers locations that stand out by their visual properties. For example, birthmarks can form clearly articulated visual entities. These landmarks are highly personal and differ in their occurrence and location across users. Their visual cues support spatial mappings, provide cues for localization, and their shapes afford different touch interactions.

To illustrate interaction on such locations that are visually different from their surroundings, we implemented a *HeartMark* (Figure 29b), a touch-sensitive heart-shaped display to augment a birthmark. The *HeartMark* notifies the user about the availability of a loved one. Touching it starts a call with that person.

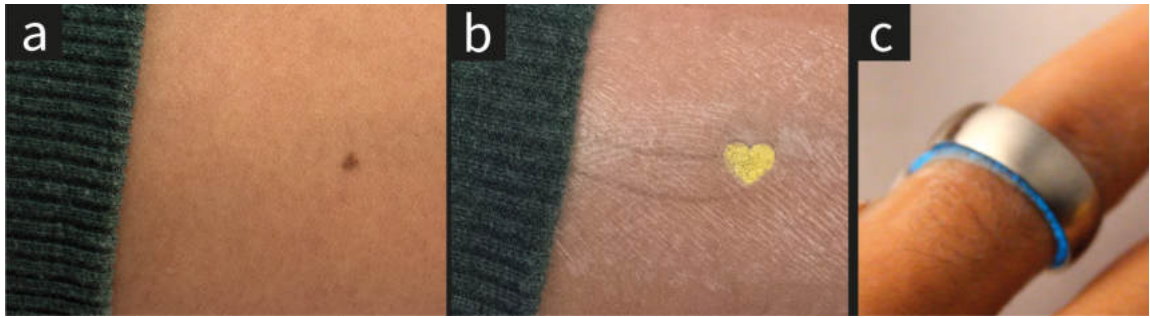


Figure 29: *SkinMarks* can augment personal locations on the skin, e.g. birthmarks (a–b), and passive accessories, e.g. a ring (c).

4.2.5 Interaction on Passive Accessories

Body-worn passive accessories provide unique tactile and visual cues and can enable novel forms of interaction. Although accessories are widely used, they have not been integrated with on-body electronics. *SkinMarks* enable interaction with passive objects in two ways: First, it enables skin illumination under and around the object using on-body displays, similar to *ScatterWatch* [371]. Second, it can make accessories touch-sensitive, through capacitance tags [386]. Touch sensing requires the accessory to be conductive; this holds for a wide variety of jewelry and other accessories. Neither interaction require modification of the passive accessory.

We implemented an augmentation for a wedding ring (Figure 29 (c)), to allow for subtle communication between both partners. Touching the ring creates a glow around the partner's ring. This is made possible by affixing an interactive tattoo at the finger segment where the ring is worn. The tattoo contains a non-exposed conductor which lies under the ring and capacitively couples with it for touch sensing. Moreover, it contains a visual display that slightly extends beyond the ring, for on-demand illumination.

4.3 TECHNICAL EVALUATION

This section presents results from technical experiments that investigate the two key technical contributions of *SkinMarks*: First, do *SkinMarks* support interaction on challenging landmarks by conforming to the skin despite high curvatures and strong elasticity? Second, do *SkinMarks* allow for precisely localized interaction on fine landmarks?

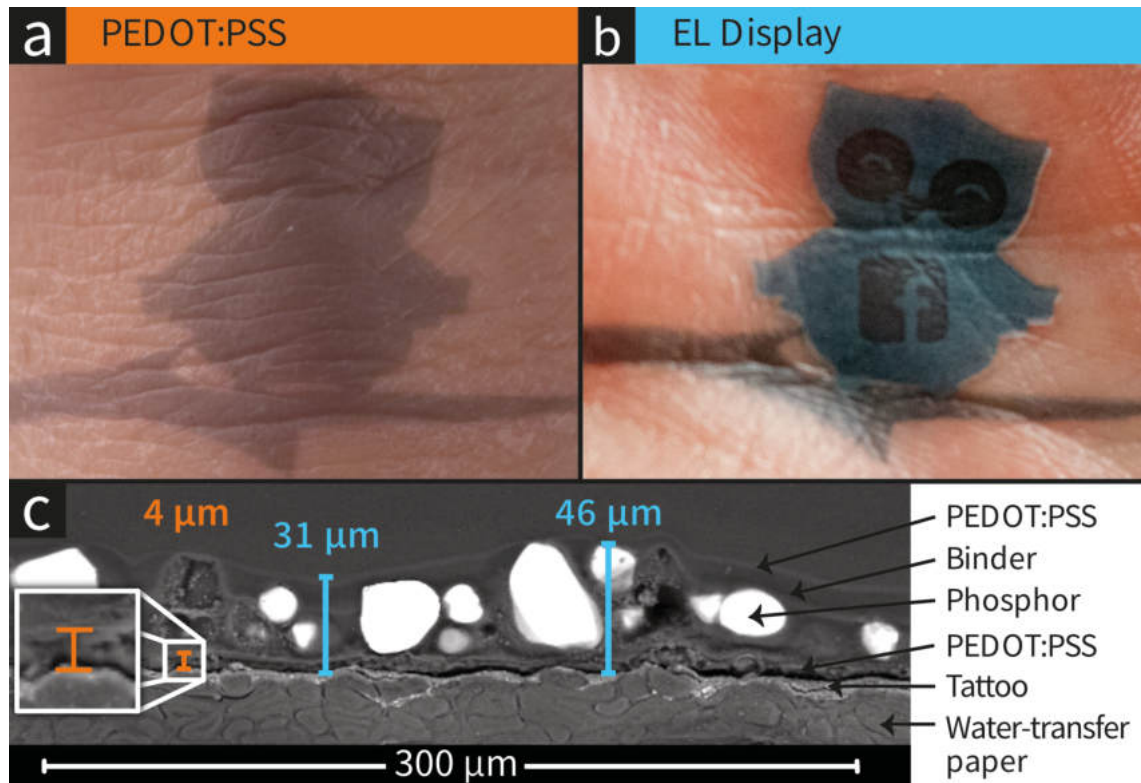


Figure 30: *SkinMarks* conform to wrinkles: (a) a tattoo with PEDOT:PSS conductor; (b) tattoo with EL display. (c) Cross-section of a tattoo with printed EL display, taken with a scanning electron microscope (SEM).

4.3.1 Conformal Form Factor

Conformal Form Factor We investigated the two main factors for conformal electronics: thickness and stretchability. To investigate the layer thickness of printed inks on a *SkinMark*, we analyzed cross-sections of printed *SkinMark* tattoos on the water-transfer paper with a Scanning Electron Microscope (SEM). Figure 7 shows the various layers of inks. A layer of PEDOT: PSS layers is approximately 1 μm thick ($\sim 4 \mu\text{m}$ with tattoo paper). A full TFEL display is between 31 μm to 46 μm thick (Figure 30 (c)). These numbers demonstrate the vastly reduced display thickness compared to prior interactive tattoos [215, 287] and TFEL displays [347, 503]. Figure 30 a&b illustrate how *SkinMark* tattoos closely conform to wrinkles. Our results confirm prior research of Jeonget al. [196], which shows that elastomer membranes of 54 μm have excellent conformality even to small wrinkles, while membranes of 36 μm have good conformality on larger wrinkles (e.g. flexure lines). Our experiments showed that the stretchability of the tattoo substrate ranges between 25–30%. PEDOT: PSS retains conductivity up to 188% strain and is reversibly stretchable up to 30% strain [280]. For comparison, the stretchability of the human epidermis is around 20% [408]. The combination of both makes *SkinMarks* intrinsically stretchable and more robust against strain than metals (e.g. [215, 287]).

4.3.2 Precise Localization: Touch Input and Tattoo Application

We validate the two necessary conditions for precisely localized input. First, can touch input be accurately sensed on sub-millimeter electrodes? Second, are users able to apply tattoos with high spatial accuracy on challenging body locations?

4.3.2.1 Touch Input on Sub-Millimeter Electrodes

Methodology: We recruited 12 voluntary participants (2 female, 10 male, 22–32 years, mean 26.8 years). Electrodes of different widths (1.0, 0.75, 0.5, and 0.25mm) were screen printed with PEDOT: PSS on tattoo paper and applied to the flexure line of the index finger of the non-dominant hand. The participants were asked to touch each line 30 times for 2 seconds to collect enough data points in the touched and non-touched state. Participants could freely choose how they touch the tattoo. The electrodes were connected to a commercial capacitive touch controller (Adafruit MPR121). This interfaced with an Arduino, which was using a serial connection to a PC for data logging. Each session took approximately 25 minutes, including 5 minutes of training.

Results: We measured the signal-to-noise ratio (SNR) of capacitive sensing for each line width. For 1 mm, the average SNR was 56.3 (SD=20.9). It was 41.2 (SD=16.4) for 0.75 mm width and 20.1 (SD=9.5) for 0.5 mm width. For the smallest electrode of 0.25 mm, the average SNR was 13.1 (SD=5.5). For each single

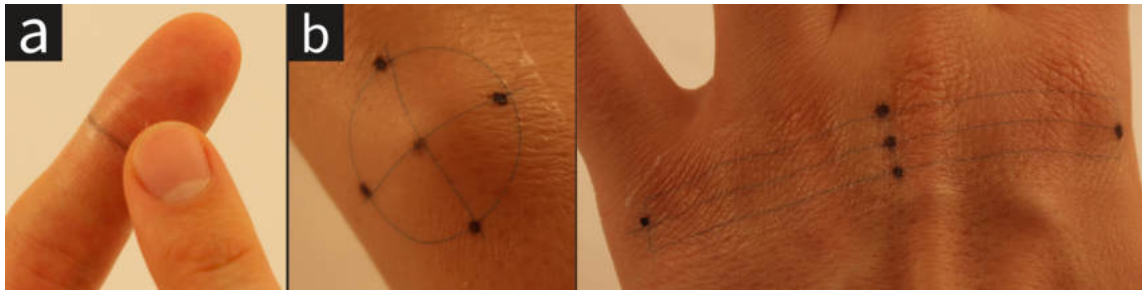


Figure 31: Study setup: (a) evaluation of touch on submillimeter electrodes and (b) of precise tattoo application.

data point, the SNR was above 7.0, which is the required SNR for robust touch sensing [79].

4.3.2.2 Precise Application of SkinMarks Tattoos

Applying temporary rub-on tattoos on planar areas is a straightforward task, but precise alignment on curved geometries of the body can be more challenging. Hence, the second key requirement for precise and accurate interaction on challenging body locations is that the user can apply the interactive rub-on tattoo on the skin with a high degree of spatial accuracy.

Methodology: We recruited six voluntary participants (1 female, 5 male, 25–28 years, mean age 26.3 years). Each participant had to precisely apply four substrates of tattoo paper at four challenging locations: knuckles (bony location with a high degree of curvature), head of ulna (bony location), flexure lines on the finger (location with fine skin microstructures), and birthmark (tiny and highly personalized location). The order of presentation of tattoos was counter-balanced. The tattoos had fine target points (see Figure 31). The participants had to align these target lines precisely with the target points that the experimenter had marked on the participant's skin. For the birthmark, the participants were free to choose any location on the forearm. We instructed the participants how to apply a temporary rub-on tattoo, before letting them apply all four tattoos on their own. We took visual surface scans to measure the error offset for each of the tattoo locations. Each session took approximately 30 minutes.

Results: The results show an inherent ability of users to apply tattoos with a millimeter or even sub-millimeter accuracy at challenging landmarks. The mean error of placement was below 1.0 mm for all locations. Most precise were birthmark (mean=0.16 mm, max=1.0 mm) and flexure line (mean=0.26 mm, max=0.7 mm), followed by knuckles (mean=0.84 mm, max=1.8 mm) and the head of ulna (mean=0.74 mm, max=2.2 mm).

4.4 DISCUSSION, LIMITATIONS AND FUTURE WORK

This section discusses practical insights, limitations, and lessons we have learned during the nine-month-long design and implementation of several iterations of prototypes.

Printing and Fabrication: Each tattoo is personalized and individually fabricated. In our experiments, fabrication of a functional tattoo required between 3–3.5 hours. Preparing the screen printing mask took the longest time (~ 2.5 h). One mask can, however, contain designs for multiple tattoo prints. The actual printing and curing is fast for touch sensor tattoos (~ 5 min) and takes between 30–60 minutes for fabricating all layers of a display tattoo. These manual steps can be largely automated using high-end industrial screen printing tools. We envision that in the near-term future a personalized interactive tattoo can be printed in less than a minute on a desktop printer.

Connector and Power: During prototyping, we found that the the connector is the weakest element in the chain. This is because the connection between printed conductors, which are slim and flexible, and external conductors, which tend to be much thicker and more rigid, is subject to strong mechanical forces. Our final solution connects each connection pad on the tattoo with a slim connector made of flexible copper tape ($\sim 30\mu\text{m}$). Applying the adhesive layer to the entire tattoo, except the connectors, helps to ensure proper connection. Aligning the tattoo on the connector can be eased by visually marking the connector areas on the backside of water-transfer tattoo paper. Future prototypes would benefit from further miniaturizing of the technology to enable a complete system within the tattoo layers. As a first step, miniaturized rigid microcontrollers (e.g., Intel Curie) could be combined with flexible batteries to enable capable, yet less flexible, areas, with on-skin advanced computation and control. Alternatively, the use of RFID/NFC [215, 240] could enable remote powering of basic sensors and allow communication through modulated backscatter. Other approaches include power harvesting of thermal energy or motion using piezo electronics, where the limited efficiency and bandwidth might still be sufficient for certain types of sensing and transmission.

Safety: Electroluminescent displays are driven using high voltage, but low-current AC [347]. We recommend using a current-limiter circuit. We found that the adhesion layer does not guarantee sufficient insulation of the current of electroluminescent (EL) displays from the skin. We recommend two additional layers of rub-on tattoo under *SkinMarks* to ensure proper electrical isolation (each layer is $3\mu\text{m}$). This approach also ensures that ink does not contact the user's skin. According to prior work [136], PEDOT: PSS does not cause skin irritations and has no long-term toxicity under direct contact.

Tattoo Application: For close conformality on challenging body locations that allow for dynamic pose changes, e.g. knuckles, we recommend applying the temporary tattoo in the flat pose. Otherwise, the tattoo application requires more

attention to avoid gaps at retracted locations, where the tattoo might not touch the skin. We also found that tattoos covering a larger area (>5 cm in one dimension) are challenging to apply on locations with high curvatures, because the water-transfer paper is relatively stiff before application. If possible, we recommend having multiple smaller tattoos covering the same area. For example, the electrodes and wires can be divided into individual tattoos for each knuckle and aligned separately.

Unintentional Input: is one of the open issues in on-body interaction. From our experience, we noticed that protruding body locations and the inner areas of the palm are more susceptible to unintentional input when compared to other locations. Body locations that retract, such as the area in-between the knuckles, seem promising to reduce the likelihood of unintentional input. Another approach consists of using more expressive gestures that are more robust by design, such as the presented directional toggle gesture or squeeze-based input.

Additional Body Locations: While this chapter presented novel interaction techniques on five different types of body locations, there are other challenging body locations and features that need to be explored. This includes even finer skin microstructures (like hair), artificial visual skin texture (like permanent tattoos, tan lines, and henna art), and a wider range of accessories (including earrings and piercings). Other skin properties, e.g., the distribution of cutaneous receptors, could also be beneficial for on-body interaction and should be investigated in future work.

Empirical Investigations: This work contributed toward enabling interaction on various challenging body locations. Future work should study *SkinMarks* in longitudinal user experiments to see how *SkinMarks* can fit in users' everyday routines. Finally, further empirical investigation needs to be conducted to evaluate the interaction benefits and user performance on non-planar and challenging body locations.

4.5 CONCLUSION

In this chapter, we have introduced *SkinMarks*, a technical enabler for interaction on small, highly curved, and deformable body locations. It expands the on-body interaction space toward more detailed interaction on challenging body areas. *SkinMarks* are temporary interactive tattoos. They sense touch on sub-millimeter electrodes, capture squeeze and bend input, and support active visual output. Through a vastly reduced tattoo thickness and increased stretchability, a *SkinMark* is sufficiently thin and flexible to conform to irregular geometry, like flexure lines and protruding bones, while still allowing the user to reference those body locations tactually or visually. We demonstrated novel interactions on five different types of body geometries including body-worn accessories advancing on-body interaction towards more detailed, highly curved, and challenging body locations.

EPIDERMAL DEVICES FOR HIGH-RESOLUTION TOUCH SENSING

The previous chapter presented *SkinMarks* devices that are highly skin-conformal and adapt to complex body geometries. However, they were limited to low-resolution touch input and single touch contact. Empirical studies show that our body affords a wider variety of touch-based interactions [499]. These interactions require high-resolution multi-touch input, which is beyond the capabilities of state-of-the-art touch sensors for the body.

The industry standard for high-resolution multi-touch input is mutual capacitance sensing [28]. Such sensors are commonplace inside objects and mobile devices. However, deploying such sensors on the human body poses several challenges: First, the human body surface is curved and deformable; hence the sensor must be very slim and flexible to conform to human skin. Second, the human body has its electro-capacitive effects, which have to be properly shielded from the body-worn sensor to acquire reliable touch input. Lastly, input locations on the body vary in their size and have various (non-rectangular) shapes; hence, the sensor should support personalization and customization.

This chapter introduces Multi-Touch Skin¹, the first high-resolution multi-touch sensor for on-body interaction. Multi-Touch Skin is thin and flexible to conform to the user's skin. In contrast to prior skin-based touch sensors that used self-capacitance [215, 287, 500], our sensor leverages on mutual-capacitance matrix sensing tailored for the body. This enables scalability and multi-touch input. Furthermore, it can be customized to diverse body geometries and is immune to body capacitance effects. More specifically, our contributions are:

We present a *fabrication approach* for realizing Multi-Touch Skin sensors with printed electronics in a simple lab setting. Based on a systematic exploration of functional inks and substrate materials, this chapter introduces the first solution to print a high-resolution multi-touch sensor with a desktop inkjet printer. We also show how to achieve very thin designs using screen printing. Based on

¹ This chapter is based on [341]. As the first author, I led the conceptual design, development of design and fabrication process for realizing the multi-touch sensors, programmed the touch controller firmware to obtain raw capacitive images, developed the design tool, designed the tactile input modalities, conducted the technical experiments, and realized the application scenarios. Dr. Anusha Withana helped in obtaining the raw capacitive images from the touch controller, performed the statistical analyses, and helped in framing the paper. Narjes Pourjafarian assisted in testing and evaluating the prototypes. She also helped in recording the mutual capacitance data for the tactile input modalities. My supervisor Jürgen Steimle advised me on the conceptual design, fabrication, design of the computational tool, evaluation, and applications. He further contributed to the structure and writing of the publication.



Figure 32: The thin and flexible multi-touch sensor can be customized in size and shape to fit various locations on the body: a) multi-touch input on the forearm for remote communication (inset shows capacitive image); b) multi-touch-enabled bracelet with an art-layer for aesthetic customization; c) input behind the ear; d) input on the palm with busy hands.

the principles from electronic circuit design and previous literature on wearable sensors [12, 135, 317, 417], we present a solution to effectively shield the slim sensor sandwich from stray capacitive noise caused by the electro-capacitive effects of the body, which is a key prerequisite for correct functioning on the body.

Moreover, we contribute a novel approach and design tool to *generate multi-touch sensor designs of custom size and custom shape*. We use these to present the first non-rectangular multi-touch sensor designs for the body.

To validate the feasibility and versatility of the approach, we have realized four *interactive prototypes and application examples*. These highlight new opportunities for on-body interaction and demonstrate that the sensor can be easily customized for use on various body locations. Empirical results from two technical evaluation studies confirm that the sensor achieves a *high signal-to-noise ratio* on the body under various grounding conditions and has a *high spatial accuracy* under different scales and when subject to strong deformation.

Overall, our results demonstrate that high-resolution multi-touch sensors can be realized in very slim and deformable form factors for the body while offering many customization options for non-conventional sensor shapes.

5.1 DESIGN REQUIREMENTS FOR MULTI-TOUCH SKIN

Human skin has properties that make it fundamentally distinct from surfaces that so far have been used for capacitive multi-touch sensors. These generate three main technical requirements for the design of the sensor:

5.1.1 *Compatible with deformable properties of skin*

Skin is deformable and has complex geometries. These natural properties vary across the body, depending on the location and the underlying anatomy (i.e. tissues, bones, etc.). They also vary between individuals. A sensor attached to the skin should be non-invasive, conformal, and compatible with the geometrical and mechanical behavior of the skin. Planar and rigid capacitive sensors used in commercial multi-touch sensors will not comply with these demands. Furthermore, mass manufacturing techniques used to make such sensors are not well-suited for the degree of customization required for a sensor designed for the human body.

5.1.2 *Robust to electro-capacitive effects of body*

The human body is conductive and hence exhibits inherent electro-capacitive effects, which interfere with capacitive sensing. These effects are often unpredictable and influenced by a variety of sources, including the movement and grounding of the body, external objects the body comes in contact with, and other environmental factors. Capacitive sensors designed to robustly work on the body should be capable to withstand these electro-capacitive effects.

5.1.3 *Leveraging unique affordances of the body*

The human body affords a variety of rich and expressive multimodal interactions [499] that go well beyond the multi-touch interactions available in common touch devices. These should be captured by a skin-based touch sensor. For instance, distinguishing between contact of nails and knuckles could capture input such as scratching and knocking, in addition to normal touch contact. Deformable areas of the body could be used for touch input of variable pressure. Lastly, tactile cues sensed by the skin allow for accurate positioning of the touching finger [139], which implies the sensor should have a high spatial resolution.

5.2 SENSOR FABRICATION

In this section, we present a fabrication approach for realizing thin and flexible multi-touch sensors for use on the body. We start by reviewing the basics of mutual-capacitance touch sensing and contribute a systematic exploration of materials

#	Conductor	Dielectric	Substrate	Technique	Functional	Fabrication Speed	Observations
1	Silver	Dielectric Paste	Tattoo Paper	Screen printing	Yes	Slow	Silver and dielectric paste are brittle
2	Carbon	Dielectric Paste	Tattoo Paper	Screen printing	Yes	Slow	Carbon and dielectric paste are brittle
3	PEDOT	Resin Binder	Tattoo Paper	Screen printing	No	Slow	High resistance of PEDOT
4	Silver	PVC film	Tattoo Paper	Screen printing	Yes	Slow	Thin sensor (70 – 160 μ m); Silver is brittle
5	Silver + PEDOT	PVC film	Tattoo Paper	Screen printing	Yes	Slow	Thin sensor (70 – 160 μ m); PEDOT increases robustness
6	Silver	PVC film	PET film	Inkjet printing	Yes	Fast	Prints within a minute; thicker sensor (~400 μ m)
7	Gold-Leaf	PVC film	Tattoo Paper	Vinyl Cutting	Yes	Slow	Gold-leaf needs larger electrode size and delicate to handle

Table 3: Results from exploration of material combinations. Recommended combinations are highlighted in bold font.

and their combinations that informed our fabrication technique. We present novel fabrication techniques for rapid iterations and high-fidelity prototyping. This includes the first technique for fabricating a mutual-capacitance multi-touch sensor on a commodity ink-jet printer. The printed sensor readily works with off-the-shelf multi-touch controllers, without requiring fine-tuning of the controller’s parameters.

5.2.1 Mutual Capacitance Touch Sensing on Skin

A mutual-capacitance-based touch sensor [28] consists of two overlaid layers of conductors: one with transmit electrodes, and another with receive electrodes. Both layers are electrically insulated from each other by a dielectric material. These electrodes are typically arranged in a 2D row-column matrix pattern creating overlapping intersections, which creates a mutual-capacitance between each transmitter (i.e. row) and receiver (i.e. column) pairs (Figure 33(b)). The transmit layer is driven by a weak alternating current (AC) signal, which is received by the receive electrodes. This received signal can be used to measure changes to the mutual-capacitance between the relevant row and column. When a human finger gets close to one of these intersections, the capacitance between the two electrodes is reduced as the electric field between them is disturbed by the finger, which can be detected as a touch-down event [132, 565]. Using a time-division multiplexing scheme [28, 93], multiple simultaneous touchpoints can be detected.

Thus far, it has been unclear how to fabricate a mutual-capacitance-based multi-touch touch sensor for use on skin, as the sensor needs to adapt to the mechanical, geometrical, and electro-capacitive aspects of the body.

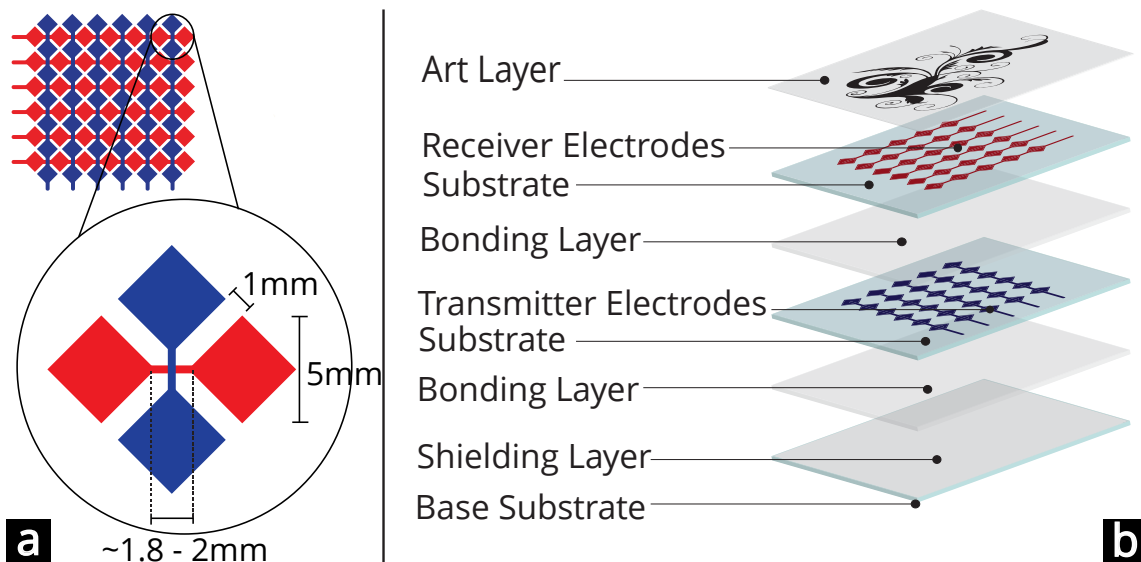


Figure 33: (a) Basic electrode design. (b) Layer-by-layer overview of the Multi-Touch Skin sensor.

Since the Multi-Touch Skin sensor is very thin and worn directly on human skin, body capacitance effects of the user will manifest as parasitic noise in the sensor readings. These are hard to control for, as changing grounding conditions, skin conductivity, and internal body composition all affect the capacitive response of the body.

For robust functioning on the body, the sensor layout must be modified. This can be achieved by adding a shielding layer as the bottom-most layer of the sensor [12, 135, 317, 417] (see Figure 33(b)). This layer acts as a fixed potential layer. It is fully covered with a conductor, and connected to the ground potential of the electrical circuitry. As demonstrated by empirical evaluation results presented in the evaluation section, this effectively masks body capacitive effects from the sensor measurements.

Hence, the main functional elements of the sensor film are three layers of conductors, patterned with electrodes and insulated by layers of dielectric material. Next, we identify suitable materials and fabrication techniques to realize them in a slim and flexible substrate.

5.2.2 Material Choices and Sensor Design

For our systematic exploration, we selected materials and fabrication techniques that have been successfully used in previous research on skin-based interfaces [215, 287, 498, 500].

Conductors: The most commonly used printable conductor is made of silver particles, which offer high conductivity at the cost of some brittleness. We used silver ink for ink-jet printing (Mitsubishi NBSIJ-MU01, $0.2\Omega/\square$ sheet resistance) and screen printing (Gwent C2131014D3, $0.1\Omega/\square$). A polymeric conductor (PEDOT-

based translucent conductor, Gwent C2100629D1) offers better stretchability and translucency with a lower conductivity ($500 - 700\text{k}\Omega/\square$). Inspired by prior work, we also used aesthetic gold leaf and conductive carbon ink (Gwent C2130925D1, $15\Omega/\square$).

Dielectric: Prior work has reported successful use of printable dielectric paste (Gwent D2070209P6) and the slimmer and transparent Resin Binder (Gwent R2070613P2). In addition, we tested simple PVC films ($\sim 7 - 15\mu\text{m}$ and $\sim 30 - 40\mu\text{m}$).

Base substrates: Temporary tattoo paper (Tattoo Decal Paper) is the slimmest material for printing used in prior work. In addition, we used transparent PET film for conductive ink-jet printing (Mitsubishi Paper Mill).

Fabrication technique: We investigated functional screen printing [347], as it is compatible with many printable materials. We tested conductive inkjet printing [222] with a commodity Canon IP100 desktop ink-jet printer, as it supports fast printing. Finally, we used vinyl cutting with gold leaf [215]. For sandwiching the layers and adhering the tattoo onto the human skin, we used the adhesive that is supplied with the temporary rub-on tattoo paper.

Table 3 summarizes our observations on functional material combinations. We started by screen printing a full stack of functional layers on a single substrate, as proposed in prior work [347, 500]. However, it became apparent that these approaches either suffer from limited mechanical robustness due to a brittle dielectric paste that forms cracks on repeated deformations (#1,2), or insufficient conductivity of the PEDOT conductor for the mutual-capacitance controller chip (#3).

We, therefore, investigated an alternative fabrication approach. It uses a separate PVC film as the dielectric. The transmitting, receiving, and shielding electrode layers are each realized on a separate tattoo paper substrate, and then bonded to the dielectric film to create a multi-layer sandwich (illustrated in Figure 33(b)). For visual customization, the sensor can optionally be covered with a printed art layer. To ensure robust bonding of layers, we recommend using 2-3 layers of tattoo paper adhesive, rather than just one. The electrode dimensions with exact spacing parameters are shown in Figure 33(a).

With this approach, we could realize functional sensors for use on skin, using all three basic fabrication techniques (approaches #4–7 in Table 3). Overall, we recommend using approach #5 if a slim sensor design has a high priority, while #6 is the best approach when the speed of fabrication is key. We used these approaches to realize all prototypes presented in this work.

5.2.2.1 High-fidelity printing

Screen printing is the preferred technique to realize a high-fidelity sensor that conforms to the user's skin, as it achieves very thin designs. We recommend printing silver overlaid with PEDOT: PSS (#5) to increase the robustness of the

traces compared to silver only (#4). Prior work has shown this bridges the gaps when tiny cracks form in the silver conductor [500].

With our approach of printing the transmitter, receiver, and shielding electrodes on separate substrates (as shown in Figure 34, we were able to realize multiple variations of Multi-Touch Skin sensors, which vary in their thickness and robustness. By choosing the dielectric PVC films of different thicknesses, the sensor can either be realized in a thinner form factor, which is more conformal to the skin while being more delicate to handle; or it can be slightly thicker, and hence offer more mechanical robustness for rapid prototyping.

For our thinnest version, we used the tattoo paper substrate for the emitter, receiver, and shielding electrode layers. Between each pair of these layers, we sandwiched a PVC film of $\sim 30\mu\text{m}$ thickness as a dielectric and insulator. This results in an overall sensor thickness of $\sim 70 - 80\mu\text{m}$. An alternative version uses a thicker PET film of $\sim 70\mu\text{m}$ thickness, resulting in an overall thickness of $\sim 150 - 160\mu\text{m}$. The increase in thickness also eased sandwiching the layers.

Because thin gold leaf (approach #7) is delicate to handle and to manually apply onto the substrate, fabricating a sensor made of gold leaf takes longer and electrodes cannot be as small as with printed silver. This decreases the effective resolution. Prior work reported a minimum size of $\sim 1.4\text{cm}$ for electrodes made of gold leaves [215], whereas our printed silver electrodes measure 5mm. We, therefore, recommend this approach only if the aesthetics of the material is a key requirement.

5.2.2.2 Rapid fabrication using ink-jet printing

The Multi-Touch Skin sensor can be fabricated using a commodity ink-jet printer and silver ink (#6 in Table 3). This is by far the fastest technique, allowing to print all layers of the sensors in less than a minute. The sensor is also very robust, as the ink-jet-printable base substrate is thick (comparable to photo paper). However, this results in an overall sensor thickness of $\sim 400\mu\text{m}$. Figure 35 shows the Multi-Touch Skin sensor of different thickness levels fabricated using various substrate materials.

5.2.3 Scalability

Mutual-capacitance sensing offers the advantage of easy scalability. We fabricated functional Multi-Touch Skin sensors with varying matrix dimensions (3×3 , 4×4 , 5×5 , 6×3 , 6×6 , 10×6) that fit commonly used areas on the human body, such as the wrist and the forearm. Based on the touch-controller specification, we identified an electrode size of 5mm and a gap spacing of 1 mm between the receiver and transmitter electrodes (Figure 33(a)) to yield robust results [318]. A controlled evaluation reported in the Evaluation section investigates the scaling effects and demonstrates the high accuracy of multi-touch sensing.

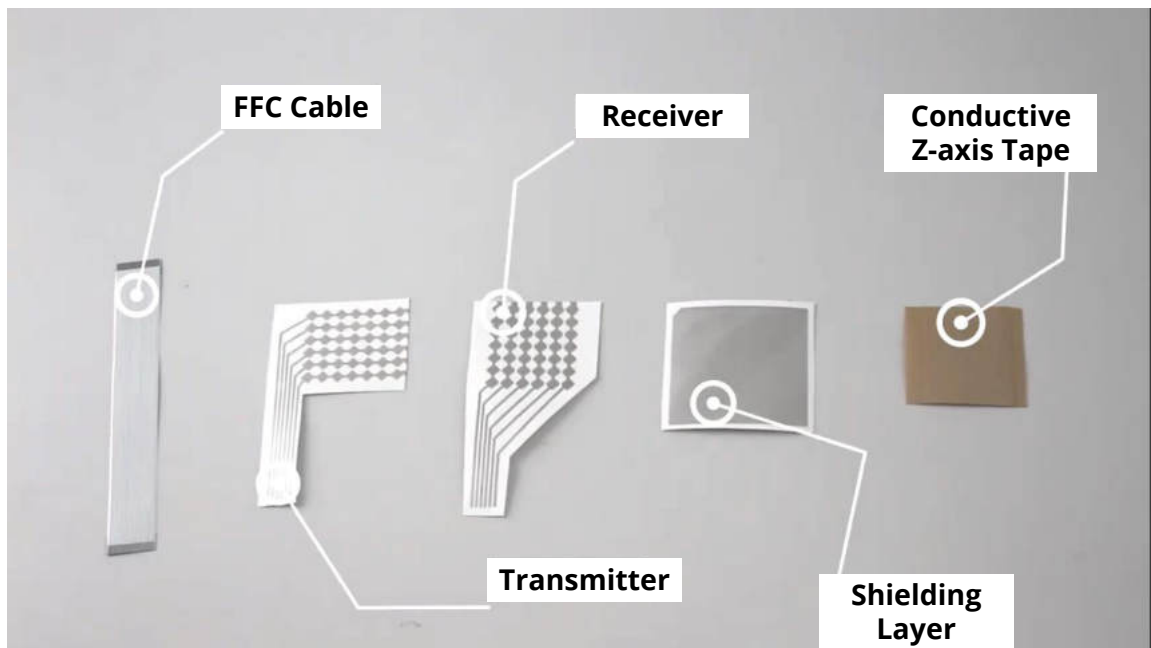


Figure 34: Overview of all the components required for preparing the interfacing the multi-touch sensor sandwich. The receiver, transmitter, and shielding layers are screen-printed onto a tattoo paper substrate. Conductive Z-axis tape is used for connecting the printed routings to a flat flexible cable (FFC) which is used for interfacing to the touch controller.

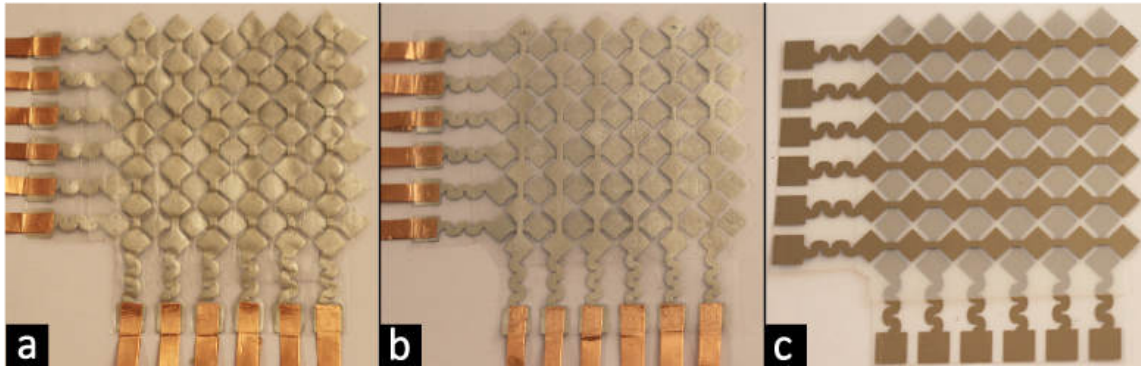


Figure 35: Multi-Touch Skin sensors with varying thickness and materials: (a) thinnest version of the sensor with tattoo-paper substrates ($\sim 70 - 80\mu\text{m}$); (b) screen-printed sensor with a thicker PET film as the substrate ($\sim 150 - 160\mu\text{m}$) (c) ink-jet printed sensor on transparent PET film ($\sim 400\mu\text{m}$)

5.3 CUSTOMIZED FORM FACTORS

The human body has varied geometric shapes. Conventional rectangular sensor designs would not fit on those various locations. A multi-touch sensor for use on the skin should be customizable to various sizes and (non-rectangular) shapes of the human body. This is not a trivial task for an interaction designer, since the intricate electrical parameters, such as electrode sizes, spacing, interconnections, and distributions of the electrodes between layers, would need assistance from electrical engineering expertise. To the best of our knowledge, prior work has not yet addressed the question of how to generate a multi-touch sensor layout for a given target shape. In this section, we introduce an approach for customizing the shape of mutual-capacitance touch sensors. We then present an interactive design tool that assists a designer in generating a functional sensor design for the desired custom shape.

5.3.1 *Generating Custom-Shaped Multi-Touch Sensor Designs*

Generating a multi-touch sensor design of a given 2D shape can be divided into two sub-tasks: first, the set of transmitter and receiver electrodes need to be generated to fit the shape; next, the interconnections between electrodes and an external connector should be generated.

Our method takes as input: 1. A polygon S defining the desired shape of the touch-sensitive area. 2. A polygon O defining the outer shape of the full sensor sheet (in addition to the touch-sensitive area, this includes additional space for routings and connector area). 3. The desired location of the connector area C in O , where a flexible flat cable will be attached for interfacing with the micro-controller (Figure 36 left).

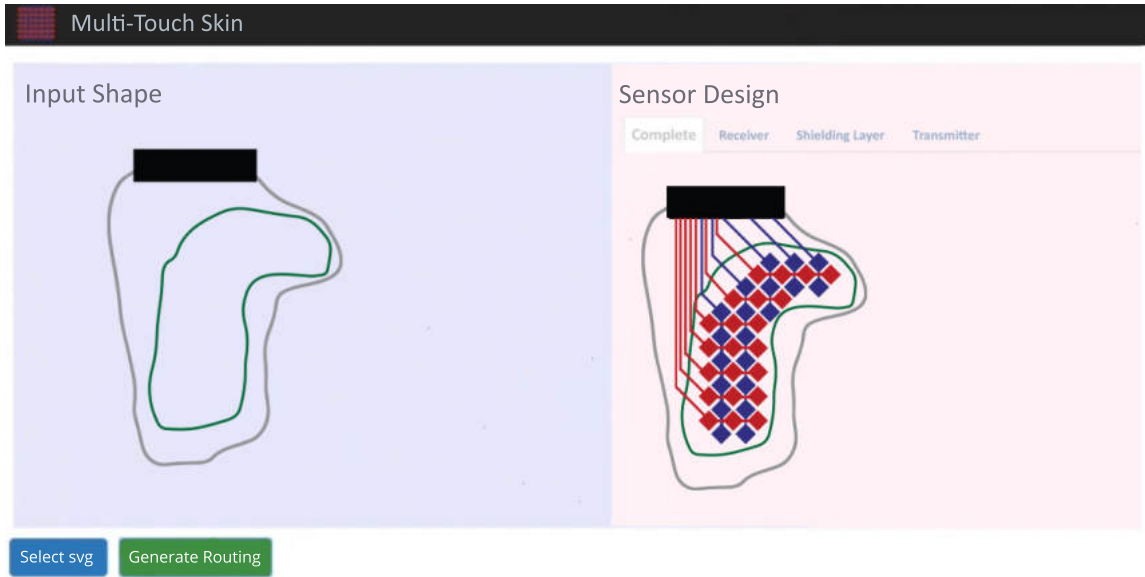


Figure 36: Screenshot of the design tool. (left) The designer specifies the touch-sensitive area S (green), the outer shape O of the full sensor sheet (gray) and the desired location of the connector C (black). (right) The tool generates the multi-touch sensor and provides the corresponding receiver, transmitter and shielding layers.

The method is based on the fact that a minimum of two adjacent electrodes of different types (one transmitter TX and one receiver RX) are required for mutual-capacitance changes to be sensed. The algorithmic steps of the electrode generation process can be summarized as follows:

1. A rectangular bounding box S is generated and filled with a rectangular sensor matrix E , using the classical row-column diamond pattern of transmitter and receiver electrodes [267].
2. For each electrode e in E : If e is fully or partially outside of S , then it is removed.
3. Flag each remaining electrode e in E with a flag f for future inspection.
4. For each electrode e in E : If e has flag f , then
 - For each neighbor electrode e' of e :
 - If e' has opposite type than e (TX vs. RX), then both e and e' are unflagged and move to next e in step 4.
 - If e' has same type as e (both RX or both TX), then move to next e' .
5. For each electrode e in E : If e has flag f , it is removed. This creates the final electrode set \bar{E} (Figure 36 right).

Next, we use the A* algorithm [82] to series-connect the transmitting and receiving electrodes, to form lines and columns, and to wire them to the connector area. Routing of traces is restricted to the polygon O , to ensure the maximum sensor dimensions are not exceeded (Figure 36 right). If there is not enough space for routing on the polygon O , the method fails and marks those electrodes that could not be routed to; otherwise, it returns the set of electrodes and the routings for the transmitting and receiving layers of the circuit.

5.3.2 Design Tool

To assist the designer in the sensor design process, we contribute a simple design tool that supports iterative design. It is implemented as a standalone web application using the JavaScript *svg.js* library² for reading and manipulating SVG files.

First, the designer uses a vector graphics application of choice to create an SVG file. It defines the desired contour of the sensor O , the shape of the functional sensor area S , and the connector placement C , using color-coded polygons.

The tool reads this input file and implements the method described above. It outputs an SVG file that contains the print layout for all the printable layers.

Our tool has been designed for “suggesting” functional sensors to the designers rather than identifying the “best” design. We followed the *designer-in-the-loop* philosophy for our tool, in which the user can quickly inspect the outcome of the algorithm and if needed, slightly modify or tweak the shape. If the algorithm fails, it marks those electrodes in gray that did not fulfill the pre-conditions or that the A* algorithm could not route to. The designer can then iteratively modify the sensor shape (O , S , and C) and re-run the algorithm until the result meets her expectations. The processing time of the algorithm to generate electrodes and routing varied between 3–8 secs for electrode numbers between 3×3 – 10×10 . Times were recorded on a portable computer (Intel Core i5).

We have successfully used our tool for generating various sensor designs of non-rectangular shapes, including the functional prototypes of our application examples (see Figure 37). None of the sensors needed any calibration of the touch controller even though the lines have different electrical and capacitive characteristics. This is because mutual capacitance measures effects at the cross-section of two electrodes, and hence effects of wire length are less influential for the sizes on the body we are interested in and are normalized by the controller. Results from our technical evaluation (see Figure 42) support this argument by showing less than 1mm change in location accuracy from 1×1 to 6×6 electrodes. This is below the human touch pointing accuracy reported in the literature (1.6mm [174]).

² <http://svgjs.com/>

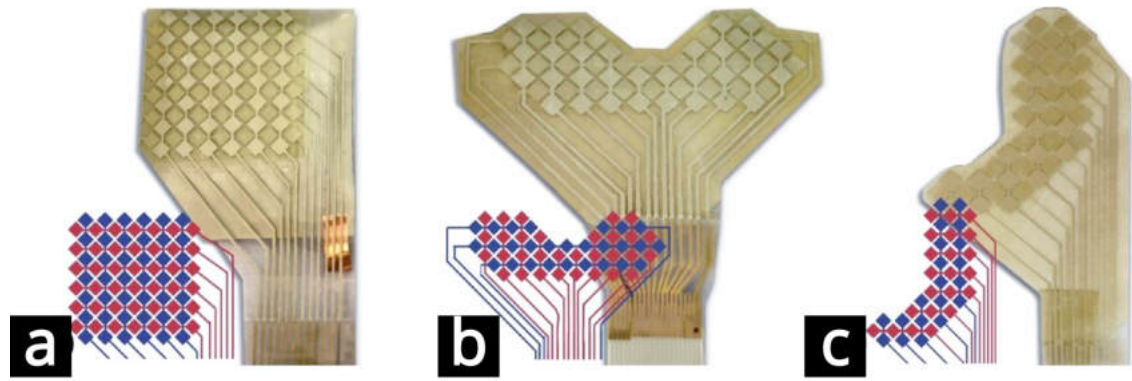


Figure 37: Functional sensor prototypes of custom rectangular and non-rectangular shapes.

5.4 INTERFACING AND DATA PROCESSING

To enable the reader to replicate a functional sensor system, we now present the implementation details, including the electrical interfacing and data processing steps.

5.4.0.1 *Electrical Interfacing and Data Capturing*

The wearable controlling unit includes a Microchip MTCH6303 mutual capacitance multi-touch sensing chip with the MTCH652 transmit booster and a Raspberry Pi Zero. MTCH6303 is connected to the Raspberry through USB. The raw mutual capacitance values are read from the controller using the libUSB library at 100 Hz as an array of 10-bit unsigned data points representing each electrode cross-point. Data is then wirelessly transmitted to a desktop computer for further processing using a WebSocket through a Wifi connection. The dimensions of the wearable controlling unit are $7 \times 4 \times 4$ cm (38)(c). Its weight is ~ 60 grams.

5.4.0.2 *Connections*

Connecting flexible electronics with rigid circuitry, such as a controlling unit, is always a challenge. Previous work typically used copper tape and jumper wires for individual point-to-point connections [500]. While this solution works for smaller matrix sizes (e.g. 3×3), it is difficult to scale to larger ones because of the large number of individual wires. To realize a more scalable approach, we used a thin and flexible flat cable (FFC) and connect it to the sensor with 3M conductive z-axis tape (see Figure 38)(c).

5.4.0.3 *Data Processing Pipeline*

We implemented a data processing pipeline to extract touchpoints and their properties (size, angle, etc.) from mutual capacitance data:

Step 1: Interpolation: Despite the relatively small number of electrodes, the sensor supports accurate spatial interpolation between cross-points. Microchip MTCH6303 senses capacitance changes for individual cross-point as continuous values spanning from 0 to 1024. By normalizing the capacitance and performing bi-linear interpolation, we create a 10x upscaled, interpolated capacitive image with continuous intensity values ranging from 0 to 1. For instance, for a sensor with 6×6 electrodes, the image has 60×60 pixels.

Step 2: Masking and Scaling: To remove noise, we mask the low-intensity pixels of the image by setting pixels with intensity less than 0.1 (10%) to 0. Then, the masked image's intensity values are linearly scaled, so that the maximum intensity is 1. This increases the contrast of the image, and highlights touch locations.

Step 3: Blob Extraction: The image is then subjected to thresholding to create a binary image. A pilot study showed that a threshold of (58%) is the most appropriate. Connected white pixels in this binary image are grouped to form blobs. Depending on the number of touch contacts, one or multiple blobs are extracted.

Figure 38(a and b) shows the results of the intermediate steps of the processing pipeline for several instances of touch input that were captured with a 6×6 sensor on the forearm.

5.5 TACTILE INPUT MODALITIES

Tactile perception on the skin is inherently multimodal. As investigated in prior work, it affords multiple modes of touch contact, which enable expressive on-body gestures [499]. In this section, we present the multi-modal sensing capabilities of Multi-Touch Skin.

Prior work has shown that raw capacitive images can be used to differentiate between different forms of touch contact, such as various finger angles [394, 519], pressure [407], through a textile overlay [403], or stemming from other people [157]. Additional modalities have been demonstrated using other sensing principles, such as acoustic for body parts (finger pad, nail, knuckle) [158] or FTIR-based optical sensing for pressure [31], yet it remains unclear how they transfer to capacitive sensing.

The capacitive response of Multi-Touch Skin is likely to differ from conventional and rigid touch sensors, not only because of the different conductive and dielectric materials we use, but also because of the effects of body capacitance and the different mechanical behavior of a sensor that is deployed on soft skin. Hence, we had to investigate if and how well our sensor can differentiate between multiple types of touch contact.

We identified a set of 10 tactile modalities that have particularly high relevance for touch input on human skin (Fig. 39 leftmost columns). Extending beyond *conventional touch* contact, it comprises contact with the *nail* for scratching gestures [499]. To account for the softness of skin and its inherent tactile feedback, we

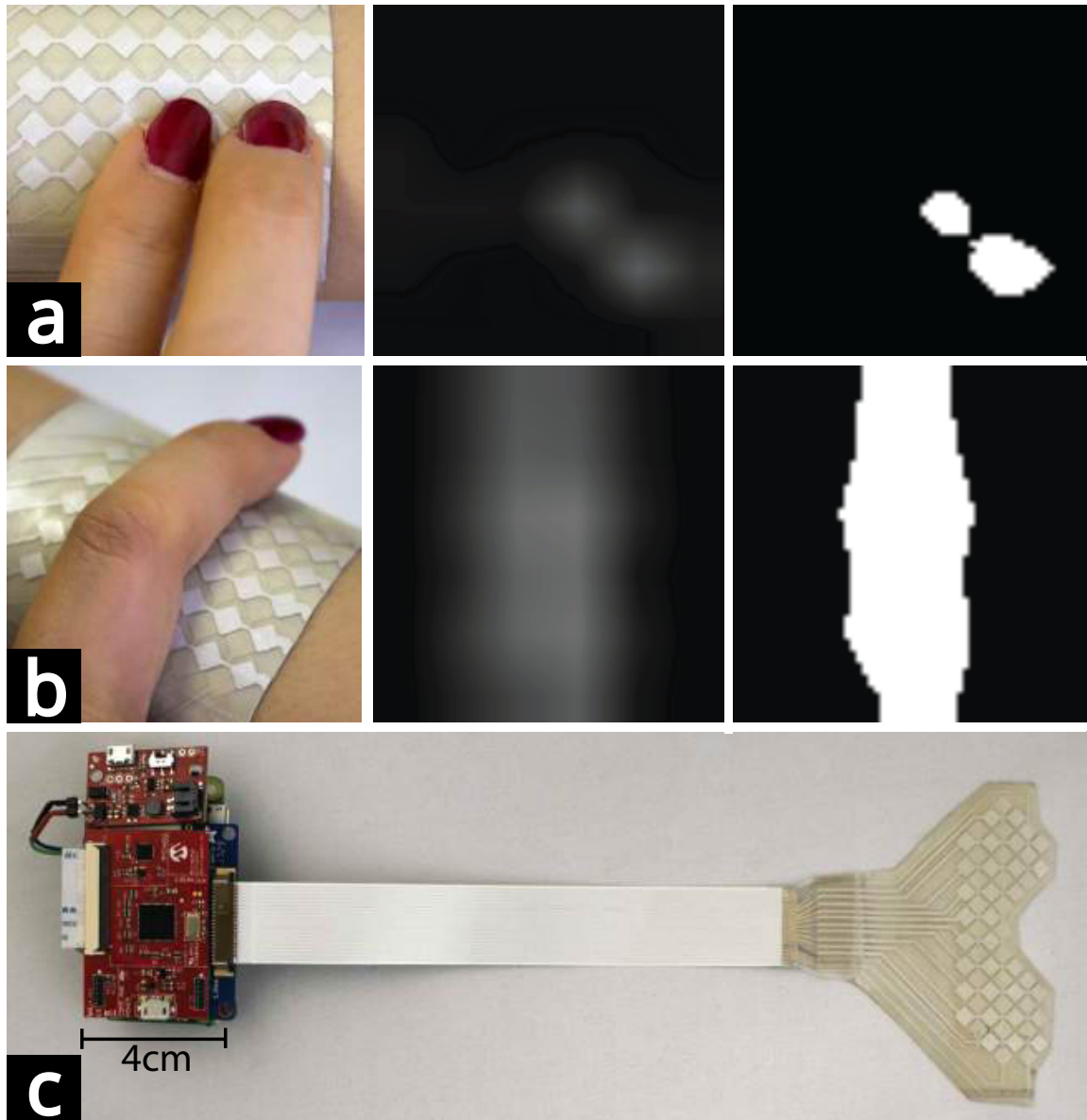


Figure 38: Detecting multi-touch input: a) minimum distance between two fingers which results in two distinct blobs, and the corresponding interpolated capacitive image and the extracted blobs; b) full finger placed on the sensor; c) the wearable hardware setup includes a Raspberry Pi Zero, the touch controller board and the Multi-Touch Skin Sensor.

differentiate between *low pressure* and *high pressure* input for these modalities. Moreover, our set includes several further variations of touch contact that extend the gesture space: contact with the *knuckle*, such as for knocking, with the *thumb*, and the full *finger*. Motivated by the results of [499] and to leverage interaction on cylindrical body areas, we furthermore included *grabbing* input, which consists of wrapping the fingers around the curved sensor. Because many body areas are covered by clothing, we also investigated touch input through a *textile overlay*. Lastly, for collaborative applications, we sought to differentiate between touch input that originates from the user who is wearing the sensor and touch input performed by *another person*.

5.5.1 Classifying Input Modalities

Our classification system builds on the data processing pipeline which was introduced before. Following the interpolation, masking, and blob extraction steps, we perform feature extraction and classification on the identified blobs for recognition of tactile input modalities.

Previous research has identified the size, shape and intensity distribution of the touch footprint to be important features for classifying the touch modality [481]. OpenCV defines blobs as an ellipse, with *location* (ie, x , y coordinates), *major* and *minor* axes, *area* and the *rotation angle*. We use the major and minor axis length of the blob as two features. The area of the blob is a derivative of axes lengths and thus not considered as an independent feature. As a third feature, we use the original intensity of the blob location from the interpolated capacitive image in step 1. Fig 39 (rightmost column) shows average feature values for the 10 modalities (major and minor axis length is normalized for image dimension). Values shown are averages from one user performing each modality three times for 500ms, resulting in 150 data samples for each modality. Given the properties of the extracted features can be highly user-dependent (e.g., blob size), we utilize a per-user trained multi-class BayesNet machine learning algorithm to classify the modalities. We used the Weka machine learning library to implement the classifier.

In order to explore the unique effects of touch input on the flexible sensor on soft skin, we conducted a pilot study with one participant who performed the 10 tactile modalities in two conditions: while the sensor is attached on the forearm and while it is resting on a rigid and planar table surface. Qualitative comparison of the features indicates that the deformability of the sensor surface on human skin contributes to observable differences in the shape, size, and intensity of blobs in the capacitive image. For instance, high-pressure touch on the rigid table yields an elongated blob; the same modality performed on the body results in a larger and more circular blob. This can be explained by the mechanical behavior of the soft surface, where the pressure causes the sensor to deform and wrap around the finger pad. Similarly, we observe a comparatively larger blob from

nail input on the body compared to the rigid surface. This is also a result of the sensor wrapping around the nail, as opposed to the smaller nail contact surface on the rigid table. Another observable effect was apparent in the grab modality. Geometrical variations of palm and finger joints do not conform to the flat and rigid table surface, resulting in multiple blobs of smaller sizes. However, the soft body surface can deform to conform with these geometrical variations and create one larger blob.

5.6 EVALUATION

Three key aspects make Multi-Touch Skin different from conventional mutual-capacitance touch sensors: 1) The sensor is designed to be in constant contact with the body, 2) the sensor is deformable to fit different geometries on the body, and 3) the sensor needs to be scaled for different body locations. To formally evaluate the sensor's functionality with regard to these key differences, we conducted two controlled technical evaluations. In addition to these two technical evaluations, we conducted a third evaluation to investigate how well the tactile input modalities scale across multiple different users.

5.6.1 *Study 1: Guarding Against Body Capacitance*

Multi-Touch Skin is very thin and worn directly on the body. The body capacitance of a person can change rapidly and in an unpredictable way. Therefore, it must be investigated if the shielding layer can effectively guard sensor readings from such changes.

5.6.1.1 *Methodology*

We collected mutual-capacitance data for 10 voluntary participants (avg. age : 26.9, SD = 2.1), with two sensor samples: one with the shielding layer (S1) and one without (S2). All other electrical and physical properties of S1 and S2 are kept the same. The sensors were consecutively placed at the same location on the non-dominant forearm of the participant. To test representative real-world situations, we collected touch data from each sensor in six different activity conditions that modified the grounding conditions, external electro-magnetic fields, and involved various types of physical movement: C1: sitting with forearm resting on the table, and legs resting on the floor; C2: same as C1 but lifting legs from the floor by ~ 20 cm for 10 seconds; C3: same as C1 but with a wooden plank of 10 cm thickness between the feet and the floor; C4: same as C1 with touching the outside of an insulated active AC wire with the non-dominant hand; C5: standing on the floor and walking at a fix location; C6: same as C1 with freely moving the non-dominant arm to the front and side of the torso. The order of all conditions and the sensors was counterbalanced.

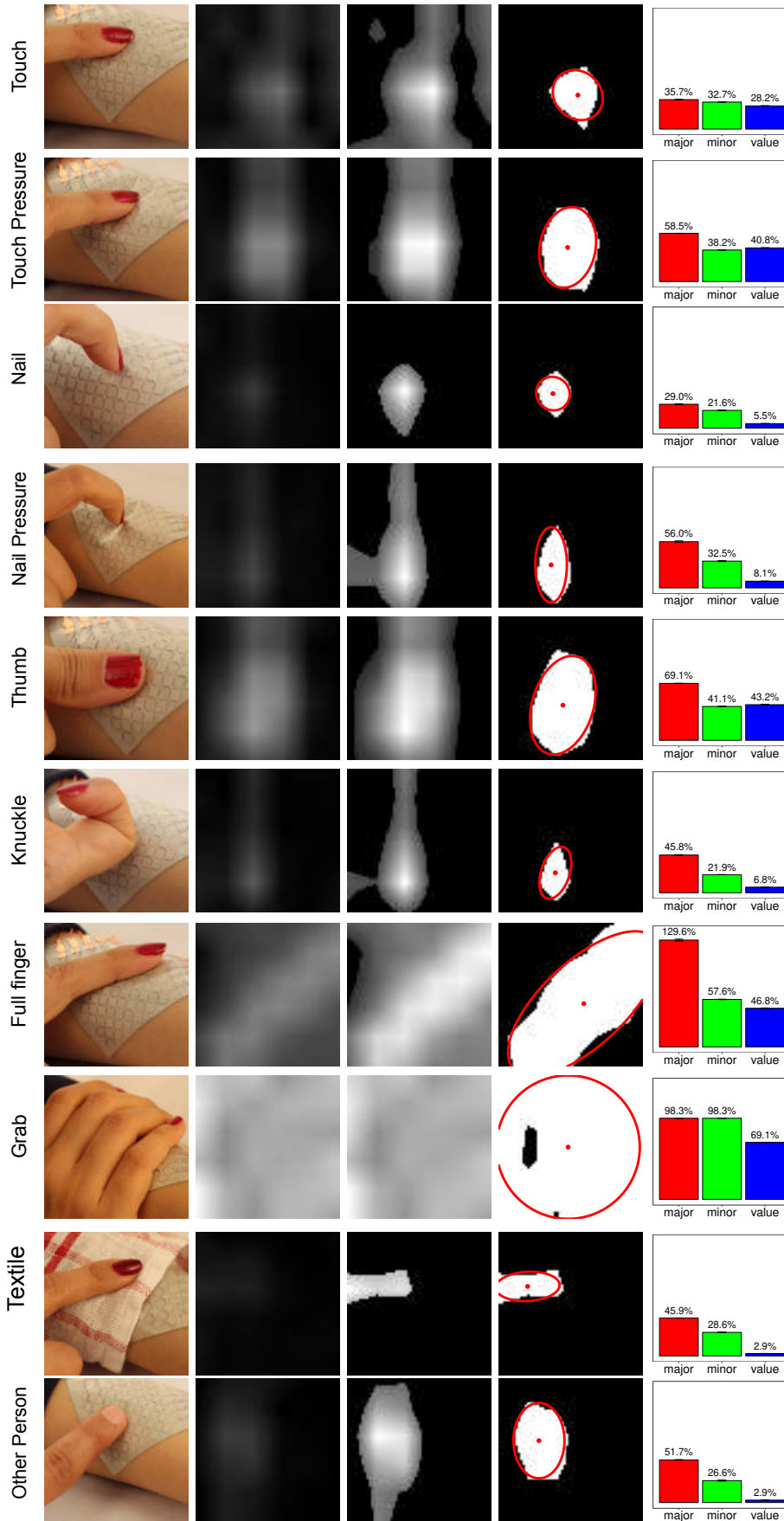


Figure 39: Tactile input modalities supported by Multi-Touch Skin. For each input modality, the interpolated, masked images are generated followed by blob extraction. Higher-level features such as major axis, minor axis, and intensity levels are extracted from the blobs and fed to a BayesNet machine learning classifier.

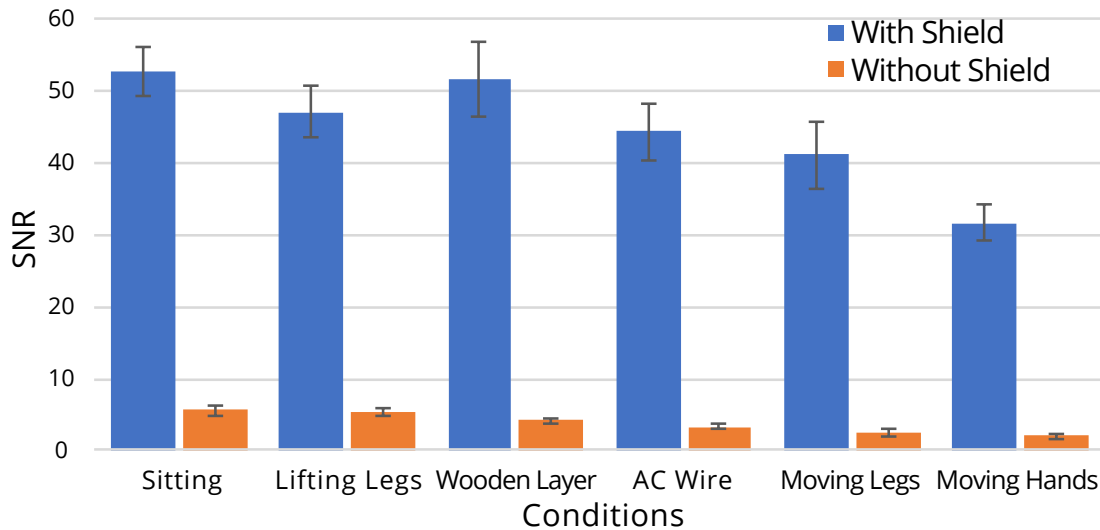


Figure 40: Signal-to-noise ratio of touch sensing on the body with and without the shielding layer.

For a given sensor and activity condition, the task consisted of repeatedly touching (5 trials) the sensor with the dominant hand's index finger for a 1s interval and releasing it for 1s, as accurately as possible. Audio guidance for touch events was given by our study software. The participants were free to touch at any location on the sensor. The mutual capacitance values were recorded for all touch and no-touch conditions, and the signal-to-noise ratio (SNR) for touch events were calculated following the method presented in [79].

5.6.1.2 Results

Figure 40 shows the signal-to-noise ratio of the sensors with and without ground layer for the various activity conditions. In all conditions, the sensor with the shielding layer achieved a high signal-to-noise ratio (SNR), with average values ranging between 52.6 and 31.6. While the results show a decrease in SNR in the case of body movement (C5 and C6) and external EM noise (C4), all values are considerably higher than 15, which is the minimum requirement for having robust touch sensing [79]. In contrast, the sensor without shielding layer had insufficient SNRs, ranging between 2.4 and 5. A two-way ANOVA confirmed a significant main effect of shielding ($p < 0.001$, $F = 639.1$). Overall, these results show that the shielding layer effectively shields the influence of body capacitance and ensures accurate functioning of the body.

5.6.2 Study 2: Flexibility and Scalability

Multi-Touch Skin will be deployed on different curvature conditions on the body and will need different scales to fit body locations. We set out to investigate how

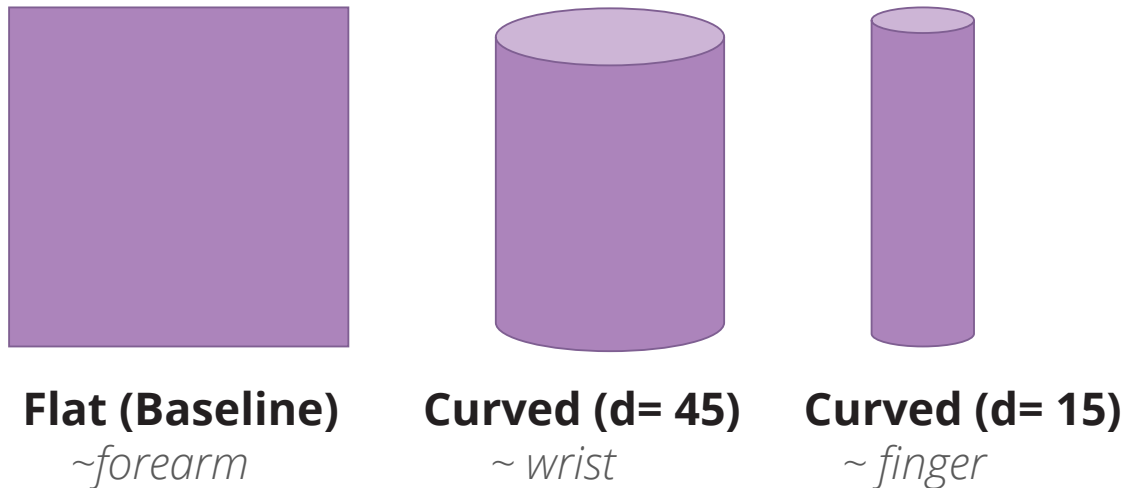


Figure 41: Illustration of the three different curvature conditions evaluated for investigating the flexibility of the sensor. Each of the curvature condition reflects placement on forearm, wrist and finger respectively.

these conditions affect the spatial accuracy of touch input.

5.6.2.1 Methodology

We conducted a technical evaluation with three curvature conditions and three sensor sizes (3×3 factorial design) to evaluate the flexibility and scalability of the sensor. The curvature conditions are informed by the curvature of body locations that are commonly used for skin interfaces: fully flat state (C_1); curved with a diameter of 45mm to reflect the typical curvature of a human wrist (C_2); and curved with a diameter of 15mm to reflect the typical curvature of a human finger (as shown in Figure 41. The scalability conditions were chosen to reflect placement of the sensor on the fingertip (2×2 electrodes with 15×15 mm size), on the wrist (4×4 electrodes, 30×30 mm), and on the forearm (6×6 electrodes, 45×45 mm). The flat condition (C_1) was chosen as the ground condition to comparatively assess the potential detrimental effects of curvature.

Testing the sensor with the human body would have created multiple sources of strong bias that would have been impossible to control: First, prior work has shown that the human error of touch targeting is 1.6mm [174]. As the expected accuracy of our sensor is higher, we would have studied human accuracy rather than the sensor's accuracy. Second, affixing the sensor on a natural body location would have made it impossible to control the curvature and angle of contact, because of continuous variations of curvature and underlying tissue at a given body location as well as involuntary body movements.

To ensure a controlled experiment setup and to be able to test the sensor's accuracy at an mm-scale, we, therefore, opted for a technical study. The sensor was affixed to a 3D printed flat (C_1) or cylindrical object (C_2 and C_3), while touch

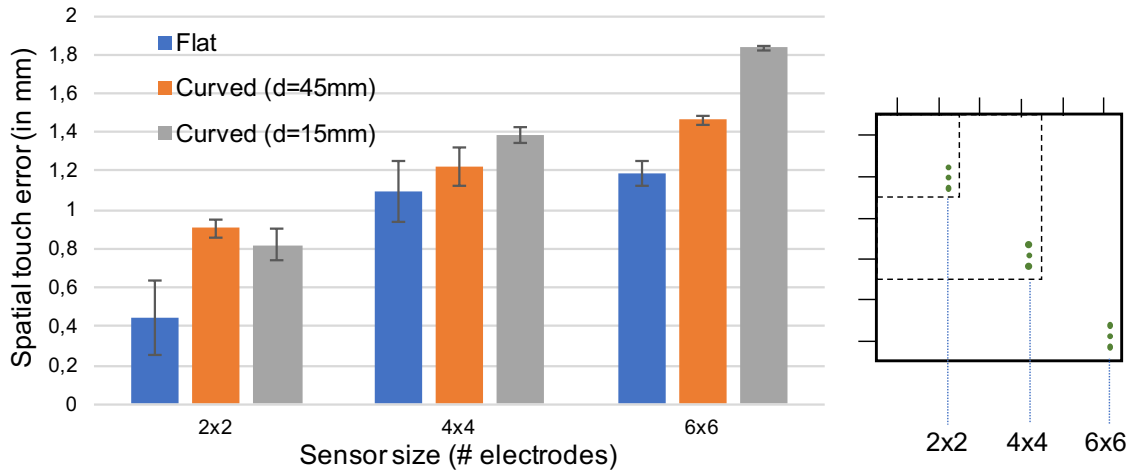


Figure 42: (a) Spatial accuracy of touch contact for different sensor sizes and curvatures. (b) The green dots show the locations on the sensor matrix which were used for evaluating the spatial accuracy.

input was performed with a conductive stylus (diameter 6mm). We verified the capacitive signal generated by the stylus is similar in intensity to a typical touch contact of a human finger. To ensure precise and reproducible measurements, we laser-cut stencils made of transparent acrylic (thickness 3mm) with holes on the target locations. Touch input was performed inside the holes with the stylus. The sensor was marked with visual markers for precisely aligning the stencil.

For each curvature condition, we measured the spatial accuracy on the sensor which reflect scale conditions 2×2 , 4×4 and 6×6 . We opted for locations that are farthest from the signal driving lines because this is the location on the sensor that has the lowest spatial accuracy. For each scale \times curvature condition, we tested three locations that were placed with 2mm distance. The locations are shown in Figure 42(b). At each of these locations, we captured three trials of two-second-long touch contact. The touch controller IC samples at 100fps , resulting in 200 data points per trial.

Overall, this resulted in 3 (curvature conditions) $\times 3$ (scale conditions) $\times 3$ (locations) $\times 3$ (trials) $\times 2$ (seconds) $\times 100$ (fps) = $16,200$ data points for our analysis. For each sample, we calculated the distance between the actual location and the interpolated location that was calculated from capacitive sensor data.

5.6.2.2 Results

The results are depicted in Figure 42. An ANOVA identified a significant main effect of curvature ($p < 0.001$, $F = 15.53$) and of sensor size ($p < 0.001$, $F = 48.39$). Not surprisingly, accuracy is highest in the flat state (avg= 0.91mm , SD= 0.41) and lowest in the most deformed state (avg= 1.35mm , SD= 0.45). Likewise, accuracy decreases with increasing sensor sizes, averaging between 0.72mm (SD= 0.28) for the 2×2 sensor and 1.49mm (SD= 0.29) for the 6×6 sensor. The lowest accuracy we

measured was 1.83mm , for the largest sensor in the most deformed state. This demonstrates that the sensors support high-resolution input in all curvature and scaling conditions. As shown in Figure 42, the smallest sensor has a sub-millimeter accuracy in all deformation states. This implies it can be used for highly precise micro-gestures, e.g., when placed on the fingertip or the finger's side.

To test whether these findings generalize to multi-touch input, we performed an additional small experiment. We compared the change in the reported locations of a touch contact when no other finger was touching the sensor and when another finger was touching the sensor on the same transmitter line or the same receiver line. We did not see any significant change. This was expected, considering the sensor is using time-division multiplexing and sequentially measuring the mutual capacitance at each cross-section. Contrary to self-capacitance sensing, the effect of a second finger on mutual-capacitance is much lower and thus can be easily discarded in the filtering phase of processing. Minimum spacing between touchpoints is hard to formally evaluate (effects of angle, pressure, etc.), but we can anecdotally report that the sensor detects two distinct blobs at a distance of $\sim 7\text{mm}$ between their centers (shown in Figure 38(a)).

5.6.3 Study 3: Evaluating Tactile Input Modalities

Multi-Touch Skin is very thin and worn directly on the body. The body capacitance of a person can change rapidly and in an unpredictable way. Therefore, it must be investigated if the shielding layer can effectively guard sensor readings from such changes.

5.6.3.1 Methodology

In a third evaluation study, we investigated the classification accuracy of the tactile modalities. To account for varying body capacitances across users and possible influences that stem from individual body geometries and skin properties, we performed a controlled experiment in which the sensor was deployed on human users.

We recruited 10 participants (5 female, mean age 27.4, $SD = 3.5$). We used a 6×6 matrix with 45×45 mm dimensions and a 5mm electrode size. The sensor was affixed using a skin-safe adhesive onto the non-dominant forearm of the participant. The participants were seated in a chair with their forearm rested on the desk. The sensor was connected to the Microchip MTCH6303 mutual-capacitance touch controller with Transmit Booster (MTCH652). For data logging, the controller was connected to a desktop computer via USB.

Initially, the experimenter calibrated the sensor by adjusting the mutual capacitance threshold values for the user to account for the varying body capacitance for each user. The participant was informed about the functionality of the sensor and was asked to try using the sensor by performing some multi-touch input.

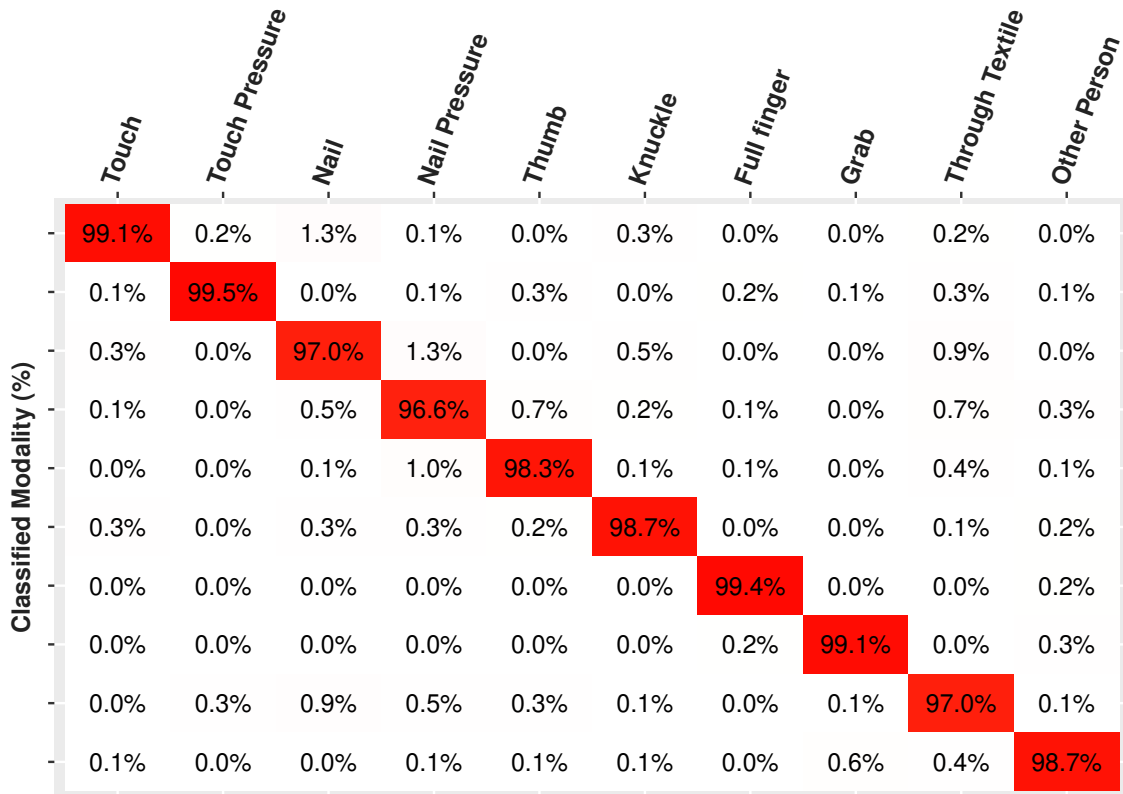


Figure 43: Confusion matrix showing the accuracy of all the input modalities.

For each of the input modalities, there was a training phase and the test phase. During the training phase, the participant tried performing the input modality. When s/he felt comfortable performing the input modality, s/he advanced to the test phase where the data was logged. For each of the input modalities, the participant performed three trials of 2 seconds long each. The participants could perform the input at any location on the sensor.

The data was recorded at 100 frames per second, resulting in overall 100 (frames) x 2 (sec.) x 3 (trials) x 12 (input modalities) x 10 (participants) = 72,000 data points. The entire study was done with a single sensor. To investigate the effects of changing body capacitance over time, two of the participants were asked to be present for a second evaluation after three days, in which they performed the same tasks. Each session took approximately 30 minutes.

5.6.3.2 Results

Results of our modality classification are shown in Fig. 43. All modalities could be classified with high accuracy of 97.0% or above.

In order to evaluate the robustness of our classification method over time, we selected two subjects from the original data set and collected data for all the modalities after three days from the initial study date. We tested the classification

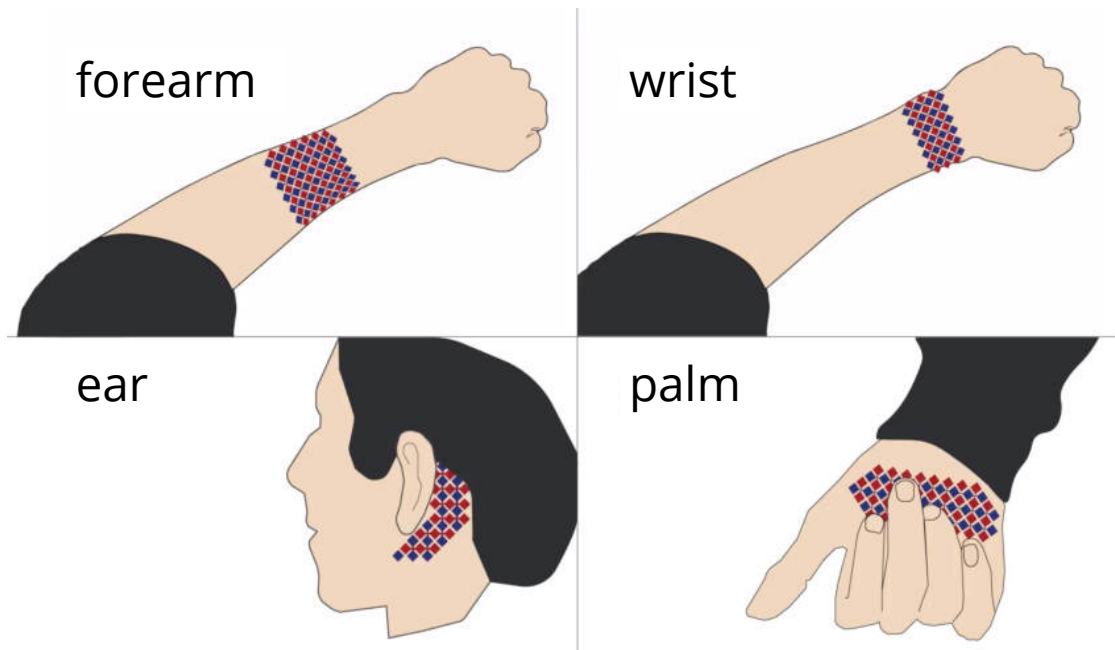


Figure 44: Multi-Touch Skin can be customized to multiple body locations. Four different body locations which were used for deploying Multi-Touch Skin

accuracies of new data against the initial training data set. The results were comparable and did not produce any significant difference to the initial accuracies.

5.7 APPLICATION EXAMPLES

To validate the fabrication approach for customized multi-touch sensor skins and to illustrate practical application scenarios, we have implemented four interactive application examples. These demonstrate the flexibility of the fabrication approach to realize various sensor sizes and shapes that are tailored for use on multiple body locations.

5.7.1 *Multi-Touch Input on the Forearm*

The forearm is one of the most prominent body locations which has been explored in HCI research. We realized a Multi-Touch Skin sensor with a 6×6 matrix of $45 \times 45 \text{mm}$ size that can be worn on the forearm (Figure 32(a)). It is used for expressive gestural input for remote communication. Prior work has identified expressive ways of skin input for remote communication [499]. The rich mutual-capacitance data of our sensor matrix now allows for the first time to detect such expressive gestures in a functional system. In addition to high-resolution single and multi-contact input, we can make use of the different blob signatures depending on the way the user touches the sensor. In our application, gestures are

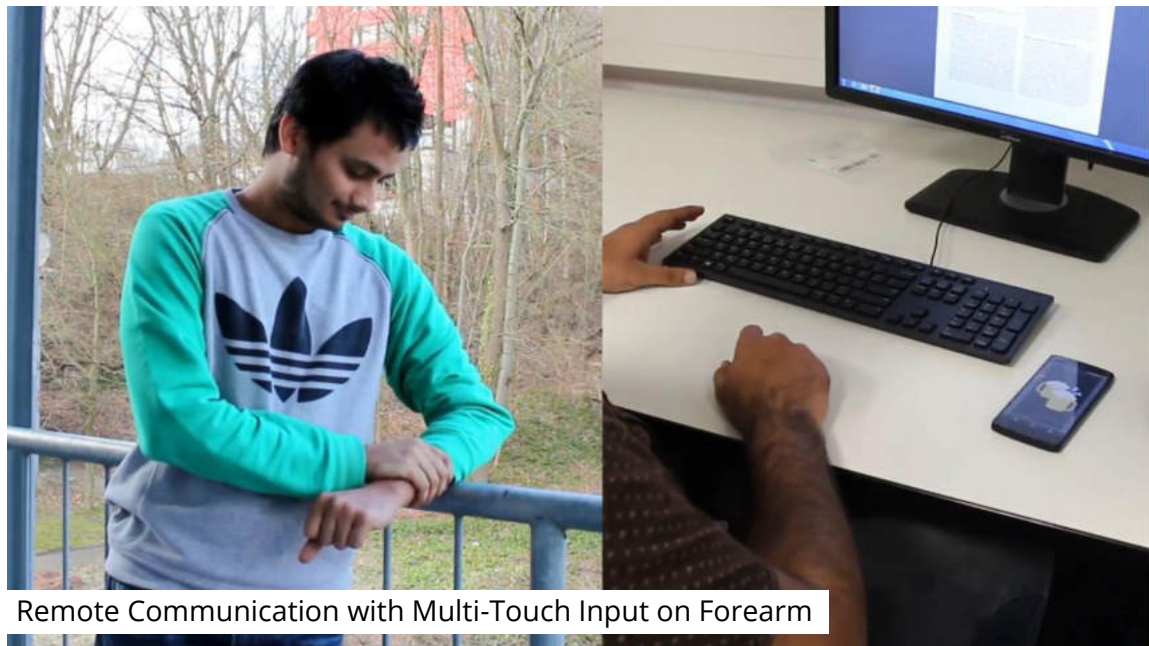


Figure 45: Multi-Touch Skin deployed on the forearm can be utilized for expressive remote communication. In this specific example, a remote user wearing a multi-touch sensor on his forearm performs a “grasp” gesture (covering his entire sensors with his hand) to send an invite to his friend for a party.

mapped to meaningful messages at the remote end. For instance, a grab gesture can be performed by covering the entire sensor with the hand to send a party invite to a friend as shown in Figure 45.

5.7.2 Multi-Touch EarStrap

Inspired from previous research on ear-based interfaces [281, 498], we fabricated a Multi-Touch Skin sensor in a non-rectangular form factor that fits behind the ear. The sensor features a 5×7 grid and has a tapered shape to match the body location (Figure 32(c)). Extending beyond prior work, it can detect continuous input along two dimensions and different types of touch contact: The user can swipe up or down to continuously set the volume. Swiping left and right switches between tracks as shown in Figure 46. Placing the entire finger flat on the sensor can pause the music track.

5.7.3 One-Handed Input while Holding an Object

The bottom area of the hand’s inner side is a promising, yet under-explored area for body-based interaction. It is accessible for multiple fingers, even while holding a thin object, such as a bag’s handle or a pen. We realized a non-rectangular

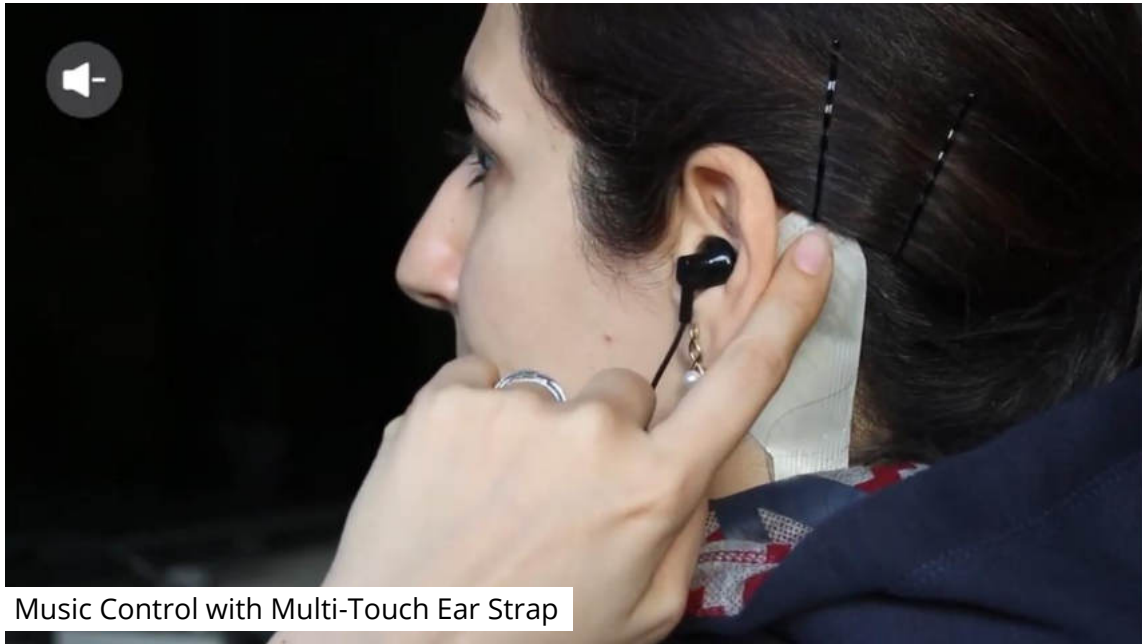


Figure 46: Multi-Touch Skin deployed on the ear to support quick access to music control. In this specific scenario, the user can perform a simple vertical and horizontal swipes to control volume or to switch music tracks.



Figure 47: Multi-Touch Skin deployed on the palm to support quick and always available input while the hands are busy. In this specific scenario, the user can perform a multi-finger tap to accept or reject calls.

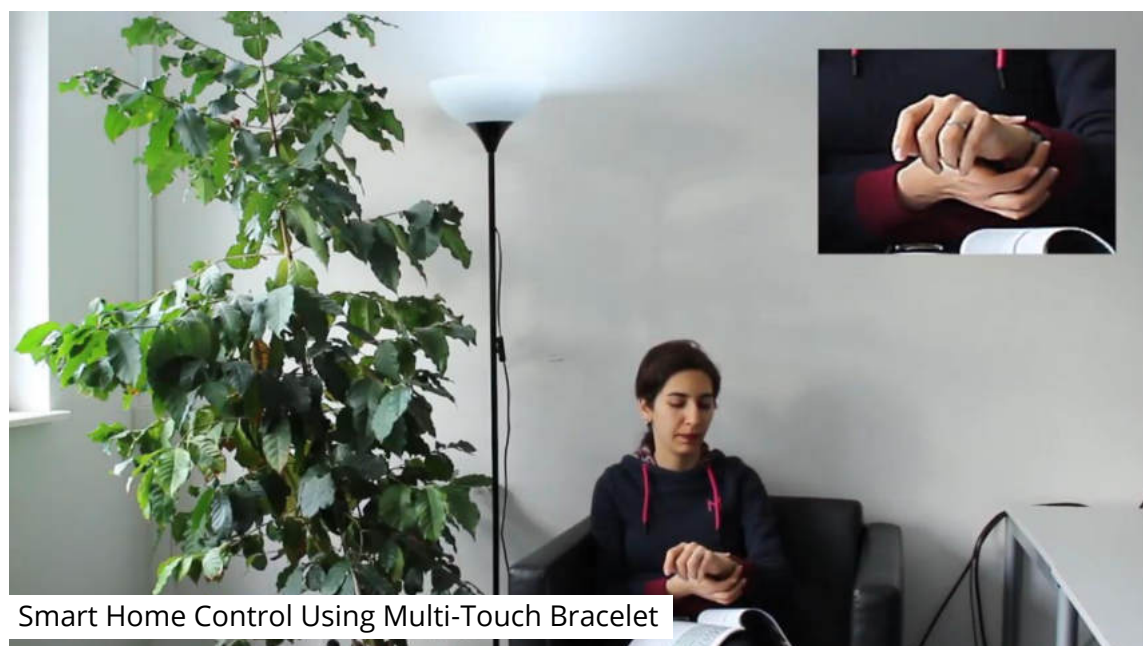


Figure 48: Multi-Touch Skin deployed on the wrist as a bracelet can be deployed in Smart Home applications. Through the Multi-Touch Bracelet, the user can control the brightness of the lamp through expressive multi-touch gestures (inset).

Multi-Touch Skin sensor for this body location, designed such that it does not occlude the palm's area. It features a 10×6 matrix with $101 \times 65\text{mm}$ in size (Figure 32(d)). In our application, the user can easily accept or reject calls when the hand is occupied, by tapping with one or two fingers on the sensor (see Figure 47. This extends the set of interactions for palm-based input [90, 141, 478].

5.7.4 *Multi-Touch Bracelet*

Previous research realizes touch buttons and single-touch sliders on a watch strap [367]. We improve by realizing a Multi-Touch Skin sensor for the wrist. The sensor features a 8×3 matrix and is $77 \times 25\text{mm}$ in size (Fig. 32(b)). In our application, the user controls a smart lamp (Philips Hue), interfaced via wifi. The user can place two fingers around the wrist and rotate to change the color of a light bulb. Swiping alongside the bracelet with two fingers controls the brightness of the lamp. Using two contacts instead of only one reduces the likelihood of false activation.

5.7.5 *Eyes-Free Text-Entry on a Fingertip Keyboard*

One-handed micro thumb-tip gestures offer new opportunities for fast, subtle, and always-available interactions especially on devices with limited input space

(e.g., wearables). Using the thumb-tip for text entry on the index finger has several unique benefits. First, the text input can be carried out using one hand, which is important in mobile scenarios, as the other hand can be occupied by a primary task. Second, the text input can be carried out unobtrusively, which can be useful in social scenarios, such as in a meeting, where alternative solutions, like texting on a device (e.g., smartphone or watch) or using speech may be socially inappropriate or prone to exposing the users' privacy. Third, the text input can be carried out without looking at the keyboard (referred to as "eyes-free"). This can lead to better performance than eyes-on input [561] and save screen real estate for devices with limited screen space. *TipText*³ is a one-handed text entry technique designed for enabling thumb-tip tapping on a miniature fingertip keyboard on the index finger. *TipText* features a QWERTY keyboard, familiar to most of today's computer users, in a 2×3 grid layout residing invisibly on the first segment of the index finger. The design of the grid layout was optimized for eyes-free input by utilizing a spatial model reflecting the users' natural spatial awareness of key locations on the index finger. The efforts of learning to type with eyes-free is largely minimized.

The design of the miniature keyboard was obtained following a series of user studies and simulations. In the first study, data was collected to understand eyes-free typing using a thumb-tip keyboard with 26 keys to inform the final keyboard design. In the next step, we explored the second option, where a keyboard design incorporates a grid layout. In this layout, keys are larger to facilitate tapping but smaller in quantity to fit themselves into the same rectangular input space of the QWERTY keyboard. T9 is an example of this approach. The major challenge of this approach is to find a keyboard layout that provides an optimal balance between tapping precision and input ambiguity. Since there are a large number of possibilities (1,146,484) of dividing the keyboard into a grid and assigning 26 letters to each of the keys in the grid, a software simulation approach was utilized in which the performance of all the possibilities was compared based on their theoretical performance. Once this was done, the top three best candidates were chosen. A second study was conducted to derive a general spatial model per grid layout. It was then used along with the language model to form a statistical decoder, which was used in the next simulation test to identify the most suitable keyboard design. Once the most suitable layout was identified, the *TipText* hardware was suitably fabricated for implementing the keyboard layout. Finally, we conducted another text-entry user study to evaluate the performance of *TipText*. We were also interested in measuring how well our keyboard design worked on a current state-of-the-art micro thumb-tip gesture sensor. The average speed of *TipText* was 11.9 WPM but participants were able to achieve 13.3 WPM in

³ This work is based on UIST'19 publication *TipText* [525] led by Zheer Xu and Pui Chung Wong from Dartmouth College, USA. I collaborated with HCI researchers from Dartmouth College led by Prof. Xing-Dong Yang to design and build the minimalistic epidermal touch sensor which was subsequently used for data collection in the publication.

the last block during the user study. This is faster than the existing finger-based one-handed text-entry technique, FingerT9 (5.42 WPM), which uses the entire body of all four fingers as the input space for a keypad. The performance of *TipText* is also comparable with DigiTouch [507], a bimanual text entry technique using the fingers of both hands (avg. 13 WPM). In the context of mobile scenarios, *TipText* has the advantage of freeing the other hand of the user for other tasks, such as carrying shopping bags. Note that our observation suggested that participants were able to pick up *TipText* fast even without seeing a keyboard. This is promising in the sense that *TipText* might be a good option for ultra-small devices without a screen. Our result shows a trend for this speed to continue growing, which suggests that expert performance could be even higher, warranting a longer-term study

In the next section, we detail the fabrication and hardware implementation of *TipText*.

5.7.5.1 *TipText* Hardware

We developed an interactive skin overlay for *TipText*. The thin and flexible device measures 2.2 × 2.2cm. It contains a printed 3×3 capacitive touch sensor matrix. The sensor features diamond-shaped electrodes of 5 mm diameter and 6.5mm center-to-center spacing. Our sensor development went through an iterative approach. We first developed a prototype using conductive inkjet printing on PET film using a Canon IP100 desktop ink-jet printer filled with conductive silver nanoparticle ink (Mitsubishi NBSIJ-MU01) [222]. Once the design was tested and its principled functionality on the finger pad confirmed, we created a second prototype with a flexible printed circuit (FPC), which gave us a more reliable reading on sensor data (Figure 8b). It is 0.025 – 0.125 mm thick and 21.5mm × 27mm wide. Finally, we developed a highly conformal version on temporary tattoo paper (30-50 μm thick). We screen printed conductive traces using silver ink (Gwent C2130809D5) overlaid with PEDOT: PSS (Gwent C2100629D1). A layer of resin binder (Gwent R2070613P2) was printed between the electrode layers to isolate them from each other. Two layers of temporary tattoos were added to insulate the sensor from the skin.

The finished sensors were controlled using an Arduino Nano with an MPR121 touch sensing chip. The raw capacitive data from each channel was transmitted at a frequency of 100Hz. Software that interpolates the electrode data was implemented in C# based on the algorithm described in the touch controller spec sheet. The sensor fabricated on the FPC (flexible printed circuit) was used for collecting the We tested *TipText* on the FPC and tattoo version and decided to use the FPC version for our user study due to its mechanical robustness and durability.

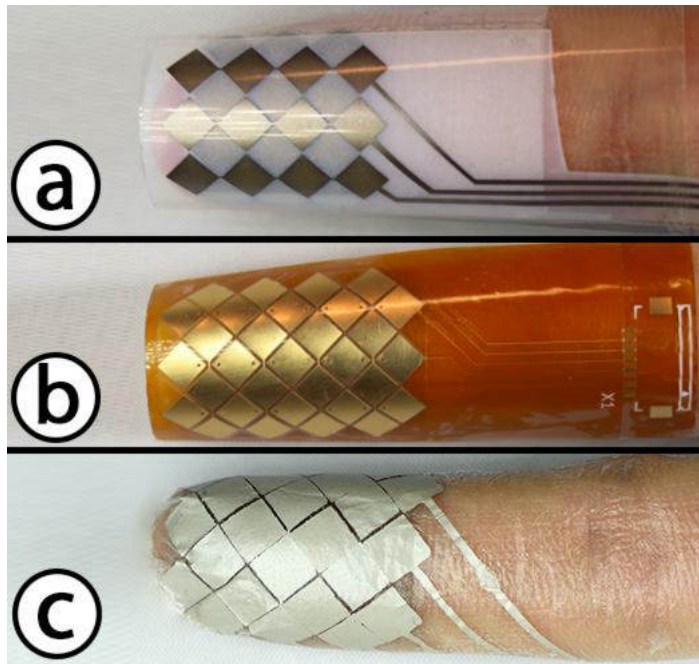


Figure 49: (a) first prototype with PET film; (b) second prototype with FPC (flexible printed circuit); (c) third prototype on temporary tattoo paper.

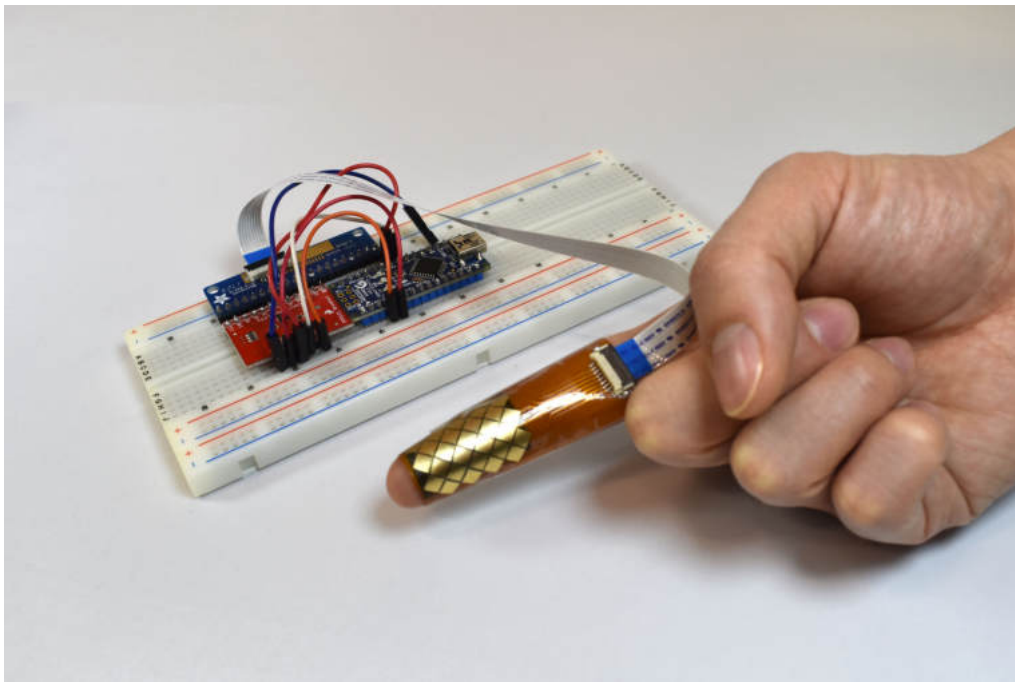


Figure 50: (a) first prototype with PET film; (b) second prototype with FPC (flexible printed circuit); (c) third prototype on temporary tattoo paper.

5.8 DISCUSSION, LIMITATIONS AND FUTURE WORK

Extreme deformations: The evaluation results showed that the sensor accurately captures touch input despite strong curvature, as it occurs for example on the finger. If worn on a joint, such as the wrist, local maxima of curvature can extend beyond this. It remains to be formally investigated to what extent the sensor can withstand such strong and repeated deformations, and if the functionality is affected. Anecdotally we can report that we tested the sensor when placed on the wrist. Despite strong bending, which created a fold on the sensor, it correctly detected touch input at all areas, except on the fold itself. The fold showed a unique capacitive signature, which lets us believe that future generations of sensors might be able to detect their deformation.

Scalability: We have formally evaluated sensor scalability up to a size of 6×6 . This reflects a typical size on many body locations. We have also realized a functional 10×6 sensor prototype. This is hinting at higher scalability but needs to be formally evaluated. Technically, the controller we used can support up to 27×18 electrodes. An important limitation of all today's skin electronics is the connection between the flexible sensor and the rigid controller. This provides a practical barrier to upscaling to significantly larger sizes. With the FFC-based connector, we have presented a novel solution that makes it easier for the HCI community to connect larger sensors.

Design tool: The design tool is limited in that it only considers full electrodes. Future versions could also consider placing partial electrodes or having non-uniform electrode sizes to more closely match the desired sensor's shape. Moreover, they could optimize the shape of the sensor and the controller placement to realize a high-quality result without design iterations. Moreover, future implementations could realize the tool as a plug-in for a vector graphics application, or even include body scanning [340], to ease design and iterative refinement.

Extended Usage: Our preliminary observations show that Multi-Touch Skin is robust and is functional over multiple days. This is supported by the fact that for study 1, we used the same sensor sample for all users; furthermore, in an informal study, three users wore the sensor on the forearm for half a workday (4-6 h) in an office setting. At the end of the experiment, we also gathered feedback on the ergonomics of the sensor. The user feedback was positive in general, highlighting the minimal invasiveness of Multi-Touch Skin. For instance, one of the participants stated: "The sensor is really thin, fits onto the skin and I cannot feel it doing my everyday tasks (P1)". These anecdotal findings show the potential of Multi-Touch Skin for using it on a daily basis. However, a more extensive "in-the-wild" investigation is required to properly understand the usability and functionality of the sensor under extended physical activities.

Accidental Input: One of the common problems of the on-skin touch input is accidental input which creates false activations. This can be a problem for Multi-Touch Skin as well. From our tests and evaluation, Multi-Touch Skin does

not get activated when there is a thick textile overlay, e.g. the sleeve of a sweater. Apart from this, the higher resolution of the sensor enables the designers to design advanced unlocking gestures which can resist false activation, which is not possible with a single electrode, self-capacitance-based touch buttons. Another approach to reduce or eliminate accidental input is to perform a longitudinal study to investigate the commonly occurring gestures in daily life and design a gesture set that avoids those.

5.9 CONCLUSION

This chapter presented Multi-Touch Skin, the first high-resolution multi-touch sensor for the body based on the principle of mutual capacitance sensing. Multi-Touch Skin is thin, flexible, and adapts to the deformable geometries of the body. A fixed potential layer added to the Multi-Touch Skin sensor makes it robust to the electro-capacitive effects of the body and makes it functional when applied to the body. Through systematic material exploration, we present multiple fabrication techniques for realizing multi-touch sensor matrices that function on the human body. To support the unique interaction affordances provided by the body, Multi-Touch Skin enables a wide range of tactile input modalities such as multi-touch, nail input, knuckle, thumb, pressure input, full-finger, and grasp input. We also presented the first computational design approach for fabricating epidermal devices. The design tool presented in this chapter assists the designer to generate multi-touch sensor designs of non-rectangular shapes. The design tool abstracts the lower-level electrode design from the higher-level design objectives reducing the expertise required for designing custom multi-touch sensors.

Three evaluation studies have been conducted to investigate the performance aspects of Multi-Touch Skin: 1) Evaluate the performance of the shielding layer in filtering the electro-capacitive effects of the body. This experiment was performed under six different grounding conditions 2) A second experiment was conducted to investigate the scaling and the flexibility aspects of the sensor. The spatial accuracy of the sensor was measured in three different curvature conditions, and 3) In the third experiment, the recognition of tactile input modalities was studied with ten participants. Results from these experiments show that Multi-Touch Skin sensors can achieve high-touch SNRs in varying grounding conditions. The spatial accuracy of the sensors is also very high indicating that these can be utilized for high-resolution touch input. Finally, with a high recognition accuracy of $\sim 97\%$, the sensor can successfully sensor ten different tactile modalities.

Taken together, Part 2 (Chapters 4 and 5) of this thesis has shown that Epidermal Devices can enable rich on-body interaction. The fabrication techniques presented in these chapters rely on simple lab equipment. Through a systematic exploration of functional materials, we provide fabrication recommendations for realizing these devices. These chapters also highlight the balance and trade-offs that need to be maintained between a high degree of skin conformality, mechanical robustness,

and the requirements of the desired application. SkinMarks devices are highly skin-conformal but do not possess a high level of mechanical robustness, while Multi-Touch Skin can be fabricated with multiple levels of mechanical robustness. The devices also possess higher levels of flexural rigidity in comparison to SkinMarks devices owing to the multiple layers of sensor sandwich (transmitter, receiver, and dielectric layers) that need to be fabricated. These observations are inline with the recommendations from Chapter 3 which highlights the trade-offs that are influenced by multiple factors such as the device type, desired skin conformality, and mechanical robustness.

One crucial advantage of epidermal devices is that they are in close contact with the body. Hence apart from serving as rich media for interaction, they can also be utilized for sensing vital bio-signals from our body. The next part of this thesis (Chapters 6 and 7) shows how epidermal devices can be designed and fabricated for sensing bio-signals from our bodies.

Part III

Part Three - Epidermal Devices for Physiological Sensing

RAPID FABRICATION OF SKIN-CONFORMAL PHYSIOLOGICAL INTERFACES

Physiological sensors are recently receiving increasing attention in the broad field of computing. While long used in areas related to health and rehabilitation [363], we are now witnessing an impressive array of new applications in interactive computing [36, 83, 121]. For instance, surface electromyography (sEMG) allows for detecting gestural input using unobtrusive wearable hardware [329, 405]. Continuous monitoring of electrocardiogram (ECG) signals informs athletes about their performance [167] and monitoring of electrodermal activity (EDA) enhances computer-mediated emotional communication [29, 36, 121, 402]. In parallel, accessible hardware platforms and toolkits make it easier than ever to implement interactive systems that include physiological sensing [1, 11, 325, 424, 434].

Despite these advances, designers seeking to develop new applications are confronted with serious restrictions at the level of the computer-body interface: commercial gel-based electrodes are non-conformal, problematic at locations that deform, and neither ergonomic nor aesthetic to wear during everyday activities. The materials community has contributed several devices that are ultra-thin and can sense multiple physiological modalities [105, 239]. However, these devices require complex fabrication processes and advanced lab equipment, which are typically inaccessible outside of specialized labs. These advanced fabrication techniques also require expertise and domain knowledge in multiple disciplines (materials science, biomedical engineering) which can make it even harder for designers, practitioners, and makers in realizing custom physiological sensing solutions.

To address this problem, we present PhysioSkin¹. We demonstrate that established digital fabrication techniques support printing customized electro-physiological sensor patches with advanced material properties that allow for accurately capturing EMG, ECG, and EDA signals. These patches readily work with off-the-shelf commodity physiological sensing toolkits (e.g. Sparkfun, Olimex,

¹ This chapter is based on [338]. As the first author, I led the conceptual design, development of design, and fabrication process for realizing the electro-physiological sensors, performed the literature survey to identify the design recommendations, conducted the technical experiments, and realized the application scenarios. Dr. Arshad Khan helped in setting up the conductive inkjet printer, helped in fabricating the devices, and in shooting the video along with student assistant Muhammad Hamid. Dr. Klaus Kruttwig prepared the soft skin adhesives that were used in the experiments and the application scenarios. My advisor Jürgen Steimle advised me on the conceptual design, fabrication, evaluation, and applications. He further contributed to the structure and writing of the publication.

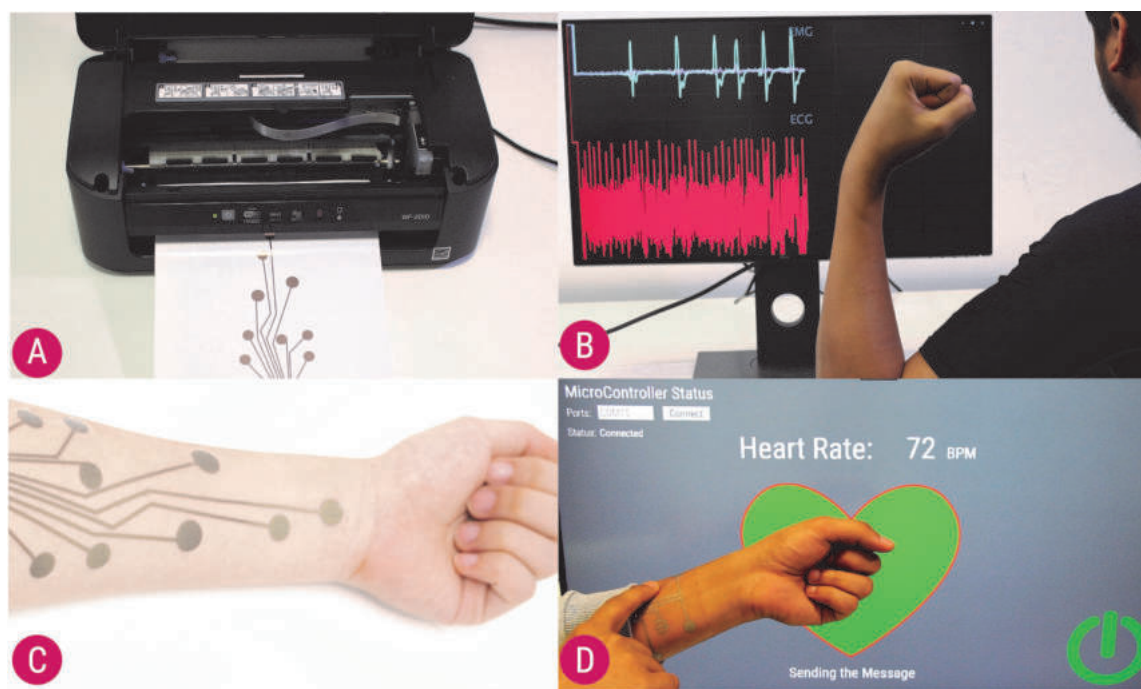


Figure 51: (a) PhysioSkin enables digital fabrication of custom electro-physiological sensing patches for monitoring EMG, ECG and EDA. (b) A custom made skin-conformal sensor. (c) A fitness tracking sportswear tracks heart rate and muscle movements. (d) Raw signal of the heart rate recorded from a temporary tattoo.

Seed Studio), eliminating the need for building custom PCBs and offering a rapid end-to-end pipeline for electro-physiological sensing.

The main contributions of this chapter are:

1. We show that the digital fabrication of skin-conformal physiological sensing patches with advanced material properties is possible within 5-20 minutes, using a desktop inkjet printer and simple lab equipment. Through a systematic exploration of materials, functional inks, and skin adhesive materials, we present multiple fabrication approaches for sensors of customized thickness, stretchability, durability, and reusability. These realized sensors are integrated into ultra-thin temporary tattoos ($\sim 1\mu\text{m}$), in stretchable TPU and PDMS materials, and textiles. Our sensors contain dry electrodes and are orders of magnitude thinner than current off-the-shelf gel-based electrodes.
2. Technical evaluation results demonstrate that sensors fabricated using these techniques achieve high a signal-to-noise ratio for EMG and ECG signals and a high Pearson correlation coefficient (with respect to commercial gel-based electrodes) for EDA signals.
3. We show how sensing of multiple electro-physiological modalities (sEMG, ECG and EDA) can be integrated in a single patch. We furthermore demonstrate how

to integrate electro-physiological sensing with user interface controls for touch input.

4. Informed from the literature in biomedical engineering, we compile coherent design recommendations for the design of electrodes for each of the modalities to pick up high-quality signals.

5. We demonstrate the practical feasibility and versatility of our approach by implementing three example applications: a textile vest for fitness tracking, a temporary tattoo for heart rate monitoring, and a PDMS-based patch for arousal logging in virtual reality environments.

6.1 RECOMMENDATIONS FOR DIGITAL DESIGN

The electro-physiological sensors investigated in this chapter work by capturing electrical biosignals with electrodes on the human skin. A prerequisite for capturing high-quality biosignals is to place electrodes at carefully chosen locations. Our approach allows the designer to define these in a digital design, made in any 2D vector graphics application. In contrast to manually placing electrodes on the body, the digital design offers both precise control and replicability.

Surface electromyography (sEMG) records muscle activity by reading the electrical potential generated by muscle cells, using two electrodes per muscle and an additional reference electrode. Electrocardiography (ECG) records the electrical activity of the heart which, amongst others, allows to identify heart rate. While it commonly involves 12 electrodes, a smaller number (3 in our implementation) is viable. Electrodermal activity (EDA) captures skin conductance, which varies with the state of sweat glands, and uses at least two electrodes.

Here we present a set of coherent design guidelines for the electrode design that we have compiled from the body of literature. Critical design choices relate to the size, location, and arrangement of electrodes:

6.1.0.1 *Electrode Size*

The contact area of the electrode influences the quality of the signal. For EMG signal acquisition, the electrodes should have a minimum surface area of 50mm^2 and a diameter of less than 10 mm [163, 315, 566]. For ECG, most prior research has typically designed electrodes in the range of 5–10 mm diameter [381, 382, 389]. For EDA signal acquisition, the recommended surface area is 1.0cm^2 [109]. We therefore select our electrodes sizes to be 10 mm diameter for EMG and ECG, and 12 mm diameter ($\sim 1.08\text{cm}^2$ area) for EDA electrodes.

6.1.0.2 *Location of Electrodes*

For EMG signals, the electrodes need to be placed on the muscle whose movement is to be captured.

For ECG measurements, electrodes are typically placed using the standard 12-electrode placement [198] or based on Einthoven's triangle arrangement [99]. However, alternate placement strategies near both wrists and the forearm have also been suggested [74, 101, 530]. Our approach is based on prior work which designed 3-electrode ECG devices on the forearm [2, 101, 152, 530]. This involves placing two electrodes on the forearm and the third electrode away from these measurement electrodes.

Since EDA electrodes measure the activity of sweat glands, they should be placed at locations that have a high density of sweat glands. The typical recommended locations are fingertips, palm (thenar and hypo-thenar eminence), foot sole and forehead [43, 109]. However, prior work has also investigated the EDA response at various other locations on the body [97], which suggests that other locations such as the forearm and wrist can deliver satisfactory performance, too.

6.1.0.3 *Inter-Electrode Distance*

The distance between the measuring electrodes plays a vital role in signal acquisition. For EMG, the two measuring electrodes should be placed along the direction of the muscle. Their recommended distance depends on how deep the muscle is present beneath the skin. For muscles present on the surface, the recommended inter-electrode distance is 25 mm; for deeper muscles, the distance is 40-50 mm [26, 314, 566]. For ECG measurements, we used inter-electrode distances from prior work [530], where the electrodes were placed around the arm with a distance interval of 3cm. For EDA measurements an inter-electrode distance of 5-6 cm has been successfully used in the previous literature [10, 97].

6.2 FABRICATION

The unique requirement for the fabrication of electro-physiological sensors is the need for low-impedance skin-contacting electrodes. This is in contrast with prior work which contributed on-skin touch sensors [215, 341, 500]. To elaborate, for on-skin touch sensing, the touch electrodes need to be well insulated and shielded from the human skin. This ensures that there is lesser noise resulting from the human body's electro-capacitive effects. On the contrary, for physiological sensing, the electrode needs to have tight low-impedance contact to pick up the bio-signals. This adds challenges, most centrally at the level of electrode materials and skin adhesives, requiring different fabrication strategies.

Commercial solutions typically use electrodes covered by conductive wet gel to improve the electrical contact; however, this makes the practical handling difficult and increases a device's thickness. Our solution uses more practical dry electrodes that we print in custom arrangements using conductive silver ink. The conformal nature of the substrates coupled with ultra-thin conductive traces ensures that the electrodes can successfully capture various bio-signals.

Soft Inkjet Printing					
Substrate	Conductor	Insulation	Skin-Contact	Thickness	Time
Tattoo Paper	Silver + PEDOT:PSS	PVP	Tattoo Adhesive	$\sim 1 \mu\text{m}$	[10-15] mins
TPU	Silver + PEDOT:PSS	PVP	SSA	[50-300] μm	[10-15] mins
PDMS	Silver + PEDOT:PSS	PVP	SSA	Custom Thickness [50-300] μm	[10-15] mins
Textile Transfer Film	Silver	PVP	Form-Fitting Garment	[1-3] μm	[25-35] mins
Instant Inkjet Printing					
Substrate	Conductor	Insulation	Skin-Contact	Thickness	Time
PET	Silver Nanoparticle	Transparent Scotch Tape	SSA	[250-300] μm	[5-10] mins

Figure 52: Overview of fabrication options with Soft inkjet and Instant inkjet printing.

Leveraging on the ease and rapidity of inkjet printing, our fabrication approach builds on printing conductive traces with a desktop inkjet printer, as previously presented by Kawahara et al. [222] and Khan et al. [225]. We contribute a systematic exploration of substrate materials, insulation mechanisms, and adhesion schemes, demonstrating for the first time that desktop inkjet fabrication can realize sensors for various electro-physiological modalities using various materials. This opens up a design space of customized levels of device thickness, elasticity, robustness, and fabrication speed. Figure 52 shows a comparative overview of all substrates and the associated compatible materials. We now present these different options.

Ultra-thin temporary tattoo sensor: Ultra-thin devices ($\sim 3\text{--}4 \mu\text{m}$) are realized by printing on commercial tattoo decal paper (SUNNYSCOPA, Printable Temporary Tattoo Paper for Laser Printer). Using the technique presented by Khan et al. [225], a layer with electrodes and connecting traces is printed using silver nanoparticle ink and heat cured. Optionally, three layers of PEDOT: PSS conductive polymer using the same design can be printed first to enhance the mechanical robustness of the brittle metallic layer. Silver traces, but not electrodes, are then insulated by printing 5 layers of PVP (Polyvinylphenol, $M_w = 11,000 \text{ g/mol}$) on top. The layers are thermally cured, as indicated in [225]. A sheet of skin adhesive film (SUNNYSCOPA) is laser cut to leave electrode locations uncovered and then bonded onto the printed tattoo sheet. The sandwich can then be transferred onto the skin.

Stretchable re-usable sensor using TPU or PDMS: While a tattoo device offers prime skin compatibility, it only supports one-time use. By using thicker elastic materials, superior robustness can be achieved while allowing for removing and reapplying the device. TPU (thermoplastic polyurethane) substrate ($\sim 50\mu\text{m}$ thick, 6.5 MPa) has high elasticity. Using the technique from [225], we print silver nanoparticle ink on TPU with added 5 layers of PVP providing the insulation. The patch can be bonded to the skin using skin adhesive film. Alternatively, one can use Soft Skin Adhesive (SSA) (MG-7-1010, Dow Corning), offering the benefit of applying and re-applying the patches multiple times.

Alternatively, PDMS (Sylgard 184, Dow Corning) offers similar mechanical properties. It is a substrate that has been extensively used for developing a wide range of epidermal devices, across disciplines. It offers great skin compatibility and can be commercially acquired or self-fabricated in custom thickness and stretchability [332]. We cast a custom PDMS film ($\sim 40\mu\text{m}$ thick, ~ 2.7 MPa) using a doctor blade. Similar to TPU, the designs can be printed with conductive inks and applied to the skin. However, as PDMS is hydrophobic a plasma treatment is required before printing on the substrate. For bonding to the skin, we used a layer of SSA as a border dressing. PVP is used for insulation.

Textile-integrated sensor: We demonstrate that printing can realize functional skin-contacting electrodes that are seamlessly integrated on a textile. Informed by [225], we use commercial textile transfer film (SKULLPAPER, Premium Textile Transfer Film) and print electrodes and electrical connections using silver. The electrical connections are insulated by printing 5-6 layers of PVP. We create a negative mask of the design and laser-cut the textile transfer film after printing. This ensures that only the electrodes and traces are transferred onto the textile, leaving all other parts of the textile unaltered. Using an iron, the film is then heat-transferred onto the textile. We recommend this fabrication approach for tight-fitting garments (e.g., bodysuits, sportswear), which ensure tight contact of the electrode with the skin.

Ultra-rapid fabrication with PET film: The last approach supports very rapid fabrication while sacrificing thin and elastic properties. This can be an acceptable trade-off for low-fidelity prototypes during early design stages. The technique uses sinter-free silver-nanoparticle ink, avoiding the need to thermally cure samples, as introduced in [222]. We print on PET film ($\sim 250\mu\text{m}$, 2.5 GPa). For electrically insulating conductive traces from the skin, we cover them using transparent scotch tape ($\sim 50\mu\text{m}$), while leaving the printed electrodes exposed. The printed sheet is adhered to the skin using SSA.

6.2.1 Hardware and Interfacing

We used-off-the shelf commercially available prototyping hardware for controlling our sensors. Olimex EMG/ECG Arduino shields [413] were used for EMG sensing. However, we can anecdotally report that our sensors worked with EMG boards

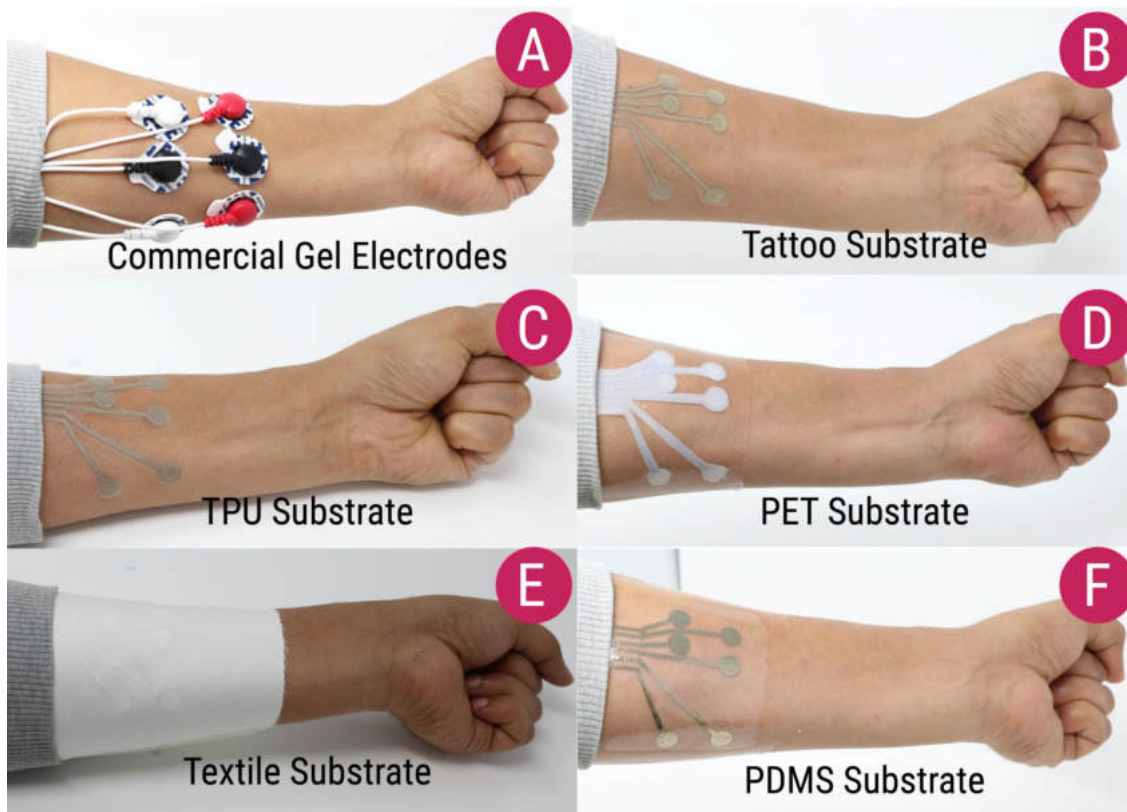


Figure 53: Conformal skin contact made by the electrodes fabricated on all the substrates.

from other manufacturers as well (Seeed Studio, Grove EMG detector [433]). Sparkfun single lead hardware monitor [424] was used for heart rate/ECG signal acquisition. For EDA monitoring, we used Grove GSR sensor [434]. Data is transmitted wirelessly from the Arduino to a laptop computer using Bluetooth low energy. A python script reads the data and offers a web server streaming interface. While our overall hardware setup can be miniaturized using a custom PCB, our goal was to ensure that the PhysioSkin overlays work with off-the-shelf hardware which is easily accessible.

Connections between the sensor patch and the controller hardware are realized using FPC connectors, to ensure a slim and compact design. The FPC connector is bonded to the printed circuit using conductive z-axis tape (Adafruit). Alternatively, connections can be realized using simple copper tape in prototypes that use only a few electrodes.

6.3 ACCURACY OF ELECTRO-PHYSIOLOGICAL SENSING

To understand how well each of these substrate materials monitors bio-signals, we conducted a detailed technical evaluation, with commercial gel-based electrodes as the baseline.

6.3.1 Method

Fabrication approach: We realized one device for each of the fabrication approaches: Tattoo decal paper, PVP, PDMS, textile, PET. The device was bonded to the participant's skin using the respective type of adhesive described above. For the baseline measurements, we used commercial gel-based electrodes (H124SG Covidien).

Sensing modalities: We tested all three modalities: sEMG, ECG, and EDA. For sEMG, the electrodes were placed on the Flexor Carpi Radialis muscle of the dominant arm. We chose this muscle since it aids in the wrist movement (flexion) [120]. ECG was measured with electrodes on the chest following Einthoven's triangle schematic [99]. The EDA electrodes were placed on the thenar and hypothenar eminence of the dominant hand since this region has a high density of sweat glands [109]. For each combination of modality and substrate, we fabricated separate devices. A device contained 3 electrodes for EMG and ECG sensing and 2 electrodes for EDA. The two measuring electrodes for EMG were on the muscle line, while the third reference electrode was placed on the posterior side of the forearm.

Task: The participants were seated in a comfortable position throughout the entire experiment. For EMG signal acquisition, the participant was asked to perform wrist flexion movement (bending the hand at the wrist such that the palm faces the arm) in a comfortable manner, like in prior work [404]. The movement was repeated five times. For ECG signal acquisition, the participant was at rest,

with the hands on the table, while a desktop computer logged the data for 300 seconds. For EDA, the participant underwent a Stroop Color Test [432, 442]. This test has been used in prior work for assessing EDA response. In brief, cognitive stimuli are presented to the subject through the use of words of different colors which are either conflicting (word and color of text are different, i.e., "blue" is written in green color) and non-conflicting (word and color of text are the same). The participant is required to state the color of the word and not read the text. The task consisted of three cycles of 1 min. rest period followed by a Stroop test. This was followed by a final 1 min. rest period. The overall experiment for EDA data collection took 9-12 minutes.

We recruited 8 participants (3 f., mean: 28.5y). The experiment took 90–120 minutes per participant. The order of FABRICATION APPROACH and SENSING MODALITIES were counterbalanced. The data for each of the modalities was sampled at 250Hz. Overall we had 8 (PARTICIPANTS) \times 6 (FABRICATION APPROACH) \times 3 (SENSING MODALITIES) = 144 sets of measurements.

6.3.2 Analysis

For EMG signals, we calculated the signal-to-noise ratio (SNR) using a double-threshold detector as stated in prior work [4]:

$$SNR = 10 * \log\left(\frac{\sigma_s^2}{\sigma_n^2} - 1\right) \quad (3)$$

where σ_s^2 and σ_n^2 are the variances of the ON and OFF states, respectively. The ON state refers to the window where the muscle activity has happened while the OFF state refers to the window where there was no activity.

The signal-to-noise ratio for ECG can be calculated as follows [101]:

$$SNR = \frac{(QRS)ECG_{p-p}}{(T - P)noise_{p-p}} \quad (4)$$

where ECG_{p-p} is peak-to-peak ECG QRS amplitude and $noise_{p-p}$ is peak-to-peak noise amplitude from T-P interval.

For the EDA response, we calculated the Pearson correlation coefficient of each fabrication approach with respect to the baseline condition, based on prior work [143].

6.3.3 Results

Overall, our results show that all fabrication approaches realized devices that can reliably capture bio-signals, with tattoo paper substrates performing the best of all fabrication approaches for all modalities. This can be explained by the fact that it has the lowest flexural rigidity of all materials used ($\sim 10^{-9}Nm$).

6.3.4 SNR of EMG Signals

It is interesting to note that all devices can accurately capture EMG signals. The minimum required SNR for obtaining good EMG measurements was reported to be 20 dB [40]. All our devices achieve SNRs that are considerably higher. PET is lowest (mean: 15.36, SD = 1.81), while Tattoo and TPU come close to commercial wet-gel electrodes. This is impressive considering our devices use dry electrodes. The raw signals for each of the substrate conditions are shown in Figure 54(a). The calculated SNR levels for all the participants are shown in Figure 54(b).

6.3.5 SNR of EDA Signals

For EDA signals, the tattoo substrate achieves a high correlation and lowest deviation (mean: 0.95, SD: 0.01), again coming close to commercial wet-gel electrodes. TPU, PDMS and Textile follow with means close to 0.9, while PET shows the least good result (mean: 0.76, sd=0.03) as shown in Figure 55(b).

6.3.6 SNR of ECG Signals

For ECG signals, the mean average SNR for commercial wet-gel electrodes was 7.45 dB while tattoo-based electrodes had a mean SNR of 6.31 dB. Figure 56(a) shows the smoothed ECG signal after applying Hanning window ($n = 11$). This result is comparable to prior work contributed in the materials community [105]. This suggests that PhysioSkin electrodes can produce meaningful ECG recordings. TPU, Textile, and PDMS follow shortly after, with mean average SNRs between 5.5 and 5.8 dB. As can be seen in Figure 56(b), the captured signal allows to clearly identify heart rate variability. PET has a considerably lower SNR. As evidenced in the plot, the signal cannot be accurately captured with PET. It is to be noted that all these measurements, including those taken with commercial wet-gel electrodes, are not suitable for clinical recordings, since the minimum required SNR for clinical ECG recordings is 20 dB [164]. This would require clinical-grade electrode placement and measuring equipment, which is outside the scope of this work.

6.4 EXAMPLE APPLICATIONS

6.4.1 Fitness Tracking Sportswear

To demonstrate rapid integration of multi-modal sensing in textiles, we implemented a custom sports vest that can track muscle movements and heart rate during exercising (see Fig. 57 and Figure 51 (c)). It uses embedded, conformal textile electrodes and circuitry that is printed and iron-transferred using the method presented above. Locations on the vest were selected such that the electrodes

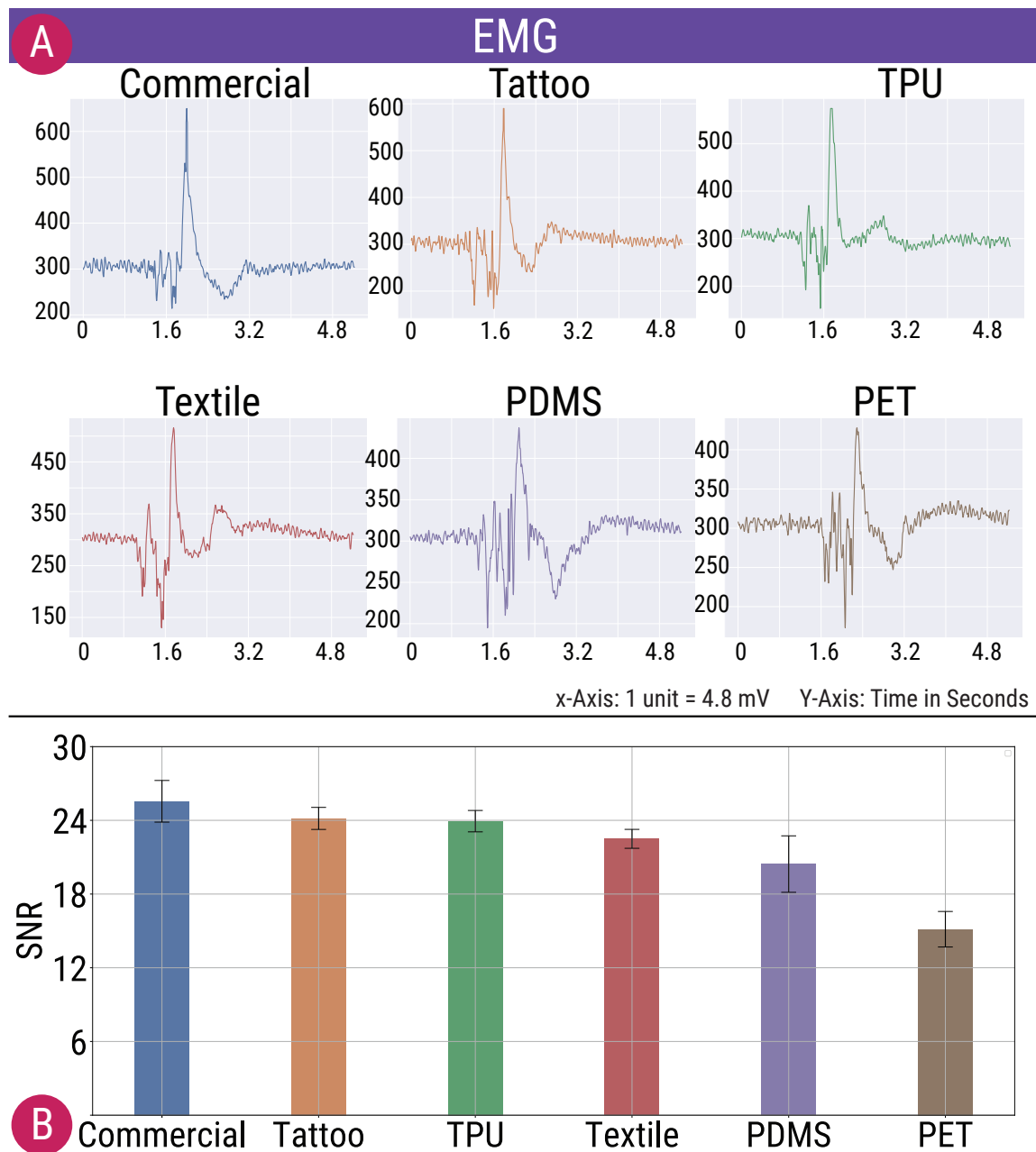


Figure 54: (a) Raw EMG signals for each of the six substrate conditions. (b) SNR levels for each of the conditions calculated for all the participants. Error bars indicate standard deviation.

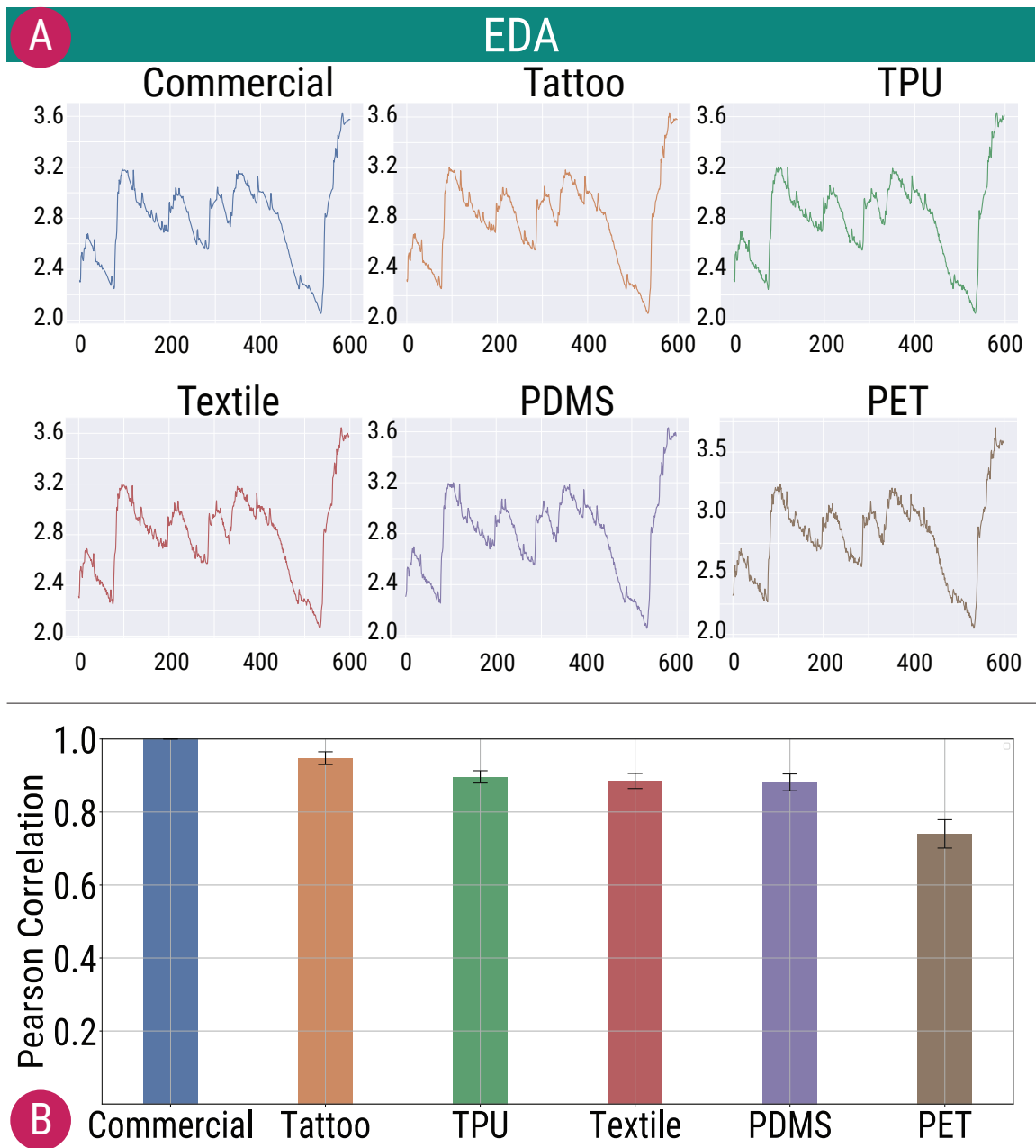


Figure 55: (a) Raw EDA signals for each of the six substrate conditions. (b) Pearson Correlation coefficients between the substrate conditions measured with respect to the commercial gel electrodes. Error bars indicate standard deviation.

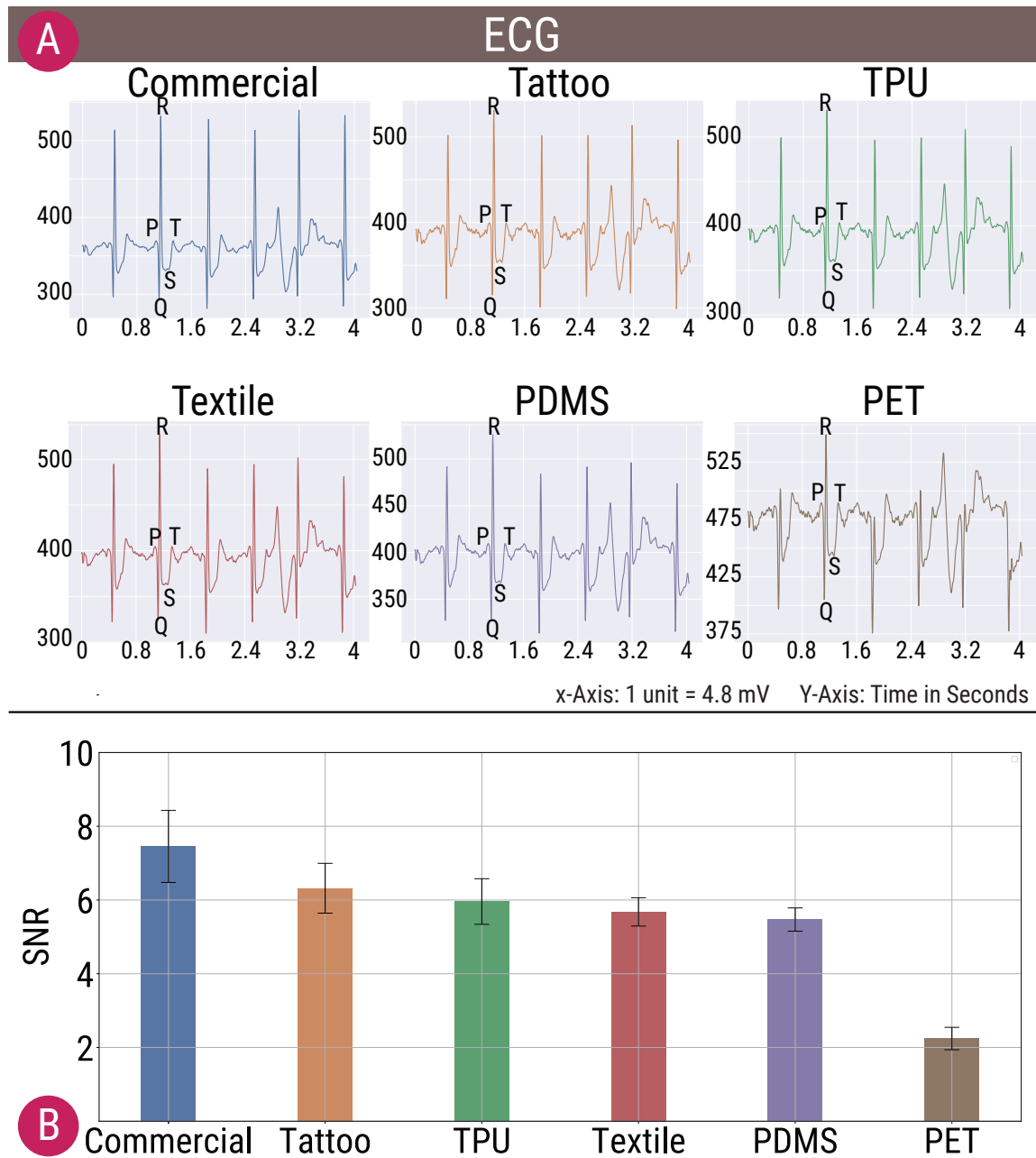


Figure 56: (a) Raw ECG signals for each of the six substrate conditions. (b) SNR levels for each of the conditions calculated for all the participants. Error bars indicate standard deviation.



Figure 57: A fitness tracking vest with electrodes for EMG and ECG sensing.

can have good electrical contact with the body. We chose two muscles for EMG monitoring: *Biceps Brachii* and the anterior part of the *Deltoid* muscle. The electrodes were placed based on the recommendations from prior work [163]. Three electrodes for ECG monitoring were placed near the chest. They are connected to an Arduino using standard copper cables. Once the digital design was made, the overall fabrication took approximately 15–20 minutes.

6.4.2 Interactive Heart Rate Sensing Tattoo

To demonstrate ultra-thin form factors and the ease of integrating input controls, we designed and fabricated a temporary tattoo that can monitor the heart rate activity (Fig. 51 (d)). It further offers two embedded touch sensors for user input. One button is used for emotional communication purposes, allowing one to send one's live heartbeat to a remote loved one. A second button offers privacy options, for turning the sensor on or off. Fabrication took approximately 25-30 minutes (including ~ 20mins of heat curing).

6.4.3 Arousal Logging in Virtual Reality Interaction

Prior work [36] suggested using ECG and EDA to sense emotional arousal and identify the magnitude of the emotional response in immersive VR environments. To realize this approach in a skin-conformal form factor, we implemented a PDMS-based device that can track ECG and the EDA on the forearm. A PDMS-based

device was fabricated based on the method described previously. The entire procedure took approximately 30–35 minutes. In our application, we developed a 360° video viewer which logs the ECG and EDA data while participants are watching the video. This could be utilized for analyzing the arousal patterns.

6.5 DISCUSSION, LIMITATIONS AND FUTURE WORK

EMG Signal Interpretation: The SNR gives a direct correlation with how well the electrodes can pick up muscle activity. From practicality aspect, prior work in biomedical engineering has recommended [40, 283] that a SNR > 20dB is recommended for detecting precise muscle activations while machine-learning based techniques need to be utilized for signals with lower SNRs (>8 dB) [283]. These findings have been confirmed for hand gesture classification, showing a 96% accuracy with 20dB SNR for 7 gestures (1 rest and 6 gestures) using only 4 features [368]. The much higher SNRs identified in our evaluation for all substrate materials (except PET) show that the EMG signals carry enough information for reliable use, e.g., in gesture recognition.

Body Locations: The quality of the signals is dependent on the body locations. In our applications examples, we have deployed the sensors at different body locations. However, the location should be chosen based on the quality of the desired signal. For example, the forearm and wrist are not the most ideal locations for ECG monitoring which results in a noisy ECG signal, however, the heart rate variability can still be detected from the signal due to the QRS peak. For a clean ECG signal with distinguishable PQRST wave, we recommend placing the electrodes near the chest, as in our textile application case.

No clinical-grade monitoring: We use hardware from commercial rapid prototyping kits for acquiring bio-signals, rather than clinical-grade hardware and materials. Our approach should not be used for clinical-grade monitoring. However, our sensors can be useful for interface designers and hobbyists for quickly prototyping custom physiological sensing solutions for entertainment computing, gesture sensing, or fitness tracking. Additionally, switching to medical-grade PDMS, can enable further designs and improve bio-compatibility. Future work could address the replacement of plasma treatment since it can alter the properties of the material and is not easily available.

Scalability: The scalability of our approach depends on the number of analog pins on the microcontroller and the size available for electrodes on the patch. We used a maximum of 5 channels and an A4-size printer.

Durability: All our substrates (except Tattoo) support usage multiple times. If the SSA adhesive is used, the patches can be easily applied and re-applied without causing pain or remove of body hairs. SSA is water-proof and can provide good adhesion for long periods. Of note, the patches used during our evaluation remained functional even after multiple days and repeated use on multiple users.

We can anecdotally report that the textile sensors can withstand multiple washing cycles; a formal study is left for future work.

Extending to other Modalities: Our results show that the electrodes can capture bio-signals when in contact with the body. We, therefore, believe that our approach should be scalable to further electro-physiological modalities e.g. EOG and EEG, which should be investigated in future work.

6.6 CONCLUSION

This chapter presented a digital fabrication approach for realizing electro physiological sensors. With a systematic exploration of materials, functional inks, and adhesives, we demonstrated that custom physiological sensors can be rapidly realized. Informed from the literature we presented a set of design recommendations that can guide designers to realize functional physiological sensing patches. We contributed a comprehensive evaluation across various material substrates, which shows that *PhysioSkin* devices can capture high-quality bio-signals, and demonstrate working implementations.

While the design recommendations that this chapter provides inform the design of multi-modal electro-physiological sensors, it is still not a trivial task to design sensor layouts encapsulating electrodes that can capture multiple bio-signal modalities. One key requirement for high-quality signal acquisition is the precise placement of measurement electrodes on the body. Precisely placing the electrodes is not trivial and is challenging for novice designers and for experts who have to rely on multiple years of experience. This chapter majorly discussed the design recommendations and the fabrication strategies for realizing electro-physiological sensors. In the next chapter, we will present a computational design and optimization approach to automatically create electro-physiological sensor layouts that can capture multiple bio-signal modalities.

COMPUTATIONAL DESIGN AND OPTIMIZATION OF ELECTRO-PHYSIOLOGICAL SENSORS

The Previous chapter presented PhysioSkin, a rapid fabrication technique for realizing skin-conformal electro-physiological sensors. In addition to these techniques, electro-physiological sensing has received a lot of attention in multiple disciplines such as materials science [105, 195, 297], biomedical engineering [494, 538], and more recently in HCI [36, 48, 338].

However, designing sensor layouts for optimal acquisition of electro-physiological signals remains a hard problem, which currently limits a more widespread deployment of this technology. The exact placement of the sensing electrodes on the user's body is critically important for acquiring high-quality signals [522], as the quality of these signals often changes drastically even with small variations in the placement. Moreover, each bio-signal poses unique requirements on valid body locations and electrode arrangements. These locations can further depend on an individual's anatomical proportions and hence differ across users [566]. This task is even more demanding if multiple bio-signals are to be captured using one device. The current state-of-the-art is designing an electrode layout manually, using iterative trial-and-error by following a set of heuristic guidelines [163, 566]. This manual approach is time-consuming and requires extensive domain expertise. Even with expert skills, electrode placements are known to be error prone [502]. Moreover, one of the key requirements for ergonomic wearability is a compact device form factor. At the same time, the device should be capable of acquiring signals with high quality. A good design solution should optimally trade-off between such conflicting design goals. Yet, manually finding such optimal trade-offs is typically not feasible, due to the complex interplay of many parameters.

We propose a computational design approach to tackle this problem (see Figure 58)¹. It automates the design of electrode layouts for epidermal electro-physiological sensors that can sense bio-signals of one or multiple modalities.

¹ This chapter is based on a recent journal article that has been accepted for publication at Nature Communications [337]. As the lead author, I contributed to the development of the concept, development of the integrated model, designed and implemented the interactive optimizer, designed, conducted, and analyzed the empirical experiments, fabricated the sensor samples, designed and developed the applications, and wrote the manuscript. Andreas Karrenbauer contributed to designing and formalizing the integrated model, the optimizer algorithm, and in writing the manuscript. Arshad Khan contributed to the fabrication of sensor samples and helped in data collection while running the application examples. Tobias Kraus contributed to the development of the concept and structure of the paper, contributed to the development of the empirical experiments and fabrication methods and to the empirical analysis, provided critical input to the project, and contributed to writing the manuscript. My advisor Jürgen Steimle conceived the overall concept, advised me in conceptualizing and designing the software tool,

It achieves two main goals: firstly, optimized sensor designs in compact form factors can be designed for supporting wearability and mobility, secondly, designs encapsulating electrodes that can measure multiple bio-signal modalities can be rapidly realized taking into account multiple constraints. Based on the desired application, designs can be optimized not only for an individual user's body but also for conflicting parameters such as signal quality and device footprint. An interactive design tool assists the user in easily specifying desired properties and aids in the rapid iterative design of multi-modal electrode layouts. To validate this approach, an optimization scheme has been designed and implemented for generating multi-modal electrode layouts, comprising three modalities: electromyography (EMG), electro-dermal activity (EDA), and electrocardiogram (ECG). The optimizer has been conceived by formulating the electrode layout design process as a geometrical optimization problem.

Optimization techniques using physics-based models have been successfully employed for optimizing device designs in prior work, such as the design of actuators [440], mechanical robots [76], and optimized meta-materials [41]. The problem investigated here poses a new class of problems since bio-signals depend on anatomical features of the human body. Therefore, an integrated predictive model has been devised that takes human anatomy into account to predict the sensing quality of multi-modal electro-physiological sensor designs. It comprises three bio-signal modalities and can be operationalized for computational optimization. The main contribution here not only lies in applying geometrical optimization for tackling the problem of electrode placement but also in identifying, formalizing, and integrating the set of rules that are inherent to electrode placement for sensing multiple modalities. We show that an optimization approach can be employed for creating compact wearable devices that can measure multiple bio-signal modalities.

The results presented here show that by using a computational design approach, multi-modal electro-physiological sensing layouts can be designed with considerably reduced device footprint while achieving high signal acquisition capability. The approach can rapidly identify optimal solutions for designs of complex combinations of electrodes for multiple modalities that comply with a desired device form factor—a task that so far was tedious and impractical even for experts. In the following, we use the placement of electrodes on the anterior side of the forearm as an example in order to demonstrate our approach and test its applicability by comparing it to conventionally obtained designs. First, we introduce an integrated predictive model for the three modalities EMG, EDA, and ECG that covers the anterior side of the forearm. The optimization problem is then formally introduced based on the model, and the algorithm is outlined. An optimizer was implemented with an interactive real-time graphical design tool that shields the user from lower-level details and exposes easy-to-use parameters

contributed to the design and analysis of the experiments, application examples. He further contributed to the structure and writing of the publication.

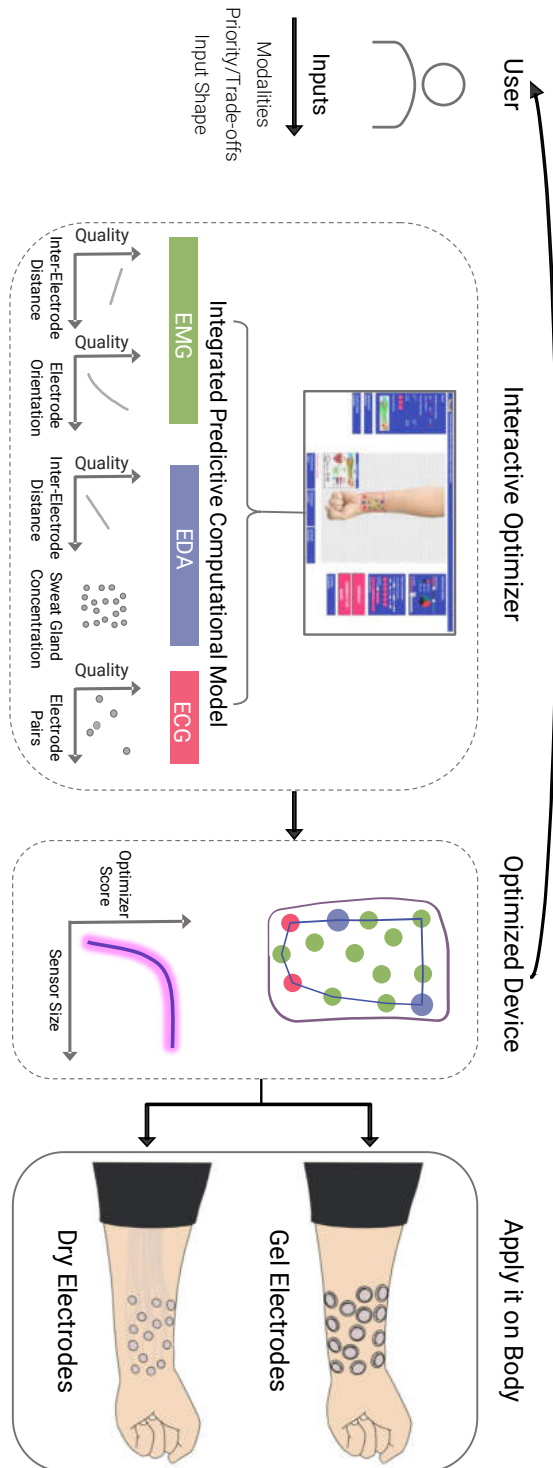


Figure 58: Overview of the concept of computational design and optimization of electro-physiological sensors. An integrated predictive model is presented which encapsulates three bio-signal modalities (EMG, EDA, and ECG). This model along with inputs from the user is fed to an optimizer which generates an optimized layout that optimally trades off between desired device size and sensing quality. An interactive software tool assists the user in specifying desired properties and inspecting the generated design in real-time. The design can be further fine-tuned by an expert while interactively inspecting its quality, allowing for a “human-in-the-loop” optimization process. The optimized device can then be realized using commercial gel electrodes or through dry electrodes fabricated on a temporary tattoo.

for the design of sensors. Designs generated by the optimizer outperform the designs created by experts using conventional placement methods. Results from an experimental validation further show that a high quantitative agreement was found between experimentally collected physiological data from multiple subjects and the prediction of the optimizer. Finally, by unifying this optimization-based design strategy with multi-material ink-jet printing, we demonstrate two application scenarios that provide a promising route towards a fully automated pipeline for the design and creation of complex multi-modal electro-physiological sensing devices.

In the next sections of this chapter, we detail the informal study which we initially conducted to understand the need for computational design tools for electrode placement. We then present the optimization principle with the underlying integrated predictive models, our evaluation studies, and application scenarios.

7.1 INFORMAL STUDY TO UNDERSTAND ELECTRODE PLACEMENT

To better understand the standard practices employed for placing electrodes to capture bio-signals, we conducted semi-structured interviews with experts from Sports Science and Rehabilitation studies.

7.1.1 *Participants*

The experts from these domains extensively use commercial gel-electrodes to capture vital bio-signals such as EMG to capture, record, monitor, and analyze muscle movements for various applications such as rehabilitation studies, improving athletic performance, and motor training. We had a total of 5 experts (1 female, 4 male, avg age:40.6, sd: 8.95). All of them have over 10+ years of experience in the field of sports and rehabilitation studies, with two persons having over 20+ years of experience in the area of sports, rehabilitation, and therapeutic medicine.

7.1.2 *Method*

We conducted semi-structured interviews with each of the participants. Initially, each expert was interviewed about their expertise, the standard methods they employ for placement of electrodes, and the typical challenges that exist with respect to electrode placement. We then asked them to design uni-modal and multi-modal electrode layouts on the forearm of the experimenter. Multi-modal electrode layouts comprised of EMG, EDA, and ECG electrodes that need to be placed on the anterior side of the forearm. Once the ideal placement locations were identified, resulting in a BASELINE solution, the next task was to shrink the size of the layout while keeping the quality of the layout reasonable. The participants were allowed to skip the task if it was deemed too challenging.

7.1.3 *Observations*

The semi-structured interviews revealed very interesting insights from the perspective of electrode placement.

7.1.3.1 *Electrode Placement is still Manual*

One of the surprising findings is that despite all the technological advancements in wearable, sensing, and software technologies, electrode placement still relies on the traditional manual placement methods. All of our participants used traditional tools such as anatomy textbooks, physical props, and models of human muscle anatomy to identify the given muscle and place the electrodes appropriately on the muscle line.

7.1.3.2 *Electrode Placement is Error-Prone*

Another limitation of the manual placement methods is that it is very error-prone, especially for novice users and practitioners with limited expertise or exposure. All our experts highlighted the need for having multiple years of experience and professional practice that enabled them to hone their electrode placement skills. This is also in line with literature that suggests that the manual placements can be error-prone [502].

7.1.3.3 *Designing Multi-Modal Electrode Layouts is Challenging*

Electrode placement for capturing bio-signals of a specific modality poses unique requirements on valid body locations and electrode arrangements. For instance, placing electrodes for acquiring EMG signals requires the electrodes to be placed on the muscles line with a specific inter-electrode distance. Our experts revealed that the complexity of this task is increased when electrodes are to be placed on multiple muscles for higher-resolution EMG sensing. When additional electrodes are included for sensing other bio-signals modalities such as EDA and ECG, the challenge is amplified. Most of our experts found it very hard to design such optimized electrode layouts.

7.1.4 *Design Implications and Requirements for Design Tools*

Based on the limitations of the manual placement strategies, and the feedback from our experts, we derive design requirements for software tools that employ computational approaches for electrode placement. We believe these recommendations can inform the design of future design tools that enable the computational placement of sensors.

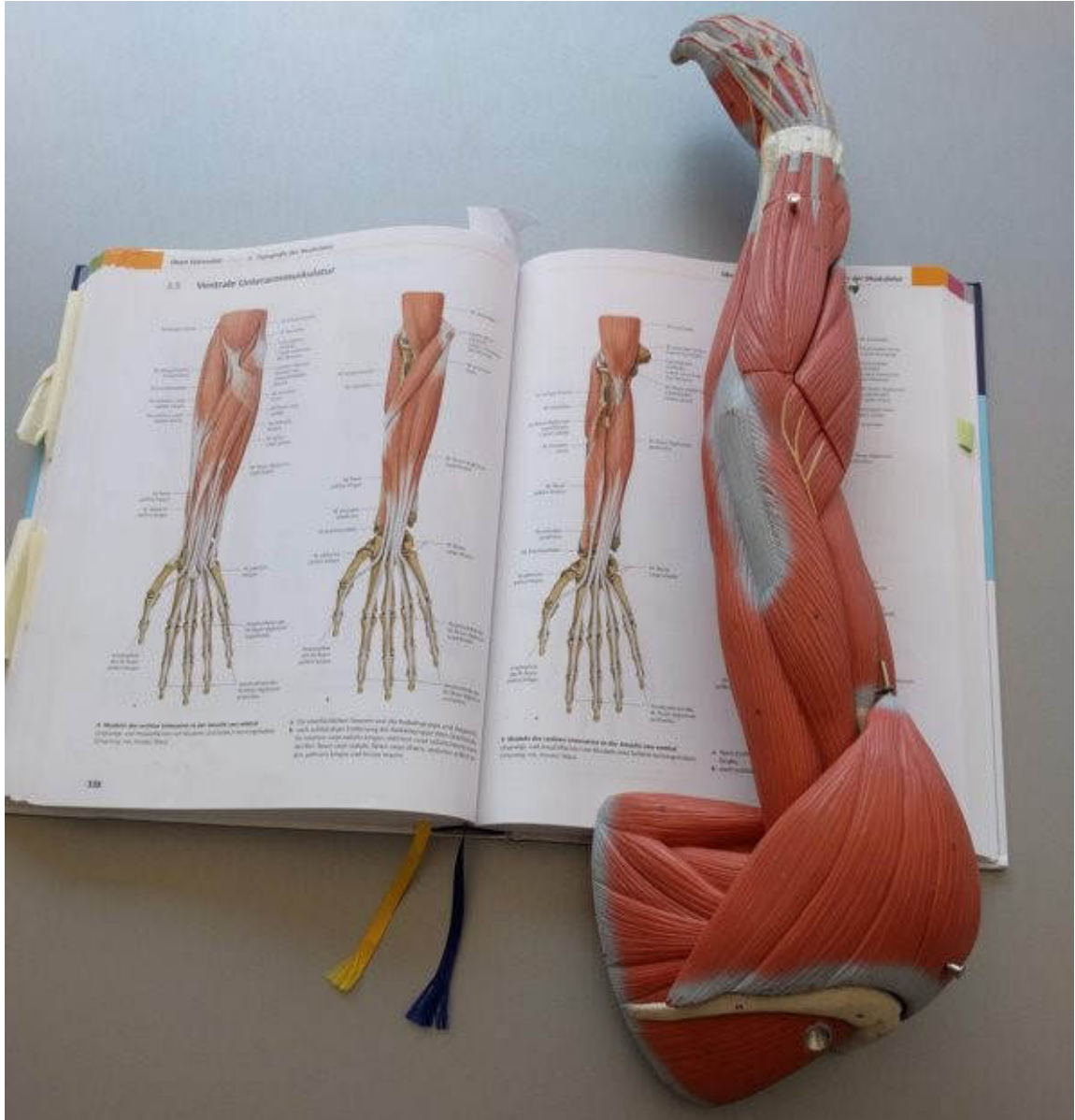


Figure 59: Physical muscular models with annotated landmarks and textbooks with placement guides used by experts in the study for placing electrodes.

7.1.4.1 *Real-Time Placement Recommendation and Quality Feedback*

The first design recommendation is the need for quickly identifying and recommending the ideal locations for electrode placement. For EMG signal acquisition, this involves placing the electrodes at specific locations on the muscle line which are often called "keypoints". These keypoints have been well documented in the literature [566] and depend on the physical dimensions of the body location. Ideal placement recommendations by a software tool can be beneficial for teaching and training practitioners in locating the best possible areas on the body for electrode placement.

7.1.4.2 *Personal Customization*

The placement of electro-physiological sensors is dependent on the physical dimensions of the body. Hence a single placement will not fit all users. The design tools should allow for personal customization by taking into account the body dimensions. Secondly, for epidermal devices, the design tools should allow designers to customize the sensor shape to fit multiple body locations.

7.1.4.3 *Support for Multiple Modalities*

Wearable health monitoring systems should incorporate multiple physiological sensing modalities to provide a holistic understanding of the user's health. To this end, multiple electrodes or sensing equipment must be encapsulated within a single device design. In our observations, all our experts found the task of optimized placement challenging where they had to place 14 measurement electrodes (10 EMG measuring five muscles, 2 EDA, and 2 ECG) within a single patch. This is attributed to the fact that the task required expertise in multiple bio-signal modalities.

7.1.4.4 *Re-Usability and Replication of a Design*

One of the limitations in the current manual electrode placement strategies is the lack of support for reusing or replicating a specific electrode placement. For instance, an expert revealed through his experience that a placement combination he experiments with his patient for rehabilitation monitoring cannot be easily replicated after a few days due to the lack of digital tools that support this workflow. This prohibits taking multiple measurements of a given electrode placement configuration in two different sessions or over multiple days because of the inherent human errors in precisely placing the electrodes at designated locations. Based on this observation, we recommend digital systems supporting electrode placement to have a mechanism for storing and retrieving the designs. These designs can then be overlaid precisely on the body to replicate the electrode placement.

7.1.4.5 *Support for Multiple Body Locations*

In our current study, we focused on the anterior side of the forearm for creating compact electrode layout designs. However, future tools should incorporate support for multiple body locations.

Based on these observations and design requirements, we contribute a computational design approach for realizing compact patches that have electrodes optimally placed for capturing bio-signals of multiple modalities. In the next sections, we firstly describe our Integrated predictive model that forms the basis for the computational optimization problem that we have formulated. Based on these, we contribute an interactive optimizer implemented as a web-based software tool.

7.2 INTEGRATED PREDICTIVE MODEL

Traditional manual placement of electro-physiological sensing electrodes relies on placing electrodes at specific locations, usually called key points, following a set of heuristic rules and placement guides presented in literature [26, 97, 101, 198, 566]. For multi-modal sensing, this typically results in either placing a dedicated device per modality at separate body locations or having large sensor sizes for sensing multiple modalities [338, 354]. For improved wearability and mobility, we demonstrate a method based on computational optimization. The optimizer produces a single device that encapsulates electrodes that can measure multiple modalities and can be worn on the forearm. The forearm has been chosen as the location for this first study since it allows to capture multiple bio-signals, supports ergonomic wearability [2, 97, 101, 405, 530] and is one of the most promising areas for human-machine interaction [118, 498, 537]. However, this approach can also be applied to other modalities and body locations.

Computational design requires a formal model of electrode performance that can be operationalized for computational optimization. Furthermore, as the optimization approach searches for a globally optimal design of multi-modal sensors, this model needs to be compatible with multiple modalities. However, the current state of the art considers different modalities separately and uses incompatible metrics. For instance, the quality of an EMG signal is commonly measured in ARV (Average Rectified Value) or RMS (Root Mean Square) value of the signal, whereas EDA signals are measured through skin conductance levels denoted in MicroSiemens (μS). This limitation is overcome with an integrated model that formalizes individual objective functions for each modality and defines cost functions for each, such that they can be combined in the overall objective function. The objective functions were formalized based on empirical findings reported from the literature for each modality. Here, we discuss our approach for constructing the models.

7.2.1 Predictive Model for EMG Electrodes

Electromyography (EMG) measures the MUAP (Motor Unit Action Potential) as an electrical potential between a ground electrode and sensing electrodes. The Surface-EMG (sEMG) measurement is a typical non-invasive method to capture MUAP by placing electrodes on the surface of the skin. For a given muscle, the EMG signal is captured by a pair of electrodes with respect to a reference electrode. The signal quality depends on a number of factors such as the electrode size, its placement with respect to the muscle line, and the distance between electrodes. From an optimization perspective, the overall optimizer score for a given muscle is normalized in the range $[0,1]$ with 0 denoting the best and 1 denoting the worst sensing quality. Our current implementation supports five muscles on the anterior side of the forearm: Flexor Carpi Radialis (FCR), Brachioradialis (BR), Palmaris Longus (PL), Pronator Quadratus (PQ), and Flexor Carpi Ulnaris (FCU).

7.2.1.1 Modelling and Identification of Muscle Lines

Given the four measurements of the forearm, the entire space of the anterior side of the forearm can be modeled as a trapezoid. From this, the muscle lines for Brachioradialis (BR), Flexor Carpi Radialis (FCR), Palmaris Longus (PL), Pronator Quadratus (PQ), and Flexor Carpi Ulnaris (FCU) can be reconstructed. The FCR muscle line can be identified as the line from the medial epicondyle to the radial styloid process [26] (which forms the diagonal of the trapezoid as shown in Figure 60). The BR muscle line can be identified as the line from the styloid process to a midpoint on the line between the lateral and medial epicondyles [26] (which is represented by the side d of the trapezoid as shown in Figure 60). The PL muscle line is the line between the medial epicondyle and the distal end of the flexor retinaculum [26] (which is represented by the line joining one corner of trapezoid a and the mid-point of b as shown in Figure 60). The PQ muscle line is identified as the horizontal muscle line situated at 2.5 cm from the wrist (Sulcus Distal Carpi) [566]. The muscle line runs parallel to the measurements a and b as shown in Figure 60. The FCU muscle line can be identified as a muscle line from the medial epicondyle and ends near the other end of the styloid process [81] (which is represented by the side c of the trapezoid as shown in Figure 60).

Given a set of forearm measurements (see Figure 60) $F = \{f_1, f_2, f_3, f_4\}$, the five muscle lines can be reconstructed based on the guides from prior work [26, 366, 566]. Based on this, a set of key points is calculated which is represented by $K_{EMG} = \{k_1, k_2, k_3, \dots, k_\ell\}$. These key points consist of ideal locations for EMG electrode placement. For EMG acquisition, the electrodes should have a minimum surface area of 50mm^2 and the diameter should not exceed 10mm [163, 315, 566]. To ensure good signal acquisition, the model incorporates electrodes which have a surface area of 50mm^2 .

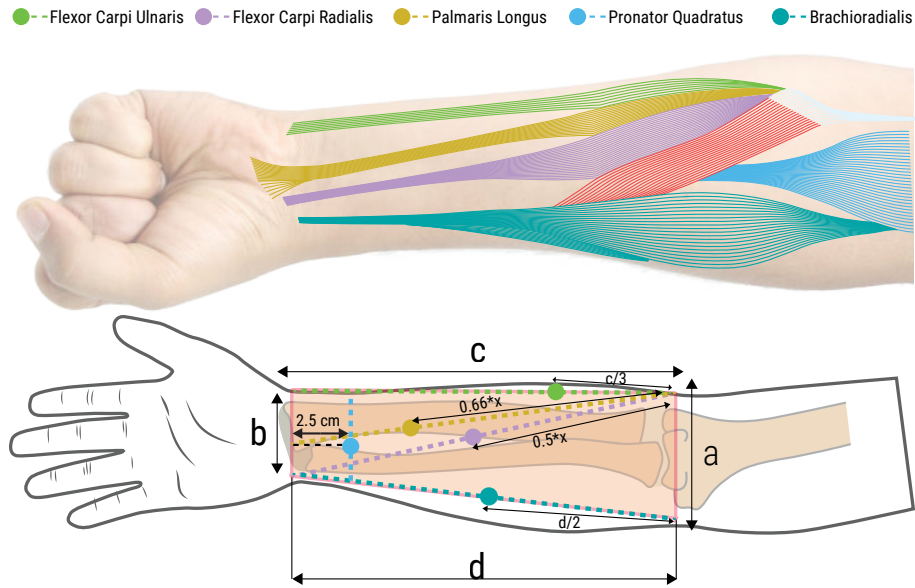


Figure 60: Key points generated for each of the muscles on the anterior side of the forearm. The electrodes need to be placed symmetrically along this key point. ("x" denotes the length of the muscle line). The four measurements a , b , c , d for the forearm form the basis for the calculation of the muscle keypoints on the anterior side of the forearm.

For a given pair of electrodes that measure the potential of a specific muscle, a series of pre-checks are made. Firstly, both electrodes need to be within a distance of 1 cm from the muscle line. This is based on the recommendation from prior work which suggests that more than 1 cm offset from the muscle line could result in a considerable decrease in signal and recognition accuracy [544]. If at least one of the electrodes is farther away, then a score of 1 is assigned. Otherwise, an additional check is made to ensure that both electrodes are not present within innervation zones. Based on the recommendations from Barbero et al. [26], Innervation Zones (IZ) are unsuitable locations to place electrodes. Hence if either of the electrodes falls within these regions, then a score of 1 is assigned. The innervation zones for muscles are well documented in the literature [26, 401].

Following successful checks for these conditions, a normalized score is calculated based on the electrode orientation with respect to the muscle line and the inter-electrode distance. The orientation of the electrodes with respect to the muscle line is calculated as follows:

$$\theta = \arccos \left(\frac{\vec{k}_i \cdot \vec{e}}{|\vec{k}| \cdot |\vec{e}|} \right) \quad (5)$$

where \vec{k} is the vector connecting the two keypoints for the specific muscle m in the set K_{EMG} (this is the vector representing the muscle line) and \vec{e} is the vector connecting the two measuring EMG electrodes e' and e'' .

Once the angle between the muscle line and the electrodes is determined, data from the literature is used to inform the model. Merletti et al. [314] showed how the quality of the EMG signal is affected by the orientation between the muscle line and the electrodes and showed that the signal drastically drops with misalignment greater than 60 degrees. The least-squares curve-fitting method has been used to derive the closest curve ($R^2 = 0.9971$) which fits the data presented in prior work [314]. Based on this, the energy function for the orientation of the electrodes is defined by:

$$\omega(\theta) = \begin{cases} 0.0057\theta + 0.000181\theta^2 & \text{if } \theta \leq 60^\circ \\ 1, & \text{otherwise} \end{cases} \quad (6)$$

If the electrode orientation is less than 60° , then the inter-electrode distance $|\vec{e}|$ is calculated for the electrode pair. The model is informed from prior literature which shows how the signal varies with respect to changes in the inter-electrode distance [314]. The data was normalized and a best fitting curve was calculated using the method of least squares ($R^2 = 0.9986$). The energy function for the inter-electrode distance $|\vec{e}|$ for an electrode pair is as follows:

$$v(|\vec{e}|) = \begin{cases} \max(0, 1.0125 - 0.0586|\vec{e}| + 0.0007|\vec{e}|^2) & \text{if } 5 < |\vec{e}| \leq 25 \\ 0 & \text{if } 25 < |\vec{e}| \leq 60 \\ 1 & \text{if } 60 < |\vec{e}| \end{cases} \quad (7)$$

Prior literature [163, 392] suggests that large inter-electrode distances (>60 mm) can create a drastic drop in the signal quality. Hence a limit of 6 cm was applied to ensure that large inter-electrode distances are not generated.

For calculating the overall score of the EMG electrodes, the inter-electrode distance and electrode orientation are taken into account. Combining equation 6 and 7, the overall energy function for a muscle m is calculated as a weighted average of the angle orientation score and the inter-electrode distance score, which is defined as:

$$O_{1i} = \begin{cases} \alpha \cdot \omega(\theta_i) + (1 - \alpha) \cdot v(|\vec{e}_i|) & \text{if } e'_i, e''_i \notin R_i \\ 1 & \text{otherwise} \end{cases} \quad (8)$$

where α and $1 - \alpha$ are the priorities assigned for both parameters and serve as the calibration parameter for EMG measurement hardware. R_m corresponds to the innervation zones which are not suitable locations for the electrode placement. In the current model, equal priorities ($\alpha = 0.5$) are given for both these factors.

For n selected muscles, the overall EMG score is then calculated as the product of the EMG weight assigned and the average of the overall muscle scores of each of the selected muscles, which can be formulated as:

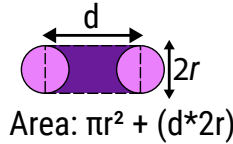


Figure 61: Total area covered between and under two EDA electrodes.

$$O_1(F, E_1, w_1, S) = w_1 \cdot \frac{1}{m} \sum_{i=1}^m O_{1i} \quad (9)$$

where $F = \{f_1, f_2, f_3, f_4\}$ is the set of forearm measurements, E_1 is the electrode set for EMG, w_1 is the weight determining the priority for EMG in the overall objective function and S is the optional input shape.

7.2.2 Predictive Model for EDA Electrodes

Electrodermal activity (EDA) measures the changes in electrical conductance of the skin and has been used as an indicator for detecting emotional responses [467]. The EDA response is influenced by the sweat gland activity which is directly proportional to the number of sweat glands (higher the number of sweat glands, higher the skin conductance levels). Hence the EDA model predicts the number of sweat glands covered between the electrodes, which determines the quality of the EDA response.

A sensor for measuring EDA typically consists of two electrodes placed on the body between which the conductance is measured. Based on the recommendations from the literature [321], the surface area of electrodes were set to 0.78 cm^2 . The quality of a given layout of electrodes for sensing EDA is based on two factors: the density of the sweat glands at a given body location and the inter-electrode distance.

Electrode location on the body: The electrodes for EDA response can be placed on various locations on the body as long as a required minimum number of sweat glands are captured. The density of sweat glands varies across the body, with higher concentrations present at fingertips, palms, and forehead. The density of sweat glands is rather a discrete function, and the forearm is reported to have about $\approx 108/\text{cm}^2$ [323]. The sweat gland concentration for various other locations is reported in the literature [323, 452]. Prior work has shown that a minimum number of sweat glands that need to be covered between EDA electrodes for maintaining functionality is 140 [143].

Estimating the Count of Sweat Glands: For two given circular electrodes, the area covered by and between the electrodes can be calculated as shown in Figure 61. Hence, if D_s is the density of sweat glands at a specific location, the number of sweat glands covered by the electrodes is given by: $N_s = (\pi r^2 + (d \times 2r)) \times D_s$.

Inter-Electrode Distance: The skin conductance level is linearly proportional to the number of sweat glands between the electrodes. This is because the glands act as resistors connected in parallel, thus bringing the skin resistance down [43].

The recommended distance between the electrodes is 5–6cm [43, 97]. For larger distances, the two electrodes risk not being on the same dermatome, which can lead to invalid readings [43]. Assuming an ideal inter-electrode distance of 6 cm, the maximum number of sweat glands that can be covered the on forearm is $N_{\max} = (\pi 0.5^2 + (6 \times 2 \times 0.5)) \times 108 \approx 733$ sweat glands.

The energy function is as follows:

$$O_2(E_2, D_s) = \begin{cases} 1 & \text{if } N_s \leq 140 \text{ or } d_s > D \\ 1 - N_s/N_{\max} & \text{otherwise} \end{cases} \quad (10)$$

where d_s is the inter-electrode distance and D is the recommended distance of 6 cm. N_s is the number of sweat glands covered by the electrodes for a given inter-electrode distance d_s and N_{\max} is the maximum number of sweat glands that can be covered on the forearm for a recommended distance of 6cm (which is ≈ 733). For inter-electrode distances larger than 6cm, a score of 1 is assigned since larger inter-electrode distances are not recommended.

7.2.3 Predictive Model for ECG Electrodes

Electrocardiogram (ECG) measures the electrical activity that occurs during a cardiac cycle. Clinically, the measurements are obtained by placing 12 electrodes near the chest [198]. More recently, 3-electrode ECG configurations on the forearm have been designed to support ambulatory and wearable devices [2, 101, 152, 530]. Our model is derived based on the mapping of ECG signals at various locations on the forearm as described in prior work [101].

To the best of our knowledge, there exist no continuous models which predict the strength of ECG signals based on the spatial configuration of the measuring electrodes on the forearm. Therefore, we adopted a discrete model based on prior work [101]. ECG measurements were taken for a set of discrete locations on the forearm. These locations were chosen from prior work [101]. Figure 62 shows the key point locations incorporated into the model and the SNRs measured with a portable ECG device for combinations of key points. The SNR measurements were highest at the upper end of the forearm since the electrodes are closer to the heart. The signals drop drastically as the electrodes are placed farther down on the forearm.

7.2.4 Predictive Model for Area

To ensure that devices with small form factors are created, an additional weight w_4 for Small Area is incorporated into the model. This Small Area weight w_4 determines the priority given to the size of the device.

For a given layout, the area of the convex hull of all electrodes is calculated based on the Graham Scan algorithm [128]. This area is then normalized with

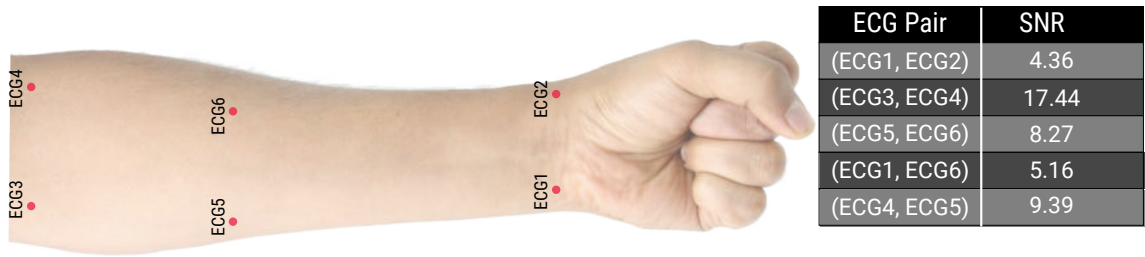


Figure 62: Key points for ECG electrode placement on the forearm and empirically measured signal quality for combinations of key points.

respect to the area of the BASELINE SOLUTION for a given combination of modalities. While we have assigned a linear cost penalty for the Area, a quadratic cost penalty can be assigned alternatively to more aggressively shrink the sensor size. The energy function is as follows:

$$O_4(E) = \frac{A(E)}{A(E_b)} \quad (11)$$

where $A(E)$ is the area of a given layout and $A(E_b)$ is the area of the Baseline solution.

7.3 COMPUTATIONAL OPTIMIZATION

The predictive model provides the basis of a computational design tool that can generate a sensor design that packs a set of electrodes for measuring one or more electro-physiological signals. Each pair of electrodes have a specific functionality; for instance, two electrodes placed on the muscle measure electric potential generated from muscle movements, while another electrode pair measures electro-dermal activity, etc. The spatial configuration of the electrodes affects the quality of the bio-signals which are to be acquired. The aim of the optimizer is to find a globally optimal solution that provides a good trade-off between signal quality and the overall size of the sensor.

7.3.1 Weight-Based Optimization

The model allows for specifying which bio-signals the sensor should be able to capture. Any combination of EMG, EDA, and ECG can be selected, the choice of EMG involves specifying the set of individual muscles for sensing. The designer can further specify weights for prioritizing or de-prioritizing bio-signals in global optimization. A higher priority implies that this bio-signal is given more weight, increasing the likelihood the corresponding electrodes are placed such that high-quality sensing is ensured. Similarly, the designer can specify a weight indicating how aggressively the optimizer seeks to create small form

factor solutions. Furthermore, if desired, the designer can specify the exact outline and position on the body that any valid design must not exceed. In this case of constrained optimization, the optimizer searches for optimal solutions only within the given input shape S which is a closed polygon.

The optimization problem was formulated as follows. Given a set of forearm measurements $F = \{f_1, f_2, f_3, f_4\}$ (see Supplementary Figure 1), an input shape S , and a set of weights $W = \{w_1, w_2, w_3, w_4\}$ which represent the priorities for EMG, EDA, ECG and Small Area respectively ($w_1 + w_2 + w_3 = 1$), an electrode set $E = \{e_1, e_2, \dots, e_n\}$ is generated. The overall global objective function of the electrode set E is:

$$O(F, W, S) = \sum_{k=1}^4 w_k \cdot O_k \quad (12)$$

which is minimized over all non-overlapping placements of the electrodes in E within the input shape S , where O_1, O_2, O_3, O_4 are the objective functions for EMG, EDA, ECG, and Small Area, respectively.

Considering the challenge of dealing with a large search space, a large number of potential solutions are possible. Monte-Carlo approaches are well suited for these kinds of problems, where sampling the entire solution space is not feasible. Here, efficient sampling of new configurations with an objective function that can be evaluated quickly can result in well-optimized solutions. Hence, Simulated Annealing (SA) [468] was used for implementing the optimization scheme. It is a probabilistic technique for approximating the global optimum of a given energy function. The annealing procedure starts with a random initial layout that is generated within the shape S . After every iteration, a neighboring layout is generated by picking a random electrode and translating it with a vector \vec{v} . The new solution is accepted if it either lowers the objective or raises it based on a randomized probability function which is given as follows:

```

c ← rand(0,1)
if c ≤ e-ΔO/T then
  accept solution
else
  reject solution
end if

```

where $\Delta O = O(t) - O(t - 1)$ is the difference in the objective function at successive annealing temperatures and T is the annealing temperature.

7.3.2 Lower-Bound Based Optimization

In addition to the weight-based optimization approach in which the user provides relative priorities through weights, an additional optimization scheme has been incorporated.

In this *Lower-Bound based optimization*, the user specifies a required reference signal value for each of the modalities. The optimizer then strives for higher quality scores than the respective lower bounds for each modality. To this end, we increase the objective function by a penalty for each modality that grows exponentially with the extent of the violation of the corresponding lower bound.

That is, we define

$$P_k := p \cdot (e^{\max(O_k - \ell_k, 0)} - 1) \quad (13)$$

where ℓ_k is the specified lower bound for modality k and p is a parameter to control the softness of the lower-bound constraints. The higher the value of p is, the harder the lower bound is enforced by the optimizer. Observe that a penalty only occurs if a lower bound is violated, i.e., $P_k = 0$ whenever $O_k \geq \ell_k$.

In this scheme, the relative weights of the modalities can be disabled such that only the area weight is used for calculating the objective function. Hence, each modality receives equal priority for achieving a quality above the corresponding lower bound. However, the user can also activate lower bounds and modality weights at the same time in a hybrid scheme.

7.4 CONCEPTION OF AN INTERACTIVE OPTIMIZER WITH A WEB-BASED SOFTWARE TOOL

A computational predictive model and optimizer are necessary but not sufficient for the rapid design of electrode layouts. To make the optimization approach accessible to a wide audience of practitioners and researchers and to ease visual analysis and rapid iterations of custom designs, an interactive software tool has been designed and implemented (see Figure 63).

7.4.1 Inputs and Constraints

The graphical tool abstracts low-level details of the model, electrode design, and optimization scheme (e.g. electrode sizes, spacing, placement, etc.), while exposing relevant parameters in an intuitive and user-friendly interface. It offers a Web-based interface that encapsulates the predictive model and automatically sets low-level parameters of the design. For instance, the size of electrodes is preset with appropriate dimensions for ensuring maximum performance, and their spacing is automatically adjusted by the optimizer. High-level parameters that allow for customizing the sensor can be adjusted through intuitive checkboxes and sliders. This offers a direct, fast, and user-friendly way of setting body dimensions, selecting the modalities the sensor will be able to capture (EMG, ECG, and/or EDA), and selecting specific muscles for EMG sensing. The sensing quality of one or multiple modalities can be easily prioritized by moving a slider. Similarly, the priority of a compact sensor vs. highest possible sensing quality can be continuously adjusted. In our current implementation, the interface was designed

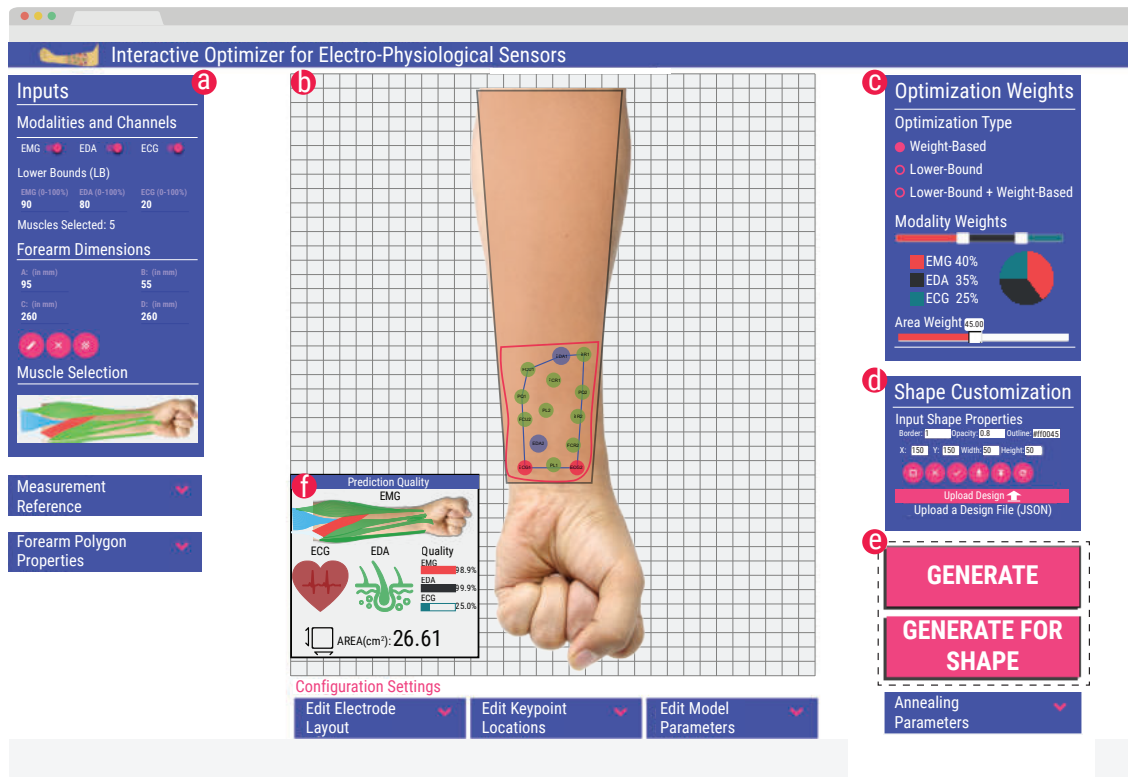


Figure 63: Screenshot of the graphical design tool for interactively generating and inspecting optimized results. (a) Input panel for selecting the modalities and muscles, setting forearm dimensions, and setting the lower bounds. (b) The canvas area where the generated designs are visualized. Designs can be fine-tuned by drawing a desired location and shape or dragging individual electrodes. (c) Panel for choosing the optimization type, weights for each of the modalities, and overall sensor area. (d) Shape customization panel for fine-tuning the properties related to the sensor shape. Additionally, this panel also allows for uploading existing designs and exporting the current designs. (e) Buttons for one-click automatic generation of the layout. The result is displayed in real-time in the canvas area. (f) Panel visualizing quality metrics for the generated layout. Advanced functionality for use by experts can be accessed through drop-down panels. This includes functions for adjusting and editing the electrodes in the generated solution, adjusting the internal parameters of the model, tweaking the optimization parameters, and adjusting the appearance of the forearm polygon. The workflow for using the tool is shown in Supplementary Video 1.

for the anterior side of the forearm. However, it can be extended to support other body sites as well based on the underlying anatomical properties (e.g. muscles lines, types, and their directions, sweat gland concentration, etc.).

7.4.1.1 User Inputs

The inputs to the model which are provided through the software tool are formalized as follows:

- **Dimensions of the Location:** The dimensions refer to the body site (the forearm in our implementation).
- **Modalities:** These involve the selection of desired modalities.
- **Individual Muscles:** These involve the set of muscles for EMG sensing.
- **Area Weight or Outline of Sensor Shape:** The shape of the sensor layout can be sketched by the user. Alternatively, if no shape is specified, the tool automatically generates the appropriate sensor layout based on the weight provided for the Small Area.
- **Weights:** These include the weights for each of the modalities. These weights can be represented as $W = \{w_1, w_2, w_3, w_4\}$ where $w_1 + w_2 + w_3 = 1$ and correspond to the weights of EMG, EDA and ECG respectively. w_4 refers to the weight for the Small Area of the sensor layout.

7.4.1.2 Derived Parameters

Based on the user inputs, the following parameters are derived:

- **Key Point Set:** Given the dimensions, modalities and the muscle selection, the keypoints set $K = \{k_1, k_2, k_3, \dots, k_n\}$ is calculated. These keypoints consist of ideal locations for EMG and ECG electrode placement.
- **Electrode Sizes:** Based on the selected modalities, the optimizer selects the size of electrodes for high-quality signal acquisition. The electrode sizes were fixed as follows: 50 mm² for EMG and ECG electrodes and 80 mm² for EDA electrodes. These sizes were chosen such that they match with the dimensions of electrodes that are commercially available.

Finally, prior literature also suggests that increasing the electrode surface area does not necessarily result in better signal quality [163, 321].

- **Electrode Set:** Based on the above three parameters, a measuring electrode set $E = \{e_1, e_2, \dots, e_\ell\}$ is generated, which contains disjoint subsets of electrodes $E_1 = \{e'_1, e''_1, \dots, e'_m, e''_m\}$ for EMG, $E_2 = \{e_{2,1}, e_{2,2}\}$ for EDA, and $E_3 = \{e_{3,1}, e_{3,2}\}$ for ECG, i.e., $E_1 \dot{\cup} E_2 \dot{\cup} E_3 \subset E$. For all these electrodes, a maximum of two

reference electrodes are required: one electrode which acts as a common reference for the EMG and one electrode which is required for the ECG. Both these electrodes need to be placed away from the forearm (preferably near the shoulder/chest) for having a high quality ECG signal.

For ensuring the validity of the generated electrode layout, the following set of constraints have been imposed:

- **Overlapping Electrodes:** To ensure that no electrodes overlap with each other, the center-to-center distance between each pair of electrodes with radii r_1 and r_2 must be greater than $r_1 + r_2$. For ensuring a safe distance between all the electrodes, the pair-wise inter-electrode distance between all pairs of electrodes was set to atleast 12mm.

To ensure that all the electrodes within a layout are inside the input region sketched by the user, the Point-in-Polygon (PIP) algorithm [108] was implemented. For all the solutions that are generated, this constraint is checked and only if it is met, the energy of the layout is calculated.

7.4.2 Selection of Search Space

By default, the search space of the optimization scheme spans the entire surface of the body site. In cases when a more precise control over the location and shape of the sensor is required, the search space can be constrained interactively. As shown in Figure 63 (b) (user sketched shape outline represented in pink color), the location and shape can be quickly specified by sketching a free-form polygonal outline on the canvas, using a mouse or a touchscreen. This defines a region that the sensor design must not exceed. Lastly, more detailed settings can be adjusted in dropdown panels, if experts wish to do so. Then, with the click of a button, the sensor design is generated and optimized for the given parameters.

7.4.3 Optimizer Results

To allow for real-time visual analysis of the result's quality, the design is immediately visualized within a few seconds, alongside metrics for the predicted quality of the sensor (see Figure 63 (b) and (f)). If the design is not fully satisfactory yet, parameters can be fine-tuned and the design re-optimized. Moreover, a basic electrode layout editor has been incorporated which enables the user to directly adjust the electrode positions if desired. The resultant quality metrics are immediately updated. These features are vital to enable a designer in-the-loop optimization [86, 341] approach: rather than simply accepting the solutions generated by the optimizer, the designer interacts in real-time with the optimizer; this allows for combining the strengths of algorithmic optimization with human creativity and knowledge of the application domain.

7.4.4 *Electrode-Agnostic Design*

Finally, to ease sensor fabrication and to ease replication, the generated design can be exported to a standard scalable vector graphics (SVG) file. This can be directly used for printing the electrode layout using conductive ink on a flexible substrate [105, 225]. Alternatively, if off-the-shelf wet-gel electrodes are going to be used, the SVG file defines a stencil for electrode placement that is printed on a transparent PET. Holes can be punched through the PET film at electrode locations, and once overlaid onto the forearm, a marker can be used for marking electrode locations on the forearm. Electrodes can then be placed on these locations on the forearm. In addition, design solutions can be saved as a JSON formatted file for later use in the design tool. These functionalities help overcome a major drawback of the classic manual placement approach by making it possible to precisely replicate a specific electrode placement.

7.5 COMPARISON OF OPTIMIZER RESULTS WITH CONVENTIONAL DESIGNS

The performance of the optimizer was experimentally validated for tasks of various complexity. The experiment had two objectives. Firstly, understand how well a computationally optimized design performs in comparison to the standard placement techniques and an expert generated solution. The second objective was to assess the efficiency and scalability of the optimizer for more complex device configurations encapsulating electrodes that measure multiple physiological modalities.

To address the first objective, electrode layouts were optimized that capture one modality only. Electromyography was selected as the most demanding modality due to its strong requirements for precise electrode placement. A combination comprising three muscles was chosen, which together support a variety of arm movements [506]: Flexor Carpi Radialis (FCR), BrachioRadiali (BR), and Palmaris Longus (PL). The following electrode layouts were compared:

- **BASELINE SOLUTION:** This is a non-optimized rule-based solution generated following the existing placement guides for EMG electrodes presented in the literature [26, 226, 401, 566]. Electrodes are placed at the respective muscle's key points, which ensures highest quality.
- **QUALITY OPTIMIZED:** The optimizer has traded-off size for achieving high-quality sensing. The following section details how this solution was generated.
- **AREA OPTIMIZED:** The optimizer has aggressively tried to reduce the size of the layout while trading-off sensing quality. The following section details how this solution was generated.

- **EXPERT GENERATED:** This solution was manually created by a human expert (a sports scientist, male, 31 years old, specializing in placing EMG electrodes for rehabilitation and performance monitoring with 6 years of professional experience). The expert was tasked to design a sensor layout for use near the wrist ensuring the smallest possible size. The expert stressed the challenging nature of creating the design for multiple muscles, in a compact form factor. The heuristic approach used by the expert was to first identify for each of the three muscles the muscle line and place the electrodes close to the wrist while ensuring the electrodes are approximately aligned with the muscle. Then, the expert aggressively reduced the inter-electrode distance, while ensuring that there was at least a 10mm distance between electrodes. He considered this minimum distance as absolutely essential to keep sensing quality at a reasonable level, which is in-line with recommendations presented in the literature [163].

7.5.1 *Validation of Optimizer*

The key goal of the experiment is to demonstrate that the optimizer generates valid and functional solutions. We were also interested in the broad spectrum of solutions that could be generated. Therefore the entire forearm space was sampled, allowing for 1) informing about the influence of the search space on the quality of the generated solutions, and 2) providing a wide range of solutions with varying levels of quality and sizes sampled across the entire forearm search space. Note that in typical usage scenarios it is not required to sample the entire forearm space; instead, an optimal solution can be directly generated by setting the desired priority for a small area, or by providing a desired shape of the sensor.

Figure 64(a) shows the sampling of the forearm space used for generating optimized solutions. Figure 64(b) shows the scatter plot of all solutions generated for the uni-modal case, plotted against their respective area.

The entire forearm was sampled at high-resolution, starting at the wrist. Two configurations were chosen: a multi-modal configuration where all the modalities were included (5 muscles, EDA and ECG), and a uni-modal configuration with EMG only (3 muscles). Starting at the wrist, the search space for the optimizer was incrementally increased by providing a bounding box as shown in Figure 4 in Supplementary Information. The height of the bounding box was increased in 1 mm increments until the box covered the entire forearm. Figure 64(a) shows the sampling of the forearm space used for generating optimized solutions. Figure 64(b) shows the scatter plot of all solutions generated for the uni-modal case, plotted against their respective area. For each 1mm increment, a solution was generated through the optimizer. The **AREA OPTIMIZED SOLUTION** was identified as the first solution that gives an optimizer score lower than 1. For obtaining the **QUALITY OPTIMIZED** solution, the search space was incrementally decreased in 1mm intervals, starting at the top of the forearm until the predicted signal quality

dropped below 0.9. The QUALITY OPTIMIZED solution was then identified as the solution which had the smallest size out of all solutions that have predicted quality of ≥ 0.95 , or ≤ 0.05 optimizer score. The annealing parameters were kept constant for all iterations. Each iteration generated a design file that contained information about the electrode layout, quality, area, and other configuration information. For the multi-modal configuration containing EMG, EDA, and ECG modalities, there were a total of 193 iterations with each iteration picking an optimal solution from a set for 15,490 randomly generated solutions, resulting in a total of 2,989,570 solutions. For the uni-modal combination involving three muscles, a total of 122 iterations were generated, resulting in a total of 1,889,780 solutions.

The smallest possible solution (AREA OPTIMIZED) for the uni-modal configuration was generated at a window of height 3cm. No solution was generated below this height since there was not enough space for the optimizer to fill all the electrodes. The solution generated by the optimizer was slightly larger in size than the EXPERT GENERATED Solution because of the constraint imposed which limits too small inter-electrode distances (the inter-electrode distances between all pairs of electrodes is kept at least 12mm). It is noteworthy that despite this constraint the optimizer was able to shrink the device size to a level that is comparable to the expert-generated design. Conversely, for identifying the solution with the best quality while having a small size, the search space was decreased in increments, until the predicted signal quality dropped below 90%. The QUALITY OPTIMIZED solution can then be easily recognized as the solution with smallest area out of all solutions that have $\geq 95\%$ predicted quality, or ≤ 0.05 optimizer score as shown in Figure 64(b).

The window height was 7.8cm for the multi-modal combination. The relatively large window height was required due to the fact that the multi-modal case requires a larger number of electrodes (14 electrodes) than compared to the uni-modal configuration (6 electrodes). It should be noted that these window heights depend on factors such as the configuration chosen, the number of electrodes to fit in, and the individual forearm dimensions.

7.5.2 Results

Figure 65(a) depicts the generated designs alongside their area and quality score predicted by the model.²

The BASELINE SOLUTION (predicted quality: 1.0) was taken as reference and the scores for other solutions were normalized with respect to this condition. The QUALITY OPTIMIZED solution achieves a signal quality almost on-par with the BASELINE SOLUTION (average quality of 0.979 [max: 0.99, min: 0.96]), while

² The optimizer score, i.e. the result of the cost function, represents the sensing quality predicted by the model. It is in the range [0,1] with 1 being worst and 0 being the best. For better clarity, we report the quality score, which is the complement ($1 - \text{Optimizer Score}$), with higher values denoting higher predicted quality.

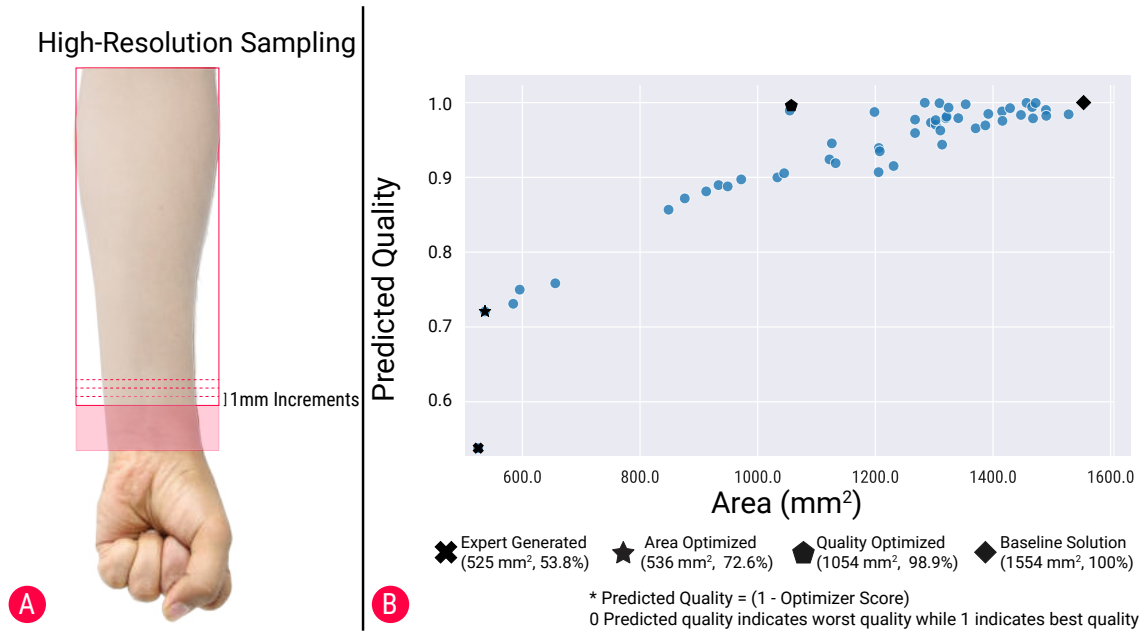


Figure 64: (a) High resolution sampling of the anterior side of the forearm in 1 mm increments starting near the wrist. (b) Scatter plot showing the entire spectrum of solutions generated by varying the search space on the forearm. The solutions have been plotted with respect to their size.

considerably shrinking the sensor area by an average of 44% across the three participants (max: 56%, min: 33%). The AREA OPTIMIZED solution yielded a lower predicted sensor quality with an average of 0.60 (max: 0.72, min: 0.54), while however being able to shrink the sensor's footprint to almost one-third of the baseline's footprint (max: 65%, min: 48%). Noteworthy, it clearly outperforms the EXPERT GENERATED solution, by offering a considerably higher predicted sensing quality (18% more) with only a minimally larger footprint (2% larger).

For achieving our second objective we were interested in how the optimizer would perform for more complex combinations involving a larger number of muscles and additional physiological modalities (EDA and ECG) resulting in a multi-modal sensor. To investigate the optimization of a multi-modal sensor, a complex combination was chosen, involving EDA and ECG modalities as well as EMG sensing for five muscles: Flexor Carpi Radialis (FCR), Brachiradialis (BR), Palmaris Longus (PL), Pronator Quadratus (PQ) and Flexor Carpi Radialis (FCU). It involves the placement of 14 measurement electrodes for acquiring signals. Arranging all these electrodes while ensuring a minimum size is a very taxing task, even for experts.

Similar to the uni-modal case described above, four electrode layouts were compared: a BASELINE solutions that is not optimized and follows the existing placement guides for EMG [26, 366, 566], EDA [97] and ECG [101] electrodes presented in the literature; a QUALITY OPTIMIZED design; an AREA OPTIMIZED design; and an EXPERT GENERATED design.

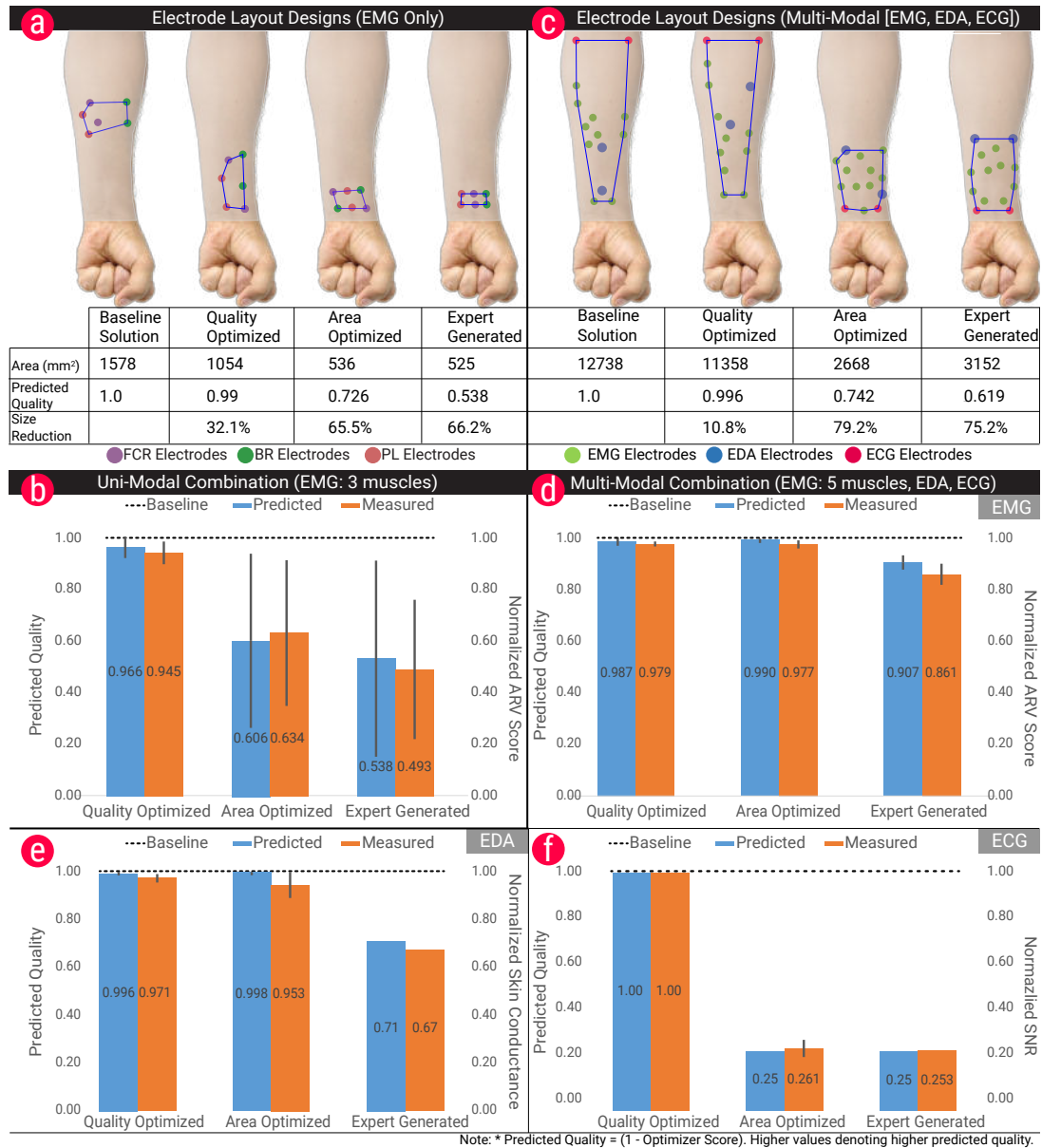


Figure 65: Comparison of the optimizer results with conventional designs and the experimentally collected physiological data. (a) Visual representation of the generated designs for the uni-modal combination, involving EMG with three muscles, alongside their area and quality score predicted by the optimizer (values are normalized w.r.t. the baseline solution). (b) Comparison of model prediction with empirically measured quality scores of EMG sensing. The model is able to accurately predict the sensing quality (values are normalized w.r.t the baseline solution). (c) Visual representation of the generated designs for the multi-modal combination, involving EMG with five muscles, EDA and ECG. (d, e, f) Modality-wise comparison of model prediction with empirically measured quality scores, for EMG, EDA, and ECG sensing, showing the model accurately predicts the sensing quality. Note: The optimizer score ranges between 0 and 1 with 0 being the best. For better clarity, the graphs plot the complement value (1 - Optimizer Score) which gives a direct measure of the quality predicted.

Figure 65(c) depicts the generated designs alongside their area and quality score predicted by the model. The average reduction in the area for QUALITY OPTIMIZED solution was 10% (max: 14.4%, min: 4.8%) with an average drop in quality of only 0.5%. This reduction is smaller compared to the uni-modal case presented above due to specifics of ECG sensing: the ECG keypoints located closer to the elbow on the upper forearm produce higher signal quality, whereas the quality decreases drastically closer to the wrist. Therefore the optimizer favors designs that span a larger area up to the forearm. The average reduction in area for the AREA OPTIMIZED solution was 75.9% (max: 79.1%, min: 68%) with an average reduction in quality of 26.2% (min: 25.6%, max: 26.7%). The AREA OPTIMIZED solution again clearly outperformed the EXPERT GENERATED design (75% reduction in size with 38% drop in quality), yielding a comparably smaller footprint while offering considerably higher predicted sensing quality than the EXPERT GENERATED design. The quality for EMG was high for all the solutions since there was enough space for electrodes to be aligned to their respective muscle lines while maintaining a good inter-electrode distance. For EDA, the key takeaway here is that the optimizer scores were very similar between AREA OPTIMIZED and QUALITY OPTIMIZED solutions, owing to the fact that a similar number of sweat glands were covered in both the AREA OPTIMIZED and QUALITY OPTIMIZED solutions. For ECG, the position of the electrodes was the same for the BASELINE SOLUTION and the QUALITY OPTIMIZED solution; therefore the difference in the SNR levels across the designs was minimal. However, for the AREA OPTIMIZED solution, the quality drops drastically since the electrode locations are located further below on the forearm.

7.6 EXPERIMENTAL VALIDATION OF OPTIMIZER'S RESULTS

To experimentally validate the optimizer's prediction quality for uni-modal optimization, EMG data were recorded for each muscle on each design. Three volunteer participants (2 female, 1 male, mean age: 28y, SD: 2.9) were recruited for the experiment. The physical measurements of the forearm were procured from the participants. QUALITY OPTIMIZED and AREA OPTIMIZED designs were generated for the participants' arm dimensions through the software tool. The EXPERT GENERATED design was manually generated for only one participant. Wet-gel electrodes (KendallTM Covidien, H135SG, Sensor Area: 50mm²) were placed on the participants' right forearm at the locations specified in the design. Wet-gel electrodes are the experimental standard for measuring physiological signals and provide a stable baseline for evaluating the predicted signal quality of the optimizer. As discussed in the later sections, our anecdotal results indicate that the quality prediction of the optimizer also generalizes to dry electrodes fabricated through conductive ink-jet printing, demonstrating a close agreement between the predicted and measured signal quality.

Muscle	Voluntary Muscle Contractions
Flexor Carpi Radialis (FCR)	The forearm was rested on a table; elbow slightly turned inward; palm upward. Wrist flexion was performed at maximal contraction level [506].
Brachioradialis (BR)	The elbow was flexed to 90 degrees. Then movement was performed from full pronation to neutral [38].
Palmaris Longus (PL)	The forearm was rested on a table with the wrist in a neutral position. Standard hypothenar abduction (maximal contraction) was performed [324].
Pronator Quadratus (PQ)	The elbow was flexed to 90 degrees in mid-air; the wrist was closed to form a fist. The movement was performed from full pronation to neutral [505].
Flexor Carpi Ulnaris (FCU)	The forearm was rested on a table; elbow slightly turned inward; palm upward. Wrist adduction was performed at maximal contraction level [504].

Table 4: Five muscles used for the experimental condition and their corresponding voluntary contraction identified from literature [506]

7.6.1 Experimental Data Collection

Commercial gel-based electrodes (Kendall™ Covidien H135SG, Sensor Area: 50mm² for EMG and ECG[224], Kendall™ Covidien H124SG, Sensor Area: 80mm² for EDA [223]) were used to experimentally evaluate the performance of the optimization technique.

7.6.1.1 EMG Data Collection

The primary functions of each of the muscles were identified from the literature. For each of the muscles, participants were instructed to perform maximal voluntary contractions, with five repetitions. Before the start of the experiment, the participants were free to perform and practice the contractions. EMG recordings were recorded using a custom hardware acquisition unit (see the section on Hardware Interfacing). Digitized signals were full-wave rectified and integrated, to calculate the Average Rectified Value (ARV). For each of the muscles, the movements performed for EMG signal capturing are described in Table 1.

7.6.1.2 EDA Data Collection

For EDA, the participant underwent a Stroop Color Test [443]. This test has been used in prior work for assessing EDA response [338]. In brief, cognitive stimuli were presented to the subject through the use of words of different colors which were either conflicting (word and color of text were different, e.g., "blue" was written in green color) and non-conflicting (word and color of text were the same). The participant was instructed to state the color of the word and not read the text. The task consisted of an initial 1 min rest period followed by a 2-3 minute long Stroop test. This was followed by a final 1 min. rest period. The reference skin conductance level was also measured for each of the conditions by placing a commercial EDA sensor consisting of dry metallic electrodes (Seed Studio Groove [434]) on the fingers. One electrode was placed on the index finger while the other electrode was placed on the middle finger.

7.6.1.3 ECG Data Collection

For ECG signal acquisition, the participant was at rest, with the hands on a table, while a commercial portable ECG device (MD100, ChoiceMed) logged the data for 30 seconds.

7.6.1.4 Hardware and Interfacing

Custom hardware setups were implemented for recording EMG and EDA signals based on existing open-source hardware specifications. For EMG, our hardware setup is based on prior work which presented solutions for recording high-quality EMG data [1, 433, 461]. The sEMG acquisition board consists of one differential amplifier (INA331IDGKT, Texas Instruments) and two zero drift amplifiers (OPA333, Texas Instruments) and can measure the EMG signal of one muscle through three electrodes (2 measurement and one reference). The acquisition board converts the analog differential signal (the EMG bio-potentials generated by muscles) attached to its inputs through a Disposable Surface Electrodes connector into a single stream of data as output. The output signal is analog and has to be discretized for digital processing. The signal is passed through an instrumentation amplifier (Gain=10) followed by a high-pass filter with a cut-off frequency of 0.2Hz. Finally, an operational amplifier with a regulated gain (in the range [5.76, 101]) was used for producing a filtered amplified signal. The electrodes (measurement and reference) are connected to the board through an audio jack (aux cable). For supporting multiple muscles, multiple sEMG boards were connected with one common reference electrode. For EDA signal acquisition an open-source hardware platform was used [434]. The hardware units were externally grounded.

7.6.2 Accuracy of Optimizer Prediction with Gel Electrodes

The EMG signals were average rectified. The peaks correspond to the signal when there was a muscle movement. For each muscle, the mean Average Rectified Signals (ARVs) were calculated across all the trials. As shown in Figure 65(b) the scores predicted by the optimizer match very closely with the experimentally measured values. Overall, there was an average 2% difference between the predicted and measured values across all the muscles and all the participants for the QUALITY OPTIMIZED condition. The difference is marginally higher for the AREA OPTIMIZED solution (2.8%) and for the EXPERT GENERATED solution (4.5%). These results show that the optimization scheme can closely predict the sensing quality of a real sensor and offers an effective way of generating highly compact designs while maintaining a high-quality signal acquisition capability.

To experimentally validate the optimizer's prediction quality for multi-modal sensors, EMG, EDA, and ECG data were recorded for each of the layout conditions. Wet-gel electrodes (Covidien, H124SG) were placed on the participants' right forearm at the locations specified in the design. Similar to the Uni-Modal combination,

the EMG signals were average rectified. For the EDA, skin conductance measurements were obtained through off-the-shelf GSR sensors by placing the electrodes on the fingertips. Finally, for the ECG measurements, a commercial portable ECG device (EKG Monitor MD100E, ChoiceMMed) was used for recording.

The experimentally measured value for EDA and ECG are skin-conductance level and SNR values respectively. The SNR values as reported in prior work [101] correspond to the ratio of the QRS wave peak-to-peak voltage to the T-P wave peak-to-peak voltage. For EMG, the difference between measured and predicted values across all participants and all muscles was 0.8% for the QUALITY OPTIMIZED layout and 1.3% for the AREA OPTIMIZED layout. For EDA signals, the average difference between the predicted and measured values was 2.5% for the QUALITY OPTIMIZED layout and 4.5% for the AREA OPTIMIZED layout.

The average difference in measured skin conductance levels between the BASELINE SOLUTION and QUALITY OPTIMIZED solutions was $0.0776\mu\text{S}$ (resulting in an average of 2.9% difference) and $0.1096\mu\text{S}$ (resulting in an average of 4.7% difference) for the BASELINE SOLUTION and AREA OPTIMIZED solution. These differences are in-line with the variance found in skin conductance levels on the forearm as reported in prior work [97]. For ECG, the difference in the predicted and measured values for the AREA OPTIMIZED and EXPERT GENERATED designs was very small as well (1.1% and 0.3% respectively). It should also be noted that, although the quality of ECG signals drops drastically near the wrist, the distinct QRS peaks can still be noticed, implying the signal can be used for measuring the Beats per minute (BPM) or heart rate variability (HRV) (Figure 75(e)).

7.6.2.1 EMG Measurements

Figures 66 and 67 show the average rectified EMG signals for the BASELINE, QUALITY OPTIMIZED, AREA OPTIMIZED and EXPERT GENERATED sensor designs for the uni-modal and multi-modal configuration respectively. Each subplot shows the data from the five movement trials for each condition and muscle. It can be noticed that for all sensor designs, muscle activation can be clearly recognized from the peaks. The quality of the signal was measured by calculating the ARV value over the window where the signal is present. One of the key observations here is that, for cases in which the Optimizer predicts the worst quality (optimizer score of 1), there is still a weak signal (see Figure 66, Expert-Generated signal for FCR). This is because the optimizer has been modeled with hard constraints (e.g. offset to muscle line of 1cm results in zero quality) to ensure that the signal quality of the resulting device is usually high.

7.6.2.2 Skin Conductance Measurements

The skin conductance levels for each of the designs are shown in Figure 68. The results show that the information is still retained, although the skin conductance levels are lower when compared to the reference level, owing to the lower density

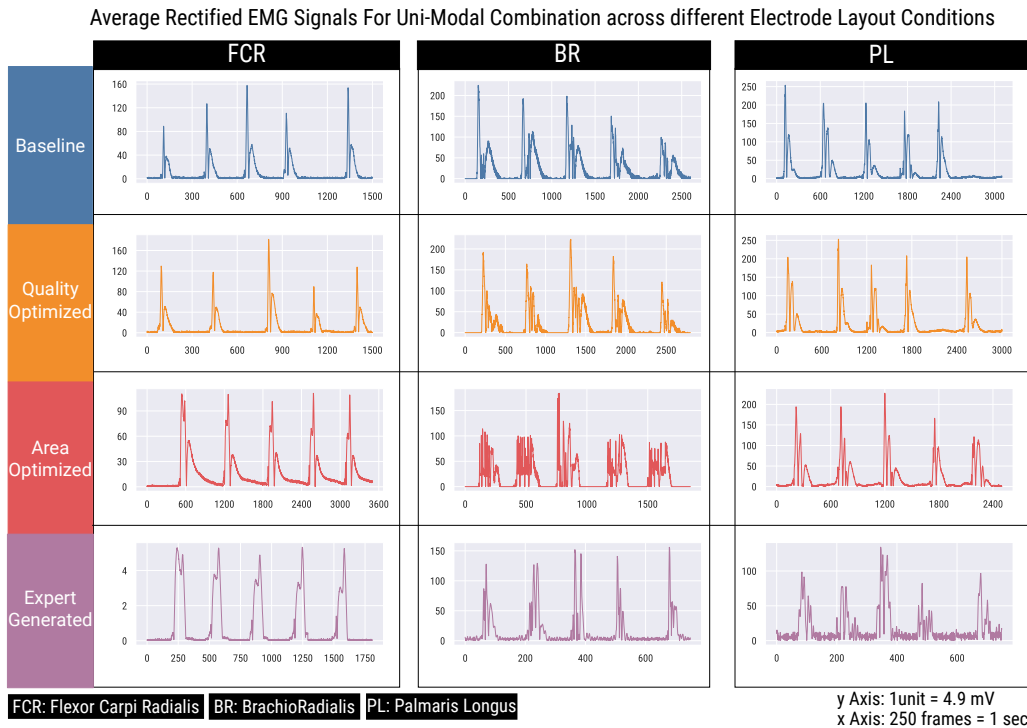


Figure 66: Average rectified EMG signals for the uni-modal combination consisting of three muscles. For each of the sensor design condition and the muscle, the predicted vs. the measured qualities have been labelled.

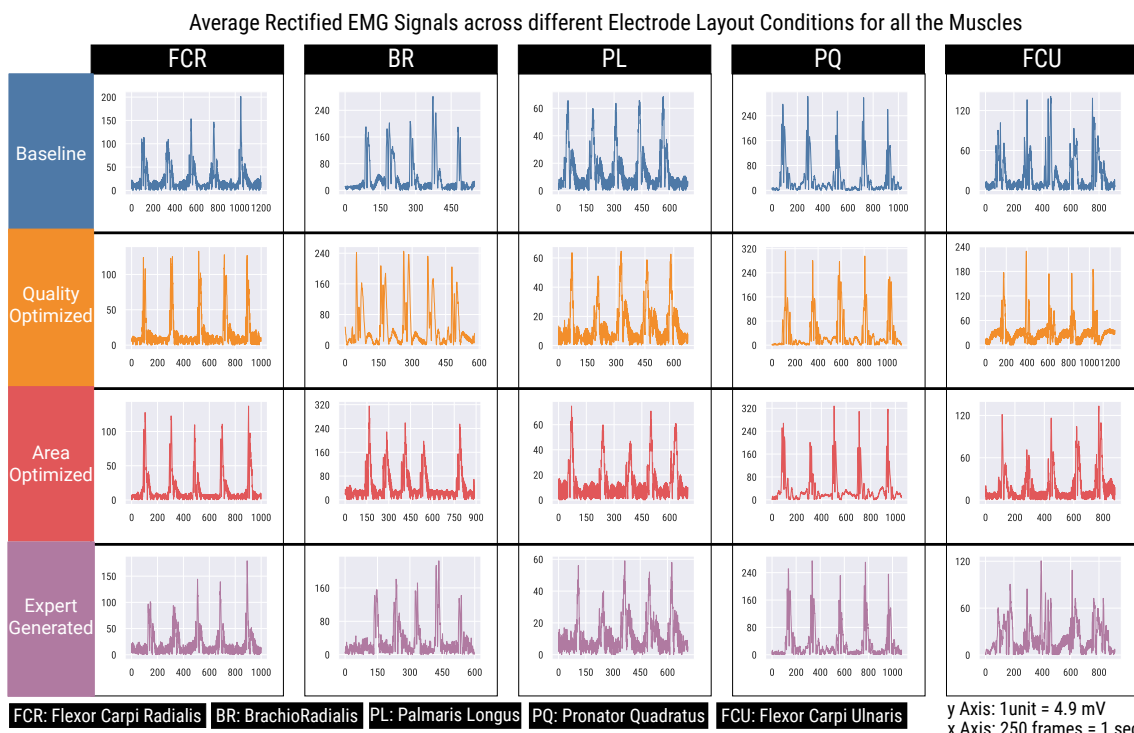


Figure 67: Average Rectified EMG signals for each of the muscles for all sensor design solutions in the multi-modal case.

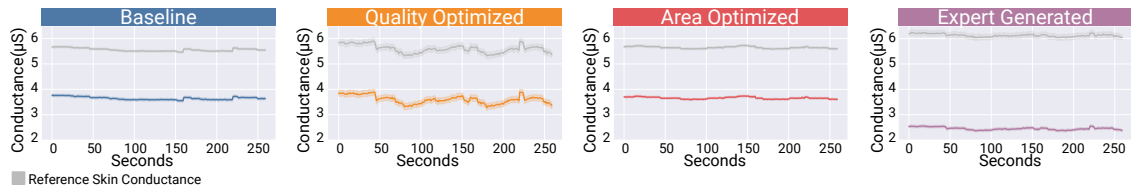


Figure 68: Raw signals of the EDA measurements for a participant for all the sensor design solutions. During each measurement, a reference measurement of skin conductance was taken by placing the electrodes on the fingertips.

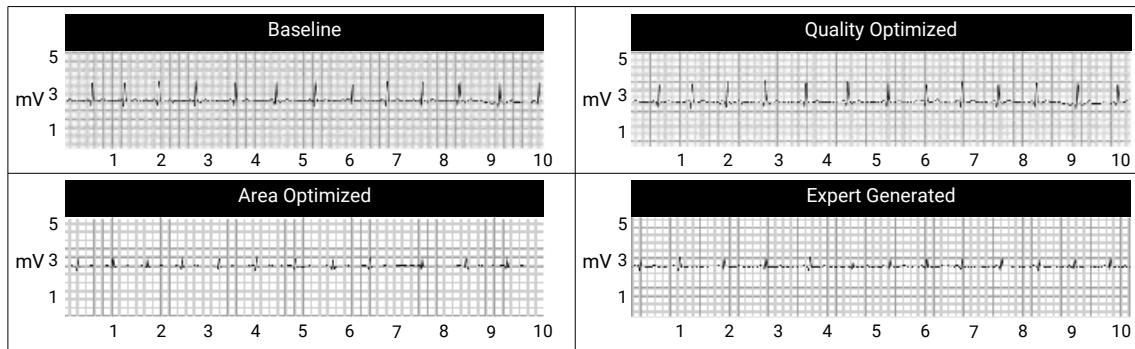


Figure 69: Raw signals of the ECG measurements for a participant for all four solutions.

of sweat glands covered by the sensor design. The average skin conductance level was $3.67\mu\text{S}$, $3.6\mu\text{S}$, $3.65\mu\text{S}$, $2.45\mu\text{S}$ for the BASELINE SOLUTION, QUALITY OPTIMIZED, AREA OPTIMIZED, and EXPERT GENERATED solutions respectively. The EXPERT GENERATED solution had a lower skin conductance level because the inter-electrode distance between the electrodes was ~ 4 cm while the other solutions had an inter-electrode distance of ~ 6 cm. The smaller inter-electrode distance resulted in a drop in the skin conductance levels because the number of sweat glands covered was lower when compared to other solutions. For all the sensor solutions, the reference skin conductance level was also measured by placing a commercial EDA sensor consisting of dry metallic electrodes (Seed Studio Groove [434]) on the fingers. One electrode was placed on the index finger while the other electrode was placed on the middle finger.

7.6.2.3 ECG Measurements

Figure 69 shows the raw ECG signals for each of the four solutions. It can be clearly seen that the BASELINE SOLUTION and QUALITY OPTIMIZED solutions have similar quality in the ECG signals. Though the SNR levels of the AREA OPTIMIZED and EXPERT OPTIMIZED are lower when compared to BASELINE SOLUTION, the signal can still be used for detecting Heart Rate Variability (HRV) which can be beneficial for various scenarios such as in applications in Virtual Reality and Human-Machine Interaction.

7.6.3 Accuracy of Optimizer Predictions for Dry Electrodes

We performed an additional experiment to understand how the optimizer's prediction scales to dry electrodes. In contrast to prior work [338] which placed electrodes at the most ideal locations, this experiment evaluates the signal quality of the electrodes when they are placed at non-ideal locations specified by the optimizer.

7.6.3.1 Fabrication of Dry Electrodes with Conductive Desktop Inkjet Printing

The fabrication method is based on the previous chapter (Chapter 6, PhysioSkin [338]) which used a desktop inkjet printer to print functional traces on various substrate materials. Commercial tattoo decal paper (SUNNYSCOPA, Printable Temporary Tattoo Paper for Laser Printer) was used as the substrate material. A layer with electrodes and connecting traces were printed using silver nanoparticle ink (Sicrys™ I40DM-106) and heat cured. An additional 3 layers of PEDOT:PSS (Orgacon™ IJ-1005, 739316) conductive polymer using the same design were printed to enhance the mechanical robustness of the brittle metallic traces. Routing traces, but not electrodes, were then insulated by printing 5 layers of PVP (Polyvinylphenol, Mw = 11,000 g/mol) on top. The layers were thermally cured. A sheet of skin adhesive film (SUNNYSCOPA) was laser cut to leave electrode locations uncovered and then bonded onto the printed tattoo sheet. The sandwich was then transferred onto the skin.

7.6.3.2 Method

The multi-modal combination was chosen for this experiment along with the AREA OPTIMIZED solution generated by the optimizer. This demanding case covered all supported modalities and muscles in a compact form factor. For comparison, signals were also captured with gel electrodes (Kendall™ Covidien H135SG, Sensor Area: 50mm² for EMG and ECG, Kendall™ Covidien H124SG, Sensor Area: 80mm² for EDA) using the same electrode layout. Overall, this experiment had the following four conditions:

- **GEL ELECTRODES - BASELINE:** The gel electrodes are placed at the most ideal locations on the forearm as specified by the BASELINE electrode layout (see main article).
- **GEL ELECTRODES - AREA OPTIMIZED:** The gel electrodes are placed at the optimized locations on the forearm as specified by the AREA OPTIMIZED electrode layout.
- **DRY ELECTRODES - BASELINE:** The dry electrodes are placed at the most ideal locations on the forearm as specified by the BASELINE solution.

- **DRY ELECTRODES - AREA OPTIMIZED:** The dry electrodes are placed at the optimized locations on the forearm as specified by the AREA OPTIMIZED solution.

For each of the conditions, the signals for EMG (for all five muscles), EDA, and ECG modalities were captured. For the dry electrodes, electrodes of circular shape were fabricated on a temporary tattoo paper substrate using the conductive ink-jet printing technique described in the Methods section. The dry electrodes had a diameter of 50 mm² for EMG and ECG modalities and 80 mm² for EDA. The same data collection method was used as described in the Methods section. One of the subjects who participated in the experimental validation of the optimizer was chosen for this experiment. To mitigate order effects, each modality was chosen at random and the order of presentation for dry and gel electrodes was chosen randomly.

7.6.3.3 Results

Figure 70 shows the comparison of the values that were predicted by the optimizer with the experimentally measured values, both for commercial gel electrodes and dry electrodes. The experimentally measured values were normalized with respect to the quality of the signal obtained in the BASELINE condition of the respective type of electrode. It can be noticed that the quantitative agreement between the optimizer prediction and the experimentally measured signal quality is at similar levels for both types of electrodes, for all three modalities. This finding suggests that the optimization approach can be generalized to different types of electrodes provided the electrodes can capture the biosignals with high quality.

Figure 71 (A) shows the absolute average rectified values of EMG signals for five muscles, captured using the BASELINE and AREA OPTIMIZED layouts with gel electrodes. Five trials were captured for each muscle in each condition. For comparison, Figure 71 (B) shows the values obtained using dry electrodes. The mean ARV of signals captured with gel electrodes (measured for both BASELINE and AREA OPTIMIZED conditions) was 1.05 V. The mean ARV of signals captured with dry electrodes (measured for both BASELINE and AREA OPTIMIZED solutions) was 0.91 V. This reduction in ARV levels is in-line with findings reported in previous work [338], which showed an average drop of ~9%. A key observation here is that while there is a drop in the signal quality for the dry electrodes in comparison to gel electrodes, the predicted and measured accuracies still are close for dry electrodes since we normalize with respect to the BASELINE solution of dry electrodes. A similar trend is also noticeable for the skin conductance measurements. It is expected that there are large variations over the course of a day. The skin conductance measurements were 9.85 μ S, and 9.56 μ S for the GEL-BASELINE and GEL - AREA OPTIMIZED conditions. The skin conductance measurements for the DRY ELECTRODES - BASELINE and DRY ELECTRODES - AREA OPTIMIZED solution were 12.76 μ S and 12.09 μ S respectively. It is interesting to

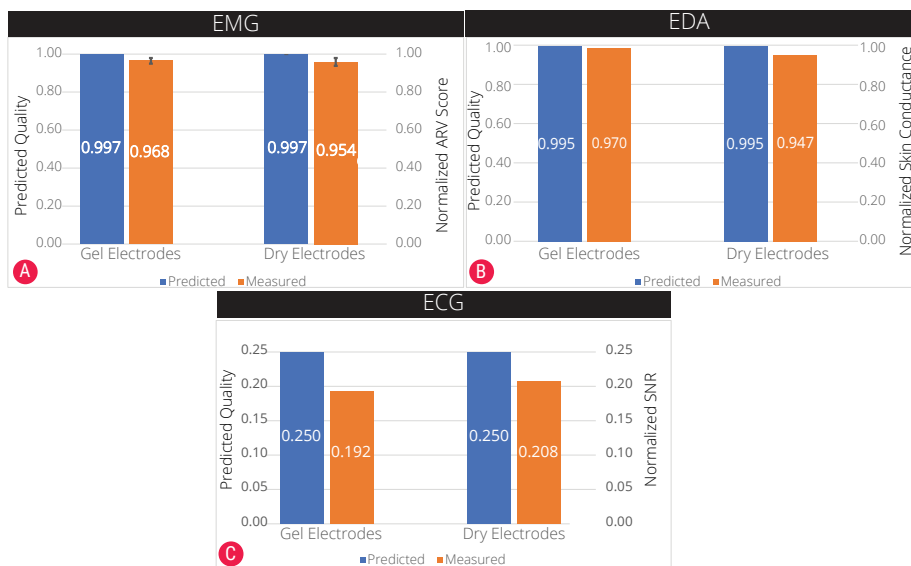


Figure 70: Accuracy of optimizer predictions for gel electrodes and dry electrodes for the AREA OPTIMIZED solution. (a) Comparison of EMG signal quality predicted by the optimizer and normalized experimental measurement, for gel electrodes and dry electrodes. (b) Comparison of EDA signal quality predicted by the optimizer and normalized experimental measurement, for gel electrodes and dry electrodes (c) Comparison of ECG signal quality predicted by the optimizer and normalized experimental measurement, for gel electrodes and dry electrodes.

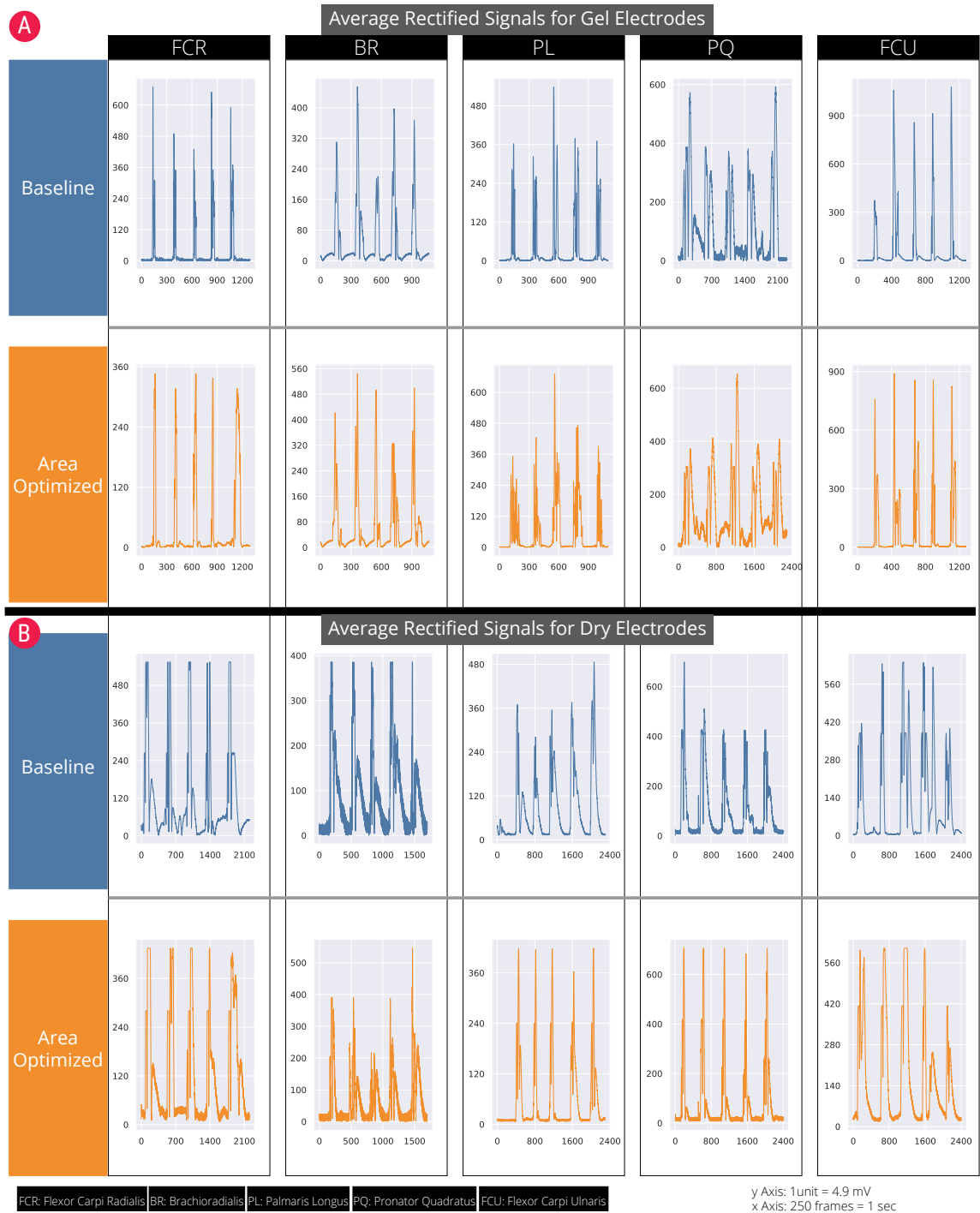


Figure 71: (a) Raw ARV signals of EMG measurements for each of the five muscles. (a) Raw ARV signals for GEL ELECTRODES -BASELINE and GEL ELECTRODES - AREA OPTIMIZED CONDITIONS. (b) Raw ARV signals for Same signals obtained with dry electrodes.

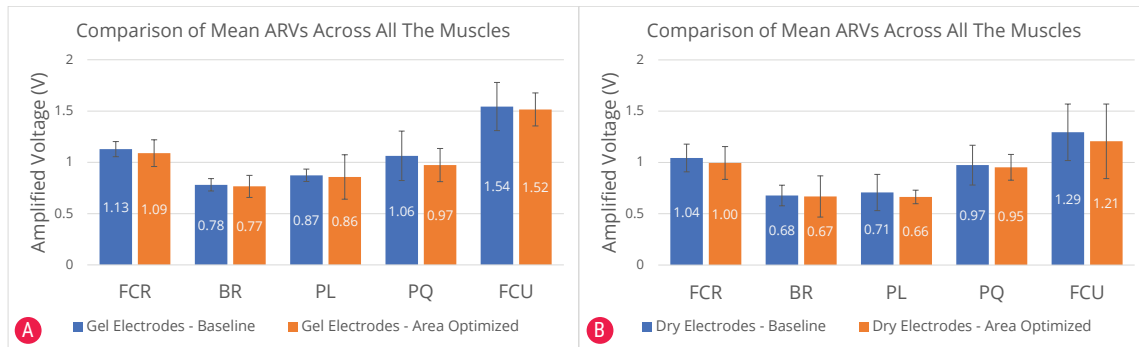


Figure 72: Magnitude of the raw ARV signals of EMG measurements for five muscles (a) Pair-wise comparison of the ARVs for the gel electrodes for BASELINE and AREA OPTIMIZED placement conditions (b) Pair-wise comparison of the ARVs for the dry electrodes for BASELINE and AREA OPTIMIZED conditions.

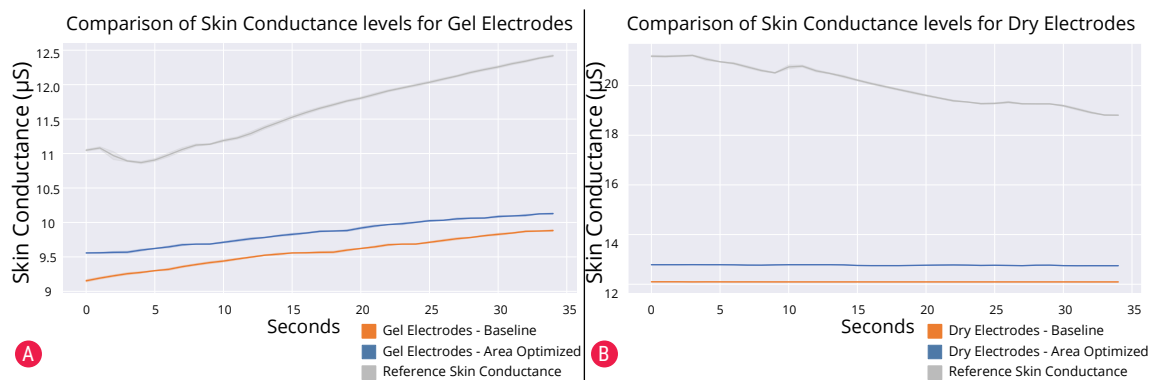


Figure 73: Raw signals of EDA measurements. (a) Skin conductance levels for the gel electrode in BASELINE and AREA OPTIMIZED conditions. (b) Skin conductance levels in the BASELINE and AREA OPTIMIZED CONDITIONS FOR THE DRY ELECTRODES.

note that while there is a change in the skin conductance levels for the BASELINE solution for the gel and dry electrodes respectively, the optimized solutions still obtain very high levels of skin conductance when compared to their respective BASELINE solutions. A similar trend is also observed for the ECG signals. The SNR levels for the GEL ELECTRODES- AREA OPTIMIZED and DRY ELECTRODES - AREA OPTIMIZED are 3.35 (sd: 0.30) and 2.67(sd:0.71) respectively. The ECG signals for each of the experimental conditions are shown in Figure 74.

7.7 APPLICATIONS

The computational design approach and the optimizer are generic. The generated designs can be implemented with either commercial gel electrodes or dry electrodes fabricated with conductive materials. Two application cases have been realized to demonstrate the benefits of the proposed approach for applications of electro-physiological sensing beyond the medical field, such as interactive

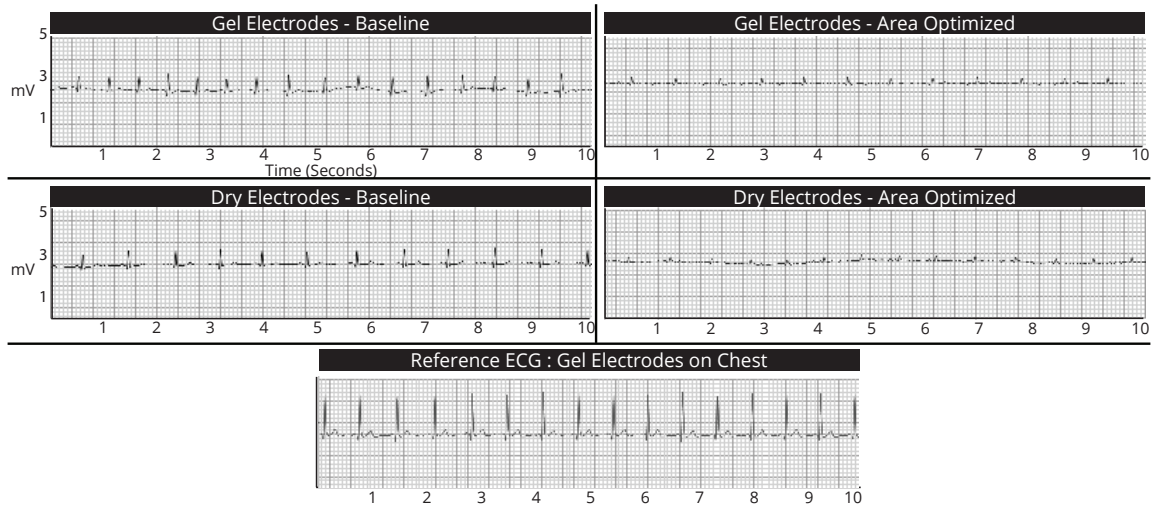


Figure 74: Raw signals of the ECG measurements showing the comparison of signals with Gel Electrodes and Dry Electrodes on the forearm.

sports devices, gaming, and virtual reality. Applications in these areas benefit from devices that have a small footprint while capturing multiple biosignals. Moreover, they impose high demands on ergonomic wearability to not obstruct body movement. These requirements can be met by integrating the computational design approach with a rapid fabrication technique [225, 338] to realize compact layouts of dry electrodes on ultra-thin temporary tattoo films.

To demonstrate an end-to-end pipeline for iterative design and rapid prototyping, a conductive ink-jet printing technique [225] has been coupled with the design tool. This combination has been utilized for fabricating an ultra-thin temporary tattoo device encapsulating EMG, EDA, and ECG electrodes. The AREA OPTIMIZED device (Figure 65 (c)) was fabricated on temporary tattoo paper for measuring EMG, EDA and ECG signals (Figure 75 (a)). Once the design was generated by the tool, a standard vector graphics application was used for creating the routing traces to connect the sensor to an external microcontroller. A flexible printed circuit (20 pins, 1mm pitch) was connected to the device with the help of a conductive z-axis tape which in turn was interfaced to two Arduino microcontrollers. One microcontroller (Arduino Uno, ATmega328P) was used to interface the five EMG channels, while another microcontroller (Arduino Uno, ATmega328P) unit interfaced with the EDA and ECG channels. Details of the hardware specifications can be found in the Methods section.

Recording physiological signals can be beneficial for personal health analytics. Inspired by new opportunities of improving physical exercising with augmented reality, an application for augmented push-up exercising has been developed. In this application, a virtual on-screen avatar performs push-ups along with the user and offers a synchronized experience using biosignals (75(b), Supplementary Video 3). When the user performs a push-up, the movement is detected through the EMG signals picked up through the temporary tattoo device on the wrist. A



Figure 75: Example applications. (a) Ultra-thin temporary tattoo with compact sensor layout generated by the optimizer and fabricated with an off-the-shelf desktop ink-jet printer. (b) Augmented reality exercising application: a virtual character performs push-up motion when the user performs a push-up. (c) A virtual reality game in which EMG-sensed gestures are used for controlling the virtual character in a first-person shooter game. (d) Raw signals of the EMG signals when performing a push-up exercise. (e) Increase in the skin conductivity levels before and after the push-ups. The shaded region represents the standard deviation. (f) Difference in the heart rate before and after performing the push-ups. (g) Raw EMG signals of the five muscles for each of the gestures used in the virtual reality game.

custom Unity application loads the virtual avatar and processes the EMG signals. When the signal corresponding to the Pronator Quadratus (PQ) muscle exceeds a threshold, a push-up is recognized (Figure 75 (d)). Then, the push-up counter is incremented, and the virtual avatar performs the push-up. The EDA and ECG signals can also be monitored. Figure 75 (f) shows the change in the heartbeat before and after performing five push-ups while Figure 75 (g) shows an increase in the skin conductance levels after performing push-ups. The computational design approach integrated with the custom fabrication pipeline enables the rapid design of a compact epidermal interface that is ergonomic to wear during physical movement. Future designs could involve designs placed at various other body locations, such as the biceps, to monitor multi-modal physiological signals while performing physically demanding activities.

The use of physiological signals in augmented or virtual reality environments is being actively explored in research [36]. Inspired by this, we developed a second application case demonstrating that a multi-modal sensor tattoo designed with the optimizer can be used as an intuitive body-based controller for gestural input in virtual reality applications. A virtual reality first-person shooter game was implemented in Unity; the interaction with the game was integrated through hand gestures that can be recognized through EMG signals. In the game, the user has to explore and shoot all the germs present in the human body (Figure 75 (c), Supplementary Video 3). Three gestures were recognized in real-time through thresholding of the signals from five EMG channels: a “Fist Clench” gesture is used to shoot a given target; a Hand pronation gesture is used to change the weapon, and a wrist flexion gesture is used for jumping. The minimally invasive form factor of the multi-modal patch can peripherally record the biosignals, without the need for dedicated sensors at multiple locations on the body. While in this scenario, we have demonstrated the use of EMG as a medium for gestural interaction, recording multi-modal physiological data can open up new possibilities for interaction and experiences in the context of augmented and virtual reality. For example, the EDA and heart rate variability data could be used for detecting the mood of the user and adapting the game’s content on the fly.

7.8 DISCUSSION

The results reported in this article demonstrate the feasibility and effectiveness of computationally designing and optimizing multi-modal electro-physiological sensor layouts. Using a computational design paradigm coupled with an optimization-based approach paves the way for automatically generating highly compact wearable devices that can monitor multiple electro-physiological modalities. With an integrated predictive model that takes into account the human anatomy, the electrode design task has been formulated as a geometric packing optimization problem. A Web-based graphical software tool allows for interactively specifying desired design parameters in a user-friendly way and for visually analyzing the

quality of generated designs. Results from the experimental evaluations show that the generated designs outperform expert-generated solutions and can considerably reduce the size of a device. Multi-modal sensors can be reduced in size by up to 79% when compared to the BASELINE SOLUTION. The sensors are also considerably smaller (19.5%) in comparison to the EXPERT GENERATED design, which suggests that the approach can create solutions that provide a very good balance between signal quality and size. Similarly, for uni-modal sensors, the AREA OPTIMIZED solution is only marginally larger (2%) but achieves considerably better quality (18.2%). The results further demonstrate high quantitative agreement between experiments and the model predictions. Two application examples were implemented and showed the feasibility of an end-to-end pipeline for computational design and fabrication of compact and ergonomic wearable sensing devices. The computational design approach is scalable to other electrophysiological modalities, provided there exists an empirically validated model that defines the placement of electrodes.

This proof-of-concept study is subject to several limitations that open a series of perspectives for future research. The model and tool are currently limited to one body location—the anterior side of the forearm. High-quality clinical-grade acquisition of ECG and EDA bio-signals is usually performed on the chest and fingertips. However, the forearm offers the benefit of superior wearability (wearability in design research is defined as the physical shape of wearables and their active relationship with the human form [118]). The forearm is one of the locations that are most unobtrusive for wearable objects [118, 339] and offer unmatched opportunities for user interaction—important benefits when considering highly practical non-medical applications such as entertainment computing, human-machine interaction, and wearable computing. While the methods presented here are expected to generalize to other body locations where continuous models are available (e.g., on the chest where continuous ECG models are available, along with placement strategies for a few muscles), there still remain several challenges to be addressed: (1) To the best of our knowledge, there exists no continuous model that evaluates ECG signals on the forearm. The discrete model used for ECG mapping in our study is simplified. Of note, this is not a limitation of the method; more advanced continuous models for ECG signals on the forearm, and other body locations, should be integrated in future studies. (2) A variety of parameters including sub-cutaneous fat levels, skin moisture levels, and variations in skin-electrode contact all affect the sensing quality [254, 399]. While the currently existing models do not consider these factors, it can be observed that the model predictions closely match the experimental measurements that were taken in the real world. It will be important for future work to develop more sophisticated models that capture more of these factors, most notably sub-cutaneous fat levels. (3) Future more advanced models could integrate additional metrics for EMG, such as RMS (Root Mean Square), Conduction Velocity, and Frequency Response. These could be beneficial for specific applications such as gait analysis, fatigue analysis, etc. Fu-

ture implementations also should expand the scope of computational design and optimization to additional electro-physiological modalities, such as EEG and EOG. (4) Currently, our model is agnostic of the type of electrode. Different electrode types can affect the signal quality due to differences in impedance, the durability of tight skin contact, or effects of skin moisture, amongst others. While the dry electrodes fabricated through our technique have low impedance and offer tight skin contact, they need to be studied more extensively with respect to the rate of degradation of the skin contact and impedance levels over an extended duration. These factors are crucial and generic for all types of dry electrodes which can be realized through various fabrication strategies. While evaluating multiple types of dry electrodes is beyond the scope of this work, this first study provides evidence that computational design approaches can be integrated with custom-fabricated dry electrodes.

For all these modalities requiring precise placement of electrodes on the body, this computational approach could pave a promising way for guiding electrode placement and reducing manual placement overhead. From an optimization perspective, our current implementation is based on Simulated Annealing which needs to be stopped after a finite number of iterations without exactly knowing how far the result is from the optimum. One approach to improve the optimization scheme in future work is to use a mixed-integer optimization that yields a rigorous lower bound on the signal quality using methods such as branch-and-bound that could serve as a benchmark.

Considering that electro-physiological sensing is becoming more widespread and is making its way into non-medical disciplines, approaches based on computational design, rather than manual heuristics for experts, promise to accelerate the widespread adoption of these sensing techniques. This first exploration unfolds a new dimension for the design of electro-physiological sensors leveraging the power of computational optimization, guided by an interactive real-time design tool. This can represent a significant step towards a fully automated and highly scalable pipeline for the design and creation of electro-physiological sensing devices.

7.9 CONCLUSION

This chapter proposed a computational approach for designing multi-modal electro-physiological sensors. By employing an optimization-based approach alongside an integrated predictive model for multiple modalities, compact sensors can be created which offer an optimal trade-off between high signal quality and small device size. The task is enabled through a graphical tool that allows for easily specifying design preferences and visually analyzing the generated designs in real-time, enabling designer-in-the-loop optimization. Our method is generic and is independent of the type of electrode material used for physiological signal acquisition. Experimental results show high quantitative agreement between the

prediction of the optimizer and experimentally collected physiological data. They demonstrate that generated designs can achieve an optimal balance between the size of the sensor and its signal acquisition capability, outperforming expert-generated solutions.

While Part 2 of this thesis focused on the computational design and fabrication of Epidermal Devices for enabling rich on-body interaction, this part (Part 3) of the thesis focuses on physiological sensing. Taken together, Chapters 6 and 7 contribute rapid fabrication and computational design methods for creating Epidermal Devices that can sense multiple modalities of bio-signals.

Part IV

Part Four - Next Steps in Epidermal Computing

NEXT STEPS FOR EPIDERMAL COMPUTING

The previous chapters in this thesis have contributed novel computational design and rapid fabrication techniques for creating Epidermal Devices. In addition, the field of HCI has seen rapid growth in the development of Epidermal Devices in the past few years. Epidermal Devices are also receiving a lot of attention in other research disciplines. With rapid technological advancements in multiple disciplines, we see a need to synthesize the main open research questions and opportunities to advance future research in this area. By systematically analyzing Epidermal Devices contributed in the HCI community, physical sciences research, and from our experiences in designing and building Epidermal Devices, we identify opportunities and challenges for advancing research in five thematic areas. This chapter builds on the multidisciplinary analysis presented in Chapter 2 to identify opportunities and challenges that enables multiple research communities to facilitate progression towards more coordinated endeavors for advancing Epidermal Computing.¹

8.1 THEMES FOR FUTURE RESEARCH

By performing a thematic analysis of these research works across disciplines, we present a synthesis of challenges and opportunities that can drive future work in this area across five thematic areas (see Figure 76):

- **Functional Materials:** We analyze the functional materials that commonly are used for building Epidermal Devices across disciplines. Based on this, we identify opportunities and challenges for sustainable materials, stretchable conductors, safety, and handling of materials.
- **Fabrication and Design Workflows:** By analyzing and understanding the fabrication mechanisms and design workflows used for realizing Epidermal Devices, we identify potential opportunities and challenges for devising new techniques that better support rapid prototyping, require only simple lab equipment, and enable easy fabrication of devices.
- **Devices and their functionality:** We compare and contrast the devices across disciplines based on their functionality and the interactions that are supported.

¹ This chapter is based on a research paper that has been submitted for ACM CHI'22. I performed the literature survey. I and my advisor Jürgen Steimle framed the definition of Epidermal Computing, derived the challenges and opportunities, and wrote the paper.

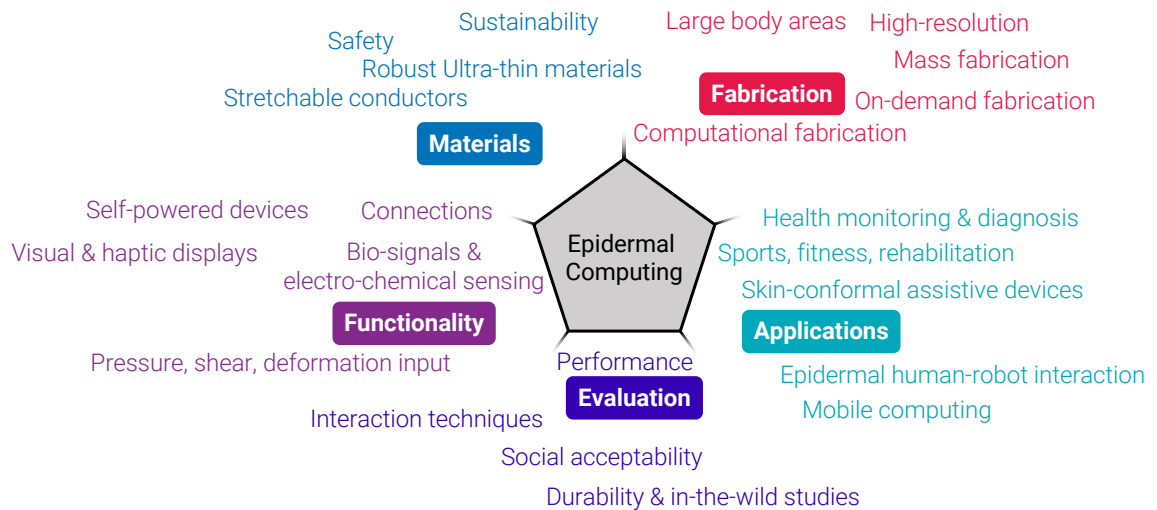


Figure 76: Opportunities and challenges for Epidermal Computing span aspects of materials, fabrication, functionality, evaluation methods, and applications.

By understanding and analyzing several device types, we identify future device functionalities that can be developed by the HCI community.

- **Evaluation Methods and Strategies:** We compare methods of evaluating technical aspects, human factors, and user interaction of Epidermal Computing Devices across disciplines. We identify the next steps with regard to fundamental empirical experiments for understanding skin-specific interactions, social acceptability, and in-the-wild studies of Epidermal Computing.
- **Applications and Real-World Deployments:** By comparing and contrasting the applications and deployments that have been targeted, we identify opportunities for potential applications that future Epidermal Devices can target.

In the following sections, we will discuss these thematic areas in turn.

8.2 MATERIALS

8.2.1 Sustainable Materials

Most materials used for Epidermal Devices today are not sustainable. For instance, rare metals are precious resources, most polymers do not biodegrade well, and multi-material sandwiches are hard to recycle. Considering that many devices are intended for one-time or short-term use, this is an issue. Here, bio-based and bio-degradable materials can open up new design space for epidermal devices, which is beginning to be explored in Materials Science [238] and in HCI [470]. By using fully bio-degradable materials like gelatin, agar-agar, etc., one might ultimately have Epidermal Devices that after use can be simply composted. Our

recent exploration takes the first step in this direction by fabricating epidermal devices with biodegradable materials such as gelatin, agar-agar, corn starch, etc.

8.2.2 *Stretchable Conductors*

A common challenge is the trade-off that exists between highly conductive materials and their stretchability. Intrinsically stretchable conductors such as PEDOT:PSS are stretchable, but typically suffer from a rather low conductivity. In contrast, metallic conductors such as silver and gold possess high conductance levels, however, they are brittle because of their high Young's modulus. A common strategy that has been employed in the Materials science community is to have composite materials, e.g. mixing liquid metals with silver particles to have highly stretchable and conductive material composites [450]. However, a downside of this approach is that the formulation process is complex and the composite material (e.g. liquid metals) might not be bio-compatible. Another approach has been to use carbon in the form of nano-tubes or nano-particles. These have been successfully demonstrated in materials and HCI research works. However, they need meticulous safety practices and a lab environment that might not be available to a large community of makers, hobbyists, and practitioners. The next step in this direction is to identify the suitable materials that are easy to handle, are bio-compatible, stretchable, conductive, and require minimal safety equipment and measures. Carbon-based composites such as graphene and graphite show a promising direction in this regard [54, 106]. Another approach that has been used is to fabricate multi-material layers composed of intrinsically conductive polymer (e.g. PEDOT:PSS) and highly conductive metals (e.g. Silver) so that the conductive polymer bridges the cracks that occur in the metal layer [500].

8.2.3 *Robust Ultra-Thin Materials*

While tattoo papers are ultra-slim and conform to complex geometries, they suffer from limited mechanical robustness. PDMS substrates on the other hand offer can be fabricated to custom thickness levels offering and can be more mechanical robust [339]. However, a key challenge that needs to be addressed is to identify substrate materials and their compositions that are ultra-thin and stretchable while being mechanically robust for a long duration (as shown in Figure 77). The same holds true for functional materials, and new explorations on functional carbon composites which include graphene and its compounds in materials science offer a promising direction in this regard [54, 106].

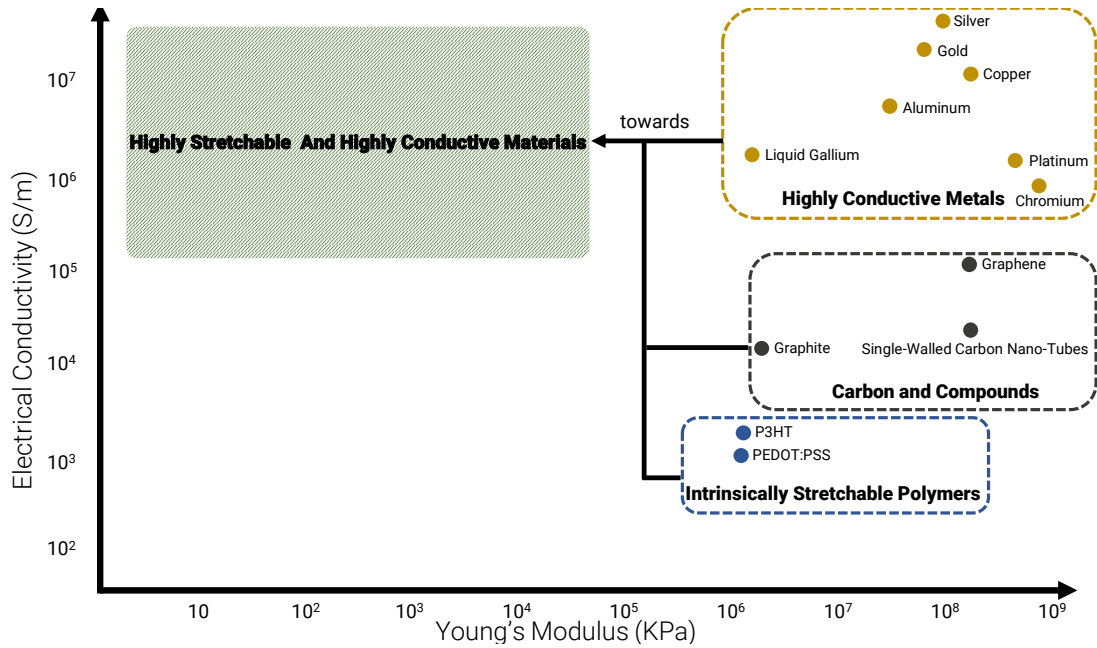


Figure 77: Most commonly used functional materials for epidermal devices, plotted against their respective electrical conductivity and Young's modulus. A key opportunity for further research is to develop highly stretchable materials that possess high electrical conductivity. Note: Young's modulus is inversely proportional to stretchability.

8.2.4 Technical and Safety Challenges for Handling Materials

Epidermal Devices are present on the surface of the human body and hence the functional materials that are used in the device should not harm the human body. While there have been several explorations of using sophisticated materials such as carbon nanotubes and liquid metals in the HCI literature, special consideration should be taken with respect to the handling of these materials as they are toxic in nature and hence not compatible with the typical standards applied in DIY processing. While safety standards and training do exist in maker spaces and fab labs, these usually cover the safe handling of machines, rather than the safe handling of materials. In the HCI and maker communities, we see the need to increase the awareness of potential hazards associated with materials and their processing and recommend lab managers to establish formal safety standards and dedicated training on material safety.

Another opportunity here is to identify, explore and investigate completely safe-to-use and bio-compatible materials. For instance, recent work in physical sciences research has demonstrated Epidermal Devices using a pencil [524].

8.3 FABRICATION

8.3.1 *Computational Fabrication*

An important direction for future work is to devise new computational design techniques that assist the designer in customizing the design for individual users, their body dimensions, and aesthetic preferences. Such techniques will need to take into account anatomical models and operationalize them for automatic optimization. This will be particularly important for functionality that depends on a specific body location, such as monitoring bio-signals. It remains a wide-open challenge of how to capture and model a user's aesthetic preferences, and operationalize them for computer-assisted device designs. These steps will pave the way for the rapid fabrication of epidermal devices that can be customized for form, shape, and aesthetics. Integrating computational design approaches with rapid prototyping techniques can facilitate on-demand mass fabrication of devices. This can enable more widespread and in-the-wild testing and evaluation of device designs, which in turn can guide the computational design and fabrication process. In addition to incorporating human-centered properties such as body dimensions and anatomical models, future tools should also explore integrating material models and finite element analysis methods which allows designers to quickly identify, predict, debug and custom-design the mechanical and electrical properties of the device.

8.3.2 *Fabricating for Large Body Areas*

Current state-of-the-art devices in HCI are usually designed for relatively small body areas and regions. Scaling up the size of such devices to enable coverage over entire, large regions of the body can open new avenues for physiological sensing. For instance, large-area, body-scale epidermal devices for electromyography (EMG) can provide robust recording capabilities across multiple muscle groups. Full-scalp or full-forehead epidermal devices for electroencephalography (EEG) can monitor electrical activity across the brain with high resolution. However, there remain three major challenges in scaling current epidermal devices in HCI for large-area electrophysiology: Firstly, the current fabrication processes used in HCI limit the size of devices to a few centimeters. Recent work in biomedical engineering has demonstrated tattoo-like electrodes for full-scalp EEG [494]. However, the microfabrication process on large thin-film wafers is expensive and requires sophisticated equipment. Secondly, without robust encapsulation, extended interconnects in direct contact with the skin can capture unwanted but substantial biopotentials that interfere with the signals collected by the measuring electrodes [63, 161]. Finally, the geometrically non-developable nature of human skin surfaces can cause wrinkles and high levels of strain on the ultrathin elec-

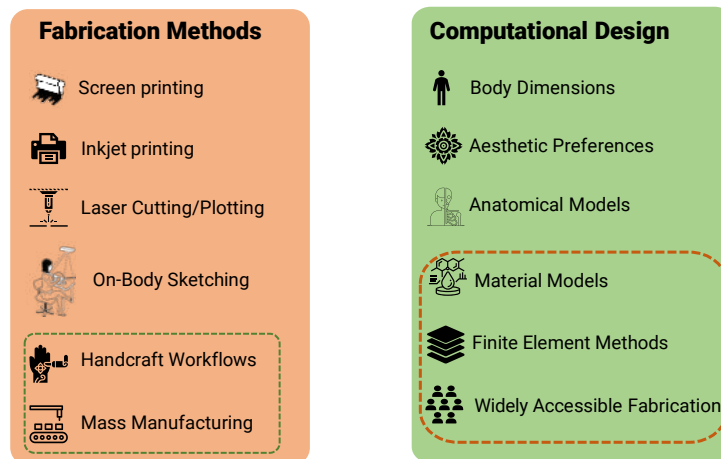


Figure 78: Key research themes for Fabricating Epidermal Devices. A number of rapid and easy-to-perform fabrication methods have been explored in HCI. For each of the fabrication methods and computational design approaches, representative research works from physical sciences and HCI research are shown. The next steps (highlighted) include the exploration of fabrication methods that leverage traditional art and handcraft-based workflows (e.g. henna tattoos) and exploration of mass manufacturing techniques. For computational design techniques, advanced design tools incorporating material properties, FEM analysis, and widely accessible fabrication methods are the next crucial steps.

trodes, which can reduce the mechanical robustness or the conformality of the devices [298, 483].

8.3.3 Supporting High Resolution and Complex Aesthetic Patterns

One of the key features of Epidermal Devices that the HCI community has focused on is the development of aesthetics for Epidermal Devices. While there are custom design tools that enable designers to create 2D aesthetic patterns [304] and support free-form sketching with a pen or a computer-controlled plotter [66, 373], most of these aesthetic designs are limited to line-arts and simple designs. Future work should look into incorporating more complex and compelling aesthetic patterns that are common in traditional handcrafts.

8.3.4 Mass Fabrication Techniques

A big next step for advancing Epidermal Computing for creating devices on a scale and for real-world deployments is to explore and identify mass manufacturing fabrication techniques. While some of the fabrication processes that have been used for Epidermal Devices have been based on mass manufacturing processes such as screen printing, they have not yet been explored on a large scale. Other techniques are not compatible or not suitable for producing devices on a large

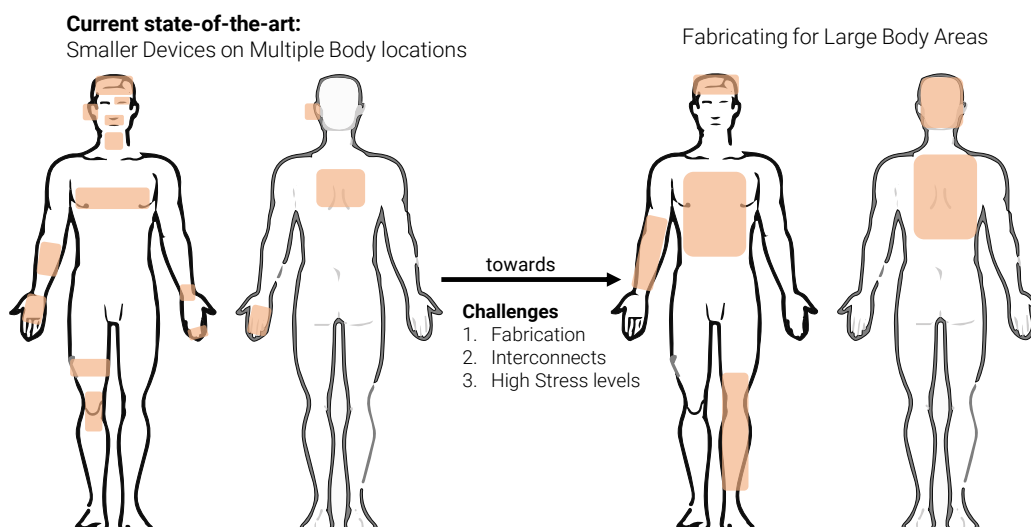


Figure 79: Current Epidermal devices are limited to a few centimeters in size. The next step is to create skin-conformable epidermal devices that cover large body areas. Representative research works from physical sciences and the HCI research community are shown.

scale. An analogy that can be compared to here is the growth of interactive textiles that leverage standard practices of mass-manufacturing textiles such as weaving, using of looms, and development of yarns [372].

8.3.5 On-Demand Fabrication Techniques

An approach orthogonal to mass manufacturing is on-demand, on-place fabrication. Epidermal devices that are personalized for a specific user might be fabricated on-demand at a local pharmacy or even at the user's home. Recent work on fabricating epidermal devices with inexpensive commodity desktop printers is making a pioneering step in this direction [225, 338]; however, more work is required until we can ultimately print an entire device on demand.

8.4 FUNCTIONALITY OF DEVICES

8.4.1 Pressure, Shear and Deformation Input

While touch contact sensing on Epidermal Devices has been intensely studied in the HCI community [215, 287, 341, 498], there is yet very little investigation of interaction using variations of pressure, shear, and deformation. These promise to further enhance the interaction vocabulary by directly building on the softness of human skin. In particular, high-resolution sensing matrices should be investigated alongside the versatile gestures and interactions they enable on diverse body

locations. This could be achieved by building onto research from material and physical sciences, and using piezo-resistive materials which have a good response to pressure [390], or employing capacitive approaches with soft dielectric materials, which provide a unique capacitive signature when normal or shear force is applied. Dense microfluidic channels and ionotronic sensing [562] is another promising alternative.

8.4.2 *Output with Visual Displays and Haptic Displays*

Further improving the quality of visual displays within interactive Epidermal Devices will be an important next step, to move past the limited quality and resolution of thermochromic or electroluminescent displays.

Printed e-ink displays and OLEDs are powerful display technologies that should be explored for Epidermal Devices. E-ink displays have been explored for wearable devices [91]; however, a key challenge is the realization of e-ink displays in skin-conformal form factors, and ideally in a simple lab environment.

Important next steps for epidermal tactile output displays comprises increasing their spatial resolution and scale. Integrating multiple forms of haptic output, for instance, pressure, skin stretch, and thermal output, in one Epidermal Device is another very promising direction, as this directly corresponds to the multi-sensory nature of human skin. Electric muscle stimulation has been widely used for providing kinesthetic feedback [219]. However, the vast majority of this work uses either commercial gel-electrodes or textile electrodes [247]. An opportunity for more ergonomically wearable systems is to use Epidermal Devices that encapsulate dry electrodes for EMS output.

8.4.3 *Bio-Signals and Electro-Chemical Sensing*

Integrating physiological sensing to a greater extent opens up interesting directions for research in HCI, which so far has been mostly concerned with user input and system feedback. For instance, deploying electro-physiological sensors that capture multiple bio-signals (e.g., EEG, ECG, EOG, EDA) at various body locations can open up opportunities for diverse applications such as continuous activity tracking, gestural interaction, or health monitoring.

Moreover, we identified that the HCI community so far is not using electrochemical sensing for capturing rich bio-signal data about the electrolyte and metabolite concentrations in the body. For instance, these comprise measuring blood glucose levels or lactate levels in sweat, which are indicators of physical activity. This poses the challenges not only of identifying the appropriate materials for sensing and sensor designs, but also identifying safe and easy-to-perform techniques for rapid prototyping that allow for encapsulating chemicals in the Epidermal Devices.

8.4.4 *Energy Harvesting and Self-Powered Devices*

Prior work in materials and physical sciences research has shown that energy can be harvested successfully for powering Epidermal Devices. Although fully untethered devices have been contributed in HCI [221, 304], self-powered devices that can harvest energy through biomechanical and physical processes are a natural and important next step for investigation. For instance, this might be achieved through triboelectric generators, which have received attention due to their easy and rapid fabrication [13] and their applicability in self-powered haptic displays [412]. However, designing devices that integrate sensing, display, and energy harvesting capabilities, all in an ultra-thin form factor, is a challenge. Computational design and optimization techniques have strong potential in helping to solve this challenge, finding optimal multi-modal device designs which have been successfully demonstrated in the HCI community can solve these challenges by taking user inputs and constraints for each of the modalities and finding an optimal design.

8.4.5 *Connections and Tethering*

Connectors and tethering the device remain a challenge, mainly because the slim and stretchable devices are not well compatible with conventional cables, jumper wires, or copper tape. This is a common problem and the most widely used approaches have been to use copper tape [500], conductive z-axis tape to connect the device to an external flexible copper-clad laminated onto a silicone [304] or to flexible printed cable [341, 510]. The latter two approaches enable easy connection of highly dense connector lines and offer flexibility, but future research should investigate the fabrication of highly stretchable connectors while supporting a large number of I/O pins. Similarly, it remains an open challenge to robustly tether multiple Epidermal Devices that are located at different body sites.

8.5 EVALUATION METHODS AND STRATEGIES

Most of the empirical work can be categorized into the following classes: Elicitation studies, social acceptability studies. However, very few of these studies actually involve epidermal devices.

8.5.1 *Understanding Skin-Specific Interactions*

Current mobile and wearable devices have matured because of numerous studies and interaction techniques that have been designed and evaluated for enabling seamless interaction [173]. Similar studies need to be designed and conducted for Epidermal Devices. Skin affords a wide variety of rich interactions such as pulling,

pushing, squeezing etc [499]. While first technologies enable such interactions, the interaction granularity of skin-specific interactions is still unknown, for e.g. what is the comfortable range and resolution with which we can perform a skin pinch gesture. Similar studies have been conducted with e-textiles [147, 218], however these studies do not translate to skin-specific interactions. Studying these questions is further complicated by the strong influence of skin location, body posture, a user's individual body anatomy, and mobility condition. The current state-of-the-art Epidermal Devices offer a viable technical platform for designing and conducting such interaction-specific studies.

8.5.2 *Performance Studies*

To gain further understanding of Epidermal Devices we need to move on to conducting studies that rigorously investigate interaction performance on Epidermal Devices. Preliminary investigations have investigated how the material stiffness of Epidermal Devices affects tactile perception [339] (described in Chapter 3). Similarly, identifying the appropriate, additional physical and mechanical properties of the devices such as surface friction and roughness to maximize input performance need to be investigated. One example is Fitt's laws studies to optimally design patches for specific body locations and body dimensions. In addition, advanced simulation studies, e.g., using biomechanical models, and FEM analysis of skin and Epidermal Devices would inform the community and designers about optimal physical and mechanical parameters to increase performance and ergonomics.

8.5.3 *Durability and In-the-wild Studies*

Typically, Epidermal Devices in HCI have been evaluated with a rather low number of participants and during short durations of use, most often in a lab setting. Testing and evaluating device functionality over multiple weeks is the major next. Preliminary investigations in this regard have been reported in physical sciences research [105, 193, 240, 537]. In-the-wild studies and field deployments help us in identifying technical issues with respect to power consumption, strong skin-conformal contact, and clean signal acquisition, but also in uncovering patterns of use in real-world contexts.

8.5.4 *Social Acceptability Studies*

Identifying what factors of Epidermal Devices increase or decrease social acceptability will provide important insights allowing to design of the next generation of devices that bring Epidermal Computing one step closer to mass adoption. While body locations are well researched [98, 188, 547], other design choices are underexplored. Social cues have been tackled in prior work [88, 179] but not systematically

evaluated. Moreover, questions related to self-expression and how personalization of devices can contribute to it [376], but also impression management [122] and also the effect of a device's visibility for bystanders need to be studied [211]. Applying and comparing design strategies for increasing social acceptability that has been presented by Koelle et al. [248] to the field of Epidermal Devices will be another important step for future work on social acceptability.

8.6 APPLICATIONS AND REAL-WORLD DEPLOYMENTS

Due to their unique form factor, intimate integration with the user's body, and low cost, Epidermal Devices open up a range of opportunities for applications and real-world deployments. These span a wide range of areas, ranging from general mobile computing and communication to supporting a user's bodily activities in sports and fitness, and ranging from health monitoring and diagnosis for the masses to more specialized areas such as assistive technologies. Exemplary application scenarios are one area where the HCI research community trumps over the physical sciences research community.

We identify a few compelling application domains where deploying Epidermal Devices can not only reveal new insights but also can have a long-term societal impact. Epidermal devices present strong opportunities in several domains, where deploying Epidermal Devices can not only reveal new insights for future generations of devices but also can have a long-term societal impact.

8.6.1 *Assistive Technologies*

The fields of assistive and accessible computing provide opportunities for further expanding the deployment of Epidermal Devices. For instance, epidermal haptic devices can be used for providing braille output through subtle localized vibrations. In this respect, empirical investigations aiming at understanding the specific needs and preferences of the target population (visually impaired, deaf and hard of hearing, or users with motor impairments) with respect to Epidermal Devices can uncover rich design guidelines. Additionally, exoskeletons are an active research area covering multiple disciplines; the development of epidermal exoskeletons that are skin-conformal and stretchable can open up opportunities for novel assistive technologies in areas such as prosthetic control, neuromotor training, and rehabilitation.

8.6.2 *Health Monitoring and Diagnosis*

Health monitoring and diagnosis is an application area that is promising and has a large potential for large-scale deployment of Epidermal Devices. When manufactured on large scale, Epidermal devices can be very cost-effective and

serve as useful tools for non-invasive measurement of health parameters. For example, recent research has successfully used Epidermal Devices for non-invasive COVID-19 testing [462]. We identify multiple opportunities for the HCI community to advance the state-of-the-art with respect to health monitoring: (1) using computational approaches for placement of devices and optimizing device designs to incorporate multiple sensing modalities, possibly even for individual users, (2) advanced signal processing and recognition algorithms for deployment in the wild and (3) machine learning techniques to continuously understand user's health from noisy or sparse sensor data. We anticipate that coupling the powerful physical capabilities of Epidermal Devices with the strengths of software-centered data processing will significantly enhance the quality and availability of data for long-term health monitoring and open up previously unseen opportunities for medical diagnosis.

8.6.3 *Sports, Fitness, and Rehabilitation*

Sports, fitness, and rehabilitation can serve as promising avenues for deploying Epidermal Devices. Research in rehabilitation studies has shown initial deployments of Epidermal Devices[355] for tracking precise body movements. Higher resolution and denser sensing patches, including full-body suits, should be developed for enabling detailed whole-body activity tracking, which can have applications in sports, fitness, and rehabilitation studies. Another area that has received limited attention is the field deployment of Epidermal Devices for athletic and sporting activities.

8.6.4 *Human-Robot Interaction*

Human-robot interaction is an active research area across multiple disciplines. We identify two major opportunities where Epidermal Devices can enhance human-robot interaction : (1) Imbuing the robot with human-like sensor capabilities: this involves designing Epidermal Devices for deployment on a robot that can capture a wide range of expressive interactions similar to the perceptual abilities of human skin, as well as devices that imitate the soft material properties of human skin to enhance human-to-robot touch contact [453]. (2) Enhancing control of robots through Epidermal Devices: controlling and manipulating robots is a complex task and this becomes even more challenging for a swarm of robots. Using skin-based interactions is a promising solution because of the human natural proprioceptive capabilities and dexterity. Preliminary work on controlling a drone through Epidermal Devices has already been reported [7].

8.6.5 *Mobile Computing*

Prior work in HCI has contributed many approaches for enriching and improving the user interaction with existing mobile and wearable devices. These explorations provide a good foundation and important lessons learned for moving to the next phase of transitioning from prototypes to commercial products. The first step in this direction is to blend these Epidermal Interfaces with existing wearable devices, for instance, soft interactive watch straps for smartwatches or as beauty accessories. Key challenges for such deployment range from identifying compelling interaction-specific use cases (e.g., eyes-free entry, inconspicuous interaction, subtle notifications without the user having to look at his mobile device or watch) to more social and personal challenges such as the aesthetic customization of the devices.

8.6.6 *Ethics, Security, and Privacy*

Security and Privacy, but also Ethics define important challenges to be considered in future applications of Epidermal Devices. Currently, no security or privacy-based features are incorporated into device designs. Unlike mobile devices which rely on security measures such as fingerprint authentication, patterns, pins, or passwords, the body provides a more sophisticated means for authentication. Bio-signal [272] and bio-impedance [75] based authentication has been explored as a promising medium for adding another layer of security for Epidermal Devices. Additionally, since Epidermal Devices are present on the body, they are already in the private space of the user, which adds another level of privacy. However, this intimate coupling with the body opens up new concerns. For one, Epidermal Devices can capture highly privacy-critical biological data about a user's body and health status. Second, the body-based output capabilities of Epidermal Devices open up new threats and ethical questions. For instance, who should be allowed to alert the user with haptic messages, and on what body locations? Under what circumstances is it legitimate to influence the user's mood through scents that are automatically disposed from Epidermal Devices? How can one avoid a hacker is getting access to an Epidermal device that through electrical muscle stimulation can control the sensorimotor functions of the victim?

Such situations of concern should be foreseen now and design decisions should be explored to counter dark patterns that might emerge in the future.

8.7 CONCLUSION

Across disciplines, there has been a rapid growth of Epidermal Devices in the last few years, embracing new technological developments and deployed in multiple domains, leading to the development of a new era of Epidermal Computing. Despite being a highly multi-disciplinary area, the field is beginning to close in

on common areas encircling new materials and fabrication, new device types, theoretical and empirical foundations, and application domains. We have identified challenges and opportunities for each of these five different themes which are key to the overall development of the area.

Our analysis builds on our own practical experiences and on an in-depth analysis of the literature that exists across multiple disciplines and research communities. This cross-disciplinary angle brings a unique perspective and helps in identifying the overarching scientific goals that transcend the boundaries of a single research community. We, therefore, believe that the challenges and opportunities presented in this paper will resonate with scientists and researchers from disciplines inside and beyond HCI, leading to coordinated efforts across disciplines. We hope that engineers, practitioners, and industry experts will recognize them for the successful commercialization of the devices. We also invite new researchers and practitioners entering the area of Epidermal Computing to use this thesis to identify and work on unsolved challenges and research problems.

While Epidermal Computing promises an exciting future, it is also very crucial to identify potential dark patterns. We have briefly discussed about these in the previous section. Previous research in HCI has identified dark patterns in interaction design [129, 130, 395] where users are deceived by the technology. We acknowledge that some of these dark patterns also apply to Epidermal Computing. We hope future work will build on our work to identify dark patterns thereby promoting safe and ethical usage of Epidermal Computing technology.

CONCLUSION

Skin is a fascinating human organ and provides several benefits for interaction. In addition to enabling rich expressive touch input, human skin acts as a biological interface for capturing bio-signals. Epidermal Devices exploit these ideal user interface properties provided by the skin for enabling rich interactions. The goal of this thesis was to advance the design and fabrication pipelines for realizing Epidermal Devices. In addition to contributing fabrication and computational design strategies, this thesis also takes the first step towards providing a deeper empirical understanding of Epidermal Devices. These empirical studies focus on how our tactile perceptions capabilities are affected while wearing Epidermal Devices.

9.1 SUMMARY

This thesis proposes Epidermal Computing as a natural successor for the current wearable computing paradigm. It advances this emerging multi-disciplinary research area by contributing novel fabrication and computational design techniques for the rapid design and development of Epidermal Devices. In particular, it advances the field in the following areas:

Material Exploration: Conventional materials used in commercial touchscreen devices are not compatible for deployment on the body. This is because, unlike commercial wearable devices, the human body is soft, malleable, and supports strong deformations. Hence, from a device design standpoint, material exploration is the first step for realizing Epidermal Devices. In addition to identifying material combinations that are stretchable while possessing high electrical conductivity, identifying other suitable materials such as insulators and skin adhesives is crucial. Chapters 4, 5, and 6 highlighted these aspects. Chapter 5 explores various material combinations including conductors and insulators suitable for creating the sensor sandwich for sensing high-resolution multi-touch input. Chapter 6 highlights the importance of skin adhesives for creating tight electrical contact with the skin for acquiring bio-signals. Through diverse material explorations, this thesis helps in better understanding the properties of functional materials that are vital for fabricating various types of Epidermal Devices.

Fabrication Techniques: Creating easy and rapid fabrication techniques is very vital for promoting the development of custom Epidermal Devices to a wider audience including researchers, practitioners, makers, and hobbyists. The primary goal of fabrication techniques used in this thesis has been to use off-the-shelf materials and simple lab equipment that is easily accessible. Screen printing was

the technique used in Chapter 4 for fabricating *SkinMarks* devices. Chapter 5 explored screen printing along with the use of other techniques such as vinyl cutting. It also explored a hybrid method where conductive inkjet printing was used for rapid prototyping and testing the designs while using screen printing for higher-fidelity prototypes. Chapter 6 built on multi-functional inkjet printing introduced in prior work [225] to create Epidermal devices for measuring electro-physiological signals. It explored multiple approaches for creating fully functional devices that comprise conductive and insulating layers. It also provides diverse fabrication strategies that are compatible with various types of base substrate materials.

Computational Design Techniques: This thesis presents the first instance of deploying computational design techniques for realizing Epidermal Device designs. Chapter 5 introduced a parametric design approach for creating multi-touch device designs in custom shapes and form factors. Given an input shape, the design tool generates the individual layers comprising diamond-shaped electrodes along with the insulating and shielding layers. The layers can subsequently be used for fabrication. Chapter 7 introduced another computational design approach - for creating custom multi-modal electro-physiological sensing patches. The design tool takes as inputs the desired modalities, muscles, priorities, or required signal quality along with an optional shape of the sensor as input and produces an optimal device design. The design tool utilizes anatomical models to create an integrated predictive model that is subsequently used by an optimizer to find device designs that optimally trade-off signal quality with the size of the device. Both these design tools abstract the lower-level technical details from the designer enabling her to focus on the device design by specifying higher-level functional objectives.

Empirical Understanding of Epidermal Devices: An empirical understanding of Epidermal Devices is crucial since this informs novel device designs. Chapter 3 provides the first step in this direction. It firstly identifies the physical metric for quantifying the tactile performance of Epidermal Devices. Three psychophysical studies are then presented to understand the effect of Epidermal Devices on passive and active tactile perception tasks. The results give new insights into the design of Epidermal Devices. Chapter 8 presents the detailed roadmap for future research on Epidermal Computing. By using a multi-disciplinary survey approach, it compares and contrasts Epidermal Devices across disciplines to identify challenges and opportunities for future research across five thematic areas: Materials, Fabrication, Device Functionality, Empirical Studies, and Application Domains.

Future work in Epidermal Computing and development of Epidermal Devices should look into the following thematic areas as highlighted in previous chapters:

- *Advanced Materials and their formulations* - Future work should look into the exploration of new materials which include stretchable conductors,

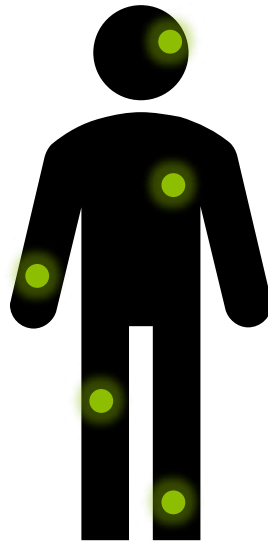


Figure 80: **Epidermal IoT** - In the future, we can envision Epidermal Devices to be an integral part of our body. These devices (highlighted in green) can be easily worn at multiple locations on the body custom-designed for a specific purpose. As a collective, they present us with an ecosystem of Epidermal Devices enabling new opportunities for sensing, computing, and interaction, in addition to giving us a holistic picture of the state of our body.

robust ultra-thin materials, sustainable materials which can be bio-sourced, biodegradable, and can be simply composted.

- *Fabrication techniques that aid rapid-prototyping* - Novel fabrication techniques that can enable mass fabrication of Epidermal Devices need to be developed. Additionally, techniques for fabricating devices that cover large body areas, computational design techniques for supporting the rapid iterative design, and fusing traditional art practices and workflows into the fabrication of Epidermal Devices remain promising avenues for future work.
- *Novel device functionality* - In addition to realizing devices with advanced capabilities in sensing deformation, developing output devices with high resolution visual and tactile display is the next natural step. In addition to these, rapid and computational fabrication of devices that can harvest power, sense biosignals, and the development of highly stretchable connectors are the next logical steps to enhance the capabilities of Epidermal Devices.
- *Empirical and human factors Studies* - While there have been empirical experiments on Epidermal Devices (with Chapter 3 contributing one of them), there are still open research questions that need to be investigated for understanding the usability of Epidermal Devices. Further empirical studies need to be conducted along multiple dimensions that include: (1) understanding skin-specific interactions and their granularity (2) performance studies that

rigorously investigate interaction performance (3) durability and in-the-wild studies (4) social acceptability studies that can inform mass adoption.

- *Real-World Deployments and Application deployments* - Epidermal Devices can be deployed in multiple application domains due to their compelling form factor. A few potential areas for deployment include (1) assistive technologies, (2) health monitoring and diagnosis, (3) sports fitness and rehabilitation, (4) human-robot interaction, and (5) mobile computing.

Overall, this thesis proposes, contributes, and lays the first foundations towards a newly emerging area of computing - **Epidermal Computing** that is a natural successor to the current wearable computing paradigm. Epidermal Devices leverage the ideal user interface properties that human skin offers to create interfaces that seamlessly blend with the human body utilizing its perceptual, mental, motor, and proprioceptive capabilities.

Going beyond this, similar to the current ecosystem of IoT (Internet-of-Things), we can envision a future where we will have a whole ecosystem of Epidermal Devices (*Epidermal IoT*) at various locations on the body, each having its functionality, but collectively presenting us with a wide range of opportunities for sensing, computing, and interaction. The contributions in this thesis serve as the basic building blocks that can enable future research to realize this vision.

BIBLIOGRAPHY

- [1] <https://www.olimex.com/Products/Duino/Shields/SHIELD-EKG-EMG/open-source-hardware>. Accessed: 2019-09-20.
- [2] Gizem Acar, Ozberk Ozturk, and Murat Kaya Yapici. "Wearable Graphene Nanotextile Embedded Smart Armband for Cardiac Monitoring." In: *2018 IEEE SENSORS*. IEEE. 2018, pp. 1–4.
- [3] Rochelle Ackerley, Ida Carlsson, Henric Wester, Håkan Olausson, and Helena Backlund Wasling. "Touch perceptions across skin sites: differences between sensitivity, direction discrimination and pleasantness." In: *Frontiers in behavioral neuroscience* 8 (2014), p. 54. ISSN: 1662-5153. DOI: [10.3389/fnbeh.2014.00054](https://doi.org/10.3389/fnbeh.2014.00054). URL: <http://www.ncbi.nlm.nih.gov/pubmed/24600368><http://www.pubmedcentral.nih.gov/articlerender.fcgi?artid=PMC3928539>.
- [4] Valentina Agostini and Marco Knaflitz. "An algorithm for the estimation of the signal-to-noise ratio in surface myoelectric signals generated during cyclic movements." In: *IEEE Transactions on Biomedical Engineering* 59.1 (2011), pp. 219–225.
- [5] Roland Aigner, Andreas Pointner, Thomas Preindl, Patrick Parzer, and Michael Haller. "Embroidered Resistive Pressure Sensors: A Novel Approach for Textile Interfaces." In: *Proceedings of the 2020 CHI Conference on Human Factors in Computing Systems*. New York, NY, USA: Association for Computing Machinery, 2020, 1–13. ISBN: 9781450367080. URL: <https://doi.org/10.1145/3313831.3376305>.
- [6] Brian Amento, Will Hill, and Loren Terveen. "The Sound of One Hand: A Wrist-Mounted Bio-Acoustic Fingertip Gesture Interface." In: *CHI '02 Extended Abstracts on Human Factors in Computing Systems*. CHI EA '02. Minneapolis, Minnesota, USA: Association for Computing Machinery, 2002, 724–725. ISBN: 1581134541. DOI: [10.1145/506443.506566](https://doi.org/10.1145/506443.506566). URL: <https://doi.org/10.1145/506443.506566>.
- [7] Shideh Kabiri Ameri, Myungsoo Kim, Irene Agnes Kuang, Withanage K Perera, Mohammed Alshiekh, Hyoyoung Jeong, Ufuk Topcu, Deji Ak-inwande, and Nanshu Lu. "Imperceptible electrooculography graphene sensor system for human–robot interface." In: *npj 2D Materials and Applications* 2.1 (2018), pp. 1–7.
- [8] Christoph Amma, Thomas Krings, Jonas Böer, and Tanja Schultz. "Advancing Muscle-Computer Interfaces with High-Density Electromyography." In: *Proceedings of the 33rd Annual ACM Conference on Human Factors in Computing Systems*. New York, NY, USA: Association for Computing Machinery,

- 2015, 929–938. ISBN: 9781450331456. URL: <https://doi.org/10.1145/2702123.2702501>.
- [9] Allison Anderson, Yigit Menguc, Robert J. Wood, and Dava Newman. “Development of the Polipo Pressure Sensing System for Dynamic Space-Suited Motion.” In: *IEEE Sensors Journal* 15.11 (2015), pp. 6229–6237. DOI: [10.1109/JSEN.2015.2449304](https://doi.org/10.1109/JSEN.2015.2449304).
- [10] AS Anusha, SP Preejith, Tony J Akl, Jayaraj Joseph, and Mohanasankar Sivaprakasam. “Dry Electrode Optimization for Wrist-based Electrodermal Activity Monitoring.” In: *2018 IEEE International Symposium on Medical Measurements and Applications (MeMeA)*. IEEE. 2018, pp. 1–6.
- [11] *Apple Watch Series 4 ECG/Heart Rate*. <https://www.apple.com/apple-watch-series-4/health/>. Accessed: 2019-09-20.
- [12] A Arogbonlo, C Usma, AZ Kouzani, and I Gibson. “Design and Fabrication of a Capacitance Based Wearable Pressure Sensor Using E-textiles.” In: *Procedia Technology* 20 (2015), pp. 270–275.
- [13] Nivedita Arora, Steven L. Zhang, Fereshteh Shahmiri, Diego Osorio, Yi-Cheng Wang, Mohit Gupta, Zhengjun Wang, Thad Starner, Zhong Lin Wang, and Gregory D. Abowd. “SATURN: A Thin and Flexible Self-Powered Microphone Leveraging Triboelectric Nanogenerator.” In: *Proc. ACM Interact. Mob. Wearable Ubiquitous Technol.* 2.2 (July 2018). DOI: [10.1145/3214263](https://doi.org/10.1145/3214263). URL: <https://doi.org/10.1145/3214263>.
- [14] Daniel Ashbrook, Patrick Baudisch, and Sean White. “Nenya: Subtle and Eyes-Free Mobile Input with a Magnetically-Tracked Finger Ring.” In: *Proceedings of the SIGCHI Conference on Human Factors in Computing Systems*. New York, NY, USA: Association for Computing Machinery, 2011, 2043–2046. ISBN: 9781450302289. URL: <https://doi.org/10.1145/1978942.1979238>.
- [15] J. B. Vallbo. “Properties of cutaneous mechanoreceptors in the human hand-related to touch sensation.” In: 1999.
- [16] Joonho Bae, Min Kyu Song, Young Jun Park, Jong Min Kim, Meilin Liu, and Zhong Lin Wang. “Fiber supercapacitors made of nanowire-fiber hybrid structures for wearable/flexible energy storage.” In: *Angewandte Chemie International Edition* 50.7 (2011), pp. 1683–1687.
- [17] Sara Bagherifard, Ali Tamayol, Pooria Mostafalu, Mohsen Akbari, Mattia Comotto, Nasim Annabi, Masoumeh Ghaderi, Sameer Sonkusale, Mehmet R Dokmeci, and Ali Khademhosseini. “Dermal patch with integrated flexible heater for on demand drug delivery.” In: *Advanced healthcare materials* 5.1 (2016), pp. 175–184.

- [18] Gilles Bailly, Jörg Müller, Michael Rohs, Daniel Wigdor, and Sven Kratz. "ShoeSense: A New Perspective on Gestural Interaction and Wearable Applications." In: *Proceedings of the SIGCHI Conference on Human Factors in Computing Systems*. CHI '12. Austin, Texas, USA: Association for Computing Machinery, 2012, 1239–1248. ISBN: 9781450310154. DOI: [10.1145/2207676.2208576](https://doi.org/10.1145/2207676.2208576). URL: <https://doi.org/10.1145/2207676.2208576>.
- [19] Ananta Narayanan Balaji and Li-Shiuan Peh. "AI-on-Skin: Enabling On-Body AI Inference for Wearable Artificial Skin Interfaces." In: *Extended Abstracts of the 2021 CHI Conference on Human Factors in Computing Systems*. New York, NY, USA: Association for Computing Machinery, 2021. ISBN: 9781450380959. URL: <https://doi.org/10.1145/3411763.3451689>.
- [20] Amay J Bandodkar, Philipp Gutruf, Jungil Choi, KunHyuck Lee, Yurina Sekine, Jonathan T Reeder, William J Jeang, Alexander J Aranyosi, Stephen P Lee, Jeffrey B Model, et al. "Battery-free, skin-interfaced microfluidic/electronic systems for simultaneous electrochemical, colorimetric, and volumetric analysis of sweat." In: *Science advances* 5.1 (2019), eaav3294.
- [21] Amay J Bandodkar, Itthipon Jeerapan, Jung-Min You, Rogelio Nuñez-Flores, and Joseph Wang. "Highly stretchable fully-printed CNT-based electrochemical sensors and biofuel cells: Combining intrinsic and design-induced stretchability." In: *Nano letters* 16.1 (2016), pp. 721–727.
- [22] Amay J. Bandodkar, Wenzhao Jia, and Joseph Wang. "Tattoo-Based Wearable Electrochemical Devices: A Review." In: *Electroanalysis* 27.3 (2015), pp. 562–572. ISSN: 10400397. DOI: [10.1002/elan.201400537](https://doi.org/10.1002/elan.201400537). URL: <http://doi.wiley.com/10.1002/elan.201400537>.
- [23] Amay J Bandodkar, Wenzhao Jia, and Joseph Wang. "Tattoo-based wearable electrochemical devices: a review." In: *Electroanalysis* 27.3 (2015), pp. 562–572.
- [24] Amay J Bandodkar, Aoife M O'Mahony, Julian Ramírez, Izabela A Samek, Sean M Anderson, Joshua R Windmiller, and Joseph Wang. "Solid-state Forensic Finger sensor for integrated sampling and detection of gunshot residue and explosives: towards 'Lab-on-a-finger'." In: *Analyst* 138.18 (2013), pp. 5288–5295.
- [25] Amay J Bandodkar, Jung-Min You, Nam-Heon Kim, Yue Gu, Rajan Kumar, AM Vinu Mohan, Jonas Kurniawan, Somayeh Imani, Tatsuo Nakagawa, Brianna Parish, et al. "Soft, stretchable, high power density electronic skin-based biofuel cells for scavenging energy from human sweat." In: *Energy & Environmental Science* 10.7 (2017), pp. 1581–1589.
- [26] Marco Barbero, Roberto Merletti, and Alberto Rainoldi. *Atlas of muscle innervation zones: understanding surface electromyography and its applications*. Springer Science & Business Media, 2012.

- [27] Lilach Bareket, Lilah Inzelberg, David Rand, Moshe David-Pur, David Rabinovich, Barak Brandes, and Yael Hanein. "Temporary-tattoo for long-term high fidelity biopotential recordings." In: *Scientific reports* 6 (2016), p. 25727.
- [28] Gary Barrett and Ryomei Omote. "Projected-capacitive touch technology." In: *Information Display* 26.3 (2010), pp. 16–21.
- [29] Sharon Baurley, Philippa Brock, Erik Geelhoed, and Andrew Moore. "Communication-Wear: user feedback as part of a co-design process." In: *International Workshop on Haptic and Audio Interaction Design*. Springer. 2007, pp. 56–68.
- [30] Judith Bell-Krotoski, Sidney Weinstein, and Curt Weinstein. "Testing Sensibility, Including Touch-Pressure, Two-point Discrimination, Point Localization, and Vibration." In: *Journal of Hand Therapy* 6.2 (1993), pp. 114–123. ISSN: 0894-1130. DOI: [10.1016/S0894-1130\(12\)80292-4](https://doi.org/10.1016/S0894-1130(12)80292-4). URL: <https://www.sciencedirect.com/science/article/pii/S0894113012802924>.
- [31] Hrvoje Benko, Andrew D. Wilson, and Patrick Baudisch. "Precise Selection Techniques for Multi-Touch Screens." In: *Proceedings of the SIGCHI Conference on Human Factors in Computing Systems*. CHI '06. Montréal, Québec, Canada: Association for Computing Machinery, 2006, 1263–1272. ISBN: 1595933727. DOI: [10.1145/1124772.1124963](https://doi.org/10.1145/1124772.1124963). URL: <https://doi.org/10.1145/1124772.1124963>.
- [32] Sheela Berchmans, Amay J Bandodkar, Wenzhao Jia, Julian Ramírez, Ying S Meng, and Joseph Wang. "An epidermal alkaline rechargeable Ag–Zn printable tattoo battery for wearable electronics." In: *Journal of Materials Chemistry A* 2.38 (2014), pp. 15788–15795.
- [33] Joanna Bergstrom-Lehtovirta, Sebastian Boring, and Kasper Hornbæk. "Placing and Recalling Virtual Items on the Skin." In: *Proceedings of the 2017 CHI Conference on Human Factors in Computing Systems*. New York, NY, USA: Association for Computing Machinery, 2017, 1497–1507. ISBN: 9781450346559. URL: <https://doi.org/10.1145/3025453.3026030>.
- [34] Joanna Bergstrom-Lehtovirta, David Coyle, Jarrod Knibbe, and Kasper Hornbæk. "I Really Did That: Sense of Agency with Touchpad, Keyboard, and On-Skin Interaction." In: *Proceedings of the 2018 CHI Conference on Human Factors in Computing Systems*. New York, NY, USA: Association for Computing Machinery, 2018, 1–8. ISBN: 9781450356206. URL: <https://doi.org/10.1145/3173574.3173952>.
- [35] Joanna Bergstrom-Lehtovirta, Kasper Hornbæk, and Sebastian Boring. "It's a Wrap: Mapping On-Skin Input to Off-Skin Displays." In: *Proceedings of the 2018 CHI Conference on Human Factors in Computing Systems*. New York, NY, USA: Association for Computing Machinery, 2018, 1–11. ISBN: 9781450356206. URL: <https://doi.org/10.1145/3173574.3174138>.

- [36] Guillermo Bernal, Tao Yang, Abhinandan Jain, and Pattie Maes. “PhysioHMD: A Conformable, Modular Toolkit for Collecting Physiological Data from Head-Mounted Displays.” In: *Proceedings of the 2018 ACM International Symposium on Wearable Computers*. ISWC '18. Singapore, Singapore: Association for Computing Machinery, 2018, 160–167. ISBN: 9781450359672. DOI: [10.1145/3267242.3267268](https://doi.org/10.1145/3267242.3267268). URL: <https://doi.org/10.1145/3267242.3267268>.
- [37] Breno Bitarello, Hugo Fuks, and João Queiroz. “New Technologies for Dynamic Tattoo Art.” In: *Proceedings of the Fifth International Conference on Tangible, Embedded, and Embodied Interaction*. TEI '11. Funchal, Portugal: Association for Computing Machinery, 2010, 313–316. ISBN: 9781450304788. DOI: [10.1145/1935701.1935774](https://doi.org/10.1145/1935701.1935774). URL: <https://doi.org/10.1145/1935701.1935774>.
- [38] Michael R Boland, Tracy Spigelman, and Tim L Uhl. “The function of brachioradialis.” In: *The Journal of hand surgery* 33.10 (2008), pp. 1853–1859. DOI: [10.1016/j.jhsa.2008.07.019](https://doi.org/10.1016/j.jhsa.2008.07.019). URL: <https://doi.org/10.1016/j.jhsa.2008.07.019>.
- [39] Giorgio E Bonacchini, Caterina Bossio, Francesco Greco, Virgilio Mattoli, Yun-Hi Kim, Guglielmo Lanzani, and Mario Caironi. “Tattoo-Paper Transfer as a Versatile Platform for All-Printed Organic Edible Electronics.” In: *Advanced Materials* 30.14 (2018), p. 1706091.
- [40] Paolo Bonato, Tommaso D’Alessio, and Marco Knaflitz. “A statistical method for the measurement of muscle activation intervals from surface myoelectric signal during gait.” In: *IEEE Transactions on biomedical engineering* 45.3 (1998), pp. 287–299.
- [41] Silvia Bonfanti, Roberto Guerra, Francesc Font-Clos, Daniel Rayneau-Kirkhope, and Stefano Zapperi. “Automatic design of mechanical metamaterial actuators.” In: *Nature Communications* 11 (1 Dec. 2020), pp. 1–10. ISSN: 20411723. DOI: [10.1038/s41467-020-17947-2](https://doi.org/10.1038/s41467-020-17947-2). URL: <https://doi.org/10.1038/s41467-020-17947-2>.
- [42] Idil Bostan, Oğuz Turan Buruk, Mert Canat, Mustafa Ozan Tezcan, Celalettin Yurdakul, Tilbe Göksun, and Oğuzhan Özcan. “Hands as a Controller: User Preferences for Hand Specific On-Skin Gestures.” In: *Proceedings of the 2017 Conference on Designing Interactive Systems*. DIS '17. Edinburgh, United Kingdom: Association for Computing Machinery, 2017, 1123–1134. ISBN: 9781450349222. DOI: [10.1145/3064663.3064766](https://doi.org/10.1145/3064663.3064766). URL: <https://doi.org/10.1145/3064663.3064766>.
- [43] Wolfram Boucsein. *Electrodermal activity*. Springer Science & Business Media, 2012.

- [44] Alexandra Bucknor, Alan Karthikesalingam, SR Markar, PJ Holt, Isabel Jones, and TG Allen-Mersh. "A comparison of the effect of different surgical gloves on objective measurement of fingertip cutaneous sensibility." In: *The Annals of The Royal College of Surgeons of England* 93.2 (2010), pp. 95–98.
- [45] Alex Butler, Shahram Izadi, and Steve Hodges. "SideSight: Multi-"touch" Interaction around Small Devices." In: *Proceedings of the 21st Annual ACM Symposium on User Interface Software and Technology*. UIST '08. Monterey, CA, USA: Association for Computing Machinery, 2008, 201–204. ISBN: 9781595939753. DOI: [10.1145/1449715.1449746](https://doi.org/10.1145/1449715.1449746). URL: <https://doi.org/10.1145/1449715.1449746>.
- [46] DK Cai, A Neyer, R Kuckuk, and HM Heise. "Optical absorption in transparent PDMS materials applied for multimode waveguides fabrication." In: *Optical materials* 30.7 (2008), pp. 1157–1161.
- [47] Le Cai, Li Song, Pingshan Luan, Qiang Zhang, Nan Zhang, Qingqing Gao, Duan Zhao, Xiao Zhang, Min Tu, Feng Yang, et al. "Super-stretchable, transparent carbon nanotube-based capacitive strain sensors for human motion detection." In: *Scientific reports* 3.1 (2013), pp. 1–9.
- [48] Andrew Carek and Christian Holz. "Naptics: Convenient and Continuous Blood Pressure Monitoring during Sleep." In: *Proceedings of the ACM on Interactive, Mobile, Wearable and Ubiquitous Technologies* 2.3 (2018), p. 96.
- [49] Lina M Castano and Alison B Flatau. "Smart fabric sensors and e-textile technologies: a review." In: *Smart Materials and structures* 23.5 (2014), p. 053001.
- [50] Edwin Chan, Teddy Seyed, Wolfgang Stuerzlinger, Xing-Dong Yang, and Frank Maurer. "User Elicitation on Single-Hand Microgestures." In: *Proceedings of the 2016 CHI Conference on Human Factors in Computing Systems*. New York, NY, USA: Association for Computing Machinery, 2016, 3403–3414. ISBN: 9781450333627. URL: <https://doi.org/10.1145/2858036.2858589>.
- [51] Liwei Chan, Yi-Ling Chen, Chi-Hao Hsieh, Rong-Hao Liang, and Bing-Yu Chen. "CyclopsRing: Enabling Whole-Hand and Context-Aware Interactions Through a Fisheye Ring." In: *Proceedings of the 28th Annual ACM Symposium on User Interface Software and Technology*. UIST '15. Charlotte, NC, USA: Association for Computing Machinery, 2015, 549–556. ISBN: 9781450337793. DOI: [10.1145/2807442.2807450](https://doi.org/10.1145/2807442.2807450). URL: <https://doi.org/10.1145/2807442.2807450>.
- [52] Liwei Chan, Chi-Hao Hsieh, Yi-Ling Chen, Shuo Yang, Da-Yuan Huang, Rong-Hao Liang, and Bing-Yu Chen. "Cyclops: Wearable and Single-Piece Full-Body Gesture Input Devices." In: *Proceedings of the 33rd Annual ACM Conference on Human Factors in Computing Systems*. CHI '15. Seoul, Republic of Korea: Association for Computing Machinery, 2015, 3001–3009. ISBN:

9781450331456. DOI: [10.1145/2702123.2702464](https://doi.org/10.1145/2702123.2702464). URL: <https://doi.org/10.1145/2702123.2702464>.
- [53] Liwei Chan, Rong-Hao Liang, Ming-Chang Tsai, Kai-Yin Cheng, Chao-Huai Su, Mike Y. Chen, Wen-Huang Cheng, and Bing-Yu Chen. "FingerPad: Private and Subtle Interaction Using Fingertips." In: *Proceedings of the 26th Annual ACM Symposium on User Interface Software and Technology*. UIST '13. St. Andrews, Scotland, United Kingdom: ACM, 2013, pp. 255–260. ISBN: 978-1-4503-2268-3. DOI: [10.1145/2501988.2502016](https://doi.org/10.1145/2501988.2502016). URL: <http://doi.acm.org/10.1145/2501988.2502016>.
- [54] Tang Chang-bin, Liu Dao-Xin, Wang Zhan, and Gao Yang. "Electro-spark alloying using graphite electrode on titanium alloy surface for biomedical applications." In: *Applied Surface Science* 257.15 (2011), pp. 6364–6371.
- [55] Christopher Chen, David Howard, Steven L. Zhang, Youngwook Do, Sienna Sun, Tingyu Cheng, Zhong Lin Wang, Gregory D. Abowd, and HyunJoo Oh. "SPIN (Self-Powered Paper Interfaces): Bridging Triboelectric Nanogenerator with Folding Paper Creases." In: *Proceedings of the Fourteenth International Conference on Tangible, Embedded, and Embodied Interaction*. TEI '20. Sydney NSW, Australia: Association for Computing Machinery, 2020, 431–442. ISBN: 9781450361071. DOI: [10.1145/3374920.3374946](https://doi.org/10.1145/3374920.3374946). URL: <https://doi.org/10.1145/3374920.3374946>.
- [56] Ke-Yu Chen, Kent Lyons, Sean White, and Shwetak Patel. "UTrack: 3D Input Using Two Magnetic Sensors." In: *Proceedings of the 26th Annual ACM Symposium on User Interface Software and Technology*. UIST '13. St. Andrews, Scotland, United Kingdom: Association for Computing Machinery, 2013, 237–244. ISBN: 9781450322683. DOI: [10.1145/2501988.2502035](https://doi.org/10.1145/2501988.2502035). URL: <https://doi.org/10.1145/2501988.2502035>.
- [57] Ke-Yu Chen, Shwetak N. Patel, and Sean Keller. "Finexus: Tracking Precise Motions of Multiple Fingertips Using Magnetic Sensing." In: *Proceedings of the 2016 CHI Conference on Human Factors in Computing Systems*. CHI '16. San Jose, California, USA: Association for Computing Machinery, 2016, 1504–1514. ISBN: 9781450333627. DOI: [10.1145/2858036.2858125](https://doi.org/10.1145/2858036.2858125). URL: <https://doi.org/10.1145/2858036.2858125>.
- [58] Xiang 'Anthony' Chen, Tovi Grossman, Daniel J. Wigdor, and George Fitzmaurice. "Duet: Exploring Joint Interactions on a Smart Phone and a Smart Watch." In: *Proceedings of the SIGCHI Conference on Human Factors in Computing Systems*. CHI '14. Toronto, Ontario, Canada: Association for Computing Machinery, 2014, 159–168. ISBN: 9781450324731. DOI: [10.1145/2556288.2556955](https://doi.org/10.1145/2556288.2556955). URL: <https://doi.org/10.1145/2556288.2556955>.

- [59] Yu-Chun Chen, Chia-Ying Liao, Shuo-wen Hsu, Da-Yuan Huang, and Bing-Yu Chen. "Exploring User Defined Gestures for Ear-Based Interactions." In: *Proc. ACM Hum.-Comput. Interact.* 4.ISS (Nov. 2020). DOI: [10.1145/3427314](https://doi.org/10.1145/3427314). URL: <https://doi.org/10.1145/3427314>.
- [60] Jingyuan Cheng, Paul Lukowicz, Niels Henze, Albrecht Schmidt, Oliver Amft, Giovanni A Salvatore, and Gerhard Tröster. "Smart textiles: From niche to mainstream." In: *IEEE Pervasive Computing* 12.3 (2013), pp. 81–84.
- [61] Tingyu Cheng et al. "Silver Tape: Inkjet-Printed Circuits Peeled-and-Transferred on Versatile Substrates." In: *Proc. ACM Interact. Mob. Wearable Ubiquitous Technol.* 4.1 (Mar. 2020). DOI: [10.1145/3381013](https://doi.org/10.1145/3381013). URL: <https://doi.org/10.1145/3381013>.
- [62] George Chernyshov, Benjamin Tag, Cedric Caremel, Feier Cao, Gemma Liu, and Kai Kunze. "Shape memory alloy wire actuators for soft, wearable haptic devices." In: *Proceedings of the 2018 ACM International Symposium on Wearable Computers*. 2018, pp. 112–119.
- [63] Yu Mike Chi, Tzyy-Ping Jung, and Gert Cauwenberghs. "Dry-contact and noncontact biopotential electrodes: Methodological review." In: *IEEE reviews in biomedical engineering* 3 (2010), pp. 106–119.
- [64] Chin-yu Chien, Rong-Hao Liang, Long-Fei Lin, Liwei Chan, and Bing-Yu Chen. "Flexibend: Enabling interactivity of multi-part, deformable fabrications using single shape-sensing strip." In: *Proceedings of the 28th Annual ACM Symposium on User Interface Software and Technology*. 2015, pp. 659–663.
- [65] Seungmoon Choi and Katherine J Kuchenbecker. "Vibrotactile display: Perception, technology, and applications." In: *Proceedings of the IEEE* 101.9 (2013), pp. 2093–2104.
- [66] Youngkyung Choi, Neung Ryu, Myung Jin Kim, Artem Dementyev, and Andrea Bianchi. "BodyPrinter: Fabricating Circuits Directly on the Skin at Arbitrary Locations Using a Wearable Compact Plotter." In: *Proceedings of the 33rd Annual ACM Symposium on User Interface Software and Technology*. UIST '20. Virtual Event, USA: Association for Computing Machinery, 2020, 554–564. ISBN: 9781450375146. DOI: [10.1145/3379337.3415840](https://doi.org/10.1145/3379337.3415840). URL: <https://doi.org/10.1145/3379337.3415840>.
- [67] Alex Chortos, Jia Liu, and Zhenan Bao. "Pursuing prosthetic electronic skin." In: *Nature materials* 15.9 (2016), p. 937.
- [68] Ho-Hsiu Chou, Amanda Nguyen, Alex Chortos, John WF To, Chien Lu, Jianguo Mei, Tadanori Kurosawa, Won-Gyu Bae, Jeffrey B-H Tok, and Zhenan Bao. "A chameleon-inspired stretchable electronic skin with interactive colour changing controlled by tactile sensing." In: *Nature communications* 6.1 (2015), pp. 1–10.

- [69] Jinsung Chun, Na-Ri Kang, Ju-Young Kim, Myoung-Sub Noh, Chong-Yun Kang, Dukhyun Choi, Sang-Woo Kim, Zhong Lin Wang, and Jeong Min Baik. "Highly anisotropic power generation in piezoelectric hemispheres composed stretchable composite film for self-powered motion sensor." In: *Nano Energy* 11 (2015), pp. 1–10.
- [70] C Cochrane, Carla Hertleer, and Anne Schwarz-Pfeiffer. "Smart textiles in health: An overview." In: *Smart textiles and their applications* (2016), pp. 9–32.
- [71] Gabe Cohn, Sidhant Gupta, Tien-Jui Lee, Dan Morris, Joshua R. Smith, Matthew S. Reynolds, Desney S. Tan, and Shwetak N. Patel. "An Ultra-Low-Power Human Body Motion Sensor Using Static Electric Field Sensing." In: *Proceedings of the 2012 ACM Conference on Ubiquitous Computing*. UbiComp '12. Pittsburgh, Pennsylvania: Association for Computing Machinery, 2012, 99–102. ISBN: 9781450312240. DOI: [10.1145/2370216.2370233](https://doi.org/10.1145/2370216.2370233). URL: <https://doi.org/10.1145/2370216.2370233>.
- [72] Gabe Cohn, Daniel Morris, Shwetak N. Patel, and Desney S. Tan. "Your Noise is My Command: Sensing Gestures Using the Body as an Antenna." In: *Proceedings of the SIGCHI Conference on Human Factors in Computing Systems*. New York, NY, USA: Association for Computing Machinery, 2011, 791–800. ISBN: 9781450302289. URL: <https://doi.org/10.1145/1978942.1979058>.
- [73] Gabe Cohn, Daniel Morris, Shwetak Patel, and Desney Tan. "Humantenna: Using the Body as an Antenna for Real-Time Whole-Body Interaction." In: *Proceedings of the SIGCHI Conference on Human Factors in Computing Systems*. New York, NY, USA: Association for Computing Machinery, 2012, 1901–1910. ISBN: 9781450310154. URL: <https://doi.org/10.1145/2207676.2208330>.
- [74] Mary Boudreau Conover. *Understanding electrocardiography*. Elsevier Health Sciences, 2002.
- [75] Cory Cornelius, Ronald Peterson, Joseph Skinner, Ryan Halter, and David Kotz. "A Wearable System That Knows Who Wears It." In: *Proceedings of the 12th Annual International Conference on Mobile Systems, Applications, and Services*. MobiSys '14. Bretton Woods, New Hampshire, USA: Association for Computing Machinery, 2014, 55–67. ISBN: 9781450327930. DOI: [10.1145/2594368.2594369](https://doi.org/10.1145/2594368.2594369). URL: <https://doi.org/10.1145/2594368.2594369>.
- [76] Stelian Coros, Bernhard Thomaszewski, Gioacchino Noris, Shinjiro Sueda, Moira Forberg, Robert W Sumner, Wojciech Matusik, and Bernd Bickel. "Computational design of mechanical characters." In: *ACM Transactions on Graphics (TOG)* 32.4 (2013), p. 83.

- [77] Vincenzo F Curto, Cormac Fay, Shirley Coyle, Robert Byrne, Corinne O'Toole, Caroline Barry, Sarah Hughes, Niall Moyna, Dermot Diamond, and Fernando Benito-Lopez. "Real-time sweat pH monitoring based on a wearable chemical barcode micro-fluidic platform incorporating ionic liquids." In: *Sensors and Actuators B: Chemical* 171 (2012), pp. 1327–1334.
- [78] Yahao Dai, Huawei Hu, Maritha Wang, Jie Xu, and Sihong Wang. "Stretchable transistors and functional circuits for human-integrated electronics." In: *Nature Electronics* 4.1 (2021), pp. 17–29.
- [79] Burke Davison. "Techniques for robust touch sensing design." In: *AN1334 Microchip Technology Inc* (2010), p. 53.
- [80] M DeMello. "Facial hair." In: *Encyclopedia of Body Adornment*. Westport, CT: Greenwood Publishing Group (2007), p. 109.
- [81] Edward F Delagi. *Anatomical guide for the electromyographer: the limbs and trunk*. Charles C. Thomas, 2011.
- [82] Daniel Delling, Peter Sanders, Dominik Schultes, and Dorothea Wagner. "Engineering Route Planning Algorithms." In: *Algorithmics of Large and Complex Networks: Design, Analysis, and Simulation*. Ed. by Jürgen Lerner, Dorothea Wagner, and Katharina A. Zweig. Berlin, Heidelberg: Springer Berlin Heidelberg, 2009, pp. 117–139. ISBN: 978-3-642-02094-0. DOI: [10.1007/978-3-642-02094-0_7](https://doi.org/10.1007/978-3-642-02094-0_7). URL: https://doi.org/10.1007/978-3-642-02094-0_7.
- [83] Artem Dementyev, Javier Hernandez, Inrak Choi, Sean Follmer, and Joseph Paradiso. "Epidermal Robots: Wearable Sensors That Climb on the Skin." In: *Proc. ACM Interact. Mob. Wearable Ubiquitous Technol.* 2.3 (Sept. 2018). DOI: [10.1145/3264912](https://doi.org/10.1145/3264912). URL: <https://doi.org/10.1145/3264912>.
- [84] Artem Dementyev and Christian Holz. "DualBlink: A Wearable Device to Continuously Detect, Track, and Actuate Blinking For Alleviating Dry Eyes and Computer Vision Syndrome." In: *Proc. ACM Interact. Mob. Wearable Ubiquitous Technol.* 1.1 (Mar. 2017). DOI: [10.1145/3053330](https://doi.org/10.1145/3053330). URL: <https://doi.org/10.1145/3053330>.
- [85] Artem Dementyev and Joseph A. Paradiso. "WristFlex: Low-Power Gesture Input with Wrist-Worn Pressure Sensors." In: *Proceedings of the 27th Annual ACM Symposium on User Interface Software and Technology*. UIST '14. Honolulu, Hawaii, USA: Association for Computing Machinery, 2014, 161–166. ISBN: 9781450330695. DOI: [10.1145/2642918.2647396](https://doi.org/10.1145/2642918.2647396). URL: <https://doi.org/10.1145/2642918.2647396>.
- [86] Ruta Desai, Ye Yuan, and Stelian Coros. "Computational abstractions for interactive design of robotic devices." In: *2017 IEEE International Conference on Robotics and Automation (ICRA)*. IEEE. 2017, pp. 1196–1203.

- [87] Laura Devendorf and Chad Di Lauro. "Adapting Double Weaving and Yarn Plying Techniques for Smart Textiles Applications." In: *Proceedings of the Thirteenth International Conference on Tangible, Embedded, and Embodied Interaction*. TEI '19. Tempe, Arizona, USA: Association for Computing Machinery, 2019, 77–85. ISBN: 9781450361965. DOI: [10.1145/3294109.3295625](https://doi.org/10.1145/3294109.3295625). URL: <https://doi.org/10.1145/3294109.3295625>.
- [88] Laura Devendorf, Joanne Lo, Noura Howell, Jung Lin Lee, Nan-Wei Gong, M. Emre Karagozler, Shiho Fukuhara, Ivan Poupyrev, Eric Paulos, and Kimiko Ryokai. "'I Don't Want to Wear a Screen': Probing Perceptions of and Possibilities for Dynamic Displays on Clothing." In: *Proceedings of the 2016 CHI Conference on Human Factors in Computing Systems*. New York, NY, USA: Association for Computing Machinery, 2016, 6028–6039. ISBN: 9781450333627. URL: <https://doi.org/10.1145/2858036.2858192>.
- [89] Travis Deyle, Szabolcs Palinko, Erika Shehan Poole, and Thad Starner. "Hambone: A bio-acoustic gesture interface." In: *2007 11th IEEE International Symposium on Wearable Computers*. IEEE, 2007, pp. 3–10.
- [90] Niloofar Dezfuli, Mohammadreza Khalilbeigi, Jochen Huber, Florian Müller, and Max Mühlhäuser. "PalmRC: Imaginary Palm-based Remote Control for Eyes-free Television Interaction." In: *Proceedings of the 10th European Conference on Interactive TV and Video*. EuroITV '12. Berlin, Germany: ACM, 2012, pp. 27–34. ISBN: 978-1-4503-1107-6. DOI: [10.1145/2325616.2325623](https://doi.org/10.1145/2325616.2325623). URL: <http://doi.acm.org/10.1145/2325616.2325623>.
- [91] Christine Dierk, Molly Jane Pearce Nicholas, and Eric Paulos. "AlterWear: Battery-Free Wearable Displays for Opportunistic Interactions." In: *Proceedings of the 2018 CHI Conference on Human Factors in Computing Systems*. New York, NY, USA: Association for Computing Machinery, 2018, 1–11. ISBN: 9781450356206. URL: <https://doi.org/10.1145/3173574.3173794>.
- [92] Christine Dierk, Sarah Sterman, Molly Jane Pearce Nicholas, and Eric Paulos. "HäIrIÖ: Human Hair as Interactive Material." In: *Proceedings of the Twelfth International Conference on Tangible, Embedded, and Embodied Interaction*. TEI '18. Stockholm, Sweden: Association for Computing Machinery, 2018, 148–157. ISBN: 9781450355681. DOI: [10.1145/3173225.3173232](https://doi.org/10.1145/3173225.3173232). URL: <https://doi.org/10.1145/3173225.3173232>.
- [93] Paul Dietz and Darren Leigh. "DiamondTouch: A Multi-user Touch Technology." In: *Proceedings of the 14th Annual ACM Symposium on User Interface Software and Technology*. UIST '01. Orlando, Florida: ACM, 2001, pp. 219–226. ISBN: 1-58113-438-X. DOI: [10.1145/502348.502389](https://doi.org/10.1145/502348.502389). URL: <http://doi.acm.org/10.1145/502348.502389>.
- [94] Laura Dipietro, Angelo M Sabatini, and Paolo Dario. "A survey of glove-based systems and their applications." In: *Ieee transactions on systems, man, and cybernetics, part c (applications and reviews)* 38.4 (2008), pp. 461–482.

- [95] David Dobbstein, Philipp Hock, and Enrico Rukzio. "Belt: An Unobtrusive Touch Input Device for Head-Worn Displays." In: *Proceedings of the 33rd Annual ACM Conference on Human Factors in Computing Systems*. New York, NY, USA: Association for Computing Machinery, 2015, 2135–2138. ISBN: 9781450331456. URL: <https://doi.org/10.1145/2702123.2702450>.
- [96] David Dobbstein, Christian Winkler, Gabriel Haas, and Enrico Rukzio. "PocketThumb: A Wearable Dual-Sided Touch Interface for Cursor-Based Control of Smart-Eyewear." In: *Proc. ACM Interact. Mob. Wearable Ubiquitous Technol.* 1.2 (June 2017). DOI: 10.1145/3090055. URL: <https://doi.org/10.1145/3090055>.
- [97] Marieke van Dooren, J.J.G. (Gert-Jan) de Vries, and Joris H. Janssen. "Emotional sweating across the body: Comparing 16 different skin conductance measurement locations." In: *Physiology & Behavior* 106.2 (2012), pp. 298–304. ISSN: 0031-9384. DOI: 10.1016/J.PHYSBEH.2012.01.020. URL: https://www.sciencedirect.com/science/article/pii/S0031938412000613?dgcid=api{_}sd{_}search-api-endpoint.
- [98] Lucy E Dunne, Halley Profita, Clint Zeagler, James Clawson, Scott Gilliland, Ellen Yi-Luen Do, and Jim Budd. "The social comfort of wearable technology and gestural interaction." In: *2014 36th annual international conference of the IEEE engineering in medicine and biology society*. IEEE, 2014, pp. 4159–4162.
- [99] Willem Einthoven, G Fahr, and A De Waart. " "U about the direction and the manifest size of the potential fluctuations in the human heart and about the influence of the heart situation on the shape of the electrocardiogram." In: *Pflügler's Archive European Journal of Physiology* 150.6 (1913), pp. 275–315.
- [100] Christoph Endres, Tim Schwartz, and Christian A. Müller. "Geremin": 2D Microgestures for Drivers Based on Electric Field Sensing." In: *Proceedings of the 16th International Conference on Intelligent User Interfaces*. IUI '11. Palo Alto, CA, USA: Association for Computing Machinery, 2011, 327–330. ISBN: 9781450304191. DOI: 10.1145/1943403.1943457. URL: <https://doi.org/10.1145/1943403.1943457>.
- [101] Omar J Escalona, Louise McFrederick, Maira Borges, Pedro Linares, Ricardo Villegas, Gilberto I Perpiñan, James McLaughlin, and David McEneaney. "Wrist and arm body surface bipolar ECG leads signal and sensor study for long-term rhythm monitoring." In: *2017 Computing in Cardiology (CinC)*. IEEE, 2017, pp. 1–4.
- [102] Ramona Fagiani, Francesco Massi, Eric Chatelet, Yves Berthier, and Adnan Akay. "Tactile perception by friction induced vibrations." In: *Tribology International* 44.10 (2011), pp. 1100–1110.
- [103] Feng-Ru Fan, Zhong-Qun Tian, and Zhong Lin Wang. "Flexible triboelectric generator." In: *Nano energy* 1.2 (2012), pp. 328–334.

- [104] Laura M. Ferrari, Sudha Sudha, Sergio Tarantino, Roberto Esposti, Francesco Bolzoni, Paolo Cavallari, Christian Cipriani, Virgilio Mattoli, and Francesco Greco. "Ultraconformable Temporary Tattoo Electrodes for Electrophysiology." In: *Advanced Science* 5.3 (2018), p. 1700771. ISSN: 21983844. DOI: [10.1002/advs.201700771](https://doi.org/10.1002/advs.201700771). URL: <http://doi.wiley.com/10.1002/advs.201700771>.
- [105] Laura M Ferrari, Sudha Sudha, Sergio Tarantino, Roberto Esposti, Francesco Bolzoni, Paolo Cavallari, Christian Cipriani, Virgilio Mattoli, and Francesco Greco. "Ultraconformable temporary tattoo electrodes for electrophysiology." In: *Advanced Science* 5.3 (2018), p. 1700771.
- [106] Filipe Vargas Ferreira, Luciana De Simone Cividanes, Felipe Sales Brito, Beatriz Rossi Canuto de Menezes, Wesley Franceschi, Evelyn Alves Nunes Simonetti, and Gilmar Patrocínio Thim. "Functionalization of graphene and applications." In: *Functionalizing graphene and carbon nanotubes*. Springer, 2016, pp. 1–29.
- [107] T Finni, Min Hu, P Kettunen, T Vilavuo, and S Cheng. "Measurement of EMG activity with textile electrodes embedded into clothing." In: *Physiological measurement* 28.11 (2007), p. 1405.
- [108] James D Foley, Foley Dan Van, Andries Van Dam, Steven K Feiner, John F Hughes, Edward Angel, and J Hughes. *Computer graphics: principles and practice*. Vol. 12110. Addison-Wesley Professional, 1996.
- [109] Don C Fowles, Margaret J Christie, Robert Edelberg, William W Grings, David T Lykken, and Peter H Venables. "Publication recommendations for electrodermal measurements." In: *Psychophysiology* 18.3 (1981), pp. 232–239.
- [110] Max by Frey. *Investigations on the sensory functions of the human skin: 1. treatise: pressure sensation and pain*. Vol. 23. 3. S. Hirzel, 1896.
- [111] Koumei Fukahori, Daisuke Sakamoto, and Takeo Igarashi. "Exploring Subtle Foot Plantar-Based Gestures with Sock-Placed Pressure Sensors." In: *Proceedings of the 33rd Annual ACM Conference on Human Factors in Computing Systems*. New York, NY, USA: Association for Computing Machinery, 2015, 3019–3028. ISBN: 9781450331456. URL: <https://doi.org/10.1145/2702123.2702308>.
- [112] Rui Fukui, Masahiko Watanabe, Tomoaki Gyota, Masamichi Shimosaka, and Tomomasa Sato. "Hand Shape Classification with a Wrist Contour Sensor: Development of a Prototype Device." In: *Proceedings of the 13th International Conference on Ubiquitous Computing*. UbiComp '11. Beijing, China: Association for Computing Machinery, 2011, 311–314. ISBN: 9781450306300. DOI: [10.1145/2030112.2030154](https://doi.org/10.1145/2030112.2030154). URL: <https://doi.org/10.1145/2030112.2030154>.

- [113] Masaaki Fukumoto and Yoshinobu Tonomura. "Whisper: A Wristwatch Style Wearable Handset." In: *Proceedings of the SIGCHI Conference on Human Factors in Computing Systems*. CHI '99. Pittsburgh, Pennsylvania, USA: Association for Computing Machinery, 1999, 112–119. ISBN: 0201485591. DOI: [10.1145/302979.303009](https://doi.org/10.1145/302979.303009). URL: <https://doi.org/10.1145/302979.303009>.
- [114] Li Gao et al. "ARTICLE Epidermal photonic devices for quantitative imaging of temperature and thermal transport characteristics of the skin." In: *Nature Communications* 5 (2014). DOI: [10.1038/ncomms5938](https://doi.org/10.1038/ncomms5938). URL: <http://rogersgroup.northwestern.edu/files/2014/ncommsephoton.pdf>.
- [115] Wei Gao, Sam Emaminejad, Hnin Yin Yin Nyein, Samyuktha Challa, Kevin Chen, Austin Peck, Hossain M Fahad, Hiroki Ota, Hiroshi Shiraki, Daisuke Kiriya, et al. "Fully integrated wearable sensor arrays for multiplexed in situ perspiration analysis." In: *Nature* 529.7587 (2016), pp. 509–514.
- [116] Jaber Nasrollah Gavvani, Amirhossein Hasani, Mohammad Nouri, Mojtaba Mahyari, and Alireza Salehi. "Highly sensitive and flexible ammonia sensor based on S and N co-doped graphene quantum dots/polyaniline hybrid at room temperature." In: *Sensors and Actuators B: Chemical* 229 (2016), pp. 239–248.
- [117] Dawit Gedamu, Ingo Paulowicz, Sören Kaps, Oleg Lupan, Sebastian Wille, Galina Haidarschin, Yogendra Kumar Mishra, and Rainer Adelung. "Rapid fabrication technique for interpenetrated ZnO nanotetrapod networks for fast UV sensors." In: *Advanced materials* 26.10 (2014), pp. 1541–1550.
- [118] Francine Gemperle, Chris Kasabach, John Stivoric, Malcolm Bauer, and Richard Martin. "Design for wearability." In: *digest of papers. Second international symposium on wearable computers (cat. No. 98EX215)*. IEEE. 1998, pp. 116–122.
- [119] George A Gescheider. *Psychophysics: the fundamentals*. Psychology Press, 2013.
- [120] Hossein Ghapanchizadeh, Siti A Ahmad, and Asnor Juraiza Ishak. "Recommended surface EMG electrode position for wrist extension and flexion." In: *2015 IEEE Student Symposium in Biomedical Engineering & Sciences (ISS-BES)*. IEEE. 2015, pp. 108–112.
- [121] Stephen Gilroy, Julie Porteous, Fred Charles, and Marc Cavazza. "PINTER: Interactive Storytelling with Physiological Input." In: *Proceedings of the 2012 ACM International Conference on Intelligent User Interfaces*. IUI '12. Lisbon, Portugal: ACM, 2012, pp. 333–334. ISBN: 978-1-4503-1048-2. DOI: [10.1145/2166966.2167039](https://doi.org/10.1145/2166966.2167039). URL: <http://doi.acm.org/10.1145/2166966.2167039>.
- [122] Erving Goffman. *The presentation of self in everyday life*. Vol. 21. Harmondsworth London, 1978.

- [123] E Bruce Goldstein and James Brockmole. *Sensation and perception*. Cengage Learning, 2016.
- [124] Jun Gong, Yu Wu, Lei Yan, Teddy Seyed, and Xing-Dong Yang. “Tessutivo: Contextual Interactions on Interactive Fabrics with Inductive Sensing.” In: *Proceedings of the 32nd Annual ACM Symposium on User Interface Software and Technology*. UIST ’19. New Orleans, LA, USA: Association for Computing Machinery, 2019, 29–41. ISBN: 9781450368162. DOI: [10.1145/3332165.3347897](https://doi.org/10.1145/3332165.3347897). URL: <https://doi.org/10.1145/3332165.3347897>.
- [125] Jun Gong, Xing-Dong Yang, and Pourang Irani. “WristWhirl: One-Handed Continuous Smartwatch Input Using Wrist Gestures.” In: *Proceedings of the 29th Annual Symposium on User Interface Software and Technology*. UIST ’16. Tokyo, Japan: Association for Computing Machinery, 2016, 861–872. ISBN: 9781450341899. DOI: [10.1145/2984511.2984563](https://doi.org/10.1145/2984511.2984563). URL: <https://doi.org/10.1145/2984511.2984563>.
- [126] Jun Gong, Yang Zhang, Xia Zhou, and Xing-Dong Yang. “Pyro: Thumb-Tip Gesture Recognition Using Pyroelectric Infrared Sensing.” In: *Proceedings of the 30th Annual ACM Symposium on User Interface Software and Technology*. UIST ’17. Québec City, QC, Canada: Association for Computing Machinery, 2017, 553–563. ISBN: 9781450349819. DOI: [10.1145/3126594.3126615](https://doi.org/10.1145/3126594.3126615). URL: <https://doi.org/10.1145/3126594.3126615>.
- [127] Ramyah Gowrishankar. “Constructing Triboelectric Textiles with Weaving.” In: *Proceedings of the 2017 ACM International Symposium on Wearable Computers*. ISWC ’17. Maui, Hawaii: Association for Computing Machinery, 2017, 170–171. ISBN: 9781450351881. DOI: [10.1145/3123021.3123037](https://doi.org/10.1145/3123021.3123037). URL: <https://doi.org/10.1145/3123021.3123037>.
- [128] Ronald L. Graham. “An efficient algorithm for determining the convex hull of a finite planar set.” In: *Information Processing Letters* 1 (1972), pp. 132–133. DOI: [10.1016/0020-0190\(72\)90045-2](https://doi.org/10.1016/0020-0190(72)90045-2). URL: [https://doi.org/10.1016/0020-0190\(72\)90045-2](https://doi.org/10.1016/0020-0190(72)90045-2).
- [129] Colin M. Gray, Yubo Kou, Bryan Battles, Joseph Hoggatt, and Austin L. Toombs. “The Dark (Patterns) Side of UX Design.” In: *Proceedings of the 2018 CHI Conference on Human Factors in Computing Systems*. New York, NY, USA: Association for Computing Machinery, 2018, 1–14. ISBN: 9781450356206. URL: <https://doi.org/10.1145/3173574.3174108>.
- [130] Saul Greenberg, Sebastian Boring, Jo Vermeulen, and Jakub Dostal. “Dark Patterns in Proxemic Interactions: A Critical Perspective.” In: *Proceedings of the 2014 Conference on Designing Interactive Systems*. DIS ’14. Vancouver, BC, Canada: Association for Computing Machinery, 2014, 523–532. ISBN: 9781450329026. DOI: [10.1145/2598510.2598541](https://doi.org/10.1145/2598510.2598541). URL: <https://doi.org/10.1145/2598510.2598541>.

- [131] Daniel Groeger and Jürgen Steimle. "LASEC: Instant Fabrication of Stretchable Circuits Using a Laser Cutter." In: *Proceedings of the 2019 CHI Conference on Human Factors in Computing Systems*. New York, NY, USA: Association for Computing Machinery, 2019, 1–14. ISBN: 9781450359702. URL: <https://doi.org/10.1145/3290605.3300929>.
- [132] Tobias Grosse-Puppendahl, Christian Holz, Gabe Cohn, Raphael Wimmer, Oskar Bechtold, Steve Hodges, Matthew S. Reynolds, and Joshua R. Smith. "Finding Common Ground: A Survey of Capacitive Sensing in Human-Computer Interaction." In: *Proceedings of the SIGCHI Conference on Human Factors in Computing Systems*. CHI '17. Denver, USA: ACM, 2017. DOI: 10.1145/3025453.3025808. URL: <http://doi.acm.org/10.1145/3025453.3025808>.
- [133] Tomas Guinovart, Amay J Bandodkar, Joshua R Windmiller, Francisco J Andrade, and Joseph Wang. "A potentiometric tattoo sensor for monitoring ammonium in sweat." In: *Analyst* 138.22 (2013), pp. 7031–7038.
- [134] Rui Guo, Xuyang Sun, Siyuan Yao, Minghui Duan, Hongzhang Wang, Jing Liu, and Zhongshan Deng. "Semi-Liquid-Metal-(Ni-EGaIn)-Based Ultraconformable Electronic Tattoo." In: *Advanced Materials Technologies* 4.8 (2019), p. 1900183.
- [135] Xiaohui Guo, Ying Huang, Xia Cai, Caixia Liu, and Ping Liu. "Capacitive wearable tactile sensor based on smart textile substrate with carbon black/silicone rubber composite dielectric." In: *Measurement Science and Technology* 27.4 (2016), p. 045105.
- [136] Yang Guo, Michael T. Otley, Mengfang Li, Xiaozheng Zhang, Sneha K. Sinha, Gregory M. Treich, and Gregory A. Sotzing. "PEDOT:PSS "Wires" Printed on Textile for Wearable Electronics." In: *ACS Applied Materials & Interfaces* 8.40 (2016). PMID: 27632390, pp. 26998–27005. DOI: 10.1021/acsami.6b08036. eprint: <https://doi.org/10.1021/acsami.6b08036>. URL: <https://doi.org/10.1021/acsami.6b08036>.
- [137] Aakar Gupta, Antony Albert Raj Irudayaraj, and Ravin Balakrishnan. "HapticClench: Investigating Squeeze Sensations Using Memory Alloys." In: *Proceedings of the 30th Annual ACM Symposium on User Interface Software and Technology*. UIST '17. Québec City, QC, Canada: Association for Computing Machinery, 2017, 109–117. ISBN: 9781450349819. DOI: 10.1145/3126594.3126598. URL: <https://doi.org/10.1145/3126594.3126598>.
- [138] Sean G. Gustafson, Bernhard Rabe, and Patrick M. Baudisch. "Understanding Palm-based Imaginary Interfaces: The Role of Visual and Tactile Cues when Browsing." In: *Proceedings of the SIGCHI Conference on Human Factors in Computing Systems*. CHI '13. Paris, France: ACM, 2013, pp. 889–898. ISBN: 978-1-4503-1899-0. DOI: 10.1145/2470654.2466114. URL: <http://doi.acm.org/10.1145/2470654.2466114>.

- [139] Sean G. Gustafson, Bernhard Rabe, and Patrick M. Baudisch. "Understanding palm-based imaginary interfaces." In: *Proceedings of the SIGCHI Conference on Human Factors in Computing Systems - CHI '13*. New York, New York, USA: ACM Press, 2013, p. 889. ISBN: 9781450318990. DOI: [10.1145/2470654.2466114](https://doi.org/10.1145/2470654.2466114). URL: <http://dl.acm.org/citation.cfm?doid=2470654.2466114>.
- [140] Sean Gustafson, Daniel Bierwirth, and Patrick Baudisch. "Imaginary Interfaces: Spatial Interaction with Empty Hands and without Visual Feedback." In: *Proceedings of the 23rd Annual ACM Symposium on User Interface Software and Technology*. UIST '10. New York, New York, USA: Association for Computing Machinery, 2010, 3–12. ISBN: 9781450302715. DOI: [10.1145/1866029.1866033](https://doi.org/10.1145/1866029.1866033). URL: <https://doi.org/10.1145/1866029.1866033>.
- [141] Sean Gustafson, Christian Holz, and Patrick Baudisch. "Imaginary phone: learning imaginary interfaces by transferring spatial memory from a familiar device." In: *Proceedings of the 24th annual ACM symposium on User Interface Software and Technology*. ACM, 2011, pp. 283–292.
- [142] Taku Hachisu, Baptiste Bourreau, and Kenji Suzuki. "EnhancedTouchX: Smart Bracelets for Augmenting Interpersonal Touch Interactions." In: *Proceedings of the 2019 CHI Conference on Human Factors in Computing Systems*. New York, NY, USA: Association for Computing Machinery, 2019, 1–12. ISBN: 9781450359702. URL: <https://doi.org/10.1145/3290605.3300551>.
- [143] Peter A Haddad, Amir Servati, Saeid Soltanian, Frank Ko, and Peyman Servati. "Effects of flexible dry electrode design on electrodermal activity stimulus response detection." In: *IEEE Transactions on Biomedical Engineering* 64.12 (2017), pp. 2979–2987.
- [144] Lenka Halámková, Jan Halánek, Vera Bocharova, Alon Szczupak, Lital Alfonta, and Evgeny Katz. "Implanted biofuel cell operating in a living snail." In: *Journal of the American Chemical Society* 134.11 (2012), pp. 5040–5043.
- [145] Skarphedinn Halldorsson, Edinson Lucumi, Rafael Gómez-Sjöberg, and Ronan MT Fleming. "Advantages and challenges of microfluidic cell culture in polydimethylsiloxane devices." In: *Biosensors and Bioelectronics* 63 (2015), pp. 218–231.
- [146] Nur Al-huda Hamdan, Jeffrey R. Blum, Florian Heller, Ravi Kanth Kosuru, and Jan Borchers. "Grabbing at an Angle: Menu Selection for Fabric Interfaces." In: *Proceedings of the 2016 ACM International Symposium on Wearable Computers*. ISWC '16. Heidelberg, Germany: Association for Computing Machinery, 2016, 1–7. ISBN: 9781450344609. DOI: [10.1145/2971763.2971786](https://doi.org/10.1145/2971763.2971786). URL: <https://doi.org/10.1145/2971763.2971786>.

- [147] Nur Al-huda Hamdan, Florian Heller, Chat Wacharamanatham, Jan Thar, and Jan Borchers. "Grabrics: A Foldable Two-Dimensional Textile Input Controller." In: *Proceedings of the 2016 CHI Conference Extended Abstracts on Human Factors in Computing Systems*. CHI EA '16. San Jose, California, USA: Association for Computing Machinery, 2016, 2497–2503. ISBN: 9781450340823. DOI: [10.1145/2851581.2892529](https://doi.org/10.1145/2851581.2892529). URL: <https://doi.org/10.1145/2851581.2892529>.
- [148] Nur Al-huda Hamdan, Simon Voelker, and Jan Borchers. "Sketch & Stitch: Interactive Embroidery for E-Textiles." In: *Proceedings of the 2018 CHI Conference on Human Factors in Computing Systems*. New York, NY, USA: Association for Computing Machinery, 2018, 1–13. ISBN: 9781450356206. URL: <https://doi.org/10.1145/3173574.3173656>.
- [149] Nur Al-huda Hamdan, Adrian Wagner, Simon Voelker, Jürgen Steimle, and Jan Borchers. "Springlets: Expressive, Flexible and Silent On-Skin Tactile Interfaces." In: *Proceedings of the 2019 CHI Conference on Human Factors in Computing Systems*. New York, NY, USA: Association for Computing Machinery, 2019, 1–14. ISBN: 9781450359702. URL: <https://doi.org/10.1145/3290605.3300718>.
- [150] Teng Han, Fraser Anderson, Pourang Irani, and Tovi Grossman. "HydroRing: Supporting Mixed Reality Haptics Using Liquid Flow." In: *Proceedings of the 31st Annual ACM Symposium on User Interface Software and Technology*. UIST '18. Berlin, Germany: Association for Computing Machinery, 2018, 913–925. ISBN: 9781450359481. DOI: [10.1145/3242587.3242667](https://doi.org/10.1145/3242587.3242667). URL: <https://doi.org/10.1145/3242587.3242667>.
- [151] Teng Han, Shubhi Bansal, Xiaochen Shi, Yanjun Chen, Baogang Quan, Feng Tian, Hongan Wang, and Sriram Subramanian. "HapBead: On-Skin Microfluidic Haptic Interface Using Tunable Bead." In: *Proceedings of the 2020 CHI Conference on Human Factors in Computing Systems*. New York, NY, USA: Association for Computing Machinery, 2020, 1–10. ISBN: 9781450367080. URL: <https://doi.org/10.1145/3313831.3376190>.
- [152] Manne Hannula, H Hinkula, and J Jauhiainen. "Development and evaluation of one arm electrode based ECG measurement system." In: *14th Nordic-Baltic Conference on Biomedical Engineering and Medical Physics*. Springer, 2008, pp. 234–237.
- [153] Chris Harrison, Hrvoje Benko, and Andrew D. Wilson. "OmniTouch: Wearable Multitouch Interaction Everywhere." In: *Proceedings of the 24th Annual ACM Symposium on User Interface Software and Technology*. UIST '11. Santa Barbara, California, USA: Association for Computing Machinery, 2011, 441–450. ISBN: 9781450307161. DOI: [10.1145/2047196.2047255](https://doi.org/10.1145/2047196.2047255). URL: <https://doi.org/10.1145/2047196.2047255>.

- [154] Chris Harrison and Scott E. Hudson. "Abracadabra: Wireless, High-Precision, and Unpowered Finger Input for Very Small Mobile Devices." In: *Proceedings of the 22nd Annual ACM Symposium on User Interface Software and Technology*. UIST '09. Victoria, BC, Canada: Association for Computing Machinery, 2009, 121–124. ISBN: 9781605587455. DOI: [10.1145/1622176.1622199](https://doi.org/10.1145/1622176.1622199). URL: <https://doi.org/10.1145/1622176.1622199>.
- [155] Chris Harrison, Shilpa Ramamurthy, and Scott E. Hudson. "On-Body Interaction: Armed and Dangerous." In: *Proceedings of the Sixth International Conference on Tangible, Embedded and Embodied Interaction*. TEI '12. Kingston, Ontario, Canada: Association for Computing Machinery, 2012, 69–76. ISBN: 9781450311748. DOI: [10.1145/2148131.2148148](https://doi.org/10.1145/2148131.2148148). URL: <https://doi.org/10.1145/2148131.2148148>.
- [156] Chris Harrison, Shilpa Ramamurthy, and Scott E. Hudson. "On-Body Interaction: Armed and Dangerous." In: *Proceedings of the Sixth International Conference on Tangible, Embedded and Embodied Interaction*. TEI '12. Kingston, Ontario, Canada: Association for Computing Machinery, 2012, 69–76. ISBN: 9781450311748. DOI: [10.1145/2148131.2148148](https://doi.org/10.1145/2148131.2148148). URL: <https://doi.org/10.1145/2148131.2148148>.
- [157] Chris Harrison, Munehiko Sato, and Ivan Poupyrev. "Capacitive Fingerprinting: Exploring User Differentiation by Sensing Electrical Properties of the Human Body." In: *Proceedings of the 25th Annual ACM Symposium on User Interface Software and Technology*. UIST '12. Cambridge, Massachusetts, USA: Association for Computing Machinery, 2012, 537–544. ISBN: 9781450315807. DOI: [10.1145/2380116.2380183](https://doi.org/10.1145/2380116.2380183). URL: <https://doi.org/10.1145/2380116.2380183>.
- [158] Chris Harrison, Julia Schwarz, and Scott E. Hudson. "TapSense: Enhancing Finger Interaction on Touch Surfaces." In: *Proceedings of the 24th Annual ACM Symposium on User Interface Software and Technology*. UIST '11. Santa Barbara, California, USA: Association for Computing Machinery, 2011, 627–636. ISBN: 9781450307161. DOI: [10.1145/2047196.2047279](https://doi.org/10.1145/2047196.2047279). URL: <https://doi.org/10.1145/2047196.2047279>.
- [159] Chris Harrison, Desney Tan, and Dan Morris. "Skinput: Appropriating the Body as an Input Surface." In: *Proceedings of the SIGCHI Conference on Human Factors in Computing Systems*. CHI '10. Atlanta, Georgia, USA: Association for Computing Machinery, 2010, 453–462. ISBN: 9781605589299. DOI: [10.1145/1753326.1753394](https://doi.org/10.1145/1753326.1753394). URL: <https://doi.org/10.1145/1753326.1753394>.
- [160] Kayla J. Heffernan, Frank Vetere, and Shanton Chang. "You Put What, Where? Hobbyist Use of Insertable Devices." In: *Proceedings of the 2016 CHI Conference on Human Factors in Computing Systems*. New York, NY, USA: Association for Computing Machinery, 2016, 1798–1809. ISBN: 9781450333627. URL: <https://doi.org/10.1145/2858036.2858392>.

- [161] Jajack Heikenfeld, Andrew Jajack, Jim Rogers, Philipp Gutruf, Lei Tian, Tingrui Pan, Ruya Li, Michelle Khine, Jintae Kim, and Juanhong Wang. "Wearable sensors: modalities, challenges, and prospects." In: *Lab on a Chip* 18.2 (2018), pp. 217–248.
- [162] Florian Heller, Stefan Ivanov, Chat Wacharamanatham, and Jan Borchers. "FabriTouch: Exploring Flexible Touch Input on Textiles." In: *Proceedings of the 2014 ACM International Symposium on Wearable Computers*. ISWC '14. Seattle, Washington: Association for Computing Machinery, 2014, 59–62. ISBN: 9781450329699. DOI: [10.1145/2634317.2634345](https://doi.org/10.1145/2634317.2634345). URL: <https://doi.org/10.1145/2634317.2634345>.
- [163] Hermie J Hermens, Bart Freriks, Catherine Disselhorst-Klug, and Günter Rau. "Development of recommendations for SEMG sensors and sensor placement procedures." In: *Journal of Electromyography and Kinesiology* 10.5 (2000), pp. 361–374. ISSN: 1050-6411. DOI: [10.1016/S1050-6411\(00\)00027-4](https://doi.org/10.1016/S1050-6411(00)00027-4). URL: <https://www.sciencedirect.com/science/article/pii/S1050641100000274?via=ihub>.
- [164] Rafael E Herrera, James T Cain, EG Cape, and Gerard J Boyle. "A high resolution ECG tool for detection of atrial and ventricular late potentials." In: *Computers in Cardiology 1996*. IEEE. 1996, pp. 629–632.
- [165] Matthew J Hertenstein and Sandra J Weiss. *The handbook of touch: Neuroscience, behavioral, and health perspectives*. Springer Publishing Company, 2011.
- [166] Mehrdad Hesar, Vikram Iyer, and Shyamnath Gollakota. "Enabling On-Body Transmissions with Commodity Devices." In: *Proceedings of the 2016 ACM International Joint Conference on Pervasive and Ubiquitous Computing*. UbiComp '16. Heidelberg, Germany: Association for Computing Machinery, 2016, 1100–1111. ISBN: 9781450344616. DOI: [10.1145/2971648.2971682](https://doi.org/10.1145/2971648.2971682). URL: <https://doi.org/10.1145/2971648.2971682>.
- [167] *HexoSkin Smart Shirts*. <https://www.hexoskin.com/>. Accessed: 2019-09-20. 2013.
- [168] Arthur Hirsch, Hadrien O Michaud, Aaron P Gerratt, Séverine De Mulatier, and Stéphanie P Lacour. "Intrinsically stretchable biphasic (solid–liquid) thin metal films." In: *Advanced Materials* 28.22 (2016), pp. 4507–4512.
- [169] My Duyen Ho, Yunzhi Ling, Lim Wei Yap, Yan Wang, Dashen Dong, Yunmeng Zhao, and Wenlong Cheng. "Percolating network of ultrathin gold nanowires and silver nanowires toward "invisible" wearable sensors for detecting emotional expression and apexcardiogram." In: *Advanced Functional Materials* 27.25 (2017), p. 1700845.

- [170] Hong Hocheng and Chao-Ming Chen. "Design, Fabrication and Failure Analysis of Stretchable Electrical Routings." In: *Sensors* 14.7 (2014), pp. 11855–11877. ISSN: 1424-8220. DOI: [10.3390/s140711855](https://doi.org/10.3390/s140711855). URL: <https://www.mdpi.com/1424-8220/14/7/11855>.
- [171] Paul Holleis, Albrecht Schmidt, Susanna Paasovaara, Arto Puikkonen, and Jonna Häkkinen. "Evaluating Capacitive Touch Input on Clothes." In: *Proceedings of the 10th International Conference on Human Computer Interaction with Mobile Devices and Services*. MobileHCI '08. Amsterdam, The Netherlands: Association for Computing Machinery, 2008, 81–90. ISBN: 9781595939524. DOI: [10.1145/1409240.1409250](https://doi.org/10.1145/1409240.1409250). URL: <https://doi.org/10.1145/1409240.1409250>.
- [172] Mark Hollins and S Ryan Risner. "Evidence for the duplex theory of tactile texture perception." In: *Perception & psychophysics* 62.4 (2000), pp. 695–705.
- [173] Christian Holz and Patrick Baudisch. "Understanding Touch." In: *Proceedings of the SIGCHI Conference on Human Factors in Computing Systems*. New York, NY, USA: Association for Computing Machinery, 2011, 2501–2510. ISBN: 9781450302289. URL: <https://doi.org/10.1145/1978942.1979308>.
- [174] Christian Holz and Patrick Baudisch. "Understanding touch." In: *Proceedings of the SIGCHI Conference on Human Factors in Computing Systems*. ACM, 2011, pp. 2501–2510.
- [175] Christian Holz, Tovi Grossman, George Fitzmaurice, and Anne Agur. "Implanted User Interfaces." In: *Proceedings of the SIGCHI Conference on Human Factors in Computing Systems*. New York, NY, USA: Association for Computing Machinery, 2012, 503–512. ISBN: 9781450310154. URL: <https://doi.org/10.1145/2207676.2207745>.
- [176] Christian Holz and Marius Knaust. "Biometric Touch Sensing: Seamlessly Augmenting Each Touch with Continuous Authentication." In: *Proceedings of the 28th Annual ACM Symposium on User Interface Software and Technology*. UIST '15. Charlotte, NC, USA: Association for Computing Machinery, 2015, 303–312. ISBN: 9781450337793. DOI: [10.1145/2807442.2807458](https://doi.org/10.1145/2807442.2807458). URL: <https://doi.org/10.1145/2807442.2807458>.
- [177] Christian Holz and Edward J Wang. "Glabella: Continuously sensing blood pressure behavior using an unobtrusive wearable device." In: *Proceedings of the ACM on Interactive, Mobile, Wearable and Ubiquitous Technologies* 1.3 (2017), p. 58.
- [178] Cedric Honnet, Hannah Perner-Wilson, Marc Teyssier, Bruno Fruchard, Jürgen Steimle, Ana C. Baptista, and Paul Strohmeier. "PolySense: Augmenting Textiles with Electrical Functionality Using In-Situ Polymerization." In: *Proceedings of the 2020 CHI Conference on Human Factors in Computing Systems*. New York, NY, USA: Association for Computing Machinery, 2020, 1–13. ISBN: 9781450367080. URL: <https://doi.org/10.1145/3313831.3376841>.

- [179] Noura Howell, Laura Devendorf, Rundong (Kevin) Tian, Tomás Vega Galvez, Nan-Wei Gong, Ivan Poupyrev, Eric Paulos, and Kimiko Ryokai. "Biosignals as Social Cues: Ambiguity and Emotional Interpretation in Social Displays of Skin Conductance." In: *Proceedings of the 2016 ACM Conference on Designing Interactive Systems*. DIS '16. Brisbane, QLD, Australia: Association for Computing Machinery, 2016, 865–870. ISBN: 9781450340311. DOI: [10.1145/2901790.2901850](https://doi.org/10.1145/2901790.2901850). URL: <https://doi.org/10.1145/2901790.2901850>.
- [180] Min-Chieh Hsiu, Chiuan Wang, Da-Yuan Huang, Jhe-Wei Lin, Yu-Chih Lin, De-Nian Yang, Yi-ping Hung, and Mike Chen. "Nail+: Sensing Fingernail Deformation to Detect Finger Force Touch Interactions on Rigid Surfaces." In: *Proceedings of the 18th International Conference on Human-Computer Interaction with Mobile Devices and Services*. MobileHCI '16. Florence, Italy: Association for Computing Machinery, 2016, 1–6. ISBN: 9781450344081. DOI: [10.1145/2935334.2935362](https://doi.org/10.1145/2935334.2935362). URL: <https://doi.org/10.1145/2935334.2935362>.
- [181] Da-Yuan Huang, Liwei Chan, Shuo Yang, Fan Wang, Rong-Hao Liang, De-Nian Yang, Yi-Ping Hung, and Bing-Yu Chen. "DigitSpace: Designing Thumb-to-Fingers Touch Interfaces for One-Handed and Eyes-Free Interactions." In: *Proceedings of the 2016 CHI Conference on Human Factors in Computing Systems*. CHI '16. San Jose, California, USA: Association for Computing Machinery, 2016, 1526–1537. ISBN: 9781450333627. DOI: [10.1145/2858036.2858483](https://doi.org/10.1145/2858036.2858483). URL: <https://doi.org/10.1145/2858036.2858483>.
- [182] Haizhou Huang, Shi Su, Nan Wu, Hao Wan, Shu Wan, Hengchang Bi, and Litao Sun. "Graphene-based sensors for human health monitoring." In: *Frontiers in chemistry* 7 (2019), p. 399.
- [183] Kunpeng Huang, Ruoja Sun, Ximeng Zhang, Md. Tahmidul Islam Molla, Margaret Dunne, Guimbretière François, and Cindy Hsin-Liu Kao. "Woven-Probe: Probing Possibilities for Weaving Fully-Integrated On-Skin Systems Deployable in the Field." In: *Proceedings of the 2021 ACM Conference on Designing Interactive Systems - DIS '21*. New York, New York, USA: ACM Press, 2016, pp. 853–864. ISBN: 9781450348476. DOI: [10.1145/3461778.3462105](https://doi.org/10.1145/3461778.3462105). URL: <https://doi.org/10.1145/3461778.3462105>.
- [184] Qijin Huang and Yong Zhu. "Printing conductive nanomaterials for flexible and stretchable electronics: A review of materials, processes, and applications." In: *Advanced Materials Technologies* 4.5 (2019), p. 1800546.
- [185] Xian Huang, Yuhao Liu, Kaile Chen, Woo-Jung Shin, Ching-Jui Lu, Gil-Woo Kong, Dwipayana Patnaik, Sang-Heon Lee, Jonathan Fajardo Cortes, and John A Rogers. "Stretchable, wireless sensors and functional substrates for epidermal characterization of sweat." In: *Small* 10.15 (2014), pp. 3083–3090.

- [186] Xian Huang, Yuhao Liu, Gil Woo Kong, Jung Hun Seo, Yinji Ma, Kyung-In Jang, Jonathan A Fan, Shimin Mao, Qiwen Chen, Daizhen Li, et al. "Epidermal radio frequency electronics for wireless power transfer." In: *Microsystems & nanoengineering* 2.1 (2016), pp. 1–9.
- [187] Gijs Huisman, Aduen Darriba Frederiks, Betsy Van Dijk, Dirk Hevlen, and Ben Krose. "The TaSST: Tactile sleeve for social touch." In: *World Haptics Conference (WHC), 2013*. IEEE. 2013, pp. 211–216.
- [188] Virve Inget, Heiko Müller, and Jonna Häkkinä. "Private and public aspects of smart jewellery: a design exploration study." In: *Proceedings of the 18th International Conference on Mobile and Ubiquitous Multimedia*. 2019, pp. 1–7.
- [189] Thomas R Insel. "Toward a neurobiology of attachment." In: *Review of general psychology* 4.2 (2000), pp. 176–185.
- [190] Lilah Inzelberg, Moshe David Pur, Stefan Schliske, Tobias Rödlmeier, Omer Granoviter, David Rand, Stanislav Steinberg, Gerardo Hernandez-Sosa, and Yael Hanein. "Printed facial skin electrodes as sensors of emotional affect." In: *Flexible and Printed Electronics* 3.4 (2018), p. 045001.
- [191] Yasha Iravantchi, Mayank Goel, and Chris Harrison. "BeamBand: Hand Gesture Sensing with Ultrasonic Beamforming." In: *Proceedings of the 2019 CHI Conference on Human Factors in Computing Systems*. CHI '19. Glasgow, Scotland Uk: Association for Computing Machinery, 2019, 1–10. ISBN: 9781450359702. DOI: [10.1145/3290605.3300245](https://doi.org/10.1145/3290605.3300245). URL: <https://doi.org/10.1145/3290605.3300245>.
- [192] Hyungkook Jeon, Seong Kyung Hong, Min Seo Kim, Seong J Cho, and Geunbae Lim. "Omni-purpose stretchable strain sensor based on a highly dense nanocracking structure for whole-body motion monitoring." In: *ACS applied materials & interfaces* 9.48 (2017), pp. 41712–41721.
- [193] Yongmin Jeon, Hye-Ryung Choi, Jeong Hyun Kwon, Seungyeop Choi, Kyung Mi Nam, Kyoung-Chan Park, and Kyung Cheol Choi. "Sandwich-structure transferable free-form OLEDs for wearable and disposable skin wound photomedicine." In: *Light: Science & Applications* 8.1 (2019), pp. 1–15.
- [194] Yongmin Jeon, Hye-Ryung Choi, Myungsub Lim, Seungyeop Choi, Hyuncheol Kim, Jeong Hyun Kwon, Kyoung-Chan Park, and Kyung Cheol Choi. "A wearable photobiomodulation patch using a flexible red-wavelength OLED and its in vitro differential cell proliferation effects." In: *Advanced Materials Technologies* 3.5 (2018), p. 1700391.
- [195] Jae-Woong Jeong, Min Ku Kim, Huanyu Cheng, Woon-Hong Yeo, Xian Huang, Yuhao Liu, Yihui Zhang, Yonggang Huang, and John A Rogers. "Capacitive epidermal electronics for electrically safe, long-term electrophysiological measurements." In: *Advanced healthcare materials* 3.5 (2014), pp. 642–648.

- [196] Jae-Woong Jeong et al. "Materials and Optimized Designs for Human-Machine Interfaces Via Epidermal Electronics." In: *Advanced Materials* 25.47 (2013), pp. 6839–6846. ISSN: 09359648. DOI: [10.1002/adma.201301921](https://doi.org/10.1002/adma.201301921). URL: <http://doi.wiley.com/10.1002/adma.201301921>.
- [197] Yu Ra Jeong, Jeonghyun Kim, Zhaoqian Xie, Yeguang Xue, Sang Min Won, Geumbee Lee, Sang Woo Jin, Soo Yeong Hong, Xue Feng, Yonggang Huang, et al. "A skin-attachable, stretchable integrated system based on liquid GaInSn for wireless human motion monitoring with multi-site sensing capabilities." In: *NPG Asia Materials* 9.10 (2017), e443–e443.
- [198] Phil Jevon. "Procedure for recording a standard 12-lead electrocardiogram." In: *British Journal of Nursing* 19.10 (2010), pp. 649–651.
- [199] Wenzhao Jia, Gabriela Valdés-Ramírez, Amay J Bhandodkar, Joshua R Windmiller, and Joseph Wang. "Epidermal biofuel cells: energy harvesting from human perspiration." In: *Angewandte Chemie International Edition* 52.28 (2013), pp. 7233–7236.
- [200] Jeyeon Jo and Cindy Hsin-Liu Kao. "SkinLace: Freestanding Lace by Machine Embroidery for On-Skin Interface." In: *Extended Abstracts of the 2021 CHI Conference on Human Factors in Computing Systems*. New York, NY, USA: Association for Computing Machinery, 2021. ISBN: 9781450380959. URL: <https://doi.org/10.1145/3411763.3451756>.
- [201] Roland S Johansson and J Randall Flanagan. "Coding and use of tactile signals from the fingertips in object manipulation tasks." In: *Nature Reviews Neuroscience* 10.5 (2009), pp. 345–359.
- [202] ID Johnston, DK McCluskey, CKL Tan, and MC Tracey. "Mechanical characterization of bulk Sylgard 184 for microfluidics and microengineering." In: *Journal of Micromechanics and Microengineering* 24.3 (2014), p. 035017.
- [203] Lynette A Jones and Nadine B Sarter. "Tactile displays: Guidance for their design and application." In: *Human factors* 50.1 (2008), pp. 90–111.
- [204] Lynette A Jones and Hong Z Tan. "Application of psychophysical techniques to haptic research." In: *IEEE transactions on haptics* 6.3 (2013), pp. 268–284.
- [205] Shideh Kabiri Ameri, Rebecca Ho, Hongwoo Jang, Li Tao, Youhua Wang, Liu Wang, David M. Schnyer, Deji Akinwande, and Nanshu Lu. "Graphene Electronic Tattoo Sensors." In: *ACS Nano* 11.8 (2017), pp. 7634–7641. ISSN: 1936-0851. DOI: [10.1021/acsnano.7b02182](https://doi.org/10.1021/acsnano.7b02182). URL: <http://pubs.acs.org/doi/10.1021/acsnano.7b02182>.
- [206] Shideh Kabiri Ameri, Rebecca Ho, Hongwoo Jang, Li Tao, Youhua Wang, Liu Wang, David M Schnyer, Deji Akinwande, and Nanshu Lu. "Graphene electronic tattoo sensors." In: *ACS nano* 11.8 (2017), pp. 7634–7641.

- [207] Martin Kaltenbrunner, Tsuyoshi Sekitani, Jonathan Reeder, Tomoyuki Yokota, Kazunori Kuribara, Takeyoshi Tokuhara, Michael Drack, Reinhard Schwödiauer, Ingrid Graz, Simona Bauer-Gogonea, et al. "An ultralightweight design for imperceptible plastic electronics." In: *Nature* 499.7459 (2013), pp. 458–463.
- [208] Martin Kaltenbrunner, Tsuyoshi Sekitani, Jonathan Reeder, Tomoyuki Yokota, Kazunori Kuribara, Takeyoshi Tokuhara, Michael Drack, Reinhard Schwödiauer, Ingrid Graz, Simona Bauer-Gogonea, et al. "An ultralightweight design for imperceptible plastic electronics." In: *Nature* 499.7459 (2013), p. 458.
- [209] Brian Byunghyun Kang, Hyungmin Choi, Haemin Lee, and Kyu-Jin Cho. "Exo-glove poly ii: A polymer-based soft wearable robot for the hand with a tendon-driven actuation system." In: *Soft robotics* 6.2 (2019), pp. 214–227.
- [210] Cindy Hsin-Liu (Cindy) Kao, Min-Wei Hung, Ximeng Zhang, Po-Chun Huang, and Chuang-Wen You. "Probing User Perceptions of On-Skin Notification Displays." In: *Proc. ACM Hum.-Comput. Interact.* 4.CSCW3 (Jan. 2021). DOI: [10.1145/3432943](https://doi.org/10.1145/3432943). URL: <https://doi.org/10.1145/3432943>.
- [211] Hsin-Liu Cindy Kao. "Hybrid Body Craft: Toward Culturally and Socially Inclusive Design for On-Skin Interfaces." In: *IEEE Pervasive Computing* 20.3 (2021), pp. 41–50.
- [212] Hsin-Liu (Cindy) Kao, Miren Bamforth, David Kim, and Chris Schmandt. "Skinmorph: Texture-Tunable on-Skin Interface through Thin, Programmable Gel." In: *Proceedings of the 2018 ACM International Symposium on Wearable Computers*. ISWC '18. Singapore, Singapore: Association for Computing Machinery, 2018, 196–203. ISBN: 9781450359672. DOI: [10.1145/3267242.3267262](https://doi.org/10.1145/3267242.3267262). URL: <https://doi.org/10.1145/3267242.3267262>.
- [213] Hsin-Liu Cindy Kao, Abdelkareem Bedri, and Kent Lyons. "SkinWire: Fabricating a Self-Contained On-Skin PCB for the Hand." In: *Proc. ACM Interact. Mob. Wearable Ubiquitous Technol.* 2.3 (Sept. 2018). DOI: [10.1145/3264926](https://doi.org/10.1145/3264926). URL: <https://doi.org/10.1145/3264926>.
- [214] Hsin-Liu (Cindy) Kao, Artem Dementyev, Joseph A. Paradiso, and Chris Schmandt. "NailO: Fingernails as an Input Surface." In: *Proceedings of the 33rd Annual ACM Conference on Human Factors in Computing Systems*. CHI '15. Seoul, Republic of Korea: Association for Computing Machinery, 2015, 3015–3018. ISBN: 9781450331456. DOI: [10.1145/2702123.2702572](https://doi.org/10.1145/2702123.2702572). URL: <https://doi.org/10.1145/2702123.2702572>.
- [215] Hsin-Liu (Cindy) Kao, Christian Holz, Asta Roseway, Andres Calvo, and Chris Schmandt. "DuoSkin." In: *Proceedings of the 2016 ACM International Symposium on Wearable Computers - ISWC '16*. New York, New York, USA: ACM Press, 2016, pp. 16–23. ISBN: 9781450344609. DOI: [10.1145/2971763.2971777](https://doi.org/10.1145/2971763.2971777). URL: <http://dl.acm.org/citation.cfm?doid=2971763.2971777>.

- [216] Hsin-Liu (Cindy) Kao, Manisha Mohan, Chris Schmandt, Joseph A. Paradiso, and Katia Vega. "ChromoSkin: Towards Interactive Cosmetics Using Thermochromic Pigments." In: *Proceedings of the 2016 CHI Conference Extended Abstracts on Human Factors in Computing Systems*. CHI EA '16. San Jose, California, USA: Association for Computing Machinery, 2016, 3703–3706. ISBN: 9781450340823. DOI: [10.1145/2851581.2890270](https://doi.org/10.1145/2851581.2890270). URL: <https://doi.org/10.1145/2851581.2890270>.
- [217] Jeffrey M Karp and Robert Langer. "Materials science: dry solution to a sticky problem." In: *Nature* 477:7362 (2011), p. 42.
- [218] Thorsten Karrer, Moritz Wittenhagen, Leonhard Lichtschlag, Florian Heller, and Jan Borchers. "Pinstripe: Eyes-Free Continuous Input on Interactive Clothing." In: *Proceedings of the SIGCHI Conference on Human Factors in Computing Systems*. New York, NY, USA: Association for Computing Machinery, 2011, 1313–1322. ISBN: 9781450302289. URL: <https://doi.org/10.1145/1978942.1979137>.
- [219] Shunichi Kasahara, Jun Nishida, and Pedro Lopes. "Preemptive Action: Accelerating Human Reaction Using Electrical Muscle Stimulation Without Compromising Agency." In: *Proceedings of the 2019 CHI Conference on Human Factors in Computing Systems*. New York, NY, USA: Association for Computing Machinery, 2019, 1–15. ISBN: 9781450359702. URL: <https://doi.org/10.1145/3290605.3300873>.
- [220] Kunihiro Kato, Hiroki Ishizuka, Hiroyuki Kajimoto, and Homei Miyashita. "Double-Sided Printed Tactile Display with Electro Stimuli and Electrostatic Forces and Its Assessment." In: *Proceedings of the 2018 CHI Conference on Human Factors in Computing Systems*. New York, NY, USA: Association for Computing Machinery, 2018, 1–12. ISBN: 9781450356206. URL: <https://doi.org/10.1145/3173574.3174024>.
- [221] Keiko Katsuragawa, Ju Wang, Ziyang Shan, Ningshan Ouyang, Omid Abari, and Daniel Vogel. "Tip-Tap: Battery-Free Discrete 2D Fingertip Input." In: *Proceedings of the 32nd Annual ACM Symposium on User Interface Software and Technology*. UIST '19. New Orleans, LA, USA: Association for Computing Machinery, 2019, 1045–1057. ISBN: 9781450368162. DOI: [10.1145/3332165.3347907](https://doi.org/10.1145/3332165.3347907). URL: <https://doi.org/10.1145/3332165.3347907>.
- [222] Yoshihiro Kawahara, Steve Hodges, Benjamin S. Cook, Cheng Zhang, and Gregory D. Abowd. "Instant Inkjet Circuits: Lab-based Inkjet Printing to Support Rapid Prototyping of UbiComp Devices." In: *Proceedings of the 2013 ACM International Joint Conference on Pervasive and Ubiquitous Computing*. UbiComp '13. Zurich, Switzerland: ACM, 2013, pp. 363–372. ISBN: 978-1-4503-1770-2. DOI: [10.1145/2493432.2493486](https://doi.org/10.1145/2493432.2493486). URL: <http://doi.acm.org/10.1145/2493432.2493486>.

- [223] Kendall Covidien H124SG. <https://bio-medical.com/media/support/H124SG.pdf>. Accessed: 2021-07-23.
- [224] Kendall Covidien H135SG. https://media.supplychain.nhs.uk/media/documents/FJE6316/Marketing/61534_FJE6316.pdf. Accessed: 2021-07-23.
- [225] Arshad Khan, Joan Sol Roo, Tobias Kraus, and Jürgen Steimle. “Soft Inkjet Circuits: Rapid Multi-Material Fabrication of Soft Circuits Using a Commodity Inkjet Printer.” In: *Proceedings of the 32nd Annual ACM Symposium on User Interface Software and Technology*. UIST '19. New Orleans, LA, USA: Association for Computing Machinery, 2019, 341–354. ISBN: 9781450368162. DOI: 10.1145/3332165.3347892. URL: <https://doi.org/10.1145/3332165.3347892>.
- [226] Zeeshan O Khokhar, Zhen G Xiao, and Carlo Menon. “Surface EMG pattern recognition for real-time control of a wrist exoskeleton.” In: *Biomedical engineering online* 9.1 (2010), p. 41.
- [227] Wolf Kienzle, Eric Whitmire, Chris Rittaler, and Hrvoje Benko. “ElectroRing: Subtle Pinch and Touch Detection with a Ring.” In: *Proceedings of the 2021 CHI Conference on Human Factors in Computing Systems*. New York, NY, USA: Association for Computing Machinery, 2021. ISBN: 9781450380966. URL: <https://doi.org/10.1145/3411764.3445094>.
- [228] D.-H. Kim et al. “Epidermal Electronics.” In: *Science* 333.6044 (2011), pp. 838–843. ISSN: 0036-8075. DOI: 10.1126/science.1206157. URL: <http://www.sciencemag.org/cgi/doi/10.1126/science.1206157>.
- [229] Dae-Hyeong Kim, Yun-Soung Kim, Jason Amsden, Bruce Panilaitis, David L Kaplan, Fiorenzo G Omenetto, Mitchell R Zakin, and John A Rogers. “Silicon electronics on silk as a path to bioresorbable, implantable devices.” In: *Applied physics letters* 95.13 (2009), p. 133701.
- [230] Dae-Hyeong Kim, Nanshu Lu, Rui Ma, Yun-Soung Kim, Rak-Hwan Kim, Shuodao Wang, Jian Wu, Sang Min Won, Hu Tao, Ahmad Islam, et al. “Epidermal electronics.” In: *science* 333.6044 (2011), pp. 838–843.
- [231] David Kim, Otmar Hilliges, Shahram Izadi, Alex D. Butler, Jiawen Chen, Iason Oikonomidis, and Patrick Olivier. “Digits: Freehand 3D Interactions Anywhere Using a Wrist-Worn Gloveless Sensor.” In: *Proceedings of the 25th Annual ACM Symposium on User Interface Software and Technology*. UIST '12. Cambridge, Massachusetts, USA: Association for Computing Machinery, 2012, 167–176. ISBN: 9781450315807. DOI: 10.1145/2380116.2380139. URL: <https://doi.org/10.1145/2380116.2380139>.
- [232] Dooyoung Kim, Junghan Kwon, Seunghyun Han, Yong-Lae Park, and Sungho Jo. “Deep full-body motion network for a soft wearable motion sensing suit.” In: *IEEE/ASME Transactions on Mechatronics* 24.1 (2018), pp. 56–66.

- [233] Eui Hyuk Kim, Hyowon Han, Seunggun Yu, Chanhoo Park, Gwangmook Kim, Beomjin Jeong, Seung Won Lee, Jong Sung Kim, Seokyeong Lee, Joohee Kim, et al. "Interactive skin display with epidermal stimuli electrode." In: *Advanced Science* 6.13 (2019), p. 1802351.
- [234] Gwangmook Kim, Sungjun Cho, Kiseok Chang, Wook Sung Kim, Hansaem Kang, Sung-Pil Ryu, Jaemin Myoung, Jinwoo Park, Cheolmin Park, and Wooyoung Shim. "Spatially pressure-mapped thermochromic interactive sensor." In: *Advanced Materials* 29.13 (2017), p. 1606120.
- [235] J. Kim et al. "Battery-free, stretchable optoelectronic systems for wireless optical characterization of the skin." In: *Science Advances* 2.8 (2016), e1600418–e1600418. ISSN: 2375-2548. DOI: [10.1126/sciadv.1600418](https://doi.org/10.1126/sciadv.1600418). URL: <http://advances.sciencemag.org/cgi/doi/10.1126/sciadv.1600418>.
- [236] Jayoung Kim, William R de Araujo, Izabela A Samek, Amay J Bhandodkar, Wenzhao Jia, Barbara Brunetti, Thiago RLC Paixao, and Joseph Wang. "Wearable temporary tattoo sensor for real-time trace metal monitoring in human sweat." In: *Electrochemistry Communications* 51 (2015), pp. 41–45.
- [237] Jayoung Kim, Alan S Campbell, and Joseph Wang. "Wearable non-invasive epidermal glucose sensors: A review." In: *Talanta* 177 (2018), pp. 163–170.
- [238] Jayoung Kim, Itthipon Jeerapan, Bianca Ciui, Martin C Hartel, Aida Martin, and Joseph Wang. "Edible electrochemistry: Food materials based electrochemical sensors." In: *Advanced healthcare materials* 6.22 (2017), p. 1700770.
- [239] Jeonghyun Kim, Philipp Gutruf, Antonio M Chiarelli, Seung Yun Heo, Kyoungyeon Cho, Zhaoqian Xie, Anthony Banks, Seungyoung Han, Kyung-In Jang, Jung Woo Lee, et al. "Miniaturized battery-free wireless systems for wearable pulse oximetry." In: *Advanced functional materials* 27.1 (2017), p. 1604373.
- [240] Jeonghyun Kim et al. "Epidermal Electronics with Advanced Capabilities in Near-Field Communication." In: *Small* 11.8 (2015), pp. 906–912. ISSN: 16136810. DOI: [10.1002/smll.201402495](https://doi.org/10.1002/smll.201402495). URL: <http://doi.wiley.com/10.1002/smll.201402495>.
- [241] Jungsoo Kim, Jiasheng He, Kent Lyons, and Thad Starner. "The gesture watch: A wireless contact-free gesture based wrist interface." In: *2007 11th IEEE International Symposium on Wearable Computers*. IEEE. 2007, pp. 15–22.
- [242] Namyun Kim, Taehoon Lim, Kwangsun Song, Sung Yang, and Jongho Lee. "Stretchable multichannel electromyography sensor array covering large area for controlling home electronics with distinguishable signals from multiple muscles." In: *ACS applied materials & interfaces* 8.32 (2016), pp. 21070–21076.

- [243] Yoonseob Kim, Jian Zhu, Bongjun Yeom, Matthew Di Prima, Xianli Su, Jin-Gyu Kim, Seung Jo Yoo, Ctirad Uher, and Nicholas A Kotov. "Stretchable nanoparticle conductors with self-organized conductive pathways." In: *Nature* 500.7460 (2013), pp. 59–63.
- [244] Konstantin Klamka, Raimund Dachselt, and Jürgen Steimle. "Rapid Iron-On User Interfaces: Hands-on Fabrication of Interactive Textile Prototypes." In: *Proceedings of the 2020 CHI Conference on Human Factors in Computing Systems*. New York, NY, USA: Association for Computing Machinery, 2020, 1–14. ISBN: 9781450367080. URL: <https://doi.org/10.1145/3313831.3376220>.
- [245] Roberta L Klatzky and Susan J Lederman. "Tactile roughness perception with a rigid link interposed between skin and surface." In: *Perception & Psychophysics* 61.4 (1999), pp. 591–607. URL: <https://link.springer.com/content/pdf/10.3758/BF03205532.pdf>.
- [246] George H Klem, Hans Otto Lüders, HH Jasper, C Elger, et al. "The twenty electrode system of the International Federation." In: *Electroencephalogr Clin Neurophysiol* 52.3 (1999), pp. 3–6.
- [247] Jarrod Knibbe, Rachel Freire, Marion Koelle, and Paul Strohmeier. "Skill-Sleeves: Designing Electrode Garments for Wearability." In: *Proceedings of the Fifteenth International Conference on Tangible, Embedded, and Embodied Interaction*. TEI '21. Salzburg, Austria: Association for Computing Machinery, 2021. ISBN: 9781450382137. DOI: 10.1145/3430524.3440652. URL: <https://doi.org/10.1145/3430524.3440652>.
- [248] Marion Koelle, Swamy Ananthanarayan, and Susanne Boll. "Social Acceptability in HCI: A Survey of Methods, Measures, and Design Strategies." In: *Proceedings of the 2020 CHI Conference on Human Factors in Computing Systems*. New York, NY, USA: Association for Computing Machinery, 2020, 1–19. ISBN: 9781450367080. URL: <https://doi.org/10.1145/3313831.3376162>.
- [249] Marion Koelle, Abdallah El Ali, Vanessa Cobus, Wilko Heuten, and Susanne CJ Boll. "All about Acceptability? Identifying Factors for the Adoption of Data Glasses." In: *Proceedings of the 2017 CHI Conference on Human Factors in Computing Systems*. New York, NY, USA: Association for Computing Machinery, 2017, 295–300. ISBN: 9781450346559. URL: <https://doi.org/10.1145/3025453.3025749>.
- [250] Marion Koelle, Matthias Kranz, and Andreas Möller. "Don't Look at Me That Way! Understanding User Attitudes Towards Data Glasses Usage." In: *Proceedings of the 17th International Conference on Human-Computer Interaction with Mobile Devices and Services*. MobileHCI '15. Copenhagen, Denmark: Association for Computing Machinery, 2015, 362–372. ISBN: 9781450336529. DOI: 10.1145/2785830.2785842. URL: <https://doi.org/10.1145/2785830.2785842>.

- [251] Paul AJ Kolarsick, Maria Ann Kolarsick, and Carolyn Goodwin. "Anatomy and physiology of the skin." In: *Journal of the Dermatology Nurses' Association* 3.4 (2011), pp. 203–213.
- [252] Lars Krutak and Aaron Deter-Wolf. *Ancient ink: The archaeology of tattooing*. University of Washington Press, 2017.
- [253] Yuki Kubo, Buntarou Shizuki, and Jiro Tanaka. "B2B-Swipe: Swipe Gesture for Rectangular Smartwatches from a Bezel to a Bezel." In: *Proceedings of the 2016 CHI Conference on Human Factors in Computing Systems*. CHI '16. San Jose, California, USA: Association for Computing Machinery, 2016, 3852–3856. ISBN: 9781450333627. DOI: [10 . 1145 / 2858036 . 2858216](https://doi.org/10.1145/2858036.2858216). URL: <https://doi.org/10.1145/2858036.2858216>.
- [254] Todd A Kuiken, MM Lowery, and NS Stoykov. "The effect of subcutaneous fat on myoelectric signal amplitude and cross-talk." In: *Prosthetics and orthotics international* 27.1 (2003), pp. 48–54. DOI: [10 . 3109 / 03093640309167976](https://doi.org/10.3109/03093640309167976).
- [255] Rajan Kumar, Jaewook Shin, Lu Yin, Jung-Min You, Ying Shirley Meng, and Joseph Wang. "All-printed, stretchable Zn-Ag₂O rechargeable battery via hyperelastic binder for self-powering wearable electronics." In: *Advanced Energy Materials* 7.8 (2017), p. 1602096.
- [256] G D Lamb. "Tactile discrimination of textured surfaces: psychophysical performance measurements in humans." In: *The Journal of Physiology* 338.1 (1983), pp. 551–565. ISSN: 00223751. DOI: [10 . 1113 / jphysiol . 1983 . sp014689](https://doi.org/10.1113/jphysiol.1983.sp014689). URL: <http://doi.wiley.com/10.1113/jphysiol.1983.sp014689>.
- [257] LD Landau and EM Lifshitz. *Theory of Elasticity, Oxford*. 1986.
- [258] Gierad Laput, Robert Xiao, Xiang 'Anthony' Chen, Scott E. Hudson, and Chris Harrison. "Skin Buttons: Cheap, Small, Low-Powered and Clickable Fixed-Icon Laser Projectors." In: *Proceedings of the 27th Annual ACM Symposium on User Interface Software and Technology*. UIST '14. Honolulu, Hawaii, USA: Association for Computing Machinery, 2014, 389–394. ISBN: 9781450330695. DOI: [10 . 1145 / 2642918 . 2647356](https://doi.org/10.1145/2642918.2647356). URL: <https://doi.org/10.1145/2642918.2647356>.
- [259] Gierad Laput, Chouchang Yang, Robert Xiao, Alanson Sample, and Chris Harrison. "EM-Sense: Touch Recognition of Uninstrumented, Electrical and Electromechanical Objects." In: *Proceedings of the 28th Annual ACM Symposium on User Interface Software and Technology*. UIST '15. Charlotte, NC, USA: Association for Computing Machinery, 2015, 157–166. ISBN: 9781450337793. DOI: [10 . 1145 / 2807442 . 2807481](https://doi.org/10.1145/2807442.2807481). URL: <https://doi.org/10.1145/2807442.2807481>.

- [260] Bryan Laulicht, Robert Langer, and Jeffrey M Karp. "Quick-release medical tape." In: *Proceedings of the National Academy of Sciences* 109.46 (2012), pp. 18803–18808.
- [261] Mathieu Le Goc, Stuart Taylor, Shahram Izadi, and Cem Keskin. "A Low-Cost Transparent Electric Field Sensor for 3d Interaction on Mobile Devices." In: *Proceedings of the SIGCHI Conference on Human Factors in Computing Systems*. CHI '14. Toronto, Ontario, Canada: Association for Computing Machinery, 2014, 3167–3170. ISBN: 9781450324731. DOI: [10.1145/2556288.2557331](https://doi.org/10.1145/2556288.2557331). URL: <https://doi.org/10.1145/2556288.2557331>.
- [262] S. J. Lederman and R. L. Klatzky. *Haptic perception: A tutorial*. 2009. DOI: [10.3758/APP.71.7.1439](https://doi.org/10.3758/APP.71.7.1439). arXiv: [NIHMS150003](https://arxiv.org/abs/NIHMS150003).
- [263] Chi Hwan Lee, Yinji Ma, Kyung-In Jang, Anthony Banks, Taisong Pan, Xue Feng, Jae Soon Kim, Daeshik Kang, Milan S Raj, Bryan L McGrane, et al. "Soft core/shell packages for stretchable electronics." In: *Advanced Functional Materials* 25.24 (2015), pp. 3698–3704.
- [264] DoYoung Lee, SooHwan Lee, and Ian Oakley. "Nailz: Sensing Hand Input with Touch Sensitive Nails." In: *Proceedings of the 2020 CHI Conference on Human Factors in Computing Systems*. CHI '20. Honolulu, HI, USA: Association for Computing Machinery, 2020, 1–13. ISBN: 9781450367080. DOI: [10.1145/3313831.3376778](https://doi.org/10.1145/3313831.3376778). URL: <https://doi.org/10.1145/3313831.3376778>.
- [265] Hyunjae Lee, Tae Kyu Choi, Young Bum Lee, Hye Rim Cho, Roozbeh Ghaffari, Liu Wang, Hyung Jin Choi, Taek Dong Chung, Nanshu Lu, Taeghwan Hyeon, et al. "A graphene-based electrochemical device with thermoresponsive microneedles for diabetes monitoring and therapy." In: *Nature nanotechnology* 11.6 (2016), pp. 566–572.
- [266] Hyunjae Lee, Changyeong Song, Yong Seok Hong, Min Sung Kim, Hye Rim Cho, Taegyung Kang, Kwangsoo Shin, Seung Hong Choi, Taeghwan Hyeon, and Dae-Hyeong Kim. "Wearable/disposable sweat-based glucose monitoring device with multistage transdermal drug delivery module." In: *Science advances* 3.3 (2017), e1601314.
- [267] J. Lee, M. T. Cole, J. C. S. Lai, and A. Nathan. "An Analysis of Electrode Patterns in Capacitive Touch Screen Panels." In: *Journal of Display Technology* 10.5 (2014), pp. 362–366. ISSN: 1551-319X. DOI: [10.1109/JDT.2014.2303980](https://doi.org/10.1109/JDT.2014.2303980).
- [268] Jae Keun Lee, Seung Ju Han, Kangil Kim, Yoon Hyuk Kim, and Sangmin Lee. "Wireless epidermal six-axis inertial measurement units for real-time joint angle estimation." In: *Applied Sciences* 10.7 (2020), p. 2240.

- [269] Stephen P Lee, Grace Ha, Don E Wright, Yinji Ma, Ellora Sen-Gupta, Natalie R Haubrich, Paul C Branche, Weihua Li, Gilbert L Huppert, Matthew Johnson, et al. "Highly flexible, wearable, and disposable cardiac biosensors for remote and ambulatory monitoring." In: *NPJ digital medicine* 1.1 (2018), pp. 1–8.
- [270] Pierre Leleux, Jean-Michel Badier, Jonathan Rivnay, Christian Bénar, Thierry Hervé, Patrick Chauvel, and George G Malliaras. "Conducting polymer electrodes for electroencephalography." In: *Advanced healthcare materials* 3.4 (2014), pp. 490–493.
- [271] Joanne Leong, Patrick Parzer, Florian Perteneder, Teo Babic, Christian Rendl, Anita Vogl, Hubert Egger, Alex Olwal, and Michael Haller. "Pro-Cover: Sensory Augmentation of Prosthetic Limbs Using Smart Textile Covers." In: *Proceedings of the 29th Annual Symposium on User Interface Software and Technology*. UIST '16. Tokyo, Japan: Association for Computing Machinery, 2016, 335–346. ISBN: 9781450341899. DOI: [10.1145/2984511.2984572](https://doi.org/10.1145/2984511.2984572). URL: <https://doi.org/10.1145/2984511.2984572>.
- [272] Qingqing Li, Penghui Dong, and Jun Zheng. "Enhancing the security of pattern unlock with surface EMG-based biometrics." In: *Applied Sciences* 10.2 (2020), p. 541.
- [273] Zhuying Li, Felix Brandmueller, Florian 'Floyd' Mueller, and Stefan Greuter. "Ingestible Games: Swallowing a Digital Sensor to Play a Game." In: *Extended Abstracts Publication of the Annual Symposium on Computer-Human Interaction in Play*. CHI PLAY '17 Extended Abstracts. Amsterdam, The Netherlands: Association for Computing Machinery, 2017, 511–518. ISBN: 9781450351119. DOI: [10.1145/3130859.3131312](https://doi.org/10.1145/3130859.3131312). URL: <https://doi.org/10.1145/3130859.3131312>.
- [274] Zhuying Li, Weikang Chen, Yan Wang, Ti Hoang, Wei Wang, Mario Boot, Stefan Greuter, and Florian 'Floyd' Mueller. "HeatCraft: Playing with Ingestible Sensors via Localised Sensations." In: *Proceedings of the 2018 Annual Symposium on Computer-Human Interaction in Play Companion Extended Abstracts*. CHI PLAY '18 Extended Abstracts. Melbourne, VIC, Australia: Association for Computing Machinery, 2018, 521–530. ISBN: 9781450359689. DOI: [10.1145/3270316.3271514](https://doi.org/10.1145/3270316.3271514). URL: <https://doi.org/10.1145/3270316.3271514>.
- [275] Jiajie Liang, Kwing Tong, and Qibing Pei. "A water-based silver-nanowire screen-print ink for the fabrication of stretchable conductors and wearable thin-film transistors." In: *Advanced Materials* 28.28 (2016), pp. 5986–5996.
- [276] Jhe-Wei Lin, Chiuan Wang, Yi Yao Huang, Kuan-Ting Chou, Hsuan-Yu Chen, Wei-Luan Tseng, and Mike Y. Chen. "BackHand: Sensing Hand Gestures via Back of the Hand." In: *Proceedings of the 28th Annual ACM Symposium on User Interface Software and Technology*. UIST '15. Charlotte,

- NC, USA: ACM, 2015, pp. 557–564. ISBN: 978-1-4503-3779-3. DOI: [10.1145/2807442.2807462](https://doi.org/10.1145/2807442.2807462). URL: <http://doi.acm.org/10.1145/2807442.2807462>.
- [277] Shaoting Lin, Changyong Cao, Qiming Wang, Mark Gonzalez, John E Dolbow, and Xuanhe Zhao. “Design of stiff, tough and stretchy hydrogel composites via nanoscale hybrid crosslinking and macroscale fiber reinforcement.” In: *Soft matter* 10.38 (2014), pp. 7519–7527.
- [278] Shu-Yang Lin, Chao-Huai Su, Kai-Yin Cheng, Rong-Hao Liang, Tzu-Hao Kuo, and Bing-Yu Chen. “Pub - Point upon Body: Exploring Eyes-Free Interaction and Methods on an Arm.” In: *Proceedings of the 24th Annual ACM Symposium on User Interface Software and Technology*. UIST '11. Santa Barbara, California, USA: Association for Computing Machinery, 2011, 481–488. ISBN: 9781450307161. DOI: [10.1145/2047196.2047259](https://doi.org/10.1145/2047196.2047259). URL: <https://doi.org/10.1145/2047196.2047259>.
- [279] Niklas Lindahl, Daniel Midtvedt, Johannes Svensson, Oleg A Nerushev, Niclas Lindvall, Andreas Isacson, and Eleanor EB Campbell. “Determination of the bending rigidity of graphene via electrostatic actuation of buckled membranes.” In: *Nano letters* 12.7 (2012), pp. 3526–3531.
- [280] Darren J. Lipomi, Jennifer A. Lee, Michael Vosgueritchian, Benjamin C.-K. Tee, John A. Bolander, and Zhenan Bao. “Electronic Properties of Transparent Conductive Films of PEDOT:PSS on Stretchable Substrates.” In: *Chemistry of Materials* 24.2 (2012), pp. 373–382. DOI: [10.1021/cm203216m](https://doi.org/10.1021/cm203216m). eprint: <https://doi.org/10.1021/cm203216m>. URL: <https://doi.org/10.1021/cm203216m>.
- [281] Roman Lissermann, Jochen Huber, Aristotelis Hadjakos, Suranga Nanayakkara, and Max Mühlhäuser. “EarPut: Augmenting Ear-Worn Devices for Ear-Based Interaction.” In: *Proceedings of the 26th Australian Computer-Human Interaction Conference on Designing Futures: The Future of Design*. OzCHI '14. Sydney, New South Wales, Australia: Association for Computing Machinery, 2014, 300–307. ISBN: 9781450306539. DOI: [10.1145/2686612.2686655](https://doi.org/10.1145/2686612.2686655). URL: <https://doi.org/10.1145/2686612.2686655>.
- [282] Fannie Liu, Mario Esparza, Maria Pavlovskaja, Geoff Kaufman, Laura Dabbish, and Andrés Monroy-Hernández. “Animo: Sharing biosignals on a smartwatch for lightweight social connection.” In: *Proceedings of the ACM on Interactive, Mobile, Wearable and Ubiquitous Technologies* 3.1 (2019), pp. 1–19.
- [283] Jie Liu, Dongwen Ying, William Z Rymer, and Ping Zhou. “Robust muscle activity onset detection using an unsupervised electromyogram learning framework.” In: *PloS one* 10.6 (2015), e0127990.

- [284] Ruibo Liu, Qijia Shao, Siqi Wang, Christina Ru, Devin Balkcom, and Xia Zhou. "Reconstructing Human Joint Motion with Computational Fabrics." In: *Proc. ACM Interact. Mob. Wearable Ubiquitous Technol.* 3.1 (Mar. 2019). DOI: [10.1145/3314406](https://doi.org/10.1145/3314406). URL: <https://doi.org/10.1145/3314406>.
- [285] Xin Liu, Katia Vega, Pattie Maes, and Joe A. Paradiso. "Wearability Factors for Skin Interfaces." In: *Proceedings of the 7th Augmented Human International Conference 2016. AH '16*. Geneva, Switzerland: Association for Computing Machinery, 2016. ISBN: 9781450336802. DOI: [10.1145/2875194.2875248](https://doi.org/10.1145/2875194.2875248). URL: <https://doi.org/10.1145/2875194.2875248>.
- [286] Yuhao Liu, Matt Pharr, and Giovanni Antonio Salvatore. "Lab-on-skin: a review of flexible and stretchable electronics for wearable health monitoring." In: *ACS nano* 11.10 (2017), pp. 9614–9635.
- [287] Joanne Lo, Doris Jung Lin Lee, Nathan Wong, David Bui, and Eric Paulos. "Skintillates." In: *Proceedings of the 2016 ACM Conference on Designing Interactive Systems - DIS '16*. New York, New York, USA: ACM Press, 2016, pp. 853–864. ISBN: 9781450340311. DOI: [10.1145/2901790.2901885](https://doi.org/10.1145/2901790.2901885). URL: <http://dl.acm.org/citation.cfm?doid=2901790.2901885>.
- [288] Johan Löfhede, Fernando Seoane, and Magnus Thordstein. "Textile electrodes for EEG recording—A pilot study." In: *Sensors* 12.12 (2012), pp. 16907–16919.
- [289] Pedro Alhais Lopes, Davide Vaz Gomes, Daniel Green Marques, Pedro Faia, Joana Góis, Tatiana F Patrício, Jorge Coelho, Arménio Serra, Aníbal T de Almeida, Carmel Majidi, et al. "Soft bioelectronic stickers: selection and evaluation of skin-interfacing electrodes." In: *Advanced healthcare materials* 8.15 (2019), p. 1900234.
- [290] Alberto Lopez, Francisco J Ferrero, Marta Valledor, Juan C Campo, and Octavian Postolache. "A study on electrode placement in EOG systems for medical applications." In: *2016 IEEE International Symposium on Medical Measurements and Applications (MeMeA)*. IEEE. 2016, pp. 1–5.
- [291] Tong Lu, Lauren Finkenauer, James Wissman, and Carmel Majidi. "Rapid prototyping for soft-matter electronics." In: *Advanced Functional Materials* 24.22 (2014), pp. 3351–3356.
- [292] Elle Luo, Ruixuan Fu, Alicia Chu, Katia Vega, and Hsin-Liu (Cindy) Kao. "Eslucent: An Eyelid Interface for Detecting Eye Blinking." In: *Proceedings of the 2020 International Symposium on Wearable Computers. ISWC '20*. Virtual Event, Mexico: Association for Computing Machinery, 2020, 58–62. ISBN: 9781450380775. DOI: [10.1145/3410531.3414298](https://doi.org/10.1145/3410531.3414298). URL: <https://doi.org/10.1145/3410531.3414298>.
- [293] Shen Luo, Valtino X Afonso, John G Webster, and Willis J Tompkins. "The electrode system in impedance-based ventilation measurement." In: *IEEE transactions on biomedical engineering* 39.11 (1992), pp. 1130–1141.

- [294] WD Lynn, OJ Escalona, and DJ McEneaney. "Arm and wrist surface potential mapping for wearable ECG rhythm recording devices: a pilot clinical study." In: *Journal of Physics: Conference Series*. Vol. 450. 1. IOP Publishing. 2013, p. 012026.
- [295] Kent Lyons. "Wearable Magnetic Field Sensing for Finger Tracking." In: *Proceedings of the 2020 International Symposium on Wearable Computers*. ISWC '20. Virtual Event, Mexico: Association for Computing Machinery, 2020, 63–67. ISBN: 9781450380775. DOI: [10.1145/3410531.3414304](https://doi.org/10.1145/3410531.3414304). URL: <https://doi.org/10.1145/3410531.3414304>.
- [296] MC10. *BioStamp*. link. Retrieved April 4, 2017 from <https://www.mc10inc.com/our-products#biostamp-npoint>. 2012.
- [297] Rui Ma, Dae-Hyeong Kim, Martin McCormick, Todd Coleman, and John Rogers. "A stretchable electrode array for non-invasive, skin-mounted measurement of electrocardiography (ECG), electromyography (EMG) and electroencephalography (EEG)." In: *2010 Annual International Conference of the IEEE Engineering in Medicine and Biology*. IEEE. 2010, pp. 6405–6408.
- [298] Carmel Majidi and Ronald S Fearing. "Adhesion of an elastic plate to a sphere." In: *Proceedings of the Royal Society A: Mathematical, Physical and Engineering Sciences* 464.2093 (2008), pp. 1309–1317.
- [299] Flavia Mancini, Armando Bauleo, Jonathan Cole, Fausta Lui, Carlo A Porro, Patrick Haggard, and Gian Domenico Iannetti. "Whole-body mapping of spatial acuity for pain and touch." In: *Annals of neurology* 75.6 (2014), pp. 917–24. ISSN: 1531-8249. DOI: [10.1002/ana.24179](https://doi.org/10.1002/ana.24179). URL: <http://www.ncbi.nlm.nih.gov/pubmed/24816757><http://www.pubmedcentral.nih.gov/articlerender.fcgi?artid=PMC4143958>.
- [300] Steve Mann. "Wearable computing." In: *Encyclopedia of Human-Computer Interaction* (2012).
- [301] Alex Mariakakis, Sifang Chen, Bichlien H. Nguyen, Kirsten Bray, Molly Blank, Jonathan Lester, Lauren Ryan, Paul Johns, Gonzalo Ramos, and Asta Roseway. "EcoPatches: Maker-Friendly Chemical-Based UV Sensing." In: *Proceedings of the 2020 ACM Designing Interactive Systems Conference*. New York, NY, USA: Association for Computing Machinery, 2020, 1983–1994. ISBN: 9781450369749. URL: <https://doi.org/10.1145/3357236.3395424>.
- [302] A Marion, E Heinsen, Robert Chin, and B Helmsø. "Wrist instrument opens new dimension in personal information." In: *Hewlett-Packard Journal* (1977), pp. 1–10.
- [303] Eric J Markvicka, Michael D Bartlett, Xiaonan Huang, and Carmel Majidi. "An autonomously electrically self-healing liquid metal–elastomer composite for robust soft-matter robotics and electronics." In: *Nature materials* 17.7 (2018), pp. 618–624.

- [304] Eric Markvicka, Guanyun Wang, Yi-Chin Lee, Gierad Laput, Carmel Majidi, and Lining Yao. "ElectroDermis: Fully Untethered, Stretchable, and Highly-Customizable Electronic Bandages." In: *Proceedings of the 2019 CHI Conference on Human Factors in Computing Systems*. New York, NY, USA: Association for Computing Machinery, 2019, 1–10. ISBN: 9781450359702. URL: <https://doi.org/10.1145/3290605.3300862>.
- [305] Werner Martienssen and Hans Warlimont. *Springer handbook of condensed matter and materials data*. Springer Science & Business Media, 2006.
- [306] Werner Martienssen and Hans Warlimont. *Springer handbook of condensed matter and materials data*. Springer Science & Business Media, 2006.
- [307] S.A. Mascaro and H.H. Asada. "Photoplethysmograph fingernail sensors for measuring finger forces without haptic obstruction." In: *IEEE Transactions on Robotics and Automation* 17.5 (2001), pp. 698–708. DOI: [10.1109/70.964669](https://doi.org/10.1109/70.964669).
- [308] Alex Mazursky, Shan-Yuan Teng, Romain Nith, and Pedro Lopes. "MagnetIO: Passive yet Interactive Soft Haptic Patches Anywhere." In: *Proceedings of the 2021 CHI Conference on Human Factors in Computing Systems*. CHI '21. Yokohama, Japan: Association for Computing Machinery, 2021. ISBN: 9781450380966. DOI: [10.1145/3411764.3445543](https://doi.org/10.1145/3411764.3445543). URL: <https://doi.org/10.1145/3411764.3445543>.
- [309] Alex Mazursky, Shan-Yuan Teng, Romain Nith, and Pedro Lopes. "MagnetIO: Passive yet Interactive Soft Haptic Patches Anywhere." In: *Proceedings of the 2021 CHI Conference on Human Factors in Computing Systems*. New York, NY, USA: Association for Computing Machinery, 2021. ISBN: 9781450380966. URL: <https://doi.org/10.1145/3411764.3445543>.
- [310] J Cooper McDonald and George M Whitesides. "Poly (dimethylsiloxane) as a material for fabricating microfluidic devices." In: *Accounts of chemical research* 35.7 (2002), pp. 491–499.
- [311] Jess McIntosh, Asier Marzo, Mike Fraser, and Carol Phillips. "EchoFlex: Hand Gesture Recognition Using Ultrasound Imaging." In: *Proceedings of the 2017 CHI Conference on Human Factors in Computing Systems*. New York, NY, USA: Association for Computing Machinery, 2017, 1923–1934. ISBN: 9781450346559. URL: <https://doi.org/10.1145/3025453.3025807>.
- [312] Jess McIntosh, Paul Strohmeier, Jarrod Knibbe, Sebastian Boring, and Kasper Hornbæk. "Magnetips: Combining Fingertip Tracking and Haptic Feedback for Around-Device Interaction." In: *Proceedings of the 2019 CHI Conference on Human Factors in Computing Systems*. New York, NY, USA: Association for Computing Machinery, 2019, 1–12. ISBN: 9781450359702. URL: <https://doi.org/10.1145/3290605.3300638>.

- [313] Yiğit Mengüç, Yong-Lae Park, Hao Pei, Daniel Vogt, Patrick M Aubin, Ethan Winchell, Lowell Fluke, Leia Stirling, Robert J Wood, and Conor J Walsh. "Wearable soft sensing suit for human gait measurement." In: *The International Journal of Robotics Research* 33.14 (2014), pp. 1748–1764.
- [314] Roberto Merletti, L Lo Conte, Elena Avignone, and Piero Guglielminotti. "Modeling of surface myoelectric signals. I. Model implementation." In: *IEEE transactions on biomedical engineering* 46.7 (1999), pp. 810–820.
- [315] Roberto Merletti, Philip A Parker, and Philip J Parker. *Electromyography: physiology, engineering, and non-invasive applications*. Vol. 11. John Wiley & Sons, 2004.
- [316] Christian Metzger, Matt Anderson, and Thad Starner. "Freedigiter: A contact-free device for gesture control." In: *Eighth International Symposium on Wearable Computers*. Vol. 1. IEEE. 2004, pp. 18–21.
- [317] Jan Meyer, Bert Arnrich, Johannes Schumm, and Gerhard Troster. "Design and modeling of a textile pressure sensor for sitting posture classification." In: *IEEE Sensors Journal* 10.8 (2010), pp. 1391–1398.
- [318] Microchip. *MTCH6301 Touch Controller Datasheet*. <http://ww1.microchip.com/downloads/en/DeviceDoc/40001663B.pdf>. Accessed: 2017-12-24.
- [319] Pranav Mistry and Pattie Maes. "SixthSense: A Wearable Gestural Interface." In: *ACM SIGGRAPH ASIA 2009 Sketches*. SIGGRAPH ASIA '09. Yokohama, Japan: Association for Computing Machinery, 2009. ISBN: 9781450379366. DOI: [10.1145/1667146.1667160](https://doi.org/10.1145/1667146.1667160). URL: <https://doi.org/10.1145/1667146.1667160>.
- [320] Pranav Mistry, Pattie Maes, and Liyan Chang. "WUW - Wear Ur World: A Wearable Gestural Interface." In: *CHI '09 Extended Abstracts on Human Factors in Computing Systems*. New York, NY, USA: Association for Computing Machinery, 2009, 4111–4116. ISBN: 9781605582474. URL: <https://doi.org/10.1145/1520340.1520626>.
- [321] David A Mitchell and Peter H Venables. "The relationship of EDA to electrode size." In: *Psychophysiology* 17.4 (1980), pp. 408–412. DOI: [10.1111/j.1469-8986.1980.tb00174.x](https://doi.org/10.1111/j.1469-8986.1980.tb00174.x). URL: <https://doi.org/10.1111/j.1469-8986.1980.tb00174.x>.
- [322] Akihito Miyamoto, Sungwon Lee, Nawalage Florence Cooray, Sunghoon Lee, Mami Mori, Naoji Matsuhisa, Hanbit Jin, Leona Yoda, Tomoyuki Yokota, Akira Itoh, et al. "Inflammation-free, gas-permeable, lightweight, stretchable on-skin electronics with nanomeshes." In: *Nature nanotechnology* 12.9 (2017), pp. 907–913.
- [323] JD Montagu and EM Coles. "Mechanism and measurement of the galvanic skin response." In: *Psychological Bulletin* 65.5 (1966), p. 261.

- [324] Colin W Moore, Jacob Fanous, and Charles L Rice. "Revisiting the functional anatomy of the palmaris longus as a thenar synergist." In: *Clinical Anatomy* 31.6 (2018), pp. 760–770. DOI: [10.1002/ca.23023](https://doi.org/10.1002/ca.23023). URL: <https://doi.org/10.1002/ca.23023>.
- [325] *Move ECG*. <https://www.withings.com/us/en/move-ecg>. Accessed: 2019-09-20.
- [326] Adiyani Mujibiya, Xiang Cao, Desney S. Tan, Dan Morris, Shwetak N. Patel, and Jun Rekimoto. "The Sound of Touch: On-body Touch and Gesture Sensing Based on Transdermal Ultrasound Propagation." In: *Proceedings of the 2013 ACM International Conference on Interactive Tabletops and Surfaces. ITS '13*. St. Andrews, Scotland, United Kingdom: ACM, 2013, pp. 189–198. ISBN: 978-1-4503-2271-3. DOI: [10.1145/2512349.2512821](https://doi.org/10.1145/2512349.2512821). URL: <http://doi.acm.org/10.1145/2512349.2512821>.
- [327] Adiyani Mujibiya and Jun Rekimoto. "Mirage: Exploring Interaction Modalities Using off-Body Static Electric Field Sensing." In: *Proceedings of the 26th Annual ACM Symposium on User Interface Software and Technology. UIST '13*. St. Andrews, Scotland, United Kingdom: Association for Computing Machinery, 2013, 211–220. ISBN: 9781450322683. DOI: [10.1145/2501988.2502031](https://doi.org/10.1145/2501988.2502031). URL: <https://doi.org/10.1145/2501988.2502031>.
- [328] Christian Müller, Shalom Goffri, Dag W Breiby, Jens W Andreasen, Henri D Chanzy, Rene AJ Janssen, Martin M Nielsen, Christopher P Radano, Henning Siringhaus, Paul Smith, et al. "Tough, semiconducting polyethylene-poly (3-hexylthiophene) diblock copolymers." In: *Advanced Functional Materials* 17.15 (2007), pp. 2674–2679.
- [329] *MyoBand EMG Gestures*. <https://support.getmyo.com/hc/en-us>. Accessed: 2019-09-20.
- [330] Anindya Nag, Nasrin Afasrimanesh, Shilun Feng, and Subhas Chandra Mukhopadhyay. "Strain induced graphite/PDMS sensors for biomedical applications." In: *Sensors and Actuators A: Physical* 271 (2018), pp. 257–269.
- [331] Steven Nagels, Raf Ramakers, Kris Luyten, and Wim Deferme. "Silicone Devices: A Scalable DIY Approach for Fabricating Self-Contained Multi-Layered Soft Circuits Using Microfluidics." In: *Proceedings of the 2018 CHI Conference on Human Factors in Computing Systems*. New York, NY, USA: Association for Computing Machinery, 2018, 1–13. ISBN: 9781450356206. URL: <https://doi.org/10.1145/3173574.3173762>.
- [332] Steven Nagels, Raf Ramakers, Kris Luyten, and Wim Deferme. "Silicone Devices: A Scalable DIY Approach for Fabricating Self-Contained Multi-Layered Soft Circuits Using Microfluidics." In: *Proceedings of the 2018 CHI Conference on Human Factors in Computing Systems*. ACM, 2018, p. 188.

- [333] Satoshi Nakamaru, Ryosuke Nakayama, Ryuma Niiyama, and Yasuaki Kakehi. "FoamSense: Design of Three Dimensional Soft Sensors with Porous Materials." In: *Proceedings of the 30th Annual ACM Symposium on User Interface Software and Technology*. UIST '17. Québec City, QC, Canada: Association for Computing Machinery, 2017, 437–447. ISBN: 9781450349819. DOI: [10.1145/3126594.3126666](https://doi.org/10.1145/3126594.3126666). URL: <https://doi.org/10.1145/3126594.3126666>.
- [334] Kei Nakatsuma, Hiroyuki Shinoda, Yasutoshi Makino, Katsunari Sato, and Takashi Maeno. "Touch Interface on Back of the Hand." In: *ACM SIGGRAPH 2011 Posters*. SIGGRAPH '11. Vancouver, British Columbia, Canada: Association for Computing Machinery, 2011. ISBN: 9781450309714. DOI: [10.1145/2037715.2037760](https://doi.org/10.1145/2037715.2037760). URL: <https://doi.org/10.1145/2037715.2037760>.
- [335] Koya Narumi, Fang Qin, Siyuan Liu, Huai-Yu Cheng, Jianzhe Gu, Yoshihiro Kawahara, Mohammad Islam, and Lining Yao. "Self-Healing UI: Mechanically and Electrically Self-Healing Materials for Sensing and Actuation Interfaces." In: *Proceedings of the 32nd Annual ACM Symposium on User Interface Software and Technology*. UIST '19. New Orleans, LA, USA: Association for Computing Machinery, 2019, 293–306. ISBN: 9781450368162. DOI: [10.1145/3332165.3347901](https://doi.org/10.1145/3332165.3347901). URL: <https://doi.org/10.1145/3332165.3347901>.
- [336] Tao Ni and Patrick Baudisch. "Disappearing Mobile Devices." In: *Proceedings of the 22nd Annual ACM Symposium on User Interface Software and Technology*. UIST '09. Victoria, BC, Canada: Association for Computing Machinery, 2009, 101–110. ISBN: 9781605587455. DOI: [10.1145/1622176.1622197](https://doi.org/10.1145/1622176.1622197). URL: <https://doi.org/10.1145/1622176.1622197>.
- [337] Aditya Shekhar Nittala, Andreas Karrenbauer, Arshad Khan, Tobias Kraus, and Jürgen Steimle. "Computational design and optimization of electrophysiological sensors." In: *Nature Communications* 12.1 (2021), pp. 1–14.
- [338] Aditya Shekhar Nittala, Arshad Khan, Klaus Kruttwig, Tobias Kraus, and Jürgen Steimle. "PhysioSkin: Rapid Fabrication of Skin-Conformal Physiological Interfaces." In: *Proceedings of the 2020 CHI Conference on Human Factors in Computing Systems*. New York, NY, USA: Association for Computing Machinery, 2020, 1–10. ISBN: 9781450367080. URL: <https://doi.org/10.1145/3313831.3376366>.
- [339] Aditya Shekhar Nittala, Klaus Kruttwig, Jaeyeon Lee, Roland Bennewitz, Eduard Arzt, and Jürgen Steimle. "Like A Second Skin: Understanding How Epidermal Devices Affect Human Tactile Perception." In: *Proceedings of the SIGCHI Conference on Human Factors in Computing Systems (CHI '19)*. ACM, May 2019. DOI: [10.1145/3290605.3300610](https://doi.org/10.1145/3290605.3300610). URL: <https://doi.org/10.1145/3290605.3300610>.

- [340] Aditya Shekhar Nittala and Jürgen Steimle. “Digital fabrication pipeline for on-body sensors: design goals and challenges.” In: *Proceedings of the 2016 ACM International Joint Conference on Pervasive and Ubiquitous Computing: Adjunct*. ACM. 2016, pp. 950–953.
- [341] Aditya Shekhar Nittala, Anusha Withana, Narjes Pourjafarian, and Jürgen Steimle. “Multi-Touch Skin: A Thin and Flexible Multi-Touch Sensor for On-Skin Input.” In: *Proceedings of the 2018 CHI Conference on Human Factors in Computing Systems*. CHI '18. Montreal QC, Canada: ACM, 2018, 33:1–33:12. ISBN: 978-1-4503-5620-6. DOI: [10.1145/3173574.3173607](https://doi.org/10.1145/3173574.3173607). URL: <http://doi.acm.org/10.1145/3173574.3173607>.
- [342] Ian Oakley, DoYoung Lee, MD. Rasel Islam, and Augusto Esteves. “Beats: Tapping Gestures for Smart Watches.” In: *Proceedings of the 33rd Annual ACM Conference on Human Factors in Computing Systems*. CHI '15. Seoul, Republic of Korea: Association for Computing Machinery, 2015, 1237–1246. ISBN: 9781450331456. DOI: [10.1145/2702123.2702226](https://doi.org/10.1145/2702123.2702226). URL: <https://doi.org/10.1145/2702123.2702226>.
- [343] Masa Ogata and Michita Imai. “SkinWatch: skin gesture interaction for smart watch.” In: *Proceedings of the 6th Augmented Human International Conference*. ACM. 2015, pp. 21–24.
- [344] Masa Ogata, Yuta Sugiura, Yasutoshi Makino, Masahiko Inami, and Michita Imai. “SenSkin: Adapting Skin as a Soft Interface.” In: *Proceedings of the 26th Annual ACM Symposium on User Interface Software and Technology*. UIST '13. St. Andrews, Scotland, United Kingdom: Association for Computing Machinery, 2013, 539–544. ISBN: 9781450322683. DOI: [10.1145/2501988.2502039](https://doi.org/10.1145/2501988.2502039). URL: <https://doi.org/10.1145/2501988.2502039>.
- [345] Uran Oh and Leah Findlater. “Design of and Subjective Response to On-Body Input for People with Visual Impairments.” In: *Proceedings of the 16th International ACM SIGACCESS Conference on Computers and Accessibility*. ASSETS '14. Rochester, New York, USA: Association for Computing Machinery, 2014, 115–122. ISBN: 9781450327206. DOI: [10.1145/2661334.2661376](https://doi.org/10.1145/2661334.2661376). URL: <https://doi.org/10.1145/2661334.2661376>.
- [346] Uran Oh and Leah Findlater. “A Performance Comparison of On-Hand versus On-Phone Nonvisual Input by Blind and Sighted Users.” In: *ACM Trans. Access. Comput.* 7.4 (Nov. 2015). ISSN: 1936-7228. DOI: [10.1145/2820616](https://doi.org/10.1145/2820616). URL: <https://doi.org/10.1145/2820616>.
- [347] Simon Olberding, Michael Wessely, and Jürgen Steimle. “PrintScreen: Fabricating Highly Customizable Thin-film Touch-displays.” In: *Proceedings of the 27th Annual ACM Symposium on User Interface Software and Technology*. UIST '14. Honolulu, Hawaii, USA: ACM, 2014, pp. 281–290. ISBN: 978-1-4503-3069-5. DOI: [10.1145/2642918.2647413](http://doi.acm.org/10.1145/2642918.2647413). URL: <http://doi.acm.org/10.1145/2642918.2647413>.

- [348] Alex Olwal, Jon Moeller, Greg Priest-Dorman, Thad Starner, and Ben Carroll. "I/O Braid: Scalable Touch-Sensitive Lighted Cords Using Spiraling, Repeating Sensing Textiles and Fiber Optics." In: *Proceedings of the 31st Annual ACM Symposium on User Interface Software and Technology*. UIST '18. Berlin, Germany: Association for Computing Machinery, 2018, 485–497. ISBN: 9781450359481. DOI: [10.1145/3242587.3242638](https://doi.org/10.1145/3242587.3242638). URL: <https://doi.org/10.1145/3242587.3242638>.
- [349] Alex Olwal, Thad Starner, and Gowa Mainini. "E-Textile Microinteractions: Augmenting Twist with Flick, Slide and Grasp Gestures for Soft Electronics." In: *Proceedings of the 2020 CHI Conference on Human Factors in Computing Systems*. New York, NY, USA: Association for Computing Machinery, 2020, 1–13. ISBN: 9781450367080. URL: <https://doi.org/10.1145/3313831.3376236>.
- [350] Luke E Osborn, Andrei Dragomir, Joseph L Betthausen, Christopher L Hunt, Harrison H Nguyen, Rahul R Kaliki, and Nitish V Thakor. "Prosthesis with neuromorphic multilayered e-dermis perceives touch and pain." In: *Science Robotics* 3.19 (2018), eaat3818.
- [351] Hiroki Ota, Kevin Chen, Yongjing Lin, Daisuke Kiriya, Hiroshi Shiraki, Zhibin Yu, Tae-Jun Ha, and Ali Javey. "Highly deformable liquid-state heterojunction sensors." In: *Nature communications* 5.1 (2014), pp. 1–9.
- [352] Johannes TB Overvelde, Yiğit Mengüç, Panagiotis Polygerinos, Yunjie Wang, Zheng Wang, Conor J Walsh, Robert J Wood, and Katia Bertoldi. "Mechanical and electrical numerical analysis of soft liquid-embedded deformation sensors analysis." In: *Extreme Mechanics Letters* 1 (2014), pp. 42–46.
- [353] Mary Packard. *Henna Sourcebook: Over 1,000 traditional designs and modern interpretations for body decorating*. Race Point Pub, 2012.
- [354] PS Pandian, K Mohanavelu, KP Safeer, TM Kotresh, DT Shakunthala, Parvati Gopal, and VC Padaki. "Smart Vest: Wearable multi-parameter remote physiological monitoring system." In: *Medical engineering & physics* 30.4 (2008), pp. 466–477.
- [355] Christina Papazian, Nick A Baicoianu, Keshia M Peters, Heather Feldner, and Katherine M Steele. "Electromyography recordings detect muscle activity before observable contractions in acute stroke care." In: *Archives of Rehabilitation Research and Clinical Translation* (2021), p. 100136.
- [356] Farshid Salemi Parizi, Eric Whitmire, and Shwetak Patel. "AuraRing: Precise Electromagnetic Finger Tracking." In: *Proc. ACM Interact. Mob. Wearable Ubiquitous Technol.* 3.4 (Dec. 2019). DOI: [10.1145/3369831](https://doi.org/10.1145/3369831). URL: <https://doi.org/10.1145/3369831>.

- [357] Heun Park, Dong Sik Kim, Soo Yeong Hong, Chulmin Kim, Jun Yeong Yun, Seung Yun Oh, Sang Woo Jin, Yu Ra Jeong, Gyu Tae Kim, and Jeong Sook Ha. "A skin-integrated transparent and stretchable strain sensor with interactive color-changing electrochromic displays." In: *Nanoscale* 9.22 (2017), pp. 7631–7640.
- [358] Steve Park, Hyunjin Kim, Michael Vosgueritchian, Sangmo Cheon, Hyeok Kim, Ja Hoon Koo, Taeho Roy Kim, Sanghyo Lee, Gregory Schwartz, Hyuk Chang, et al. "Stretchable energy-harvesting tactile electronic skin capable of differentiating multiple mechanical stimuli modes." In: *Advanced Materials* 26.43 (2014), pp. 7324–7332.
- [359] Yong-Lae Park, Bor-Rong Chen, and Robert J Wood. "Design and fabrication of soft artificial skin using embedded microchannels and liquid conductors." In: *IEEE Sensors journal* 12.8 (2012), pp. 2711–2718.
- [360] Yong-Lae Park, Carmel Majidi, Rebecca Kramer, Phillippe Bérard, and Robert J Wood. "Hyperelastic pressure sensing with a liquid-embedded elastomer." In: *Journal of micromechanics and microengineering* 20.12 (2010), p. 125029.
- [361] Patrick Parzer, Adwait Sharma, Anita Vogl, Jürgen Steimle, Alex Olwal, and Michael Haller. "SmartSleeve: Real-Time Sensing of Surface and Deformation Gestures on Flexible, Interactive Textiles, Using a Hybrid Gesture Detection Pipeline." In: *Proceedings of the 30th Annual ACM Symposium on User Interface Software and Technology*. UIST '17. Québec City, QC, Canada: Association for Computing Machinery, 2017, 565–577. ISBN: 9781450349819. DOI: [10.1145/3126594.3126652](https://doi.org/10.1145/3126594.3126652). URL: <https://doi.org/10.1145/3126594.3126652>.
- [362] Patrick Parzer et al. "RESi: A Highly Flexible, Pressure-Sensitive, Imperceptible Textile Interface Based on Resistive Yarns." In: *Proceedings of the 31st Annual ACM Symposium on User Interface Software and Technology*. UIST '18. Berlin, Germany: Association for Computing Machinery, 2018, 745–756. ISBN: 9781450359481. DOI: [10.1145/3242587.3242664](https://doi.org/10.1145/3242587.3242664). URL: <https://doi.org/10.1145/3242587.3242664>.
- [363] Shyamal Patel, Hyung Park, Paolo Bonato, Leighton Chan, and Mary Rodgers. "A review of wearable sensors and systems with application in rehabilitation." In: *Journal of neuroengineering and rehabilitation* 9.1 (2012), p. 21.
- [364] Roshan Lalitha Peiris, Yuan-Ling Feng, Liwei Chan, and Kouta Minamizawa. "ThermalBracelet: Exploring Thermal Haptic Feedback Around the Wrist." In: *Proceedings of the 2019 CHI Conference on Human Factors in Computing Systems*. CHI '19. Glasgow, Scotland Uk: Association for Computing Machinery, 2019, 1–11. ISBN: 9781450359702. DOI: [10.1145/3290605.3300400](https://doi.org/10.1145/3290605.3300400). URL: <https://doi.org/10.1145/3290605.3300400>.

- [365] A. Pentland. "Miniature computers built into clothes , shoes and eyeglasses may become the " smartest " new fashion accessories." In: 1999.
- [366] AO Perotto, EF Delagi, J Iazzetti, and D Morrison. "Anatomical Guide for the Electromyographer: The Limbs and Trunk , Charles C." In: *Thomas, Springfield, IL* (1994).
- [367] Simon T Perrault, Eric Lecolinet, James Eagan, and Yves Guiard. "Watchit: simple gestures and eyes-free interaction for wristwatches and bracelets." In: *Proceedings of the SIGCHI Conference on Human Factors in Computing Systems*. ACM. 2013, pp. 1451–1460.
- [368] Angkoon Phinyomark, Chusak Limsakul, and Pornchai Phukpattaranont. "A novel feature extraction for robust EMG pattern recognition." In: *arXiv preprint arXiv:0912.3973* (2009).
- [369] Erin Piateski and Lynette Jones. "Vibrotactile pattern recognition on the arm and torso." In: *Eurohaptics Conference, 2005 and Symposium on Haptic Interfaces for Virtual Environment and Teleoperator Systems, 2005. World Haptics 2005. First Joint*. IEEE. 2005, pp. 90–95.
- [370] Nicola Piva, Francesco Greco, Michele Garbugli, Antonio Iacchetti, Virgilio Mattoli, and Mario Caironi. "Tattoo-Like Transferable Hole Selective Electrodes for Highly Efficient, Solution-Processed Organic Indoor Photovoltaics." In: *Advanced Electronic Materials* 4.10 (2018), p. 1700325.
- [371] Henning Pohl, Justyna Medrek, and Michael Rohs. "ScatterWatch: Subtle Notifications via Indirect Illumination Scattered in the Skin." In: *Proceedings of the 18th International Conference on Human-Computer Interaction with Mobile Devices and Services. MobileHCI '16*. Florence, Italy: Association for Computing Machinery, 2016, 7–16. ISBN: 9781450344081. DOI: [10.1145/2935334.2935351](https://doi.org/10.1145/2935334.2935351). URL: <https://doi.org/10.1145/2935334.2935351>.
- [372] Ivan Poupyrev, Nan-Wei Gong, Shiho Fukuhara, Mustafa Emre Karagozler, Carsten Schwesig, and Karen E Robinson. "Project Jacquard: interactive digital textiles at scale." In: *Proceedings of the 2016 CHI Conference on Human Factors in Computing Systems*. 2016, pp. 4216–4227.
- [373] Narjes Pourjafarian, Marion Koelle, Bruno Fruchard, Sahar Mavali, Konstantin Klamka, Daniel Groeger, Paul Strohmeier, and Jürgen Steimle. "BodyStylus: Freehand On-Body Design and Fabrication of Epidermal Interfaces." In: *Proceedings of the 2021 CHI Conference on Human Factors in Computing Systems*. CHI '21. Yokohama, Japan: Association for Computing Machinery, 2021. ISBN: 9781450380966. DOI: [10.1145/3411764.3445475](https://doi.org/10.1145/3411764.3445475). URL: <https://doi.org/10.1145/3411764.3445475>.
- [374] Mark R Prausnitz and Robert Langer. "Transdermal drug delivery." In: *Nature biotechnology* 26.11 (2008), pp. 1261–1268.

- [375] Halley P. Profita, James Clawson, Scott Gilliland, Clint Zeagler, Thad Starner, Jim Budd, and Ellen Yi-Luen Do. "Don't Mind Me Touching My Wrist: A Case Study of Interacting with on-Body Technology in Public." In: *Proceedings of the 2013 International Symposium on Wearable Computers*. ISWC '13. Zurich, Switzerland: Association for Computing Machinery, 2013, 89–96. ISBN: 9781450321273. DOI: 10.1145/2493988.2494331. URL: <https://doi.org/10.1145/2493988.2494331>.
- [376] Halley P. Profita, Abigale Stangl, Laura Matuszewska, Sigrunn Sky, Raja Kushalnagar, and Shaun K. Kane. "'Wear It Loud': How and Why Hearing Aid and Cochlear Implant Users Customize Their Devices." In: *ACM Trans. Access. Comput.* 11.3 (Sept. 2018). ISSN: 1936-7228. DOI: 10.1145/3214382. URL: <https://doi.org/10.1145/3214382>.
- [377] Halley Profita, Nicholas Farrow, and Nikolaus Correll. "Flutter: An Exploration of an Assistive Garment Using Distributed Sensing, Computation and Actuation." In: *Proceedings of the Ninth International Conference on Tangible, Embedded, and Embodied Interaction*. TEI '15. Stanford, California, USA: Association for Computing Machinery, 2015, 359–362. ISBN: 9781450333054. DOI: 10.1145/2677199.2680586. URL: <https://doi.org/10.1145/2677199.2680586>.
- [378] Jorge-Luis Pérez-Medina, Santiago Villarreal, and Jean Vanderdonckt. "A Gesture Elicitation Study of Nose-Based Gestures." In: *Sensors* 20.24 (2020). ISSN: 1424-8220. DOI: 10.3390/s20247118. URL: <https://www.mdpi.com/1424-8220/20/24/7118>.
- [379] Fang Qin, Huai-Yu Cheng, Rachel Sneeringer, Maria Vlachostergiou, Sampada Acharya, Haolin Liu, Carmel Majidi, Mohammad Islam, and Lining Yao. "ExoForm: Shape Memory and Self-Fusing Semi-Rigid Wearables." In: *Extended Abstracts of the 2021 CHI Conference on Human Factors in Computing Systems*. New York, NY, USA: Association for Computing Machinery, 2021. ISBN: 9781450380959. URL: <https://doi.org/10.1145/3411763.3451818>.
- [380] Jody Ranck. "The wearable computing market: a global analysis." In: *Gigaom Pro* (2012), pp. 1–26.
- [381] Linda Rattfält. *Smartware electrodes for ECG measurements -Design, evaluation and signal processing*. 1546. 2013. ISBN: 9789175195070.
- [382] Linda Rattfält, Fredrik Björefors, David Nilsson, Xin Wang, Petronella Norberg, Per Ask, and Linda Rattfalt@liu Se. *Properties of screen printed electrocardiography smartware electrodes investigated in an electro-chemical cell*. Tech. rep. DOI: 10.1186/1475-925X-12-64. URL: <http://www.biomedical-engineering-online.com/content/12/1/64>.
- [383] AV Rawlings and CR Harding. "Moisturization and skin barrier function." In: *Dermatologic therapy* 17 (2004), pp. 43–48.

- [384] Giacomo Reina, José Miguel González-Domínguez, Alejandro Criado, Ester Vázquez, Alberto Bianco, and Maurizio Prato. "Promises, facts and challenges for graphene in biomedical applications." In: *Chemical Society Reviews* 46.15 (2017), pp. 4400–4416.
- [385] Jun Rekimoto. "Gesturewrist and gesturepad: Unobtrusive wearable interaction devices." In: *Proceedings Fifth International Symposium on Wearable Computers*. IEEE. 2001, pp. 21–27.
- [386] Jun Rekimoto. "SmartSkin: An Infrastructure for Freehand Manipulation on Interactive Surfaces." In: *Proceedings of the SIGCHI Conference on Human Factors in Computing Systems*. CHI '02. Minneapolis, Minnesota, USA: Association for Computing Machinery, 2002, 113–120. ISBN: 1581134533. DOI: [10.1145/503376.503397](https://doi.org/10.1145/503376.503397). URL: <https://doi.org/10.1145/503376.503397>.
- [387] Tian-Ling Ren, He Tian, Dan Xie, and Yi Yang. "Flexible graphite-on-paper piezoresistive sensors." In: *Sensors* 12.5 (2012), pp. 6685–6694.
- [388] Christian Rendl, Patrick Greindl, Michael Haller, Martin Zirkl, Barbara Stadlober, and Paul Hartmann. "PyzoFlex: Printed Piezoelectric Pressure Sensing Foil." In: *Proceedings of the 25th Annual ACM Symposium on User Interface Software and Technology*. UIST '12. Cambridge, Massachusetts, USA: Association for Computing Machinery, 2012, 509–518. ISBN: 9781450315807. DOI: [10.1145/2380116.2380180](https://doi.org/10.1145/2380116.2380180). URL: <https://doi.org/10.1145/2380116.2380180>.
- [389] Bersain A Reyes, Hugo F Posada-Quintero, Justin R Bales, Amanda L Clement, George D Pins, Albert Swiston, Jarno Riistama, John P Florian, Barbara Shykoff, Michael Qin, et al. "Novel electrodes for underwater ECG monitoring." In: *IEEE Transactions on Biomedical Engineering* 61.6 (2014), pp. 1863–1876.
- [390] You Seung Rim, Sang-Hoon Bae, Huajun Chen, Nicholas De Marco, and Yang Yang. "Recent progress in materials and devices toward printable and flexible sensors." In: *Advanced Materials* 28.22 (2016), pp. 4415–4440.
- [391] Bruna Goveia da Rocha, Oscar Tomico, Panos Markopoulos, and Daniel Tetteroo. "Crafting Research Products through Digital Machine Embroidery." In: *Proceedings of the 2020 ACM Designing Interactive Systems Conference*. New York, NY, USA: Association for Computing Machinery, 2020, 341–350. ISBN: 9781450369749. URL: <https://doi.org/10.1145/3357236.3395443>.
- [392] K Roeleveld, DF Stegeman, HM Vingerhoets, and A van Oosterom. "Motor unit potential contribution to surface electromyography." In: *Acta physiologica scandinavica* 160.2 (1997), pp. 175–183. DOI: [10.1046/j.1365-201X.1997.00152..](https://doi.org/10.1046/j.1365-201X.1997.00152..) URL: <https://doi.org/10.1046/j.1365-201X.1997.00152..>
- [393] John Rogers, George Malliaras, and Takao Someya. "Biomedical devices go wild." In: *Science Advances* 4.9 (2018).

- [394] Simon Rogers, John Williamson, Craig Stewart, and Roderick Murray-Smith. "AnglePose: Robust, Precise Capacitive Touch Tracking via 3d Orientation Estimation." In: *Proceedings of the SIGCHI Conference on Human Factors in Computing Systems*. CHI '11. Vancouver, BC, Canada: Association for Computing Machinery, 2011, 2575–2584. ISBN: 9781450302289. DOI: [10.1145/1978942.1979318](https://doi.org/10.1145/1978942.1979318). URL: <https://doi.org/10.1145/1978942.1979318>.
- [395] Yvonne Rogers, Paul Dourish, Patrick Olivier, Margot Brereton, and Jodi Forlizzi. "The Dark Side of Interaction Design." In: *Extended Abstracts of the 2020 CHI Conference on Human Factors in Computing Systems*. CHI EA '20. Honolulu, HI, USA: Association for Computing Machinery, 2020, 1–4. ISBN: 9781450368193. DOI: [10.1145/3334480.3381070](https://doi.org/10.1145/3334480.3381070). URL: <https://doi.org/10.1145/3334480.3381070>.
- [396] Daniel P Rose, Michael E Ratterman, Daniel K Griffin, Linlin Hou, Nancy Kelley-Loughnane, Rajesh R Naik, Joshua A Hagen, Ian Papautsky, and Jason C Heikenfeld. "Adhesive RFID sensor patch for monitoring of sweat electrolytes." In: *IEEE Transactions on Biomedical Engineering* 62.6 (2014), pp. 1457–1465.
- [397] Anne Roudaut, Stéphane Huot, and Eric Lecolinet. "TapTap and MagStick: Improving One-Handed Target Acquisition on Small Touch-Screens." In: *Proceedings of the Working Conference on Advanced Visual Interfaces*. AVI '08. Napoli, Italy: Association for Computing Machinery, 2008, 146–153. ISBN: 9781605581415. DOI: [10.1145/1385569.1385594](https://doi.org/10.1145/1385569.1385594). URL: <https://doi.org/10.1145/1385569.1385594>.
- [398] Thijs Roumen, Simon T. Perrault, and Shengdong Zhao. "NotiRing: A Comparative Study of Notification Channels for Wearable Interactive Rings." In: *Proceedings of the 33rd Annual ACM Conference on Human Factors in Computing Systems*. CHI '15. Seoul, Republic of Korea: Association for Computing Machinery, 2015, 2497–2500. ISBN: 9781450331456. DOI: [10.1145/2702123.2702350](https://doi.org/10.1145/2702123.2702350). URL: <https://doi.org/10.1145/2702123.2702350>.
- [399] Serge H Roy, Gianluca De Luca, M Samuel Cheng, A Johansson, L Donald Gilmore, and Carlo J De Luca. "Electro-mechanical stability of surface EMG sensors." In: *Medical & biological engineering & computing* 45.5 (2007), pp. 447–457. DOI: [10.1007/s11517-007-0168-z](https://doi.org/10.1007/s11517-007-0168-z). URL: <https://doi.org/10.1007/s11517-007-0168-z>.
- [400] Deepak Ranjan Sahoo, Timothy Neate, Yutaka Tokuda, Jennifer Pearson, Simon Robinson, Sriram Subramanian, and Matt Jones. "Tangible Drops: A Visio-Tactile Display Using Actuated Liquid-Metal Droplets." In: *Proceedings of the 2018 CHI Conference on Human Factors in Computing Systems*. New York, NY, USA: Association for Computing Machinery, 2018, 1–14. ISBN: 9781450356206. URL: <https://doi.org/10.1145/3173574.3173751>.

- [401] Kenji Saitou, Tadashi Masuda, Daisaku Michikami, Ryuhei Kojima, and Morihiko Okada. "Innervation zones of the upper and lower limb muscles estimated by using multichannel surface EMG." In: *Journal of human ergology* 29.1-2 (2000), pp. 35–52.
- [402] Shigeru Sakurazawa, Naofumi Yoshida, and Nagisa Munekata. "Entertainment Feature of a Game Using Skin Conductance Response." In: *Proceedings of the 2004 ACM SIGCHI International Conference on Advances in Computer Entertainment Technology*. ACE '04. Singapore: ACM, 2004, pp. 181–186. ISBN: 1-58113-882-2. DOI: [10.1145/1067343.1067365](https://doi.org/10.1145/1067343.1067365). URL: <http://doi.acm.org/10.1145/1067343.1067365>.
- [403] T. Scott Saponas, Chris Harrison, and Hrvoje Benko. "PocketTouch: Through-Fabric Capacitive Touch Input." In: *Proceedings of the 24th Annual ACM Symposium on User Interface Software and Technology*. UIST '11. Santa Barbara, California, USA: Association for Computing Machinery, 2011, 303–308. ISBN: 9781450307161. DOI: [10.1145/2047196.2047235](https://doi.org/10.1145/2047196.2047235). URL: <https://doi.org/10.1145/2047196.2047235>.
- [404] T Scott Saponas, Desney S Tan, Dan Morris, Ravin Balakrishnan, Jim Turner, and James A Landay. "Enabling always-available input with muscle-computer interfaces." In: *Proceedings of the 22nd annual ACM symposium on User Interface Software and Technology*. ACM. 2009, pp. 167–176.
- [405] T. Scott Saponas, Desney S. Tan, Dan Morris, Jim Turner, and James A. Landay. "Making Muscle-Computer Interfaces More Practical." In: *Proceedings of the SIGCHI Conference on Human Factors in Computing Systems*. CHI '10. Atlanta, Georgia, USA: Association for Computing Machinery, 2010, 851–854. ISBN: 9781605589299. DOI: [10.1145/1753326.1753451](https://doi.org/10.1145/1753326.1753451). URL: <https://doi.org/10.1145/1753326.1753451>.
- [406] Stefan Schneegass and Alexandra Voit. "GestureSleeve: Using Touch Sensitive Fabrics for Gestural Input on the Forearm for Controlling Smartwatches." In: *Proceedings of the 2016 ACM International Symposium on Wearable Computers*. ISWC '16. Heidelberg, Germany: Association for Computing Machinery, 2016, 108–115. ISBN: 9781450344609. DOI: [10.1145/2971763.2971797](https://doi.org/10.1145/2971763.2971797). URL: <https://doi.org/10.1145/2971763.2971797>.
- [407] Karsten Seipp and Kate Devlin. "One-Touch Pose Detection on Touchscreen Smartphones." In: *Proceedings of the 2015 International Conference on Interactive Tabletops and Surfaces*. ITS '15. Madeira, Portugal: Association for Computing Machinery, 2015, 51–54. ISBN: 9781450338998. DOI: [10.1145/2817721.2817739](https://doi.org/10.1145/2817721.2817739). URL: <https://doi.org/10.1145/2817721.2817739>.
- [408] Tsuyoshi Sekitani, Martin Kaltenbrunner, Tomoyuki Yokota, and Takao Someya. "Imperceptible Electronic Skin." In: *Information Display* 30.1 (2014), pp. 20–25. DOI: <https://doi.org/10.1002/j.2637-496X.2014.tb00680.x>. eprint: <https://sid.onlinelibrary.wiley.com/doi/pdf/10.1002/j>.

- 2637-496X.2014.tb00680.x. URL: <https://sid.onlinelibrary.wiley.com/doi/abs/10.1002/j.2637-496X.2014.tb00680.x>.
- [409] Marcos Serrano, Barrett Ens, Xing-Dong Yang, and Pourang Irani. "Desktop-Gluey: Augmenting Desktop Environments with Wearable Devices." In: *Proceedings of the 17th International Conference on Human-Computer Interaction with Mobile Devices and Services Adjunct*. MobileHCI '15. Copenhagen, Denmark: Association for Computing Machinery, 2015, 1175-1178. ISBN: 9781450336536. DOI: 10.1145/2786567.2794348. URL: <https://doi.org/10.1145/2786567.2794348>.
- [410] Fereshteh Shahmiri, Chaoyu Chen, Anandghan Waghmare, Dingtian Zhang, Shivan Mittal, Steven L. Zhang, Yi-Cheng Wang, Zhong Lin Wang, Thad E. Starner, and Gregory D. Abowd. "Serpentine: A Self-Powered Reversibly Deformable Cord Sensor for Human Input." In: *Proceedings of the 2019 CHI Conference on Human Factors in Computing Systems*. New York, NY, USA: Association for Computing Machinery, 2019, 1-14. ISBN: 9781450359702. URL: <https://doi.org/10.1145/3290605.3300775>.
- [411] Adwait Sharma, Joan Sol Roo, and Jürgen Steimle. "Grasping Microgestures: Eliciting Single-Hand Microgestures for Handheld Objects." In: *Proceedings of the 2019 CHI Conference on Human Factors in Computing Systems*. New York, NY, USA: Association for Computing Machinery, 2019, 1-13. ISBN: 9781450359702. URL: <https://doi.org/10.1145/3290605.3300632>.
- [412] Yuxiang Shi, Fan Wang, Jingwen Tian, Shuyao Li, Engang Fu, Jinhui Nie, Rui Lei, Yafei Ding, Xiangyu Chen, and Zhong Lin Wang. "Self-powered electro-tactile system for virtual tactile experiences." In: *Science Advances* 7.6 (2021), eabe2943.
- [413] Olimex EKG-EMG Shield. *Open Source EMG-ECG Shields*. Last Accessed: 2020-01-08. 2020. URL: <https://www.olimex.com/Products/Duino/Shields/SHIELD-EKG-EMG/open-source-hardware>.
- [414] Roy Shilkrot, Jochen Huber, Wong Meng Ee, Pattie Maes, and Suranga Chandima Nanayakkara. "FingerReader: A Wearable Device to Explore Printed Text on the Go." In: *Proceedings of the 33rd Annual ACM Conference on Human Factors in Computing Systems*. New York, NY, USA: Association for Computing Machinery, 2015, 2363-2372. ISBN: 9781450331456. URL: <https://doi.org/10.1145/2702123.2702421>.
- [415] Roy Shilkrot, Jochen Huber, Jürgen Steimle, Suranga Nanayakkara, and Pattie Maes. "Digital Digits: A Comprehensive Survey of Finger Augmentation Devices." In: *ACM Comput. Surv.* 48.2 (Nov. 2015). ISSN: 0360-0300. DOI: 10.1145/2828993. URL: <https://doi.org/10.1145/2828993>.

- [416] Youngbo Aram Shim, Jaeyeon Lee, and Geehyuk Lee. "Exploring Multimodal Watch-Back Tactile Display Using Wind and Vibration." In: *Proceedings of the 2018 CHI Conference on Human Factors in Computing Systems*. CHI '18. Montreal QC, Canada: Association for Computing Machinery, 2018, 1–12. ISBN: 9781450356206. DOI: [10.1145/3173574.3173706](https://doi.org/10.1145/3173574.3173706). URL: <https://doi.org/10.1145/3173574.3173706>.
- [417] Gurashish Singh, Alexander Nelson, Ryan Robucci, Chintan Patel, and Nilanjan Banerjee. "Inviz: Low-power personalized gesture recognition using wearable textile capacitive sensor arrays." In: *Pervasive Computing and Communications (PerCom), 2015 IEEE International Conference on*. IEEE, 2015, pp. 198–206.
- [418] Joshua Smith, Tom White, Christopher Dodge, Joseph Paradiso, Neil Gershenfeld, and David Allport. "Electric field sensing for graphical interfaces." In: *IEEE Computer Graphics and Applications* 18.3 (1998), pp. 54–60.
- [419] Mohamed Soliman, Franziska Mueller, Lena Hegemann, Joan Sol Roo, Christian Theobalt, and Jürgen Steimle. "FingerInput: Capturing Expressive Single-Hand Thumb-to-Finger Microgestures." In: *Proceedings of the 2018 ACM International Conference on Interactive Surfaces and Spaces*. ISS '18. Tokyo, Japan: Association for Computing Machinery, 2018, 177–187. ISBN: 9781450356947. DOI: [10.1145/3279778.3279799](https://doi.org/10.1145/3279778.3279799). URL: <https://doi.org/10.1145/3279778.3279799>.
- [420] Donghee Son, Ja Hoon Koo, Jun-Kyul Song, Jaemin Kim, Mincheol Lee, Hyung Joon Shim, Minjoon Park, Minbaek Lee, Ji Hoon Kim, and Dae-Hyeong Kim. "Stretchable carbon nanotube charge-trap floating-gate memory and logic devices for wearable electronics." In: *ACS nano* 9.5 (2015), pp. 5585–5593.
- [421] Jie Song, Fabrizio Pece, Gábor Sörös, Marion Koelle, and Otmar Hilliges. "Joint Estimation of 3D Hand Position and Gestures from Monocular Video for Mobile Interaction." In: *Proceedings of the 33rd Annual ACM Conference on Human Factors in Computing Systems*. CHI '15. Seoul, Republic of Korea: Association for Computing Machinery, 2015, 3657–3660. ISBN: 9781450331456. DOI: [10.1145/2702123.2702601](https://doi.org/10.1145/2702123.2702601). URL: <https://doi.org/10.1145/2702123.2702601>.
- [422] Jie Song, Gábor Sörös, Fabrizio Pece, Sean Ryan Fanello, Shahram Izadi, Cem Keskin, and Otmar Hilliges. "In-Air Gestures around Unmodified Mobile Devices." In: *Proceedings of the 27th Annual ACM Symposium on User Interface Software and Technology*. UIST '14. Honolulu, Hawaii, USA: Association for Computing Machinery, 2014, 319–329. ISBN: 9781450330695. DOI: [10.1145/2642918.2647373](https://doi.org/10.1145/2642918.2647373). URL: <https://doi.org/10.1145/2642918.2647373>.

- [423] Fernando Soto, Rupesh K Mishra, Robert Chrostowski, Aida Martin, and Joseph Wang. "Epidermal Tattoo Patch for Ultrasound-Based Transdermal Microballistic Delivery." In: *Advanced Materials Technologies* 2.12 (2017), p. 1700210.
- [424] Sparkfun. *SparkFun Single Lead Heart Rate Monitor*. <https://learn.sparkfun.com/tutorials/ad8232-heart-rate-monitor-hookup-guide/all>. Last Accessed: 2020-01-08. 2020.
- [425] Srinath Sridhar, Anders Markussen, Antti Oulasvirta, Christian Theobalt, and Sebastian Boring. "WatchSense: On- and Above-Skin Input Sensing through a Wearable Depth Sensor." In: *Proceedings of the 2017 CHI Conference on Human Factors in Computing Systems*. New York, NY, USA: Association for Computing Machinery, 2017, 3891–3902. ISBN: 9781450346559. URL: <https://doi.org/10.1145/3025453.3026005>.
- [426] Susan Standring. *Gray's anatomy e-book: the anatomical basis of clinical practice*. Elsevier Health Sciences, 2020.
- [427] NE Stankova, PA Atanasov, Ru G Nikov, RG Nikov, NN Nedyalkov, TR Stoyanchoy, N Fukata, KN Kolev, EI Valova, JS Georgieva, et al. "Optical properties of polydimethylsiloxane (PDMS) during nanosecond laser processing." In: *Applied Surface Science* 374 (2016), pp. 96–103.
- [428] Thad Starner, Jake Auxier, Daniel Ashbrook, and Maribeth Gandy. "The gesture pendant: A self-illuminating, wearable, infrared computer vision system for home automation control and medical monitoring." In: *Digest of Papers. Fourth International Symposium on Wearable Computers*. IEEE. 2000, pp. 87–94.
- [429] Paul Strohmeier, Jarrod Knibbe, Sebastian Boring, and Kasper Hornbæk. "ZPatch: Hybrid Resistive/Capacitive ETextile Input." In: *Proceedings of the Twelfth International Conference on Tangible, Embedded, and Embodied Interaction*. TEI '18. Stockholm, Sweden: Association for Computing Machinery, 2018, 188–198. ISBN: 9781450355681. DOI: [10.1145/3173225.3173242](https://doi.org/10.1145/3173225.3173242). URL: <https://doi.org/10.1145/3173225.3173242>.
- [430] Paul Strohmeier and Jess McIntosh. "Novel Input and Output Opportunities Using an Implanted Magnet." In: *Proceedings of the Augmented Humans International Conference*. AHs '20. Kaiserslautern, Germany: Association for Computing Machinery, 2020. ISBN: 9781450376037. DOI: [10.1145/3384657.3384785](https://doi.org/10.1145/3384657.3384785). URL: <https://doi.org/10.1145/3384657.3384785>.
- [431] Paul Strohmeier, Narjes Pourjafarian, Marion Koelle, Cedric Honnet, Bruno Fruchard, and Jürgen Steimle. "Sketching On-Body Interactions Using Piezo-Resistive Kinesiology Tape." In: *Proceedings of the Augmented Humans International Conference*. AHs '20. Kaiserslautern, Germany: Association for Computing Machinery, 2020. ISBN: 9781450376037. DOI: [10.1145/3384657.3384774](https://doi.org/10.1145/3384657.3384774). URL: <https://doi.org/10.1145/3384657.3384774>.

- [432] J Ridley Stroop. "Studies of interference in serial verbal reactions." In: *Journal of Experimental Psychology: General* 121.1 (1992), p. 15.
- [433] Seeed Studio. *Groove EMG Detector*. http://wiki.seeedstudio.com/Grove-EMG_Detector/. Last Accessed: 2020-01-08. 2020.
- [434] Seeed Studio. *Groove GSR Sensor*. http://wiki.seeedstudio.com/Grove-GSR_Sensor/. Last Accessed: 2020-01-08. 2020.
- [435] David J Sturman and David Zeltzer. "A survey of glove-based input." In: *IEEE Computer graphics and Applications* 14.1 (1994), pp. 30–39.
- [436] Chao-Huai Su, Liwei Chan, Chien-Ting Weng, Rong-Hao Liang, Kai-Yin Cheng, and Bing-Yu Chen. "NailDisplay: Bringing an Always Available Visual Display to Fingertips." In: *Proceedings of the SIGCHI Conference on Human Factors in Computing Systems*. CHI '13. Paris, France: Association for Computing Machinery, 2013, 1461–1464. ISBN: 9781450318990. DOI: 10.1145/2470654.2466193. URL: <https://doi.org/10.1145/2470654.2466193>.
- [437] Yuta Sugiura, Fumihiko Nakamura, Wataru Kawai, Takashi Kikuchi, and Maki Sugimoto. "Behind the palm: Hand gesture recognition through measuring skin deformation on back of hand by using optical sensors." In: *2017 56th Annual Conference of the Society of Instrument and Control Engineers of Japan (SICE)*. 2017, pp. 1082–1087. DOI: 10.23919/SICE.2017.8105457.
- [438] Mimi Sun, Yanan Gu, Xinyi Pei, Jingjuan Wang, Jian Liu, Chongbo Ma, Jing Bai, and Ming Zhou. "A flexible and wearable epidermal ethanol biofuel cell for on-body and real-time bioenergy harvesting from human sweat." In: *Nano Energy* 86 (2021), p. 106061.
- [439] Ruoqia Sun, Ryosuke Onose, Margaret Dunne, Andrea Ling, Amanda Denham, and Hsin-Liu (Cindy) Kao. "Weaving a Second Skin: Exploring Opportunities for Crafting On-Skin Interfaces Through Weaving." In: *Proceedings of the 2020 ACM Designing Interactive Systems Conference*. New York, NY, USA: Association for Computing Machinery, 2020, 365–377. ISBN: 9781450369749. URL: <https://doi.org/10.1145/3357236.3395548>.
- [440] Subramanian Sundaram, Melina Skouras, David S Kim, Louise van den Heuvel, and Wojciech Matusik. "Topology optimization and 3D printing of multimaterial magnetic actuators and displays." In: *Science advances* 5.7 (2019), eaaw1160.
- [441] Kenji Suzuki, Taku Hachisu, and Kazuki Iida. "EnhancedTouch: A Smart Bracelet for Enhancing Human-Human Physical Touch." In: *Proceedings of the 2016 CHI Conference on Human Factors in Computing Systems*. New York, NY, USA: Association for Computing Machinery, 2016, 1282–1293. ISBN: 9781450333627. URL: <https://doi.org/10.1145/2858036.2858439>.

- [442] Miroslav Svetlak, Petr Bob, Michal Cernik, and Miloslav Kukleta. "Electrodermal complexity during the Stroop colour word test." In: *Autonomic Neuroscience* 152.1-2 (2010), pp. 101–107.
- [443] Miroslav Svetlak, Petr Bob, Michal Cernik, and Miloslav Kukleta. "Electrodermal complexity during the Stroop colour word test." In: *Autonomic Neuroscience* 152.1-2 (2010), pp. 101–107. DOI: [10.1016/j.autneu.2009.10.003](https://doi.org/10.1016/j.autneu.2009.10.003).
- [444] Paul Sweetman. "Anchoring the (postmodern) self? Body modification, fashion and identity." In: *Body & society* 5.2-3 (1999), pp. 51–76.
- [445] W H Talbot, I Darian-Smith, H H Kornhuber, and V B Mountcastle. "The sense of flutter-vibration: comparison of the human capacity with response patterns of mechanoreceptive afferents from the monkey hand." In: *Journal of Neurophysiology* 31.2 (1968). PMID: 4972033, pp. 301–334. DOI: [10.1152/jn.1968.31.2.301](https://doi.org/10.1152/jn.1968.31.2.301). eprint: <https://doi.org/10.1152/jn.1968.31.2.301>. URL: <https://doi.org/10.1152/jn.1968.31.2.301>.
- [446] Emi Tamaki, Takashi Miyak, and Jun Rekimoto. "BrainyHand: A Wearable Computing Device without HMD and It's Interaction Techniques." In: *Proceedings of the International Conference on Advanced Visual Interfaces*. AVI '10. Roma, Italy: Association for Computing Machinery, 2010, 387–388. ISBN: 9781450300766. DOI: [10.1145/1842993.1843070](https://doi.org/10.1145/1842993.1843070). URL: <https://doi.org/10.1145/1842993.1843070>.
- [447] Matthew Wei Ming Tan, Gurunathan Thangavel, and Pooi See Lee. "Enhancing dynamic actuation performance of dielectric elastomer actuators by tuning viscoelastic effects with polar crosslinking." In: *NPG Asia Materials* 11.1 (2019), pp. 1–10.
- [448] Weijun Tao, Tao Liu, Rencheng Zheng, and Hutian Feng. "Gait analysis using wearable sensors." In: *Sensors* 12.2 (2012), pp. 2255–2283.
- [449] Mahmoud Tavakoli, Mohammad H. Malakooti, Hugo Paisana, Yunsik Ohm, Daniel Green Marques, Pedro Alhais Lopes, Ana P. Piedade, Anibal T. de Almeida, and Carmel Majidi. "EGaIn-Assisted Room-Temperature Sintering of Silver Nanoparticles for Stretchable, Inkjet-Printed, Thin-Film Electronics." In: *Advanced Materials* (2018), p. 1801852. ISSN: 09359648. DOI: [10.1002/adma.201801852](https://doi.org/10.1002/adma.201801852). URL: <http://doi.wiley.com/10.1002/adma.201801852>.
- [450] Mahmoud Tavakoli, Mohammad H Malakooti, Hugo Paisana, Yunsik Ohm, Daniel Green Marques, Pedro Alhais Lopes, Ana P Piedade, Anibal T de Almeida, and Carmel Majidi. "Fabrication of Soft and Stretchable Electronics Through Integration of Printed Silver Nanoparticles and Liquid Metal Alloy." In: *Smart Materials, Adaptive Structures and Intelligent Systems*. Vol. 51951. American Society of Mechanical Engineers. 2018, V002To8A006.

- [451] MM Taylor and Susan J Lederman. "Tactile roughness of grooved surfaces: A model and the effect of friction." In: *Perception & Psychophysics* 17.1 (1975), pp. 23–36.
- [452] Nigel AS Taylor and Christiano A Machado-Moreira. "Regional variations in transepidermal water loss, eccrine sweat gland density, sweat secretion rates and electrolyte composition in resting and exercising humans." In: *Extreme physiology & medicine* 2.1 (2013), p. 4. DOI: [10.1186/2046-7648-2-4](https://doi.org/10.1186/2046-7648-2-4).
- [453] Marc Teyssier, Brice Parilyusan, Anne Roudaut, and Jürgen Steimle. "Human-like artificial skin sensor for physical human-robot interaction." In: *2021 IEEE International Conference on Robotics and Automation (ICRA)*. IEEE. 2021.
- [454] Shilpa K Thanawala and Manoj K Chaudhury. "Surface modification of silicone elastomer using perfluorinated ether." In: *Langmuir* 16.3 (2000), pp. 1256–1260.
- [455] Xavier Thomas. "Silicone adhesives in healthcare applications." In: *Dow Corning Healthcare Industry* (2003), pp. 1–6.
- [456] Edward O Thorp. "The invention of the first wearable computer." In: *Digest of Papers. Second international symposium on wearable computers (Cat. No. 98EX215)*. IEEE. 1998, pp. 4–8.
- [457] Yutaka Tokuda, Jose Luis Berna Moya, Gianluca Memoli, Timothy Neate, Deepak Ranjan Sahoo, Simon Robinson, Jennifer Pearson, Matt Jones, and Sriram Subramanian. "Programmable Liquid Matter: 2D Shape Deformation of Highly Conductive Liquid Metals in a Dynamic Electric Field." In: *Proceedings of the 2017 ACM International Conference on Interactive Surfaces and Spaces. ISS '17*. Brighton, United Kingdom: Association for Computing Machinery, 2017, 142–150. ISBN: 9781450346917. DOI: [10.1145/3132272.3134132](https://doi.org/10.1145/3132272.3134132). URL: <https://doi.org/10.1145/3132272.3134132>.
- [458] Yutaka Tokuda, Deepak Ranjan Sahoo, Matt Jones, Sriram Subramanian, and Anusha Withana. "Flowcuits: Crafting Tangible and Interactive Electrical Components with Liquid Metal Circuits." In: *Proceedings of the Fifteenth International Conference on Tangible, Embedded, and Embodied Interaction. TEI '21*. Salzburg, Austria: Association for Computing Machinery, 2021. ISBN: 9781450382137. DOI: [10.1145/3430524.3440654](https://doi.org/10.1145/3430524.3440654). URL: <https://doi.org/10.1145/3430524.3440654>.
- [459] Aaron Toney, Barrie Mulley, Bruce H Thomas, and Wayne Piekarski. "Social weight: designing to minimise the social consequences arising from technology use by the mobile professional." In: *Personal and Ubiquitous Computing* 7.5 (2003), pp. 309–320.

- [460] Jonathan Tong, Oliver Mao, and Daniel Goldreich. "Two-Point Orientation Discrimination Versus the Traditional Two-Point Test for Tactile Spatial Acuity Assessment." In: *Frontiers in Human Neuroscience* 7 (2013), p. 579. ISSN: 1662-5161. DOI: [10.3389/fnhum.2013.00579](https://doi.org/10.3389/fnhum.2013.00579). URL: <http://journal.frontiersin.org/article/10.3389/fnhum.2013.00579/abstract>.
- [461] Sergio Fuentes del Toro, Yuyang Wei, Ester Olmeda, Lei Ren, Wei Guowu, and Vicente Díaz. "Validation of a low-cost electromyography (EMG) system via a commercial and accurate EMG device: Pilot study." In: *Sensors* 19.23 (2019), p. 5214. DOI: [10.3390/s19235214](https://doi.org/10.3390/s19235214).
- [462] Rebeca M Torrente-Rodríguez, Heather Lukas, Jiaobing Tu, Jihong Min, Yiran Yang, Changhao Xu, Harry B Rossiter, and Wei Gao. "SARS-CoV-2 RapidPlex: a graphene-based multiplexed telemedicine platform for rapid and low-cost COVID-19 diagnosis and monitoring." In: *Matter* 3.6 (2020), pp. 1981–1998.
- [463] Van-Thai Tran, Yuefan Wei, Hongyi Yang, Zhaoyao Zhan, and Hejun Du. "All-inkjet-printed flexible ZnO micro photodetector for a wearable UV monitoring device." In: *Nanotechnology* 28.9 (2017), p. 095204.
- [464] Tran Quang Trung, Le Thai Duy, Subramanian Ramasundaram, and Nae-Eung Lee. "Transparent, stretchable, and rapid-response humidity sensor for body-attachable wearable electronics." In: *Nano Research* 10.6 (2017), pp. 2021–2033.
- [465] Tran Quang Trung, Subramaniyan Ramasundaram, Byeong-Ung Hwang, and Nae-Eung Lee. "An all-elastomeric transparent and stretchable temperature sensor for body-attachable wearable electronics." In: *Advanced materials* 28.3 (2016), pp. 502–509.
- [466] Samuli Tuominen and Matti Mantysalo. "Screen printed temporary tattoos for skin-mounted electronics." In: *2019 IEEE 69th Electronic Components and Technology Conference (ECTC)*. IEEE. 2019, pp. 1252–1257.
- [467] Gaetano Valenza, Antonio Lanatà, Enzo Pasquale Scilingo, and Danilo De Rossi. "Towards a smart glove: Arousal recognition based on textile electrodermal response." In: *2010 Annual International Conference of the IEEE Engineering in Medicine and Biology*. IEEE. 2010, pp. 3598–3601.
- [468] Peter JM Van Laarhoven and Emile HL Aarts. "Simulated annealing." In: *Simulated annealing: Theory and applications*. Springer, 1987, pp. 7–15.
- [469] Jean Vanderdonckt, Nathan Magrofuoco, Suzanne Kieffer, Jorge Pérez, Ysabelle Rase, Paolo Roselli, and Santiago Villarreal. "Head and shoulders gestures: Exploring user-defined gestures with upper body." In: *International Conference on Human-Computer Interaction*. Springer. 2019, pp. 192–213.

- [470] Eldy S. Lazaro Vasquez and Katia Vega. "Myco-Accessories: Sustainable Wearables with Biodegradable Materials." In: *Proceedings of the 23rd International Symposium on Wearable Computers*. ISWC '19. London, United Kingdom: Association for Computing Machinery, 2019, 306–311. ISBN: 9781450368704. DOI: [10.1145/3341163.3346938](https://doi.org/10.1145/3341163.3346938). URL: <https://doi.org/10.1145/3341163.3346938>.
- [471] Thamarai Selvan Vasu and Tanmay K Bhandakkar. "Semi-analytical solution to plane strain loading of elastic layered coating on an elastic substrate." In: *Sadhana* 40.7 (2015), pp. 2221–2238.
- [472] Katia Fabiola Canepa Vega and Hugo Fuks. "Empowering electronic divas through beauty technology." In: *International Conference of Design, User Experience, and Usability*. Springer. 2013, pp. 237–245.
- [473] Katia Vega, Marcio Cunha, and Hugo Fuks. "Hairware: The Conscious Use of Unconscious Auto-Contact Behaviors." In: *Proceedings of the 20th International Conference on Intelligent User Interfaces*. IUI '15. Atlanta, Georgia, USA: Association for Computing Machinery, 2015, 78–86. ISBN: 9781450333061. DOI: [10.1145/2678025.2701404](https://doi.org/10.1145/2678025.2701404). URL: <https://doi.org/10.1145/2678025.2701404>.
- [474] Dong-Bach Vo, Eric Lecolinet, and Yves Guiard. "Belly Gestures: Body Centric Gestures on the Abdomen." In: *Proceedings of the 8th Nordic Conference on Human-Computer Interaction: Fun, Fast, Foundational*. NordiCHI '14. Helsinki, Finland: Association for Computing Machinery, 2014, 687–696. ISBN: 9781450325424. DOI: [10.1145/2639189.2639210](https://doi.org/10.1145/2639189.2639210). URL: <https://doi.org/10.1145/2639189.2639210>.
- [475] Anita Vogl, Patrick Parzer, Teo Babic, Joanne Leong, Alex Olwal, and Michael Haller. "StretchEBand: Enabling Fabric-Based Interactions through Rapid Fabrication of Textile Stretch Sensors." In: *Proceedings of the 2017 CHI Conference on Human Factors in Computing Systems*. CHI '17. Denver, Colorado, USA: Association for Computing Machinery, 2017, 2617–2627. ISBN: 9781450346559. DOI: [10.1145/3025453.3025938](https://doi.org/10.1145/3025453.3025938). URL: <https://doi.org/10.1145/3025453.3025938>.
- [476] Julie Wagner, Mathieu Nancel, Sean Gustafson, Stéphane Huot, and Wendy E Mackay. *A Body-centric Design Space for Multi-surface Interaction*. Tech. rep. 2013. URL: <https://hal.inria.fr/hal-00789169>.
- [477] Akira Wakita, Akito Nakano, and Nobuhiro Kobayashi. "Programmable Blobs: A Rheologic Interface for Organic Shape Design." In: *Proceedings of the Fifth International Conference on Tangible, Embedded, and Embodied Interaction*. TEI '11. Funchal, Portugal: Association for Computing Machinery,

- 2010, 273–276. ISBN: 9781450304788. DOI: [10.1145/1935701.1935760](https://doi.org/10.1145/1935701.1935760). URL: <https://doi.org/10.1145/1935701.1935760>.
- [478] Cheng-Yao Wang, Wei-Chen Chu, Po-Tsung Chiu, Min-Chieh Hsiu, Yih-Harn Chiang, and Mike Y. Chen. “PalmType: Using Palms as Keyboards for Smart Glasses.” In: *Proceedings of the 17th International Conference on Human-Computer Interaction with Mobile Devices and Services*. MobileHCI ’15. Copenhagen, Denmark: Association for Computing Machinery, 2015, 153–160. ISBN: 9781450336529. DOI: [10.1145/2785830.2785886](https://doi.org/10.1145/2785830.2785886). URL: <https://doi.org/10.1145/2785830.2785886>.
- [479] Edward Jay Wang, William Li, Doug Hawkins, Terry Gernsheimer, Colette Norby-Slycord, and Shwetak N. Patel. “HemaApp: Noninvasive Blood Screening of Hemoglobin Using Smartphone Cameras.” In: *Proceedings of the 2016 ACM International Joint Conference on Pervasive and Ubiquitous Computing*. UbiComp ’16. Heidelberg, Germany: Association for Computing Machinery, 2016, 593–604. ISBN: 9781450344616. DOI: [10.1145/2971648.2971653](https://doi.org/10.1145/2971648.2971653). URL: <https://doi.org/10.1145/2971648.2971653>.
- [480] Edward Jay Wang, Junyi Zhu, Mohit Jain, Tien-Jui Lee, Elliot Saba, Lama Nachman, and Shwetak N Patel. “Seismo: Blood pressure monitoring using built-in smartphone accelerometer and camera.” In: *Proceedings of the 2018 CHI Conference on Human Factors in Computing Systems*. ACM. 2018, p. 425.
- [481] Feng Wang and Xiangshi Ren. “Empirical Evaluation for Finger Input Properties in Multi-Touch Interaction.” In: *Proceedings of the SIGCHI Conference on Human Factors in Computing Systems*. CHI ’09. Boston, MA, USA: Association for Computing Machinery, 2009, 1063–1072. ISBN: 9781605582467. DOI: [10.1145/1518701.1518864](https://doi.org/10.1145/1518701.1518864). URL: <https://doi.org/10.1145/1518701.1518864>.
- [482] Hao Wang, Giorgia Pastorin, and Chengkuo Lee. “Toward self-powered wearable adhesive skin patch with bendable microneedle array for transdermal drug delivery.” In: *Advanced Science* 3.9 (2016), p. 1500441.
- [483] Liu Wang, Shutao Qiao, Shideh Kabiri Ameri, Hyoyoung Jeong, and Nanshu Lu. “A thin elastic membrane conformed to a soft and rough substrate subjected to stretching/compression.” In: *Journal of Applied Mechanics* 84.11 (2017).
- [484] Saiwen Wang, Jie Song, Jaime Lien, Ivan Poupyrev, and Otmar Hilliges. “Interacting with Soli: Exploring Fine-Grained Dynamic Gesture Recognition in the Radio-Frequency Spectrum.” In: *Proceedings of the 29th Annual Symposium on User Interface Software and Technology*. UIST ’16. Tokyo, Japan: Association for Computing Machinery, 2016, 851–860. ISBN: 9781450341899. DOI: [10.1145/2984511.2984565](https://doi.org/10.1145/2984511.2984565). URL: <https://doi.org/10.1145/2984511.2984565>.

- [485] Sihong Wang, Jin Young Oh, Jie Xu, Helen Tran, and Zhenan Bao. "Skin-inspired electronics: an emerging paradigm." In: *Accounts of chemical research* 51.5 (2018), pp. 1033–1045.
- [486] Sihong Wang, Jie Xu, Weichen Wang, Ging-Ji Nathan Wang, Reza Rastak, Francisco Molina-Lopez, Jong Won Chung, Simiao Niu, Vivian R Feig, Jeffery Lopez, et al. "Skin electronics from scalable fabrication of an intrinsically stretchable transistor array." In: *Nature* 555:7694 (2018), pp. 83–88.
- [487] Sihong Wang et al. "Skin electronics from scalable fabrication of an intrinsically stretchable transistor array." In: (2018). DOI: [10.1038/nature25494](https://doi.org/10.1038/nature25494). URL: <https://www.nature.com/articles/nature25494.pdf>.
- [488] Yan Wang, Sunghoon Lee, Tomoyuki Yokota, Haoyang Wang, Zhi Jiang, Jiabin Wang, Mari Koizumi, and Takao Someya. "A durable nanomesh on-skin strain gauge for natural skin motion monitoring with minimum mechanical constraints." In: *Science advances* 6.33 (2020), eabb7043.
- [489] Yanan Wang, Shijian Luo, Hebo Gong, Fei Xu, Rujia Chen, Shuai Liu, and Preben Hansen. "SKIN+: Fabricating Soft Fluidic User Interfaces for Enhancing On-Skin Experiences and Interactions." In: *Extended Abstracts of the 2018 CHI Conference on Human Factors in Computing Systems*. ACM, 2018, LBW111.
- [490] Yanan Wang, Shijian Luo, Hebo Gong, Fei Xu, Rujia Chen, Shuai Liu, and Preben Hansen. "<i>SKIN+</i>: Fabricating Soft Fluidic User Interfaces for Enhancing On-Skin Experiences and Interactions." In: *Extended Abstracts of the 2018 CHI Conference on Human Factors in Computing Systems*. CHI EA '18. Montreal QC, Canada: Association for Computing Machinery, 2018, 1–6. ISBN: 9781450356213. DOI: [10.1145/3170427.3188443](https://doi.org/10.1145/3170427.3188443). URL: <https://doi.org/10.1145/3170427.3188443>.
- [491] Yanan Wang, Shijian Luo, Yujia Lu, Hebo Gong, Yexing Zhou, Shuai Liu, and Preben Hansen. "AnimSkin: Fabricating Epidermis with Interactive, Functional and Aesthetic Color Animation." In: *Proceedings of the 2017 Conference on Designing Interactive Systems*. DIS '17. Edinburgh, United Kingdom: Association for Computing Machinery, 2017, 397–401. ISBN: 9781450349222. DOI: [10.1145/3064663.3064687](https://doi.org/10.1145/3064663.3064687). URL: <https://doi.org/10.1145/3064663.3064687>.
- [492] Yanan Wang, Shijian Luo, Yujia Lu, Hebo Gong, Yexing Zhou, Shuai Liu, and Preben Hansen. "AnimSkin: Fabricating Epidermis with Interactive, Functional and Aesthetic Color Animation." In: *Proceedings of the 2017 Conference on Designing Interactive Systems*. ACM, 2017, pp. 397–401.

- [493] Youhua Wang, Yitao Qiu, Shideh Kabiri Ameri, Hongwoo Jang, Zhaohe Dai, Yong An Huang, and Nanshu Lu. "Low-cost, μm -thick, tape-free electronic tattoo sensors with minimized motion and sweat artifacts." In: *npj Flexible Electronics* 2.1 (2018), p. 6. ISSN: 23974621. DOI: [10.1038/s41528-017-0019-4](https://doi.org/10.1038/s41528-017-0019-4). URL: www.nature.com/npjflexelectron.
- [494] Youhua Wang, Lang Yin, Yunzhao Bai, Siyi Liu, Liu Wang, Ying Zhou, Chao Hou, Zhaoyu Yang, Hao Wu, Jiayi Ma, et al. "Electrically compensated, tattoo-like electrodes for epidermal electrophysiology at scale." In: *Science advances* 6.43 (2020), eabdo996.
- [495] Kevin Warwick. "Transhumanism: some practical possibilities." In: *FifF Kommunikation* 2016.2 (2016), pp. 24–27.
- [496] Kevin Warwick, Dimitris Xydias, Slawomir J Nasuto, Victor M Becerra, Mark W Hammond, Julia Downes, Simon Marshall, and Benjamin J Whalley. "Controlling a mobile robot with a biological brain." In: *Defence Science Journal* 60.1 (2010), pp. 5–14.
- [497] R. Chad Webb et al. "Ultrathin conformal devices for precise and continuous thermal characterization of human skin." In: *Nature Materials* 12.10 (2013), pp. 938–944. ISSN: 1476-1122. DOI: [10.1038/nmat3755](https://doi.org/10.1038/nmat3755). URL: <http://www.nature.com/articles/nmat3755>.
- [498] Martin Weigel, Tong Lu, Gilles Bailly, Antti Oulasvirta, Carmel Majidi, and Jürgen Steimle. "iSkin." In: *Proceedings of the 33rd Annual ACM Conference on Human Factors in Computing Systems - CHI '15*. New York, New York, USA: ACM Press, 2015, pp. 2991–3000. ISBN: 9781450331456. DOI: [10.1145/2702123.2702391](https://doi.org/10.1145/2702123.2702391). URL: <http://dl.acm.org/citation.cfm?doid=2702123.2702391>.
- [499] Martin Weigel, Vikram Mehta, and Jürgen Steimle. "More Than Touch: Understanding How People Use Skin As an Input Surface for Mobile Computing." In: *Proceedings of the SIGCHI Conference on Human Factors in Computing Systems*. CHI '14. Toronto, Ontario, Canada: ACM, 2014, pp. 179–188. ISBN: 978-1-4503-2473-1. DOI: [10.1145/2556288.2557239](https://doi.org/10.1145/2556288.2557239). URL: <http://doi.acm.org/10.1145/2556288.2557239>.
- [500] Martin Weigel, Aditya Shekhar Nittala, Alex Olwal, and Jürgen Steimle. "SkinMarks: Enabling Interactions on Body Landmarks Using Conformal Skin Electronics." In: *Proceedings of the 2017 CHI Conference on Human Factors in Computing Systems*. CHI '17. Denver, Colorado, USA: ACM, 2017, pp. 3095–3105. ISBN: 978-1-4503-4655-9. DOI: [10.1145/3025453.3025704](https://doi.org/10.1145/3025453.3025704). URL: <http://doi.acm.org/10.1145/3025453.3025704>.
- [501] Martin Weigel and Jürgen Steimle. "DeformWear: Deformation Input on Tiny Wearable Devices." In: *Proc. ACM Interact. Mob. Wearable Ubiquitous Technol.* 1.2 (June 2017). DOI: [10.1145/3090093](https://doi.org/10.1145/3090093). URL: <https://doi.org/10.1145/3090093>.

- [502] William Wenger and Paul Kligfield. "Variability of precordial electrode placement during routine electrocardiography." In: *Journal of electrocardiology* 29.3 (1996), pp. 179–184.
- [503] Michael Wessely, Theophanis Tsandilas, and Wendy E. Mackay. "Stretchis: Fabricating Highly Stretchable User Interfaces." In: *Proceedings of the 29th Annual Symposium on User Interface Software and Technology*. UIST '16. Tokyo, Japan: Association for Computing Machinery, 2016, 697–704. ISBN: 9781450341899. DOI: [10.1145/2984511.2984521](https://doi.org/10.1145/2984511.2984521). URL: <https://doi.org/10.1145/2984511.2984521>.
- [504] *Wheeless' Textbook of Orthopaedics Flexor Carpi Ulnaris*. http://www.wheelessonline.com/ortho/flexor_carpi_ulnaris. Last Accessed: 2021-07-23. 2020.
- [505] *Wheeless' Textbook of Orthopaedics Pronator Quadratus*. http://www.wheelessonline.com/ortho/pronator_quadratus. Last Accessed: 2021-07-23. 2020.
- [506] Clifford R Wheeless. *Wheeless' textbook of orthopaedics*. CR Wheeless, MD, 1996.
- [507] Eric Whitmire, Mohit Jain, Divye Jain, Greg Nelson, Ravi Karkar, Shwetak Patel, and Mayank Goel. "DigiTouch: Reconfigurable Thumb-to-Finger Input and Text Entry on Head-Mounted Displays." In: *Proc. ACM Interact. Mob. Wearable Ubiquitous Technol.* 1.3 (Sept. 2017). DOI: [10.1145/3130978](https://doi.org/10.1145/3130978). URL: <https://doi.org/10.1145/3130978>.
- [508] Wikiversity. *WikiJournal of Medicine/Medical gallery of Blausen Medical 2014* — Wikiversity, [Online; accessed 19-May-2021]. 2018. URL: [\url{https://en.wikiversity.org/w/index.php?title=WikiJournal_of_Medicine/Medical_gallery_of_Blausen_Medical_2014&oldid=1862791}](https://en.wikiversity.org/w/index.php?title=WikiJournal_of_Medicine/Medical_gallery_of_Blausen_Medical_2014&oldid=1862791).
- [509] Mathias Wilhelm, Daniel Krakowczyk, Frank Trollmann, and Sahin Albayrak. "ERing: Multiple Finger Gesture Recognition with One Ring Using an Electric Field." In: *Proceedings of the 2nd International Workshop on Sensor-Based Activity Recognition and Interaction*. iWOAR '15. Rostock, Germany: Association for Computing Machinery, 2015. ISBN: 9781450334549. DOI: [10.1145/2790044.2790047](https://doi.org/10.1145/2790044.2790047). URL: <https://doi.org/10.1145/2790044.2790047>.
- [510] Anusha Withana, Daniel Groeger, and Jürgen Steimle. "Tacttoo: A Thin and Feel-Through Tattoo for On-Skin Tactile Output." In: *Proceedings of the 31st Annual ACM Symposium on User Interface Software and Technology*. UIST '18. Berlin, Germany: ACM, 2018, pp. 365–378. ISBN: 978-1-4503-5948-1. DOI: [10.1145/3242587.3242645](https://doi.org/10.1145/3242587.3242645). URL: <http://doi.acm.org/10.1145/3242587.3242645>.

- [511] Anusha Withana, Roshan Peiris, Nipuna Samarasekara, and Suranga Nanayakkara. "ZSense: Enabling Shallow Depth Gesture Recognition for Greater Input Expressivity on Smart Wearables." In: *Proceedings of the 33rd Annual ACM Conference on Human Factors in Computing Systems*. New York, NY, USA: Association for Computing Machinery, 2015, 3661–3670. ISBN: 9781450331456. URL: <https://doi.org/10.1145/2702123.2702371>.
- [512] Jacob O Wobbrock, Leah Findlater, Darren Gergle, and James J Higgins. "The aligned rank transform for nonparametric factorial analyses using only anova procedures." In: *Proceedings of the SIGCHI conference on human factors in computing systems*. ACM. 2011, pp. 143–146.
- [513] Marc P Wolf, Georgette B Salieb-Beugelaar, and Patrick Hunziker. "PDMS with designer functionalities—Properties, modifications strategies, and applications." In: *Progress in Polymer Science* 83 (2018), pp. 97–134.
- [514] Pui Chung Wong, Kening Zhu, Xing-Dong Yang, and Hongbo Fu. "Exploring Eyes-Free Bezel-Initiated Swipe on Round Smartwatches." In: *Proceedings of the 2020 CHI Conference on Human Factors in Computing Systems*. CHI '20. Honolulu, HI, USA: Association for Computing Machinery, 2020, 1–11. ISBN: 9781450367080. DOI: 10.1145/3313831.3376393. URL: <https://doi.org/10.1145/3313831.3376393>.
- [515] Te-Yen Wu, Zheer Xu, Xing-Dong Yang, Steve Hodges, and Teddy Seyed. "Project Tasca: Enabling Touch and Contextual Interactions with a Pocket-Based Textile Sensor." In: *Proceedings of the 2021 CHI Conference on Human Factors in Computing Systems*. CHI '21. Yokohama, Japan: Association for Computing Machinery, 2021. ISBN: 9781450380966. DOI: 10.1145/3411764.3445712. URL: <https://doi.org/10.1145/3411764.3445712>.
- [516] Haijun Xia, Tovi Grossman, and George Fitzmaurice. "NanoStylus: Enhancing Input on Ultra-Small Displays with a Finger-Mounted Stylus." In: *Proceedings of the 28th Annual ACM Symposium on User Interface Software and Technology*. UIST '15. Charlotte, NC, USA: Association for Computing Machinery, 2015, 447–456. ISBN: 9781450337793. DOI: 10.1145/2807442.2807500. URL: <https://doi.org/10.1145/2807442.2807500>.
- [517] Robert Xiao, Teng Cao, Ning Guo, Jun Zhuo, Yang Zhang, and Chris Harrison. "LumiWatch: On-Arm Projected Graphics and Touch Input." In: *Proceedings of the 2018 CHI Conference on Human Factors in Computing Systems*. ACM. 2018, p. 95.
- [518] Robert Xiao, Gierad Laput, and Chris Harrison. "Expanding the Input Expressivity of Smartwatches with Mechanical Pan, Twist, Tilt and Click." In: *Proceedings of the SIGCHI Conference on Human Factors in Computing Systems*. CHI '14. Toronto, Ontario, Canada: Association for Computing Machinery, 2014, 193–196. ISBN: 9781450324731. DOI: 10.1145/2556288.2557017. URL: <https://doi.org/10.1145/2556288.2557017>.

- [519] Robert Xiao, Julia Schwarz, and Chris Harrison. "Estimating 3D Finger Angle on Commodity Touchscreens." In: *Proceedings of the 2015 International Conference on Interactive Tabletops and Surfaces*. ITS '15. Madeira, Portugal: Association for Computing Machinery, 2015, 47–50. ISBN: 9781450338998. DOI: [10.1145/2817721.2817737](https://doi.org/10.1145/2817721.2817737). URL: <https://doi.org/10.1145/2817721.2817737>.
- [520] Gang Xu, Yanli Lu, Chen Cheng, Xin Li, Jie Xu, Zhaoyang Liu, Jinglong Liu, Guang Liu, Zhenghan Shi, Zetao Chen, et al. "Battery-Free and Wireless Smart Wound Dressing for Wound Infection Monitoring and Electrically Controlled On-Demand Drug Delivery." In: *Advanced Functional Materials* (2021), p. 2100852.
- [521] PJ Xu, H Zhang, and XM Tao. "Textile-structured electrodes for electrocardiogram." In: *Textile Progress* 40.4 (2008), pp. 183–213.
- [522] Shuai Xu, Arun Jayaraman, and John A Rogers. *Skin sensors are the future of health care*. 2019.
- [523] Xuhai Xu, Haitian Shi, Xin Yi, WenJia Liu, Yukang Yan, Yuanchun Shi, Alex Mariakakis, Jennifer Mankoff, and Anind K. Dey. "EarBuddy: Enabling On-Face Interaction via Wireless Earbuds." In: *Proceedings of the 2020 CHI Conference on Human Factors in Computing Systems*. New York, NY, USA: Association for Computing Machinery, 2020, 1–14. ISBN: 9781450367080. URL: <https://doi.org/10.1145/3313831.3376836>.
- [524] Yadong Xu, Ganggang Zhao, Liang Zhu, Qihui Fei, Zhe Zhang, Zanyu Chen, Fufei An, Yangyang Chen, Yun Ling, Peijun Guo, et al. "Pencil–paper on-skin electronics." In: *Proceedings of the National Academy of Sciences* 117.31 (2020), pp. 18292–18301.
- [525] Zheer Xu, Pui Chung Wong, Jun Gong, Te-Yen Wu, Aditya Shekhar Nittala, Xiaojun Bi, Jürgen Steimle, Hongbo Fu, Kening Zhu, and Xing-Dong Yang. "TipText: Eyes-Free Text Entry on a Fingertip Keyboard." In: *Proceedings of the 32nd Annual ACM Symposium on User Interface Software and Technology*. UIST '19. New Orleans, LA, USA: Association for Computing Machinery, 2019, 883–899. ISBN: 9781450368162. DOI: [10.1145/3332165.3347865](https://doi.org/10.1145/3332165.3347865). URL: <https://doi.org/10.1145/3332165.3347865>.
- [526] Takeo Yamada, Yuhei Hayamizu, Yuki Yamamoto, Yoshiki Yomogida, Ali Izadi-Najafabadi, Don N Futaba, and Kenji Hata. "A stretchable carbon nanotube strain sensor for human-motion detection." In: *Nature nanotechnology* 6.5 (2011), pp. 296–301.
- [527] Koki Yamashita, Takashi Kikuchi, Katsutoshi Masai, Maki Sugimoto, Bruce H. Thomas, and Yuta Sugiura. "CheekInput: Turning Your Cheek into an Input Surface by Embedded Optical Sensors on a Head-Mounted Display." In: *Proceedings of the 23rd ACM Symposium on Virtual Reality Software and Technology*. VRST '17. Gothenburg, Sweden: Association for Computing

- Machinery, 2017. ISBN: 9781450355483. DOI: [10.1145/3139131.3139146](https://doi.org/10.1145/3139131.3139146). URL: <https://doi.org/10.1145/3139131.3139146>.
- [528] Yuki Yamato, Yutaro Suzuki, Kodai Sekimori, Buntarou Shizuki, and Shin Takahashi. "Hand Gesture Interaction with a Low-Resolution Infrared Image Sensor on an Inner Wrist." In: *Proceedings of the International Conference on Advanced Visual Interfaces*. AVI '20. Salerno, Italy: Association for Computing Machinery, 2020. ISBN: 9781450375351. DOI: [10.1145/3399715.3399858](https://doi.org/10.1145/3399715.3399858). URL: <https://doi.org/10.1145/3399715.3399858>.
- [529] Canhui Yang and Zhigang Suo. "Hydrogel ionotronics." In: *Nature Reviews Materials* 3.6 (2018), pp. 125–142.
- [530] Hung-Chi Yang, Tsung-Fu Chien, Shang-Hao Liu, and Hsuan-Han Chiang. "Study of Single-Arm Electrode for ECG Measurement Using Flexible Print Circuit." In: ().
- [531] Shixuan Yang, Ying-Chen Chen, Luke Nicolini, Praveenkumar Pasupathy, Jacob Sacks, Becky Su, Russell Yang, Daniel Sanchez, Yao-Feng Chang, Pulin Wang, et al. "'Cut-and-paste' manufacture of multiparametric epidermal sensor systems." In: *Advanced Materials* 27.41 (2015), pp. 6423–6430.
- [532] Weiqing Yang, Jun Chen, Guang Zhu, Jin Yang, Peng Bai, Yuanjie Su, Qingsheng Jing, Xia Cao, and Zhong Lin Wang. "Harvesting energy from the natural vibration of human walking." In: *ACS nano* 7.12 (2013), pp. 11317–11324.
- [533] Shanshan Yao and Yong Zhu. "Wearable multifunctional sensors using printed stretchable conductors made of silver nanowires." In: *Nanoscale* 6.4 (2014), pp. 2345–2352.
- [534] Hui-Shyong Yeo, Gergely Flamich, Patrick Schrempf, David Harris-Birtill, and Aaron Quigley. "RadarCat: Radar Categorization for Input and Interaction." In: *Proceedings of the 29th Annual Symposium on User Interface Software and Technology*. UIST '16. Tokyo, Japan: Association for Computing Machinery, 2016, 833–841. ISBN: 9781450341899. DOI: [10.1145/2984511.2984515](https://doi.org/10.1145/2984511.2984515). URL: <https://doi.org/10.1145/2984511.2984515>.
- [535] Hui-Shyong Yeo, Erwin Wu, Juyoung Lee, Aaron Quigley, and Hideki Koike. "Opisthenar: Hand Poses and Finger Tapping Recognition by Observing Back of Hand Using Embedded Wrist Camera." In: *Proceedings of the 32nd Annual ACM Symposium on User Interface Software and Technology*. UIST '19. New Orleans, LA, USA: Association for Computing Machinery, 2019, 963–971. ISBN: 9781450368162. DOI: [10.1145/3332165.3347867](https://doi.org/10.1145/3332165.3347867). URL: <https://doi.org/10.1145/3332165.3347867>.
- [536] Joo Chuan Yeo, Zhuangjian Liu, Zhi-Qian Zhang, Pan Zhang, Zhiping Wang, and Chwee Teck Lim. "Wearable mechanotransduced tactile sensor for haptic perception." In: *Advanced Materials Technologies* 2.6 (2017), p. 1700006.

- [537] Woon-Hong Yeo et al. "Multifunctional Epidermal Electronics Printed Directly Onto the Skin." In: *Advanced Materials* 25.20 (2013), pp. 2773–2778. ISSN: 09359648. DOI: [10.1002/adma.201204426](https://doi.org/10.1002/adma.201204426). URL: <http://doi.wiley.com/10.1002/adma.201204426>.
- [538] Tomoyuki Yokota et al. "Ultraflexible, large-area, physiological temperature sensors for multipoint measurements." In: *Proceedings of the National Academy of Sciences* 112.47 (2015), pp. 14533–14538. ISSN: 0027-8424. DOI: [10.1073/pnas.1515650112](https://doi.org/10.1073/pnas.1515650112). eprint: <http://www.pnas.org/content/112/47/14533.full.pdf>. URL: <http://www.pnas.org/content/112/47/14533>.
- [539] Sang Ho Yoon, Ke Huo, Vinh P. Nguyen, and Karthik Ramani. "TIMMi: Finger-Worn Textile Input Device with Multimodal Sensing in Mobile Interaction." In: *Proceedings of the Ninth International Conference on Tangible, Embedded, and Embodied Interaction*. TEI '15. Stanford, California, USA: Association for Computing Machinery, 2015, 269–272. ISBN: 9781450333054. DOI: [10.1145/2677199.2680560](https://doi.org/10.1145/2677199.2680560). URL: <https://doi.org/10.1145/2677199.2680560>.
- [540] Sang Ho Yoon, Ke Huo, and Karthik Ramani. "Wearable textile input device with multimodal sensing for eyes-free mobile interaction during daily activities." In: *Pervasive and Mobile Computing* 33 (2016), pp. 17–31.
- [541] Sang Ho Yoon, Siyuan Ma, Woo Suk Lee, Shantanu Thakurdesai, Di Sun, Flávio P. Ribeiro, and James D. Holbery. "HapSense: A Soft Haptic I/O Device with Uninterrupted Dual Functionalities of Force Sensing and Vibrotactile Actuation." In: *Proceedings of the 32nd Annual ACM Symposium on User Interface Software and Technology*. UIST '19. New Orleans, LA, USA: Association for Computing Machinery, 2019, 949–961. ISBN: 9781450368162. DOI: [10.1145/3332165.3347888](https://doi.org/10.1145/3332165.3347888). URL: <https://doi.org/10.1145/3332165.3347888>.
- [542] Chuang-Wen You, Min-Wei Hung, Ximeng Zhang, Po-Chun Huang, and Hsin-Liu (Cindy) Kao. "Online Survey Study on Social Perceptions towards Color-Changing on-Skin Displays." In: *Proceedings of the 2020 International Symposium on Wearable Computers*. ISWC '20. Virtual Event, Mexico: Association for Computing Machinery, 2020, 90–95. ISBN: 9781450380775. DOI: [10.1145/3410531.3414301](https://doi.org/10.1145/3410531.3414301). URL: <https://doi.org/10.1145/3410531.3414301>.
- [543] Chuang-Wen You, Ya-Fang Lin, Elle Luo, Hung-Yeh Lin, and Hsin-Liu (Cindy) Kao. "Understanding Social Perceptions towards Interacting with On-Skin Interfaces in Public." In: *Proceedings of the 23rd International Symposium on Wearable Computers*. ISWC '19. London, United Kingdom: Association for Computing Machinery, 2019, 244–253. ISBN: 9781450368704. DOI: [10.1145/3341163.3347751](https://doi.org/10.1145/3341163.3347751). URL: <https://doi.org/10.1145/3341163.3347751>.

- [544] Aaron J Young, Levi J Hargrove, and Todd A Kuiken. "The effects of electrode size and orientation on the sensitivity of myoelectric pattern recognition systems to electrode shift." In: *IEEE Transactions on Biomedical Engineering* 58.9 (2011), pp. 2537–2544. DOI: [10.1109/TBME.2011.2159216](https://doi.org/10.1109/TBME.2011.2159216).
- [545] Xinge Yu et al. "Skin-integrated wireless haptic interfaces for virtual and augmented reality." In: *Nature* 575.7783 (2019), pp. 473–479. ISSN: 14764687. DOI: [10.1038/s41586-019-1687-0](https://doi.org/10.1038/s41586-019-1687-0). URL: <https://doi.org/10.1038/s41586-019-1687-0>.
- [546] Hyunwoo Yuk, Teng Zhang, German Alberto Parada, Xinyue Liu, and Xuanhe Zhao. "Skin-inspired hydrogel–elastomer hybrids with robust interfaces and functional microstructures." In: *Nature communications* 7.1 (2016), pp. 1–11.
- [547] Clint Zeagler. "Where to Wear It: Functional, Technical, and Social Considerations in on-Body Location for Wearable Technology 20 Years of Designing for Wearability." In: *Proceedings of the 2017 ACM International Symposium on Wearable Computers*. ISWC '17. Maui, Hawaii: Association for Computing Machinery, 2017, 150–157. ISBN: 9781450351881. DOI: [10.1145/3123021.3123042](https://doi.org/10.1145/3123021.3123042). URL: <https://doi.org/10.1145/3123021.3123042>.
- [548] Abdelkader Zebda, Chantal Gondran, Alan Le Goff, Michael Holzinger, Philippe Cinquin, and Serge Cosnier. "Mediatorless high-power glucose biofuel cells based on compressed carbon nanotube-enzyme electrodes." In: *Nature communications* 2.1 (2011), pp. 1–6.
- [549] Cheng Zhang, Sinan Hersek, Yiming Pu, Danrui Sun, Qiuyue Xue, Thad E. Starner, Gregory D. Abowd, and Omer T. Inan. "Bioacoustics-Based Human-Body-Mediated Communication." In: *Computer* 50.2 (2017), pp. 36–46. DOI: [10.1109/MC.2017.43](https://doi.org/10.1109/MC.2017.43).
- [550] Jinnan Zhang, Yanghua Cao, Min Qiao, Lingmei Ai, Kaize Sun, Qing Mi, Siyao Zang, Yong Zuo, Xueguang Yuan, and Qi Wang. "Human motion monitoring in sports using wearable graphene-coated fiber sensors." In: *Sensors and Actuators A: Physical* 274 (2018), pp. 132–140.
- [551] Yang Zhang and Chris Harrison. "Tomo: Wearable, Low-Cost Electrical Impedance Tomography for Hand Gesture Recognition." In: *Proceedings of the 28th Annual ACM Symposium on User Interface Software and Technology*. UIST '15. Charlotte, NC, USA: Association for Computing Machinery, 2015, 167–173. ISBN: 9781450337793. DOI: [10.1145/2807442.2807480](https://doi.org/10.1145/2807442.2807480). URL: <https://doi.org/10.1145/2807442.2807480>.
- [552] Yang Zhang, Wolf Kienzle, Yanjun Ma, Shiu S. Ng, Hrvoje Benko, and Chris Harrison. "ActiTouch: Robust Touch Detection for On-Skin AR/VR Interfaces." In: *Proceedings of the 32nd Annual ACM Symposium on User Interface Software and Technology*. UIST '19. New Orleans, LA, USA: Association for Computing Machinery, 2019, 1151–1159. ISBN: 9781450368162.

- DOI: [10.1145/3332165.3347869](https://doi.org/10.1145/3332165.3347869). URL: <https://doi.org/10.1145/3332165.3347869>.
- [553] Yang Zhang, Junhan Zhou, Gierad Laput, and Chris Harrison. "SkinTrack: Using the Body as an Electrical Waveguide for Continuous Finger Tracking on the Skin." In: *Proceedings of the 2016 CHI Conference on Human Factors in Computing Systems*. CHI '16. San Jose, California, USA: Association for Computing Machinery, 2016, 1491–1503. ISBN: 9781450333627. DOI: [10.1145/2858036.2858082](https://doi.org/10.1145/2858036.2858082). URL: <https://doi.org/10.1145/2858036.2858082>.
- [554] Chaoshan Zhao, Yunlei Zhou, Shaoqiang Gu, Shitai Cao, Jiachen Wang, Menghu Zhang, Youzhi Wu, and Desheng Kong. "Fully Screen-Printed, Multicolor, and Stretchable Electroluminescent Displays for Epidermal Electronics." In: *ACS Applied Materials & Interfaces* 12.42 (2020), pp. 47902–47910.
- [555] Junwen Zhong, Yuan Ma, Yu Song, Qize Zhong, Yao Chu, Ilbey Karakurt, David B Bogy, and Liwei Lin. "A flexible piezoelectret actuator/sensor patch for mechanical human-machine interfaces." In: *ACS nano* 13.6 (2019), pp. 7107–7116.
- [556] Bo Zhou, Jingyuan Cheng, Mathias Sundholm, and Paul Lukowicz. "From smart clothing to smart table cloth: Design and implementation of a large scale, textile pressure matrix sensor." In: *International conference on architecture of computing systems*. Springer. 2014, pp. 159–170.
- [557] Guangmin Zhou, Lu Li, Chaoqun Ma, Shaogang Wang, Ying Shi, Nikhil Koratkar, Wencai Ren, Feng Li, and Hui-Ming Cheng. "A graphene foam electrode with high sulfur loading for flexible and high energy Li-S batteries." In: *Nano Energy* 11 (2015), pp. 356–365.
- [558] Junhan Zhou, Yang Zhang, Gierad Laput, and Chris Harrison. "AuraSense: Enabling Expressive Around-Smartwatch Interactions with Electric Field Sensing." In: *Proceedings of the 29th Annual Symposium on User Interface Software and Technology*. UIST '16. Tokyo, Japan: Association for Computing Machinery, 2016, 81–86. ISBN: 9781450341899. DOI: [10.1145/2984511.2984568](https://doi.org/10.1145/2984511.2984568). URL: <https://doi.org/10.1145/2984511.2984568>.
- [559] Zhihao Zhou, Kyle Chen, Xiaoshi Li, Songlin Zhang, Yufen Wu, Yihao Zhou, Keyu Meng, Chenchen Sun, Qiang He, Wenjing Fan, et al. "Sign-to-speech translation using machine-learning-assisted stretchable sensor arrays." In: *Nature Electronics* 3.9 (2020), pp. 571–578.
- [560] JH Zhu. "So, R. Mays, S. Desai, WR Barnes, B. Pourdeyhimi, and M. D. Dickey." In: *Adv. Funct. Mater* 23 (2013), p. 2308.

- [561] Suwen Zhu, Jingjie Zheng, Shumin Zhai, and Xiaojun Bi. "I'sFree: Eyes-Free Gesture Typing via a Touch-Enabled Remote Control." In: *Proceedings of the 2019 CHI Conference on Human Factors in Computing Systems*. New York, NY, USA: Association for Computing Machinery, 2019, 1–12. ISBN: 9781450359702. URL: <https://doi.org/10.1145/3290605.3300678>.
- [562] Zijie Zhu, Ruya Li, and Tingrui Pan. "EIS: A wearable device for epidermal pressure sensing." In: *2018 IEEE Haptics Symposium (HAPTICS)*. IEEE, 2018, pp. 1–6.
- [563] T. G. Zimmerman. "Personal Area Networks: Near-field intrabody communication." In: *IBM Systems Journal* 35.3.4 (1996), pp. 609–617. DOI: [10.1147/sj.353.0609](https://doi.org/10.1147/sj.353.0609).
- [564] Thomas G. Zimmerman, Jaron Lanier, Chuck Blanchard, Steve Bryson, and Young Harvill. "A Hand Gesture Interface Device." In: *SIGCHI Bull.* 18.4 (May 1986), 189–192. ISSN: 0736-6906. DOI: [10.1145/1165387.275628](https://doi.org/10.1145/1165387.275628). URL: <https://doi.org/10.1145/1165387.275628>.
- [565] Thomas G Zimmerman, Joshua R Smith, Joseph A Paradiso, David Allport, and Neil Gershenfeld. "Applying electric field sensing to human-computer interfaces." In: *Proceedings of the SIGCHI conference on Human factors in computing systems*. ACM Press/Addison-Wesley Publishing Co. 1995, pp. 280–287.
- [566] P Zipp. *Recommendations for the Standardization of Lead Positions in Surface Electromyography**. Tech. rep. 1982, pp. 41–54. URL: <https://link.springer.com/content/pdf/10.1007/BF00952243.pdf>.
- [567] D Zrnic and DS Swatik. "On the resistivity and surface tension of the eutectic alloy of gallium and indium." In: *Journal of the less common metals* 18.1 (1969), pp. 67–68.
- [568] Alessandra Zucca, Christian Cipriani, Sergio Tarantino, Davide Ricci, Virgilio Mattoli, and Francesco Greco. "Tattoo conductive polymer nanosheets for skin-contact applications." In: *Advanced healthcare materials* 4.7 (2015), pp. 983–990.